CANADIAN THESES ON MICROFICHE

THÈSES CANADIENNES SUR MICROFICHE

National Library of Canada
Collections Development Branch

Canadian Theses on
Microfiche Service

Ottawa, Canada
K1A 0N4

Bibliothèque nationale du Canada
Direction du développement des collections

Service des thèses canadiennes
sur microfiche

NOTICE

The quality of this microfiche is heavily dependent upon the quality of the original thesis submitted for microfilming. Every effort has been made to ensure the highest quality of reproduction possible.

If pages are missing, contact the university which granted the degree.

Some pages may have indistinct print especially if the original pages were typed with a poor typewriter ribbon or if the university sent us an inferior photocopy.

Previously copyrighted materials (journal articles, published tests, etc.) are not filmed.

Reproduction in full or in part of this film is governed by the Canadian Copyright Act, R.S.C. 1970, c. C-30. Please read the authorization forms which accompany this thesis.

AVIS

La qualité de cette microfiche dépend grandement de la qualité de la thèse soumise au microfilmage. Nous avons tout fait pour assurer une qualité supérieure de reproduction.

S'il manque des pages, veuillez communiquer avec l'université qui a conféré le grade.

La qualité d'impression de certaines pages peut laisser à désirer, surtout si les pages originales ont été dactylographiées à l'aide d'un ruban usé ou si l'université nous a fait parvenir une photocopie de qualité inférieure.

Les documents qui font déjà l'objet d'un droit d'auteur (articles de revue, examens publiés, etc.) ne sont pas microfilmés.

La reproduction, même partielle, de ce microfilm est soumise à la Loi canadienne sur le droit d'auteur, SRC 1970, c. C-30. Veuillez prendre connaissance des formules d'autorisation qui accompagnent cette thèse.

THIS DISSERTATION
HAS BEEN MICROFILMED
EXACTLY AS RECEIVED

LA THÈSE A ÉTÉ
MICROFILMÉE TELLE QUE
NOUS L'AVONS REÇUE

Canada

NL 339 (r. 86/09)

National Library of Canada
Bibliothèque nationale du Canada

Ottawa, Canada
K1A 0N4

TC –

ISBN 0-315-21278-0

CANADIAN THESES ON MICROFICHE SERVICE – SERVICE DES THÈSES CANADIENNES SUR MICROFICHE

PERMISION TO MICROFILM – AUTORISATION DE MICROFILMER

• Please print or type – Écrire en lettres moulées ou dactylographier

AUTHOR – AUTEUR

Full Name of Author – Nom complet de l'auteur

NG, KWOK-CHOI SAMUEL

Date of Birth – Date de naissance

3rd January 1955

Canadian Citizen – Citoyen canadien

☐ Yes / Oui ☑ No / Non

Country of Birth – Lieu de naissance

HONG KONG

Permanent Address – Résidence fixe

c/o DEPARTMENT OF GEOLOGY
UNIVERSITY OF ALBERTA
EDMONTON, ALBERTA T6G 2E3

THESIS – THÈSE

Title of Thesis – Titre de la thèse

STRATIGRAPHY, SEDIMENTOLOGY AND DIAGENESIS OF THE UPPER MISSISSIPPIAN TO PERMIAN STRATA OF THE TALBOT LAKE AREA, JASPER NATIONAL PARK, ALBERTA

Degree for which thesis was presented
Grade pour lequel cette thèse fut présentée

Master of Science

Year this degree conferred
Année d'obtention de ce grade

SPRING, 1985

University – Université

UNIVERSITY OF ALBERTA

Name of Supervisor – Nom du directeur de thèse

Dr. BRIAN JONES

AUTHORIZATION – AUTORISATION

Permission is hereby granted to the NATIONAL LIBRARY OF CANADA to **microfilm** this thesis and to **lend** or **sell copies of the film.**

The author reserves other publication rights, and neither the thesis nor extensive extracts from it may be printed or otherwise reproduced without the author's written permission.

L'autorisation est, par la présente, accordée à la BIBLIOTHÈQUE NATIONALE DU CANADA de **microfilmer** cette thèse et de **prêter** ou de **vendre des exemplaires du film.**

L'auteur se réserve les autres droits de publication; ni la thèse ni de longs extraits de celle-ci ne doivent être imprimés ou autrement reproduits sans l'autorisation écrite de l'auteur.

ATTACH FORM TO THESIS – VEUILLEZ JOINDRE CE FORMULAIRE À LA THÈSE

Signature

Ng Kwok Choi

Date

24 April, 1985

Canada

THE UNIVERSITY OF ALBERTA

STRATIGRAPHY, SEDIMENTOLOGY AND DIAGENESIS OF THE UPPER MISSISSIPPIAN TO PERMIAN STRATA OF THE TALBOT LAKE AREA, JASPER NATIONAL PARK, ALBERTA

by

KWOK-CHOI SAMUEL NG

A THESIS

SUBMITTED TO THE FACULTY OF GRADUATE STUDIES AND RESEARCH IN PARTIAL FULFILMENT OF THE REQUIREMENTS FOR THE DEGREE OF MASTER OF SCIENCE

DEPARTMENT OF GEOLOGY

EDMONTON, ALBERTA

SPRING, 1985

THE UNIVERSITY OF ALBERTA

RELEASE FORM

NAME OF AUTHOR KWOK-CHOI SAMUEL NG

TITLE OF THESIS STRATIGRAPHY, SEDIMENTOLOGY AND DIAGENESIS OF THE UPPER MISSISSIPPIAN TO PERMIAN STRATA OF THE TALBOT LAKE AREA, JASPER NATIONAL PARK, ALBERTA

DEGREE FOR WHICH THESIS WAS PRESENTED MASTER OF SCIENCE

YEAR THIS DEGREE GRANTED SPRING, 1985

Permission is hereby granted to THE UNIVERSITY OF ALBERTA LIBRARY to reproduce single copies of this thesis and to lend or sell such copies for private, scholarly or scientific research purposes only.

The author reserves other publication rights, and neither the thesis nor extensive extracts from it may be printed or otherwise reproduced without the author's written permission.

(SIGNED) Ng Kwok Choi

PERMANENT ADDRESS:

DEPARTMENT OF GEOLOGY

U OF ALBERTA

EDMONTON

DATED April 24 1985

THE UNIVERSITY OF ALBERTA

FACULTY OF GRADUATE STUDIES AND RESEARCH

The undersigned certify that they have read, and recommend to the Faculty of Graduate Studies and Research, for acceptance, a thesis entitled STRATIGRAPHY, SEDIMENTOLOGY AND DIAGENESIS OF THE UPPER MISSISSIPPIAN TO PERMIAN STRATA OF THE TALBOT LAKE AREA, JASPER NATIONAL PARK, ALBERTA submitted by KWOK-CHOI SAMUEL NG in partial fulfilment of the requirements for the degree of MASTER OF SCIENCE in GEOLOGY.

.....

Supervisor

.....

.....

.....

Date April 18, 1985

ABSTRACT

In the Talbot Lake area, the Upper Mississippian carbonate sequence comprises, in ascending order, the Turner Valley, Mount Head and Etherington formations. The contact between the latter two formations is defined by a paraconformity. A major disconformity separates the Upper Mississippian carbonates and the Upper Permian Ishbel Group, which consists of the Ranger Canyon and Mowitch formations. The post-Mississippian disconformity displays paleotopographic relief as well as paleokarstic features which are indicative of relative drop in sea level in Late Mississippian time.

Those fossils, lithologies, textural characters and sedimentary structures that are preserved; permit the following environmental interpretation: Turner Valley Formation - open marine shoal grading to lagoonal; Mount Head Formation - shallow subtidal grading to lower supratidal; Etherington Formation - upper intertidal grading to supratidal; Ranger Canyon Formation - upper intertidal to supratidal; Mowitch Formation - deltaic progradation over a shallow carbonate shelf.

The Upper Mississippian dolostones underwent two phases of early replacive dolomitization, multiple stages of silicification (replacement and cementation), multiphase calcite and dolomite cementation, dedolomitization, hematite replacement, pyrite formation, internal sedimentation, stylolitization, and fracturing. The Ranger Canyon Formation

underwent early incipient dolomitization and pervasive silicification followed by late stage dedolomitization. The Mowitch Formation is characterized by phosphatization.

The Upper Mississippian and Permian successions originated by sedimentation associated with successive shallowing-upward tidal flat sequences. These prograding sequences permit the development of hypersaline conditions as well as provide additional land area for meteoric fresh water recharge. A diagenetic realm comprising sea water, fresh water and hypersaline brine is probably responsible for the complex diagenetic patterns of the rocks. Ground water lens expansion and contraction related to Late Mississippian and Late Permian maximum regressions also had significant impact on the diagenetic regime.

ACKNOWLEDGEMENTS

I express my sincere thanks to my supervisor, Dr. Brian Jones, for introducing me to the 'wonderland' of carbonate sedimentology and for his advice, guidance and encouragement throughout the course of the research. Dr. Jones' editorial skills have helped to improve this thesis immensely. His computer expertise has also alleviated me from some of the draftings.

The field work and research for this thesis were supported by grants from the Boreal Institute for Northern Studies and NSERC A6090 (to Jones). Financial assistance was provided by the University of Alberta through teaching assistantships. Permit to collect rock samples in Jasper National Park was issued by Parks Canada. To these organizations I offer my thanks.

I acknowledge my fellow graduate students, Quentin Goodbody and Franz Nentwich in particular, for their many hours of academic and non-academic, enlightening discussions. I am indebted to Cheryl Squair for her able assistance in the field. My appreciation is also extended to Dr. Charles Stelck who pointed out some important geological features in the Mount Greenock section; May Poon who typed parts of this thesis; Elsie Tsang and Leni Honsaker for their office supports; and Dr. Charles Stelck, Dr. Fred Longstaffe and Dr. Peter Kershaw who reviewed and gave valuable comments on the thesis.

Table of Contents

Chapter		Page
I.	INTRODUCTION	1
	A. OBJECTIVES	2
	B. METHOD OF STUDY	2
	C. TECTONIC SETTING	5
	D. STRATIGRAPHIC SETTING	7
	E. PREVIOUS STUDIES AND FORMATIONAL NOMENCLATURE	8
	F. CLASSIFICATION SYSTEM	12
	CARBONATE AND CLASTIC ROCKS	12
	PORE TYPES	14
	CRYSTALLINE CARBONATE FABRICS	15
	UNCONFORMITIES	15
II.	MISSISSIPPIAN STRATIGRAPHY AND SEDIMENTOLOGY	17
	A. INTRODUCTION	17
	B. TURNER VALLEY FORMATION	17
	BOUNDARIES	18
	LITHOLOGIES AND FAUNA	18
	POROSITY	21
	DISTRIBUTION OF LITHOTYPES	21
	DEPOSITIONAL ENVIRONMENTS	22
	C. MOUNT HEAD FORMATION	23
	BOUNDARIES	24
	LITHOLOGIES AND FAUNA	24
	POROSITY	32
	DISTRIBUTION OF LITHOTYPES	33
	DEPOSITIONAL ENVIRONMENTS	34

D. ETHERINGTON FORMATION 38
BOUNDARIES 38
LITHOLOGIES AND FAUNA 39
POROSITY 46
DISTRIBUTION OF LITHOTYPES 46
DEPOSITIONAL ENVIRONMENTS 47
III. MISSISSIPPIAN - PERMIAN BOUNDARY 52
A. PALEOTOPOGRAPHIC RELIEF 52
B. PALEOKARSTIC FEATURES 53
SOIL COVER 56
JOINTS AND BEDDING PLANES 56
C. CHERT CONGLOMERATE 58
D. BASAL INTRACLAST AND CONGLOMERATE 59
E. DEPOSITIONAL ENVIRONMENTS 60
IV. PERMIAN STRATIGRAPHY AND SEDIMENTOLOGY 62
A. RANGER CANYON FORMATION 62
BOUNDARIES 62
LITHOLOGIES AND FAUNA 63
DEPOSITIONAL ENVIRONMENTS 67
B. MOWITCH FORMATION 69
BOUNDARIES 69
LITHOLOGIES AND FAUNA 69
DEPOSITIONAL ENVIRONMENTS 71
V. STRATIGRAPHY AND SEDIMENTOLOGY: SYNOPSIS 73
A. INTRODUCTION 73
B. STRATIGRAPHIC CORRELATION 74
C. ENVIRONMENTAL RECONSTRUCTION 79

D. CORRELATION WITH GLOBAL SEA LEVEL CHANGES 85

VI. REPLACIVE DOLOMITIZATION 88

A. SELECTIVE DOLOMITIZATION 88

PETROGRAPHY OF DOLOMITE 88

TIMING OF SELECTIVE DOLOMITIZATION 88

MECHANISM OF SELECTIVE DOLOMITIZATION 90

B. PERVASIVE DOLOMITIZATION 91

PETROGRAPHY OF DOLOMITE 91

TIMING OF PERVASIVE DOLOMITIZATION 93

STAGES OF PERVASIVE, MATRIX DOLOMITIZATION .95

MECHANISM OF PHASE I MATRIX DOLOMITIZATION .97

MECHANISM OF PHASE II MATRIX DOLOMITIZATION 104

VII. SILICIFICATION - REPLACEMENT AND CEMENTATION 109

A. CHERT DISTRIBUTION IN MISSISSIPPIAN CARBONATES 109

B. PETROGRAPHY OF CHERTS 111

MICROCRYSTALLINE QUARTZ 111

LENGTH-FAST CHALCEDONY 112

QUARTZINE 113

MEGACRYSTALLINE QUARTZ 114

C. SOURCE OF SILICA 116

D. TIMING OF SILICIFICATION 118

RANGER CANYON FORMATION 118

MISSISSIPPIAN CARBONATES 120

E. MECHANISM OF SILICIFICATION 122

VIII. CARBONATE CEMENTATION 128

A. INTRODUCTION 128

B. LEACHING 130
C. PETROGRAPHY OF CARBONATE CEMENTS 131
CLEAR, NONFERROAN DOLOMITE 131
FERROAN DOLOMITE 132
COARSE DOLOMITE SPAR 133
MICROSTALACTITIC CALCITE 133
COARSE CALCITE SPAR 134
D. MECHANISM OF CARBONATE CEMENTATION 135
IX. DEDOLOMITIZATION AND OTHER DIAGENETIC PROCESSES .142
A. DEDOLOMITIZATION 142
PETROLOGY OF DEDOLOMITE 142
MECHANISM OF DEDOLOMITIZATION 144
B. HEMATITE REPLACEMENT ("HEMATITIZATION") 147
C. PYRITE FORMATION 148
D. INTERNAL SEDIMENTATION 149
E. PRESSURE SOLUTION 150
F. FRACTURING 151
G. PHOSPHATIZATION 152
X. DIAGENESIS: SYNOPSIS 154
A. EFFECT OF THE DEPOSITIONAL ENVIRONMENTS 158
B. DOLOMITIZATION VERSUS SILICIFICATION 159
FACTORS CONTROLLING DOLOMITIZATION 159
FACTORS CONTROLLING SILICIFICATION 160
C. CARBONATE CEMENTATION PATTERN 161
D. POROSITY DESTRUCTION BY DOLOMITIZATION 163
XI. CONCLUSION 165
XII. LIST OF PLATES: Plates 1 to 26 171

XIII. REFERENCES 224

XIV. APPENDIX 243

LIST OF FIGURES

Figure 1. Index and location map.....Page 4

Figure 2. Map showing position of studied sections and relationship to major thrust sheets.....6

Figure 3. Generalized stratigraphic column: Middle Mississippian to Triassic strata.....10

Figure 4. Formation nomenclature: Pennsylvanian to Permian strata.....13

Figure 5. Geological section: Talbot Lake...(in rear pocket)

Figure 6. Geological section: Mount Greenock(in rear pocket)

Figure 7. Geological section: Cinquefoil Mountain...(in rear pocket)

Figure 8. Geological section: Snaring River.(in rear pocket)

Figure 9. Correlation of sections: Mount Greenock...(in rear pocket)

Figure 10. Correlation of sections: Talbot Lake.....(in rear pocket)

Figure 11. Correlation of sections: Cinquefoil Mountain .(in rear pocket)

Figure 12. Schematic diagram showing paleokarstic features55

Figure 13. Schematic representation of sedimentary strata before and after thrusting.....75

Figure 14. Stratigraphic correlation of the studied sections.....76

Figure 15. Composite stratigraphic column: major lithotypes and shallowing-upward sequences.....81

Figure 16. Schematic block diagram: depositional

environments of the Upper Mississippian successions...82
Figure 17. Correlations of sedimentary breaks with Global sea level lowstands.....86
Figure 18. Variations of dolomite/calcite ratio, dolomite grain size and silica content.....89
Figure 19. Major occurrences of cements.....129
Figure 20. Occurrences of silica after evaporites, dedolomite, hematite and pyrite.....143
Figure 21. Suggested diagenetic pathway: lower Turner Valley Formation.....155
Figure 22. Suggested diagenetic pathway: upper Turner Valley to Etherington formations.....156
Figure 23. Suggested diagenetic pathway: Upper Permian Ranger Canyon Formation.....157

I. INTRODUCTION

Although a number of studies have dealt with the Mississippian-Pennsylvanian-Permian sequences of the Rocky Mountains, few have tried to unravel the complex depositional environments and subsequent diagenetic modifications of the strata. Such studies are particularly scarce for the Jasper area.

The nature and timing of sediment deposition in a sedimentary basin are influenced by factors such as tectonics, eustasy, climate and paleoceanography (Payton, 1977). Thus, the net result of these interacting processes manifested in the stratigraphic record can be used to reconstruct the original depositional environments.

Carbonate minerals are susceptible to alteration both mechanically and chemically because of their metastability (Bathurst, 1975). These diagenetic modifications continue until the carbonate sediments reach depths at which burial metamorphism prevailed. Fabrics recording the diagenetic history, especially those associated with subaerial exposure, therefore, are of extreme value in the interpretation of post-depositional environmental changes.

A study of case histories also shows that in addition to the forming of paleogeomorphic traps with subaerially erosional surface, this surface of discontiuity is also an important pathway for oil migration (Yan and Zhai, 1980; Watson, 1982). Similarly, ore grade deposits of many mineral commodities (For example, lead-zinc ore) are commonly

associated with karst terrains (Quinlan, 1972)

A. OBJECTIVES

In the context of the points outlined in the introduction, the aims of this thesis are:

1. to study the stratigraphy of the Upper Mississippian to Permian sequence exposed around Talbot Lake;
2. to determine the original depositional environments of the above-mentioned strata;
3. to document the unconformities present in the sequence, and to assess the conditions under which the paleotopographic surfaces developed;
4. to evaluate the diagenetic history which the sediments underwent, with emphasis on the diagenetic signatures associated with the subaerial exposure.

Although the main focus of this study is on outcrops exposed around Talbot Lake, Jasper National Park, the results will have general significance in establishing criteria for the interpretation of paleoenvironments and the recognition of subaerial exposures. Furthermore, the Turner Valley strata are hydrocarbon-bearing to the southeast of the study area (Thomas and Glaister, 1960).

B. METHOD OF STUDY

The fieldwork was carried out in two stages. The reconnaissance phase was conducted in October, 1983, during which four outcrops near Talbot Lake, which constitute the

basis for the present study, were identified (Fig. 1). These exposures, namely, Talbot Lake, Mount Greenock, Cinquefoil Mountain, and Snaring River, were named according to the nearest named geographic features.

Detail mapping and measurement were completed in May and June, 1984. Geological sections of the four locations were described and measured. Where applicable, the base of Turner Valley Formation was chosen as the lower limit of the study sequence. Attempts were also made to identify the sedimentary breaks in order to facilitate the stratigraphic analysis.

In order to examine the paleotopographic relief of the post-Misssissippian unconformity, transverses along depositional strikes were measured in the Talbot Lake, Mount Greenock, and Cinquefoil Mountain sections. Beds which were distinctive and could be traced out in the field were chosen as datum planes.

Two hundred samples representative of identifiable rock units were collected from the study area. They were cut and polished, and 150 thin sections were prepared for macroscopic and microscopic examination. The thin sections were impregnated with blue epoxy to facilitate the identification of original pore spaces. Staining for calcite and ferrous iron constituents using Alizarin Red-S and potassium ferricyanide respectively were applied to all thin sections according to procedures described by Dickson (1965).

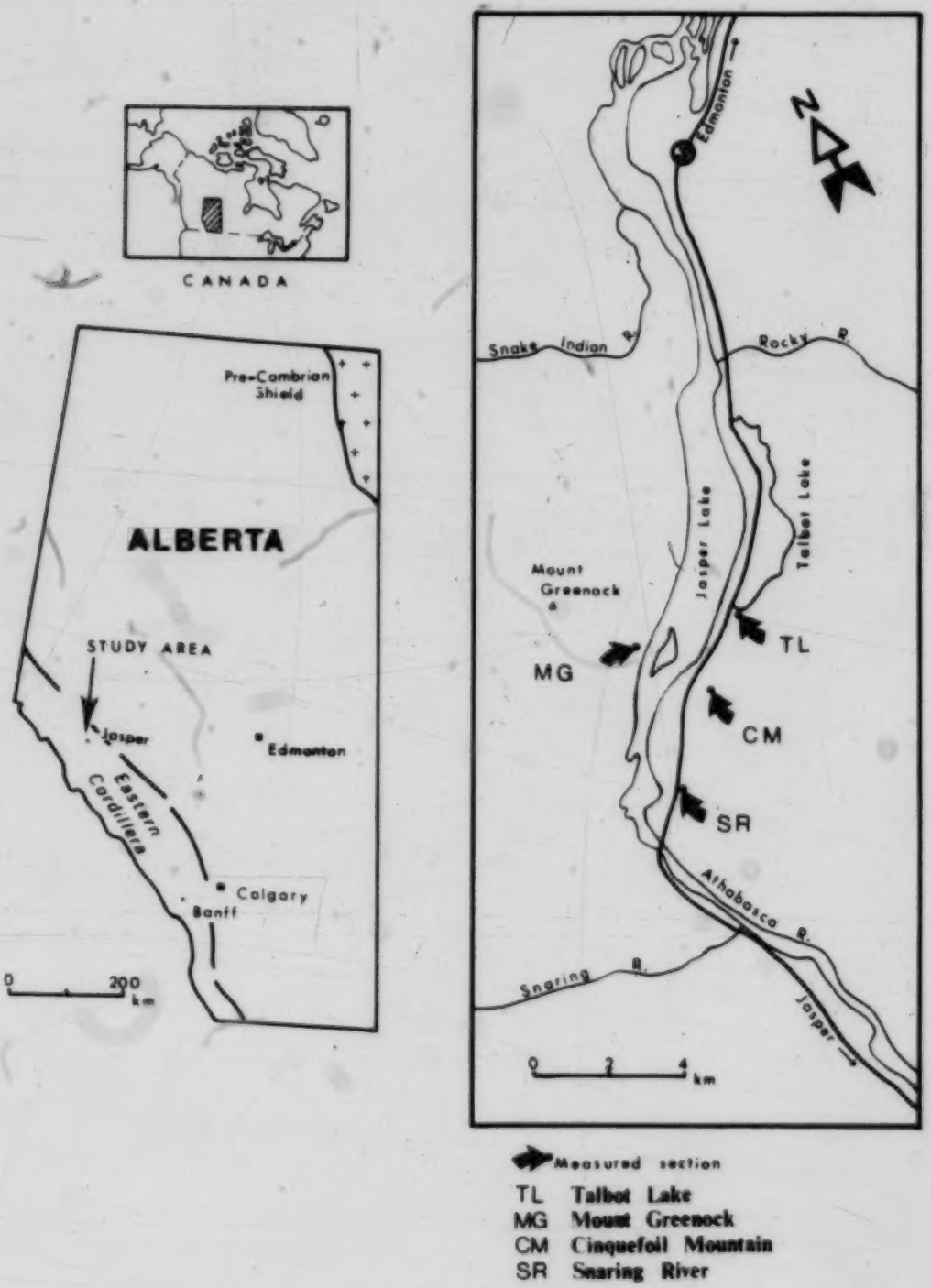

Figure 1. Index and location map.

C. TECTONIC SETTING

The study area is located in the Front Ranges of the Rocky Mountain Belt. Each of the four exposed sections are located in adjacent thrust units (Fig. 2) separated by thrust faults that trend northwest-southeast (Mountjoy, 1961). In the Canadian Rockies, hydrocarbon accumulations are located at the lead edges of the thrust sheet (Foothills) in the Upper Mississippian carbonates and Mesozoic clastics (Dahlstrom, 1970). The subcrops in the Front Ranges should provide a useful surface analogue to the subsurface hydrocarbon-bearing strata.

A need exists to study the tectonic evolution of the sedimentary basin during and after the sediments were laid down. It has been suggested that changes in continental configuration over time can be attributed to plate tectonic processes which in turn influence eustatic sea level changes (Flemming and Roberts, 1973). In addition to providing an insight in the environment of deposition, information regarding the source of sediments and post-depositional environment can be extracted from this general study.

The Rocky Mountain Belt forms the southeastern, cratonward portion of the Eastern Canadian Cordillera, which is defined by a broad linear valley system at its western margin (Zeigler, 1969). Thick westward expanding wedges of sediments were deposited in a passive margin setting during Early Cambrian to Early Jurassic times. Late Jurassic to Tertiary strata accumulated in an eastward migrating

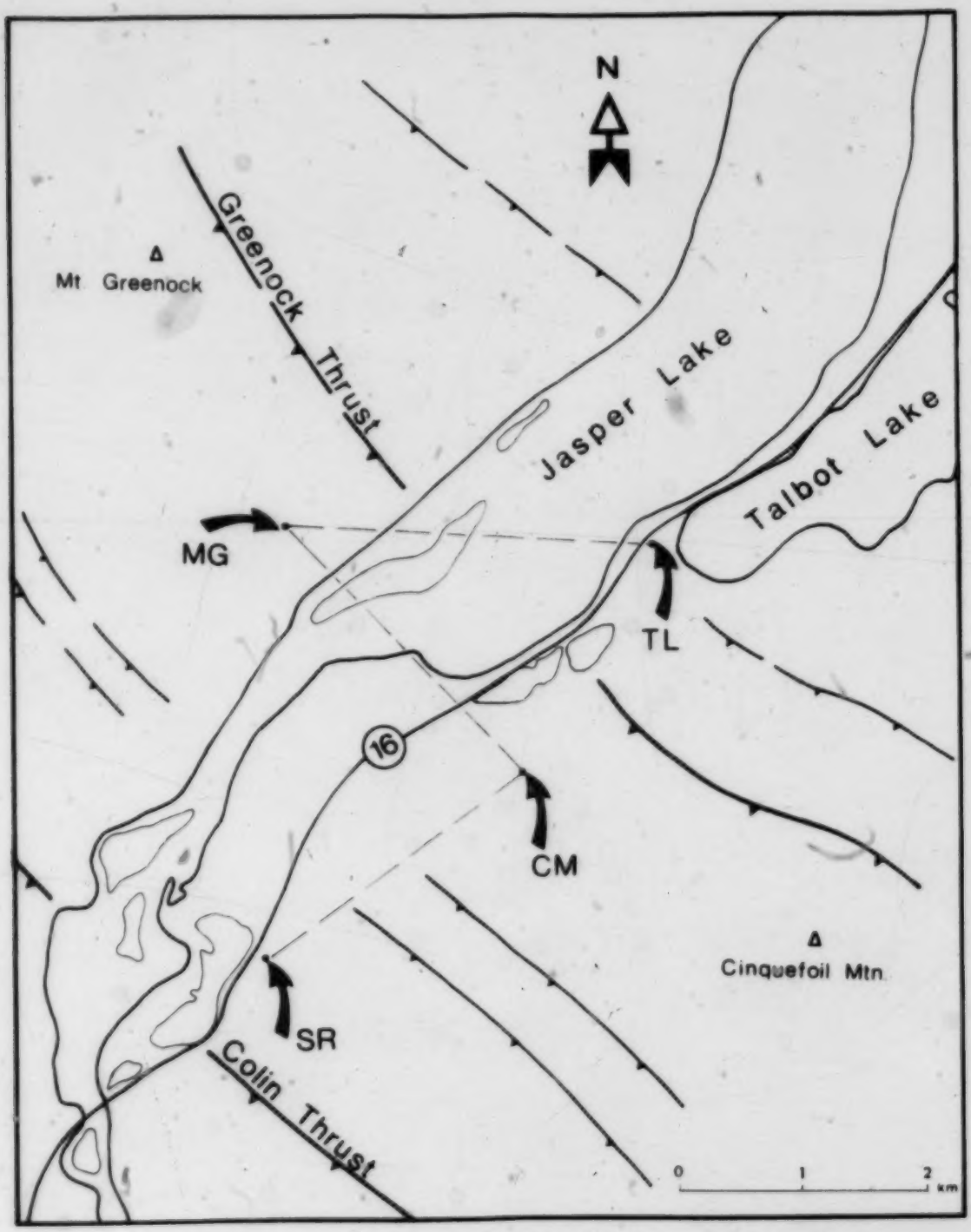

Figure 2. Map showing position of studied sections and their relationship to the major thrust sheets in the study area.

foredeep. The last major orogeny occurred in the Early Eocene (Douglas *et al.*, 1976; Bally, 1975).

Using Plate-tectonic concepts, Monger *et al.* (1972) suggested that Devonian-Mississippian time showed the first evidence of clastic detritus shed eastward onto the rocks that can be linked physically with the Rocky Mountain Belt. This eastward clastic source may have provided the silica source and nutrients for the thriving of sponge spicules and vertebrate fauna in the Upper Mississippian to Upper Permian times.

Based primarily on seismic reflection data, Bally *et al.* (1966) and Dahlstrom (1970) concluded that the Rocky Mountain thrust-fold assemblage is of basement-detached tectonics. In general, such faulting only causes slight to moderate disruption allowing reservoir continuity and migration pathways to remain intact (Harding and Lowell, 1979). Hence, the strata were not subjected to high temperature metamorphic events during the Laramide orogeny.

D. STRATIGRAPHIC SETTING

Studies of Quaternary and Recent carbonates have yielded an immense amount of information which allows a more realistic and reliable modelling of the ancient depositional and diagenetic environments (Bathurst, 1975). There is, however, no existing model of epeiric seas to guide the investigation of the ancient carbonates deposited in such settings.

The epeiric seas were characterized by their great width, the low order of slopes, and the extreme shallowness of the waters (Irwin, 1965). This physiographic situation would have important consequences in the nearshore zone (Irwin, 1965; Hallam, 1981). The following parameters must be taken into account in the interpretation of ancient depositional environments: (1) the negligible tidal range and wind-generated wave action; (2) the tendency towards stagnation of the water; (3) the abnormally high salinity of the sea water; and (4) the high organic productivities.

During Paleozoic and most of Mesozoic times, deposition in the extensive shallow seas formed sediment wedges. The reduction in thickness from west to east (landward) is a characteristic of the sequences throughout the outcrop belt in the Front Ranges (Oswald, 1968; MacRae and McGugan, 1977). There is also a depositional thinning towards the north (Douglas *et al.*, 1976). Futhermore, continuous but diachronous rock bodies of considerable extent formed as a result of marine transgression over such a shallow shelf.

E. PREVIOUS STUDIES AND FORMATIONAL NOMENCLATURE

Correlation of the Permo-Carboniferous successions in the Rocky Mountain Front Ranges has been made difficult due to several episodes of post-depositional erosion and to a lesser extent by original depositional thinning. Furthermore, the facies appear to change abruptly across the various thrust units as a result of the horizontal movement

on the thrusts.

The group and formation names established for the Permo-Carboniferous sequence were defined at different localities in the Banff area of the Southern Rockies. There is a significant difference between the sequences around Banff and around Jasper (Fig. 3).

The detailed stratigraphic and paleontological investigation of the Mount Greenock area by Brown (1952) was the first major study of the Permo-Carboniferous strata in the Jasper area. Brown (1952) subdivided the exposed section into, in ascending order, the Banff, Rundle and Greenock formations. Since then, numerous modifications through correlations between Banff and Jasper area have been suggested by applying the formation names in use in Southern Alberta (Moore, 1958; Drummond, 1961; Nelson and Rudy, 1961; Green, 1962). Several sections exposed along the Athabasca Valley were also examined by other workers (McGugan and Rapson, 1961b; Walasko *et al.*, 1964). The Cadomin section located in the Foothills belt to the southeast was studied by Macqueen (1966).

At Mount Greenock, Hawryszko and Hamilton (1964) applied the name Debolt Formation for the strata which are stratigraphically equivalent to the Turner Valley and Mount Head formations of the Banff area. They also proposed the Jasper Lake Member for a local crinoidal unit in the upper part of the Shunda Formation. Mountjoy (1965) argued that this member should be part of the overlying Turner Valley

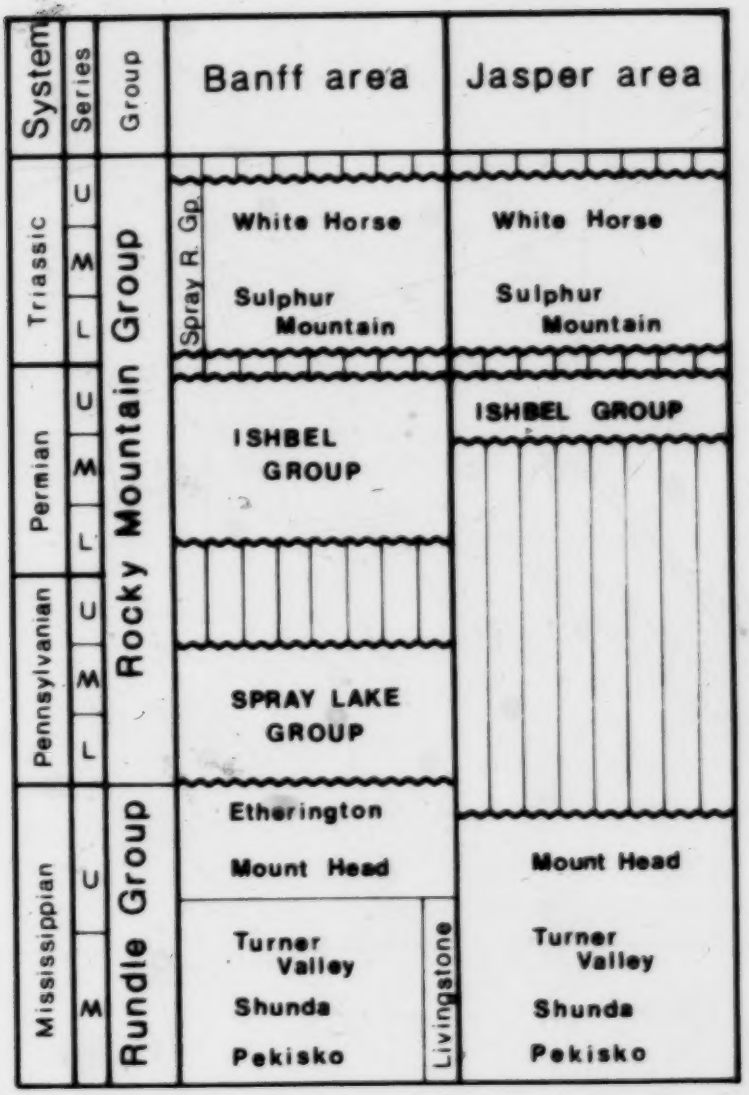

Figure 3. Generalized stratigraphic column of the Middle Mississippian to Triassic strata of the Rocky Mountain Front Ranges (compiled from references discussed in text).

Formation and that a new member name was not justifiable. Since its usage has been the subject of controversy, it is not used in this study. The Elkton Member which is widely used in the subsurface studies is equivalent to the lower Turner Valley Formation (Penner, 1957).

Douglas (1953) introduced the Etherington Formation for a thin section of arenaceous limestone and dolostone of Chesterian age in the Mount Head area. This formation was included as the top of the Rundle Group. Nelson's (1962) review of this particular formation in the Tunnel Mountain and Mount Rae sections (Southern Rockies) was essentially in agreement with that of Douglas and Harker (1958). This formation, however, has not been reported from the Jasper area.

The stratigraphic terminology of the Pennsylvanian and Permian strata of the Rocky Mountain Front Ranges was well established by McGugan and others in a series of studies (McGugan and Rapson, 1961a, 1962, 1963a; McGugan, 1963, 1968; McGugan *et al.*, 1968). They subdivided the Pennsylvanian to Permian Rocky Mountain Group into, in ascending order, the Tunnel Mountain (restricted), Kananaskis, and Ishbel formations (McGugan and Rapson, 1961a). The Ishbel Formation was later elevated to a group status to encompass the Belcourt, Johnston Canyon, Telford, Ross Creek, Ranger Canyon, and Mowitch formations (McGugan and Rapson, 1963a).

In the Jasper area, the Rocky Mountain Group was only alluded to by several workers (Nelson and Rudy, 1961; Hawryszko and Hamilton, 1964; Walasko *et al.*, 1964). Studies by McGugan and Rapson (1961b, 1963b) constituted the major work for the extension of the formational nomenclature of the Southern Rockies to the Jasper area (Fig. 4). They suggested that the Tunnel Mountain and Kananaskis formations were not recognisable, and that the Johnston Canyon, Telford, and Ross Creek formations were also missing in the Jasper area (McGugan and Rapson, 1963a, 1963b).

It appears that the Belcourt Formation which is characterized by fusulinid beds with the underlying breccio-conglomerate is also missing in the Jasper area (Forbes and McGugan, 1959). A breccio-conglomerate very similar in character was found by Forbes and McGugan (1959) in a small fault block in the Jasper National Park area; however, this finding was not substantiated in a later study by McGugan and Rapson (1961b).

F. CLASSIFICATION SYSTEM

CARBONATE AND CLASTIC ROCKS

The polygenetic origin of carbonate rocks has resulted in many attempts to develop a comprehensive classification system to fit all the possible conditions and parameters. Thus it is necessary to specify the schemes used in this study.

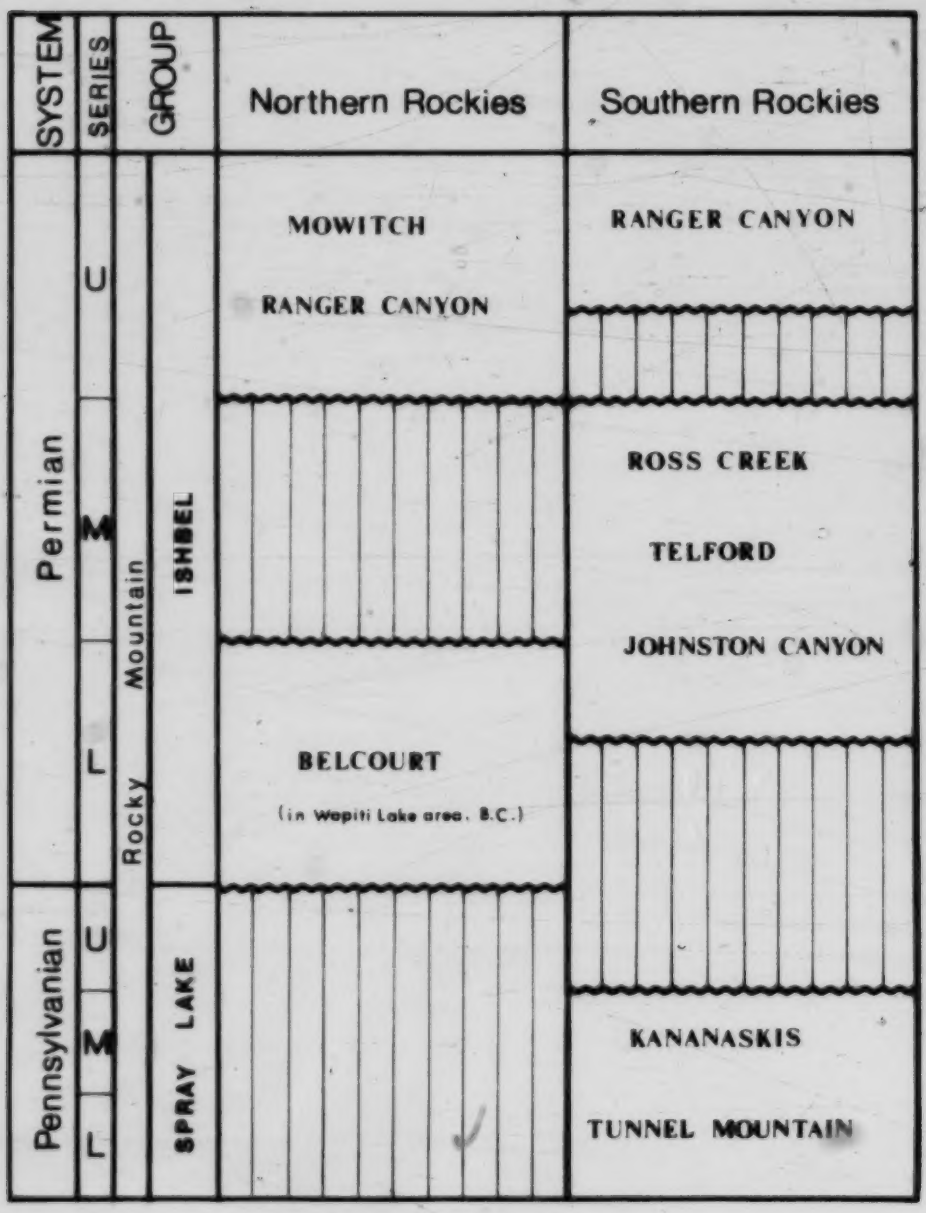

Figure 4. Formation nomenclature of the Pennsylvanian to Permian strata of the Rocky Mountain Front Ranges (after McGugan and Rapson, 1963a).

Dunham's classification (1962) is herein used to describe dolomitized limestones in which the original depositional texture was not totally obliterated by dolomitization or other diagenetic processes. Micrite (<0.02 mm), however, is used as synonymous to lime mud or mudstone following Bathurst (1975). In dolostones where depositional textures are not recognisable, Folk's classification (1962) according to grain size is used. The above two systems were slightly modified according to the allochemical constituents, for examples, oölitic grainstone and intraclastic fine crystalline dolostone.

Folk's classification (1968) for clastic rocks is used for the sandstone units in the succession. This scheme was chosen because it also provides the provenance significance of the clastic components.

PORE TYPES

Most limestones have been through multiple stages of porosity creation and destruction (Murray, 1960). Like carbonates classification schemes, a plethora of classification systems for pores have been proposed over the past two decades (Reeckmann and Friedman, 1982). Although Choquette and Pray (1970) offered one of the most comprehensive genetic classification, it is considered adequate to simply classify the pore types in relation to the depositional fabric for most practical purposes.

Primary pore types include intergranular and intragranular porosity. Secondary porosity encompasses the fabric selective intergranular and intragranular, in addition to the fracture and intercrystalline types. The latter is mainly caused by dolomitization.

CRYSTALLINE CARBONATE FABRICS

The terminology of crystalline carbonate fabrics proposed by Friedman (1965) provides a concise petrograghic description of the carbonates in which the depositional textures and fabrics have been obscured by dolomitization, recrystallization and/or cementation. A more elaborate classification system was recently suggested by Gregg and Sibley (1984) to furnish both the morphologic relationships among individual dolomite crystals as well as the genetic importance of crystal boundaries, such as straight, curved or irregular. In the present study, the purely descriptive terms xenotopic, hypidiotopic, idiotopic, porphyrotopic and poikilotopic, are employed strictly in accordance to Friedman's (1965) definitions.

UNCONFORMITIES

An unconformity is a surface of erosion or nondeposition that separates younger strata from older rocks and represents a break in the continuity of the geologic record. The most widely adopted classification scheme is the one first outlined by Dunbar and Rodgers (1957). The four

major categories of unconformity classified by Dunbar and Rodgers (1957) on the basis of the angularity and parallelism of the strata above and below the unconformity are angular unconformity, disconformity, paraconformity and nonconformity. Among the four types, only disconformity and paraconformity are pertinent to the present studies.

A disconformity, which is of regional extent, is an unconformity in which the beds above and below are parallel yet show some evidence of nondeposition and accompanying erosion. A paraconformity, which is usually of local extent or significance, is an unconformity in which the beds above and below are parallel, but there is no apparent erosional break or the contact is a simple bedding plane. The presence of an unconformity, therefore, is defined by either missing time from an absolute or an evolutionary reference, or by missing time-stratigraphic intervals as defined by temporal events (Chenoweth, 1972).

II. MISSISSIPPIAN STRATIGRAPHY AND SEDIMENTOLOGY

A. INTRODUCTION

In all the measured sections, the strata trend northwest-southeast and dip 60-80° to the southwest. The thrusts separating the sections strike in approximately the same orientation (Fig. 2).

Fossil identification is difficult because of extensive recrystallization, dolomitization and silicification. Futhermore, fossils are rare in the Mount Head and Etherington formations. The lack of adequate and reliable paleontological data means that the stratigraphic correlation must rely heavily on the sedimentary breaks and lithologic similarity of the equivalent sequences.

On the basis of lithologic comparison and stratigraphic succession, the Upper Mississippian carbonate succession of the study area is divided into three formations, namely, the Turner Valley, Mount Head, and Etherington formations of the Rundle Group. These formation names are abbreviated as TV, MH, and E for the Turner Valley, Mount Head, and Etherington formations respectively.

B. TURNER VALLEY FORMATION

The exposures of the Turner Valley Formation in the Talbot Lake and Mount Greenock sections are very good. Unfortunately, this formation is largely covered by vegetation and displaced by thrusting in the Cinquefoil

Mountain and Snaring River sections.

BOUNDARIES

At Talbot Lake, the conformable contact with the underlying Shunda Formation is placed at the top of the black, very thin, carbonaceous, calcareous shale unit (Fig. 5, Plate 1) which probably records the maximum shallowing during late Osagean time. This contact is covered at the Mount Greenock section located along the pipe-line cut. Mountjoy (1965), however, noted that the basal contact in this area shows channel filling of at least 0.3 m deep.

The upper boundary of the formation, which appears gradational in both sections, is placed at the base of a thin intraclastic dolostone unit and at a yellowish brown, very thin, recessive weathered seam in the Talbot Lake and Mount Greenock sections respectively (Figs. 5 and 6, Plate 2).

LITHOLOGIES AND FAUNA

In general, the constituents of the Turner Valley Formation (Figs. 5 and 6) are similar to those described in other studies (Douglas and Harker, 1958; Drummond, 1961; Walasko *et al.*, 1964; Macqueen, 1966; Bamber *et al.*, 1968). It is formed of thick bedded echinoderm-bryozoan grainstone and packstone.

Based on the allochemical constituents, the Turner Valley Formation is divided into four basic lithotypes: (1)

echinoderm-bryozoan grainstone, (2) skeletal grainstone, (3) oölitic grainstone, and (4) skeletal wackestone-packstone. All these lithotypes are partially or completely dolomitized.

LITHOTYPE TV1: ECHINODERM-BRYOZOAN GRAINSTONE

Crinoid columnals and plates and fenestrate bryozoan fragments dominate (>80%) in the light grey grainstone (Plates 3A and 3B). The bioclasts are generally sand sized, poorly sorted and aligned parallel to bedding. Other allochems include fragments of brachiopods, solitary corals, foraminifera, ostracods, and calcispheres. The rocks are extensively dolomitized leaving only 'ghost' structure of the allochems for identification.

LITHOTYPE TV2: SKELETAL GRAINSTONE

This grey coloured skeletal dolostone has diverse allochemical constituents. Crinoid and bryozoan fragments are the dominant fossils (>50%), but locally fragments of brachiopods, molluscs (gastropods and pelecypods), ostracods, solitary corals, foraminifera, calcispheres, ooids and peloids occur (Plates 3C and 3D). Colonial corals are present but most have been leached out (Plate 4A). Cross-bedding is present near the upper part of the skeletal grainstone (Plate 4B).

Syntaxial calcite growth on crinoidal skeletons and preferential dolomitization of micrite and peloids is

common. The partially dolomitized allochems generally retain some of their features and these permit their identification.

LITHOTYPE TV3: OÖLITIC GRAINSTONE

Oöids constitute over 80% of the grains in this lithotype (Plate 3E). The oöids are of medium sand sized and fairly well sorted. Crinoid fragments also occur.

The oöids have been pervasively dolomitized. Their vague outlines are defined by the distribution of relic inclusions in the dolomite rhombs or the presence of microspar calcite cement filling interstitial voids around the oöids (Plate 3F). Although the internal structures are completely obliterated by dolomitization, these oöids probably had a concentric fabric similar to those found in the partially dolomitized skeletal grainstones.

LITHOTYPE TV4: SKELETAL WACKESTONE-PACKSTONE

The allochems are predominately echinoderm and bryozoan fragments (average 20%) with minor constituents of unidentified fossil debris and peloids. Alternating crinoid rich and micrite laminae are ubiquitous. Evidence of sediment reworking by infaunal organisms is present; however, the process was not intensive enough to destroy the laminated character of the rock. Mottled textures (Plate 4C) and pseudonodules (Plate 4D) caused by bioturbation are common.

This lithotype has been completely dolomitized and only 'ghost' structures remain for identification. Minor silicification of possibly fossil fragments is evident in thin sections. Dedolomite and quartz pseudomorph after anhydrite are present in this lithotype in the Talbot Lake and Mount Greenock sections respectively.

POROSITY

Intercrystalline and secondary intragranular porosity, resulting from dolomitization and leaching respectively, are well developed in the completely dolomitized grainstones. Dolomite selectively replaced the micrite in the partially dolomitized grainstones. The intercrystalline porosity is further supplemented by subsequent leaching of the skeletal and/or oöid grains. Leaching, however, is rare in the partially dolomitized rocks. These pore types were also recorded in the subsurface in the oil-bearing Elkton Member (Thomas and Glaister, 1960).

Brecciated zones in the lower part of the formation are usually tightly cemented by secondary calcite. The upper wackestone and packstone units have no appreciable porosity.

DISTRIBUTION OF LITHOTYPES

In the Talbot Lake area (Fig. 5), the skeletal grainstone (TV2) forms the lower massive unit of the formation and is overlain by a thin unit (<1 m thick) of oölitic grainstone (TV3). The lithotypes TV2 and TV3 are not

present in the Mount Greenock section. In the latter section (Fig. 6), the lower part of the formation is formed of thick bedded, resistant, dolomitic echinoderm-bryozoan grainstone (TV1). The skeletal wackestone-packstone (TV4) forms the upper one-third of the Turner Valley Formation (Figs. 5 and 6).

DEPOSITIONAL ENVIRONMENTS

Becher and Moore (1976) noted that micrite might have several discrete origins; however, it responds in much the same manner as its clastic counterparts - terrigenous clays - to the winnowing activity of currents. Thus, the low micrite content, and the abundance of normal marine fauna of the echinoderm-bryozoan and skeletal grainstones indicate that they were deposited in a shallow, open marine water, well within the zone of wave agitation. The open marine setting is well exemplified by the abundance of crinoid and bryozoan which prosper in clear water with good circulation (Tasch, 1973). Wilson (1975) suggested that such deposits represent carbonate shoal development near platform margin.

The cross-bedded crinodal grainstones occur where the uppermost beds of the skeletal grainstones (TV2) grade into the clean oölitic grainstones. This further reflects the decrease of water depth and increasing agitation as the carbonate shoal continued its build-up toward sea level. Newell *et al.* (1960) suggested that the optimum zone of oöid production was in shallow water less than two meters deep.

The end of oöid formation was succeeded by the deposition of laminated wackestone. This probably represents a decrease in energy level and sedimentation on the lee side of the shoal. This quiet, shallow water depositional regime is reflected by the flat laminations, thin bedding, and abundance of micrite. Skeletal laminae were probably produced by the periodic influx of debris derived from the carbonate shoal. The low degree of bioturbation is probably due to the high mobility of the substrate near the shoal.

At the Mount Greenock section, the evidence for the pre-existing evaporite minerals present in the uppermost unit of the the Turner Valley Formation further corroborate the interpretation of shoaling-upward as a consequence of high rate of carbonate sedimentation relative to sea level rise. The hypersaline conditions were probably created by the shoal acting as a barrier which reduced sea water circulation in the lagoon.

C. MOUNT HEAD FORMATION

The Mount Head Formation is well exposed in the Talbot Lake and Mount Greenock sections. Some covered intervals are due to differential weathering related to a series of east-west trending fault. At Cinquefoil Mountain, vegetation and loose debris cover most of the lower part of the section except for the prominent cherty dolostone ridges. Thrusting has displaced the lower portion of the formation in the Snaring River section.

BOUNDARIES

The lower contact with the Turner Valley Formation is placed at the base of an intraclastic unit (Fig. 5, Plate 2) and a weathered seam at the top of the skeletal wackestone (TV4) at the Talbot Lake and Mount Greenock sections respectively. The base of a thin chert pebble bed denotes the upper boundary of the Mount Head Formation at the Talbot Lake section (Fig. 5). This unit probably represents a short erosional break. The upper contact at other sections is placed at the base of a thin intraclastic dolostone unit.

LITHOLOGIES AND FAUNA

Studies by Macqueen and Bamber (1968) demonstrated that the Mount Head Formation exhibits a significant facies change westward and northward from the type area at Highwood Range, South Rocky Mountain Front Ranges. The six member subdivision of the formation (Douglas, 1953, 1958) is not recognisable north of Bow Valley (Macqueen and Bamber, 1968). In the northern Rockies, it was described as sparsely fossiliferous, in part cherty, microcrystalline to fine crystalline and argillaceous dolostone (McGugan and Rapson, 1961b; Walasko *et al.*, 1964; Macqueen, 1966).

The weathered light grey to grey dolostone appears unfossiliferous and monotonous in the outcrops studied along the Athabasca Valleys. Careful field examination and laboratory studies, however, do reveal some distinct features of the Mount Head Formation. These diagnostic

lithologic features and stratigraphic successions seem to have importance in the environmental reconstruction of the succession.

Although the Mount Head Formation varies from section to section (Figs. 5, 6 and 7), even along the same range as in the case of Mount Greenock and Cinquefoil Mountain, seven distinct lithotypes are present: (1) intraclastic dolostone, (2) echinoderm-bryozoan grainstone, (3) skeletal fine to medium crystalline dolostone, (4) cherty bryozoan dolostone, (5) cherty algal dolostone, (6) fine crystalline dolostone, and (7) dolostone-argillaceous dolostone.

LITHOTYPE MH1: INTRACLASTIC DOLOSTONE

The term 'intraclast' is used according to Folk's definition (1962) to embrace all types of reworked, penecontemporaneous carbonate sediment originating from within the depositional environment. It is synonymous with erosional intraclast (Laporte, 1969), flat pebble conglomerate (Sepkoski, 1982) and basal transgression lag (Enos, 1983).

The lithology of the intraclasts is identical to that of the underlying bed suggesting that they originated by erosion and resedimentation of earlier deposited sediment. They are essentially dolostone clasts of fine crystalline dolomite. The clasts range from a few millimeters up to 3 cm in length. The intraclasts invariably have a circular to elliptical shape, and are usually imbricated or flat-lying (Plate

4E).

The matrix is formed of medium crystalline dolomite with approximately 20% skeletal debris. Most of the fossils have been leached out and the cavities filled by dolomite and calcite cements. The intraclast-matrix boundaries are not sharp, implying that both the clasts and matrix were dolomitized contemporaneous and the different dolomite grain size simply reflects the difference in the original sediments.

LITHOTYPE MH2: ECHINODERM-BRYOZOAN GRAINSTONE (DOLOSTONE)

Crinoid stems and ossicles and fenestrate bryozoan fragments dominate the biota of this light grey dolostone. Solitary corals are present in the Talbot Lake exposures. Allochems are mostly medium to coarse sand sized, poorly sorted, and show some degree of alignment parallel to bedding.

The internal structures of the bioclasts are completely destroyed by leaching, dolomitization or silicification; nevertheless, the external 'ghost' structures permit their identification. Matrix dolomites are generally medium crystalline and display a xenotopic fabric.

LITHOTYPE MH3: SKELETAL FINE-MEDIUM CRYSTALLINE DOLOSTONE

This lithotype is a grey, fine to medium crystalline dolostone with about 10 to 20% fossil fragments. Crinoid ossicles are the most abundant of the identifiable bioclasts, but subordinate amounts of bryozoan debris and brachiopod fragments are present. These fossil fragments are commonly replaced by medium crystalline dolomite. The matrix is formed of fine to medium crystalline dolomite. Lucia and Murray (1967), in a study of crinoidal rocks of the Mississippian Harmattan Field in Alberta, noted that dolomite selectively replaced a crinoidal sediment that had a high micrite content. Therefore, the skeletal dolostone is thought to have originally been a skeletal wackestone.

Biogenic reworking of the sediments is emphasized by the mottled textures. Chert occurs as dark bluish grey, discontinuous stringers or bands, while the associated matrix dolomite becomes finer grained. The characteristic central canal of the monoaxon sponge spicules in the chert are readily identified in thin sections or in polished slabs.

In the Mount Greenock section, this lithotype includes a distinct lithology (<1 m thick). It is a dark grey dolomite with evenly spaced, pencil-thin laminae of cryptocrystalline chert (Plate 4F). This remarkable cyclic lamination resembles the 'pin-stripe' laminations described by Folk (1973) in the Devonian Caballos chert.

LITHOTYPE MH4: CHERTY BRYOZOAN DOLOSTONE

Chert which occurs as silicified organic components constitutes 15-30% of the rock. The chert is dominated by silicified fragments of robust ramose bryozoan giving the rock a 'ragged' appearance (Plates 5A, 5B and 5C). Other silicified fossils of much less abundance are crinoids, gastropods, brachiopods, bivalves, and sponges (Plates 5D, 5E and 5F). Sponge spicules are evident in the chertified portion of the rock. The matrix is formed of cherty, finely crystalline xenotopic dolomite. Based on Murray and Lucia's (1967) studies the matrix dolomite probably originated as lime mudstone.

Preferential silicification of the fossils is probably due to the fossil fragments having a higher porosity than the surrounding matrix. The selective replacement of fossils by silica has also been documented by Siedlecka (1972) and Jacka (1974).

LITHOTYPE MH5: CHERTY ALGAL DOLOSTONE

This lithotype together with the cherty bryozoan dolostone (MH4) form the prominent ridges of the Mount Head Formation (Plate 6A). The chert laminae, which are a few millimeters to 2-3 cm thick, are interlayered with finely crystalline dolomite (Plates 3B, 3C and 3D). Minor 'domal' shaped chert layers are present in the Talbot Lake section. Sponge spicules occur in the chert laminae.

The cherts of this lithotype are similar to the ribbon cherts in the Ordovician Aleman Formation, southwestern New Mexico which Geeslin and Chafetz (1982) interpreted as silicified stromatolitic layers. Geeslin and Chafetz (1982) also suggested that the algal layers were preferentially silicified because of locally enhanced porosity which provides avenue for silica-rich fluids. Numerous examples of fossil algae were also described by Toomey and Babcock (1983) in Precambrian and Paleozoic carbonates.

Quartz nodules (Plate 6F) occur on the upper surface of the dolostone ridge (50 m from base of section) in the Cinquefoil Mountain exposures. No detail study has been made, but the morphological features of these nodules appear analogous to those described by other workers from other carbonate sequences (Siedlecka, 1972; Chowns and Elkins, 1974; Milliken, 1979; Geeslin and Chafetz, 1982). They all concluded that the nodules were formed by silicification of former evaporite nodules.

LITHOTYPE MH6: FINE CRYSTALLINE DOLOSTONE

Lithologically, the unfossiliferous light grey dolostone is formed of fine to very fine crystalline xenotopic dolomite. The fact that the dolomite rhombs are all of equal size suggests that the rock was originally deposited as micrite. This unit is characterized by the presence of bird's-eye structures

which are planar to irregular augen-shaped (Plates 7A and 7B).

The bird's-eye vugs are filled with dolomite and calcite cement. Microstalactitic calcite cement is also present in some of the voids. Lath-like relics in the dolomite cement suggests that the vugs were initially filled with evaporite minerals. Silicification of the dolomite cements is common.

Minor amounts of silicified fossils such as gastropods, bivalves, crinoid and bryozoan fragments are present. The gastropods and bivalves are of small sized and thin shelled species (Plate 7C).

LITHOTYPE MH7: DOLOSTONE-ARGILLACEOUS DOLOSTONE

This lithotype consists of interbedded dolostone and argillaceous dolostone. This phenomenon is particularly well developed in the Mount Greenock and Cinquefoil Mountain section, where the thin bedded to laminated argillaceous dolostones are preferentially weathered out (Plate 7F). The dolostones are unfossiliferous and the matrix is generally fine to very fine crystalline dolomite with local silicified patches.

LITHOTYPES IN SNARING RIVER SECTION

The strata thought to be stratigraphically equivalent to the uppermost beds of the Mount Head Formation in the Mount Greenock area comprise three lithotypes: (1) massive medium crystalline dolostone,

(2) laminated fine crystalline dolostone and (3) quartzitic fine crystalline dolostone (Fig 8).

1. LITHOTYPE MH8: MASSIVE MEDIUM CRYSTALLINE DOLOSTONE

This light grey dolostone is composed of medium crystalline dolomite with patches of coarse crystalline dolomite that are probably dolomitized allochems. The identity of these allochems is impossible because of the obliteration of both the internal and external structures by dolomitization. Their irregular outline and size, however, suggest that they may be peloids. If this is the case, the original rock was probably a peloidal packstone or grainstone.

An extensively burrowed surface occurs at about 0.75 m above the base of the Snaring River section (Fig. 8). These are essentially horizontal burrows (Plate 7D). The surface is overlain by lithologically similar strata which is porous due to leaching of the allochems.

2. LITHOTYPE MH9: LAMINATED FINE CRYSTALLINE DOLOSTONE

This lithotype is a grey, thin bedded to laminated, fine crystalline dolostone. Bioturbation is common but not intense enough to destroy the fine laminae. Abundant pyrite is commonly associated with the burrows.

3. LITHOTYPE MH10: QUARTZITIC FINE CRYSTALLINE

DOLOSTONE

This lithotype is characterized by the presence of euhedral authigenic quartz (approximately 10%) and pyrite crystals. The quartz crystals are randomly distributed in the fine crystalline dolomite matrix, but tend to be concentrated near a chert band which appears to be bioturbated (Plate 7E). Relic inclusions, which are common in the quartz, are too fine to be resolved by petrographic microscope. The quartz crystals were probably formed by authigenic quartz replacement of carbonates. The dark grey, silt sized internal sediments resting on calcite spar cements in voids are probably marine sediments infiltrated into the open pore network. Chert occurs as nodules parallel to bedding (Plate 6E).

POROSITY

In general, porosity development in the Mount Head Formation is poor. Microscopically visible porosity is confined to the echinoderm-bryozoan dolostone and skeletal dolostone where dolomitization was the dominant post-depositional diagenetic process. Intercrystalline and secondary intragranular porosity are the main pore types. Where silicification is common the pores were completely occlued by silica, dolomite or calcite cements. Intercrystalline and secondary intragranular porosity are

the main pore types.

Pores in the bird's-eye structures were generally filled by secondary cements. Fractures probably related to late Laramide orogeny were mostly cemented by coarse dolomite or sparry calcite.

DISTRIBUTION OF LITHOTYPES

The basal unit of the Mount Head Formation is a thin (20 cm thick) intraclastic dolostone (MH1) in the Mount Greenock area. Directly overlying this basal unit is slightly bioturbated skeletal medium crystalline dolostone (MH3).

Grading upward, two repetitive cycles are present (Figs. 5, 6 and 7) Each successive sequence comprises, from bottom upward, the echinoderm-bryozoan grainstone (MH2), skeletal fine to medium crystalline dolostone (MH3), cherty bryozoan dolostone (MH4), cherty algal dolostone (MH5), and fine crystalline dolostone (MH6). The echinoderm-bryozoan grainstone locally occurs as thin units in the skeletal dolostone (MH3). The Mount Head Formation in the Greenock Range is capped by a 8-10 m thick unit of interbedded dolostone and argillaceous dolostone (MH7).

The resistant, light grey, thick bedded cherty dolostones (MH4 and MH5) form the prominent ribs of the Mount Head Formation. These cherty dolostone ridges range from three to seven meters thick.

In the Snaring River section (Fig. 8), the exposed upper Mount Head Formation appears different to that of the other sections. In ascending order, it comprises massive medium crystalline dolostone (MH8), laminated fine crystalline dolostone (MH9), and quartzitic fine crystalline dolostone (MH10).

DEPOSITIONAL ENVIRONMENTS

There is a distinct variation in the stratigraphy of the Mount Head Formation from section to section. Changes are evident even in the Mount Greenock and Cinquefoil Mountain sections which are located along the same range on the overhanging block of the Mount Greenock thrust. Such variations suggest that deposition occurred in a shallow water environment (Hite, 1970; Folk, 1973; James, 1984).

The basal intraclastic dolostone records the marine incursion onto land and erosion and redeposition of the underlying sediments. Grading upward into the bioturbated medium crystalline dolostone, it records the onset of deposition of the Mount Head Formation in a subtidal environment. This is then followed by two repetitive sequences.

The cyclic phenomenon is interpreted as shallowing-upward sequences that range from shallow marine to supratidal conditions. The abundance of echinoderm and fenestrate bryozoan fragments of the grainstones indicates a shallow marine, moderate to high energy environment. The

inconsistent vertical and horizontal extent of these skeletal sand units suggest tidal channel deposits rather than carbonate shoals. Channel migration caused a decrease in current energy and hence skeletal wackestone deposition (lithotype MH3).

The pin-striped chert-dolomite laminations in the skeletal dolostone of the stratigraphically lower, shallowing-upward sequence probably represents a locally developed hypersaline environment similar to that described by Folk (1973) in the Devonian Caballos chert. He suggested that the laminations were probably silicified varved evaporites and dolomite deposited in shallow water or lagoonal environments. The cyclic precipitation of dolomite, silica or evaporites were resulted from changes in water chemistry due to seasonal fluctuations (Folk, 1973).

The high energy intertidal zone is manifested by the thick accumulation of robust ramose bryozoan stems, and low faunal diversity. According to Cheetham (1971), the robust nature of the bryozoan stems probably represents morphological adaptation to rapidly moving water. Boardman (1960) also noted that calcareous mudstone facies, suggesting a shallow, rough water environment was the optimum environment for ramose trepostomes development. Furthermore, the low biotic diversity may suggest that the high energy condition perhaps may have been adverse for other marine fauna.

The bryozoan colonies are all fragmented, not in growth position, and randomly oriented. Thomsen (1976), in a study of the lower Danian bryozoan mounds in Darlby Kint, Denmark, suggested that where currents were strong, the bryozoan population thrived. The dense bryozoan colonies served to trap and bind sediment (Tasch, 1973; Thomsen, 1976). After death the bryozoan colonies were eventually embedded in the micrite layer without any significant transportation. Fragmentation was probably caused by overburden weight (Thomsen, 1976) and current activity.

Preservation of algal lamination and bird's-eye structures denotes the end of the first shallowing-upward sequence with an upper intertidal to supratidal environment. The laminated cherts are morphologically similar to the algal mat deposits found in the modern carbonate environments (Davies, 1970; Hardie and Ginsburg, 1977; Shinn, 1983). Preservation of these laminae is restricted to supratidal and upper intertidal zones where conditions are not favourable for gastropods, a common algal predator (James, 1984). These algal laminations probably represent seasonal cyclic repetition as a result of alternating flooding and deposition of micrite and algal mat growth (Davies, 1970; Shinn, 1983). Laporte (1967, 1969) suggested that the laminated sediments found in the lower Devonian Manlius Formation were formed by the successive periodic flooding of the supratidal environment by unusually high tides. Algal mats then developed on the newly deposited

micrite layer as water receded.

Bird's-eye structures were recognised by Illing (1959) in the course of his study of the Mississippian Shunda Formation. Illing (1959) suggested six possible origins for their formation. Through laboratory experiments and core examinations of modern sediments, Shinn (1968a, 1983) concluded that bird's-eye structures are best preserved in the upper tidal zones. Therefore, their presence in the Mount Head Formation are good indicators of upper intertidal to supratidal environments. Such depositional settings are corroborated by the reduced size and thin shell of the gastropods and bivalves which probably indicate an adverse environment.

Laporte (1967) and James (1984) suggested that the repetitive occurrence of shallowing-upward sequence in a carbonate succession is a good indicator of shallow shelf, tidal flat environment. Alternating beds of dolostone and argillaceous dolostone which cap the Mount Head Formation further supports the shallow water depositional settings.

In the Snaring River section, the massive medium crystalline dolostone grades upward into laminated fine crystalline dolostone, suggesting a shallowing-upward sequence in a relatively distal shelf environment. Burrowed hardground and lack of any diagnostic sedimentary structures are evidence for submarine depositional setting (Shinn, 1969; Heckel, 1972; Howard, 1972). Therefore, the extensively burrowed surface is probably a submarine

hardground indicating an early lithification of sand-sized sediments. Furthermore, the intimate linkage of the pyrite and burrows suggests that they probably formed as a consequence of bacterial attack on interstitial organic matter in a locally developed reducing environment as suggested by Friedman and Sanders (1978). The Snaring River sequence was probably deposited in a subtidal to intertidal zone, possibly in a lagoonal setting.

D. ETHERINGTON FORMATION

The Etherington Formation is the youngest formation of the Mississippian carbonate succession. Exposure of the formation is generally good in all four measured sections, except for certain intervals in the Talbot Lake and Cinquefoil Mountain sections which are covered by loose debris.

BOUNDARIES

In the Talbot Lake section, the lower contact is placed at the base of a chert pebble bed (Fig 5). The lower boundary is placed at the base of a intraclastic dolostone unit in the other sections (Figs. 6, 7 and 8). The upper boundary is marked by a distinct disconformity (Figs. 5, 6, 7 and 8). A condensed conglomerate sequence directly overlies the disconformity.

LITHOLOGIES AND FAUNA

The Etherington Formation of Chesterian age was divided into three parts and the lithology was described as cherty arenaceous limestone to fine crystalline dolostone (Douglas, 1953, 1958). Scott (1964) noted the facies change from east to west in the Southern Rocky Mountains and the presence of numerous thin intraformational breccias and conglomerates. There has been some confusions regarding the use of this formational nomenclature (Nelson, 1962). McGugan and Rapson (1961a) proposed the Tunnel Mountain Formation (restricted) to include only the clastics and the Etherington Formation for the lower carbonates. The Etherington Formation has not been reported in the Northern Rocky Mountains.

On the basis of the lithologic characteristics and stratigrahpic succession, it seems justifiable to use the 'Etherington Formation' for the topmost 10-15 meters of the Mississippian sequence identified in the studied sections (Figs. 5, 6, 7 and 8). The usage of this term may be considered a temporary measure pending further study.

In general, the Etherington Formation is formed of resistant, thinly to moderately bedded, in part siliceous, fine crystalline dolostone. Since the vertical sequence of units from section to section (Figs. 5, 6, 7 and 8) is seemingly without order, the discussion below is to highlight the lithotypes which are of importance in environmental interpretation. The bracketed location name denotes the place of occurrence.

LITHOTYPE E1: CHERT PEBBLE BED (Talbot Lake)

The chert pebbles (and granules) are mostly angular to subangular fragments of tabular shape up to 3-4 cm long. Subordinate clasts are angular fragments of fine crystalline dolostone which generally constitute less than 5% of the clast content (Plates 8A and 8B). Despite the general random distribution of these chert pebbles, minor degrees of imbrication are apparent in the elongated fragments.

The matrix is formed of very fine to fine crystalline dolomite with 10-15% of fine sand sized quartz grains. These detrital quartz grains are partially dolomitized around their grain boundaries. Silica replacement of possibly fossil fragments, and dolomite and silica cementation of voids are common.

Small, ramifying solution channels are present on the pebble bed surface. These small caverns were filled with an admixture of subrounded fragments of chert and dolostone, and quartz grains (Plate 8C).

LITHOTYPE E2: INTRACLASTIC-INTRALAMINATED DOLOSTONE (Greenock Range)

This lithotype is formed of intercalated intraclastic and intralaminated dolostone (Plate 8D). Low angle, ripple cross-lamination and truncation are present in the lower part of the intraclastic dolostones (Plate 8F). Locally, the dolostone clasts show chaotic arrangement (Plate 8E).

The intraclasts are generally thin, elliptical in shape and have rounded edges. They are composed of fine crystalline dolomite similar in composition and fabric to the matrix, which is medium crystalline dolomite with less than 5% quartz grains. Very minor amounts of laminated phosphate fragments are identified in thin sections.

The intralaminated dolostone is formed of fine to medium crystalline dolomite. The internal laminations resemble the plane bed form structure described by Allen (1970).

This lithotype locally occurs as small lenses which consist of relatively smaller clasts (average 1 cm in length). They probably represent local events such as levee crests or tidal channels environments (Hardie and Ginsburg, 1977).

LITHOTYPE E3: INTRACLASTIC DOLOSTONE (Snaring River)

The intraclasts in this lithotype are laminated and exhibit pseudo-anticline structures (Plate 8G). This usage follows the definition given by Assereto and Kendall (1977), who described pseudo-anticline as any antiform structure formed by the expansion of indurated carbonate where the process and environment responsible for expansion cannot be established. Thin section examination reveals that the dark grey laminae are composed of fine crystalline dolomite, whereas the dolomite crystals in the light grey laminae are slightly

coarser.

The intraclasts are embedded in a matrix of fine to medium crystalline dolomite. Quartz and pyrite crystals are abundant. Most quartz grains are subrounded, but some have pinacoid or tabular crystal shape with partial etching of the grain boundaries. Very fine inclusions are common in the quartz grains. The grain shapes suggest that they were probably quartz pseudomorphs after gypsum crystals which were reworked from the underlying sediments.

LITHOTYPE E4: INTRACLASTIC BRACHIOPOD DOLOSTONE (Snaring River)

Along with the elliptical, round-edged, fine crystalline dolostone clasts, abundant brachiopod shells are present. The dolostone clasts are 1-5 cm in length, but large, more angular clasts longer than 10 cm are present (Plate 8H). Phosphate fragments, mostly tooth-like structures, become more common toward the top. The matrix is fine to medium crystalline dolomite grading upward into predominantly medium crystalline dolomite.

Both the intraclasts and brachiopod shells are flat-lying and parallel to bedding. The shells are preferentially oriented in a convex-down position. A small channel occurs in the uppermost part of the intraclastic dolostone.

The rock underwent a complex sequence of diagenesis. Brachiopod shells were all silicified, but the parallel fibrous structures were largely retained. Stylolitization with concentration of pyrite and late fractures cemented by coarse crystalline dolomite are common. Iron oxide rosettes also occurs. The crystal morphology suggests that they were probably iron oxide filling voids created by dissolution of radiating clusters of authigenic gypsum crystals.

LITHOTYPE E5: CHERTY STROMATOLITIC DOLOSTONE (Talbot Lake and Greenock Range)

In the Talbot Lake section, this lithotype is formed of chertified mounds in very fine crystalline dolostone. These domal structures (average 0.3 m in diameter) exposed along bedding planes are laterally linked in a polygonal fashion and locally form large colonies (Plate 9A). The relief of these domes are generally less that 0.3 m. Muir *et al*. (1980) and Geeslin and Chafetz (1982) also described chertified stromatolites in ancient carbonates.

Hardie and Ginsburg (1977) suggested that substrate irregularites are the main attribute for the development of domal shape in algal stromatolites. Therefore, the doming of the stromatolites in the Talbot Lake area probably were caused by growth over pre-existing surface irregularities.

Single mounds and isolated small colonies of stromatolites are present in the section at Cinquefoil Mountain section (Plates 9B and 9C), while a thick (0.5-1.0 m) continuous unit of very low relief (<10 cm) occurs in the Mount Greenock section. These cherty stromatolites are near the top of the formation. Distinct, small, hemispherical domal stromatolites (Plate 9D) displaying well preserved internal structure are found in the Mount Greenock area. Thin section examination shows that the differentially weathered pattern corresponds to alternating layers of thin chert and relatively thicker dolomite laminae.

Like the cherty algal dolostone (MH5), the algal stromatolites are preferentially silicified probably because of their porous and permeable structure.

LITHOTYPE E6: SILICEOUS DOLOSTONE (Talbot Lake, Greenock Rangeand Snaring River)

The rock is a mosaic of interlocking fine to very fine crystalline xenotopic dolomite and coarser silica grains. Less than 10% of silt to fine sand size detrital quartz grains are present. The detrital quartz content decreases upward and towards the Greenock Range. The detrital quartz grains are commonly concentrated along stylolite seams. Local preservation of siliceous sponge spicules (monoaxon) is the only identifiable fauna. Other unidentifiable fossil fragments were mostly leached out and subsequently filled by silica and/or

dolomite cement.

The silicification pattern in the siliceous dolostone appears quite intricate. The interweaving of different silica types is hard to understand. Silica constituents commonly include white cryptocrystalline chert, grey microcrystalline chert and small round patches of fibrous chalcedony (Plate 9E).

In the Talbot Lake area, another interesting characteristic of the siliceous dolostone is the presence of pisolith-like silica/dolomite structures. Dunham (1969a) defined a pisolith as a grain of unspecified origin, larger than 2 mm, and having concentric structure. Most pisoliths in the siliceous dolostone were completely replaced by silica but dolomite relics are evident. Large pisoliths appear as compound grains bounded together by dark micritic (algal?) laminae. Hair-line pores following the pisolith boundaries are common. Thin sections studies under plane light show some relic zonings with right angle re-entrants. These pisoliths appear similar to the algal and aragonite encrusted pisoids described by Wright (1981) in the Lower Carboniferous Llanelly Formation, even though they are mineralogically different.

LITHOTYPE E7: QUARTZITIC DOLOSTONE (Mount Greenock)

The matrix of the quartzitic dolostone is formed of very fine crystalline xenotopic dolomite. Euhedral quartz crystals occur both singly or in cluster (Plate

9F). Dolomite relics are usually confined around the edges of the euhedras. Raidating quartz clusters commonly have a central portion of partly microflamboyant megaquartz (Milliken, 1979), whereas quartz crystals filling voids show cleavage planes and sawtooth, right-angled grain boundaries.

Other quartz crystals having a well defined rectangular outline also are present. These crystals are typically zoned. Minor inclusions are present in some of the cloudy crystals.

LITHOTYPE E8: CHERTY BRYOZOAN DOLOSTONE (Greenock Range)

This lithotype is similar to that found in the Mount Head formation (MH4) but is far less conspicuous. It is composed of randomly oriented, chertified ramose bryozoan stems in a fine crystalline dolomite matrix. Bryozoan branches constitute about 10% of the dolostone.

POROSITY

The dolostones in the Etherington Formation are generally tight with very poor porosity. This is in part due to the unfossiliferous nature of the formation, and is largely attributed to the pervasive dolomitization and silicification.

DISTRIBUTION OF LITHOTYPES

Significant variation of the lithotypes occurs between the studied sections. In the Talbot Lake area (Fig. 5),

directly overlying the basal chert pebble bed (E1) is a unit of cherty stromatolitic dolostone (E5). This grades upward into the siliceous dolostone (E6) which forms the upper part of the Etherington Formation.

The lithotypes in the Greenock Range (Figs. 6 and 7) are more diverse. In ascending order, the formation comprises the intraclastic-intralaminated dolostone (E2), siliceous dolostone (E6) and stromatolitic dolostone (E5). Two thin beds (20 cm thick) of quartzitic dolostone (E7) are intercalated with the siliceous dolostone in the lower part of the formation. A unit of cherty bryozoan dolostone (E8) which is less prominent than lithotype MH4 is also present.

In the Snaring River section (Fig. 8), the Etherington Formation is composed of the basal intraclastic dolostone (E3), and thin bedded siliceous dolostone (E6). The intraclastic brachiopod dolostone (E4) occurs at about 6 m below the post-Mississippian disconformity. A very thin (10 cm thick) greenish grey shale occurs near the top of the formation.

DEPOSITIONAL ENVIRONMENTS

The apparent variations of the vertical sequence across the studied sections probably reflects a shallow water depositional environment. Significant facies shifts forming a complex record of erosion, nondeposition, onlap and/or offlap can be caused by a minor changes in sea level (Laporte, 1967; Kendall and Schlager, 1981; James and

Mountjoy, 1983). The abundance of siliceous sponge spicules and scarcity of other faunas further support a nearshore, very shallow water environment (Cavoroc and Ferm, 1968; Rapson-McGugan, 1970).

A period of slow rate of sedimentation and early lithification is shown by the formation of lithified sediments and mini-pseudoanticlines. The chert pebble bed (E1) and intraclastic units (E2 and E3) mark the onset of marine transgression. The clasts were probably formed by periodic storm-induced current activities similar to those described by Laporte (1969), Ball (1971), Sepkoski (1982), and Shinn (1983) in other areas.

The dolostone intraclasts show no evidence of plastic deformation and must have been formed by penecontemporaneous erosion and redeposition of the partially lithified underlying beds. Modern intraclasts have been observed forming on tidal flats of northwestern Andros Island, Bahamas (Hardie and Ginsburg, 1977). Uniform clasts orientation is probably effected by tidal currents and/or wave movement after deposition (Lindholm, 1980). In addition to the sediment reworking and resedimentation, the proximal section (Talbot Lake) also experienced a brief episode of subaerial exposure that resulted in microkarst development. The tabular nature of the chert fragments suggests that they were probably derived from the underlying chertified algal laminae. As the internal laminations of the intralaminated units resemble the plane bed form structure described by

Allen (1970), they also suggest a high energy, very shallow water environment.

The post-depositional diagenetic changes and mechanical transport have made it difficult to establish the environment in which the mini-pseudoanticlines developed. On the basis of the stratigraphic succession, it is thought that they were probably formed in a submarine environment under the force of calcite crystallization (Shinn, 1969; Bathurst, 1975; Assereto and Kendall, 1977), although process related to growth of evaporite minerals is also possible. These pseudoanticlinal intraclasts again record a period of slow sedimentation and early lithification followed by reworking and redeposition in response to sea incursion onto land.

The chertified mounds in lithotype E5 probably were algal stromatolites similar to those found in modern carbonate environments (Davies, 1970; Bathurst, 1975; von der Broch, 1976; Hardie and Ginsburg, 1977). The algal domes are valuable indicators of depositional environments (Bathurst, 1975). The mounds of subtidal to lower intertidal stromatolites are largest and grade into laterally continuous mats in lower supratidal zones (Shinn, 1983; James, 1984). Logan (1961) also concluded that the domal relief of the algal stromatolites equals the tidal range. In this context, the generally low, laterally linked colonies of algal stromatolites, and algal mats in the Etherington Formation strongly suggests an upper intertidal to lower

supratidal depositional environment.

The most distal section (Snaring River) displays a different sequence; however, the unfossiliferous, light grey, thin bedded to laminated dolostone probably originated in a shallow water environment. The intraclastic brachiopod dolostone further supports an intertidal zone well within the agitated zone. Like the other intaclastic units, the intraclastic brachiopod dolostone probably was formed by erosion and redeposition of the partially lithified underlying beds due to storm activities. The high energy regime is further supported by the predominately convex-down orientation of the brachiopod shells. Jeffery and Aligner (1982) noted that the dominant convex-down position of bioclastic shells implies periodic influx of shell-rich sediment due to storm events, rapid sedimentation from suspension, and no subsequent reworking due to immediate burial.

The greenish grey thin shale which occurs near the top of the formation suggests a fining-upward sequence which means an upward decrease in energy. This thin shale unit of limited vertical extent is thought to have deposited in a quiet lagoonal environment.

The evidence for the existence of evaporite minerals associated with very fine crystalline dolomite is a valuable diagenetic indicator which suggests an arid tidal flat setting (Lucia, 1972; Friedman, 1980). Thus, the fine crystalline nature of the dolomite is additional evidence

for an upper tidal flat depositional environment. Many workers have noted that modern dolomite in the higher parts of the tidal flat is commonly very fine crystalline regardless of the various mechanisms they proposed for its formation (Curtis *et al.*, 1963; Deffeyes *et al.*, 1965; Hardie, 1977; Friedman, 1980; McKenzie *et al.*, 1980).

The presence of quartz pseudomorphs after previous evaporites further suggests that the deposition of the Etherington Formation was dominately in an arid supratidal environment. The lines of evidence for the now vanished evaporites are (1) the nodular feature of the partially silicified dolostone, (2) the replacement of the pisolitic structures by fibrous silica, (3) the right-angled grain boundaries of the void-filling quartz crystals, and (4) the quartz pseudomorphs after the rectangular crystals. In an arid climate, interstitial growth of evaporite minerals by displacement or replacement in the host sediments is a common phenomenon of tidal flat environments (Kinsman, 1969; Lucia, 1972; James, 1984; Kendall, 1984). This diagenetic process is in response to hypersalinity of groundwater due to high evaporation rate and sediment permeability barrier. The evaporite minerals are commonly calcitized or removed by percolating meteoric water of low salinity (Lucia, 1972; Muir *et al.*, 1980; James, 1984; Kendall, 1984).

III. MISSISSIPPIAN - PERMIAN BOUNDARY

The top of the Mississippian carbonate succession is marked by a major disconformity which is overlain by a distinct chert conglomerate. Above this unit are the chert and clastic sequences of the Permian Ishbel Group (McGugan and Rapson, 1963a). This means that the 4-13 m thick basal conglomerate represents a condensed sequence of Pennsylvanian and Lower Permian strata - a span of about 70 million years.

A. PALEOTOPOGRAPHIC RELIEF

In order to determine the topographic relief of the post-Mississippian disconformity, profiles were measured along strike in the Mount Greenock, Talbot Lake and Cinquefoil sections. Datum planes were chosen such that they could be traced out easily along strike in the field. They are stratigraphically close to the paleotopographic surface such that the effects of structural movement between the time of deposition of the datum horizon and the time of emergence is at a minimum. At Talbot Lake, the top of the thin, planar, chert pebble bed (E1) is the datum plane; while at Mount Greenock and Cinquefoil Mountain, the top of the prominent cherty dolostone unit (MH5 of the stratigraphically higher shallowing-upward sequence) is the base of the measurement.

In the Mount Greenock section, the conglomerate is commonly hidden in a gully by loose debris or vegetation,

and only small (1 m across) outcrops serve to identify its existence (Fig. 9). Exposures in the other two areas are much better. The surface irregularity of the disconformity (Figs. 10 and 11; Plates 10A, 10B and 10C) is best shown in transverses T2 to TG (Talbot Lake, Fig. 10) and C1 to CF (Cinquefoil Mountain, Fig. 11).

The disconformity has a relief of at least 5 m in the Cinquefoil Mountain area and 10 m in the Talbot Lake area. Furthermore, the profiles demonstrate that the contact between the conglomerate and the overlying chert is a planar surface parallel to the datum plane (Figs. 9, 10 and 11). The paleotopographic relief was probably generated by erosion. Deposition of the overlying Permian sequence must have begun after the top of the conglomerate was peneplaned by marine transgression.

B. PALEOKARSTIC FEATURES

It is well known that karst develops readily in subaerially exposed carbonate rocks. Karsting is controlled and produced by dissolution and migration of calcium carbonate in meteoric water and is therefore largely a diagenetic process (Esteban and Klappa, 1983).

The length of time during which the post-Mississippian disconformity was developed should have led to a prominent paleokarstic surface as might be expected from comparison with modern karst terrain. It is only under careful examination of the contact between the carbonate and the

chert conglomerate that some subtle features are discernible. These are believed to represent remnants of surface-developed paleokarstic surface (Wright, 1982) that was later modified by erosion. Recognisable paleokarstic features include (Fig. 12):

1. The presence of small troughs (0.5 m wide) with irregular, steeply sloping walls which are commonly filled with chert cobble conglomerate (Plate 11A);
2. the presence of narrow, irregular dolostone ridges (10 cm wide) surrounded by chert conglomerate on both sides (Plate 11B);
3. the contacts between the Mississippian siliceous dolostone and overlying conglomerate commonly are irregular and at high angle to the bedding plane (Plate 11C). Some sharp contacts are evidently joints and/or fissures control (Plate 11D);
4. the presence of sandstone lenses in the underlying siliceous dolostone (Plate 11E). The sandstone is a fairly well sorted fine to medium grained chert arenite with minor pebble sized angular chert fragments. Vague stratifications due to differential concentration of dark chert grains are present (Plate 11F).

The poor exposure of these subdued paleokarst landforms has rendered it impossible to determine their lateral and vertical extents. It is feasible, however, to assess the factors which controlled their formation.

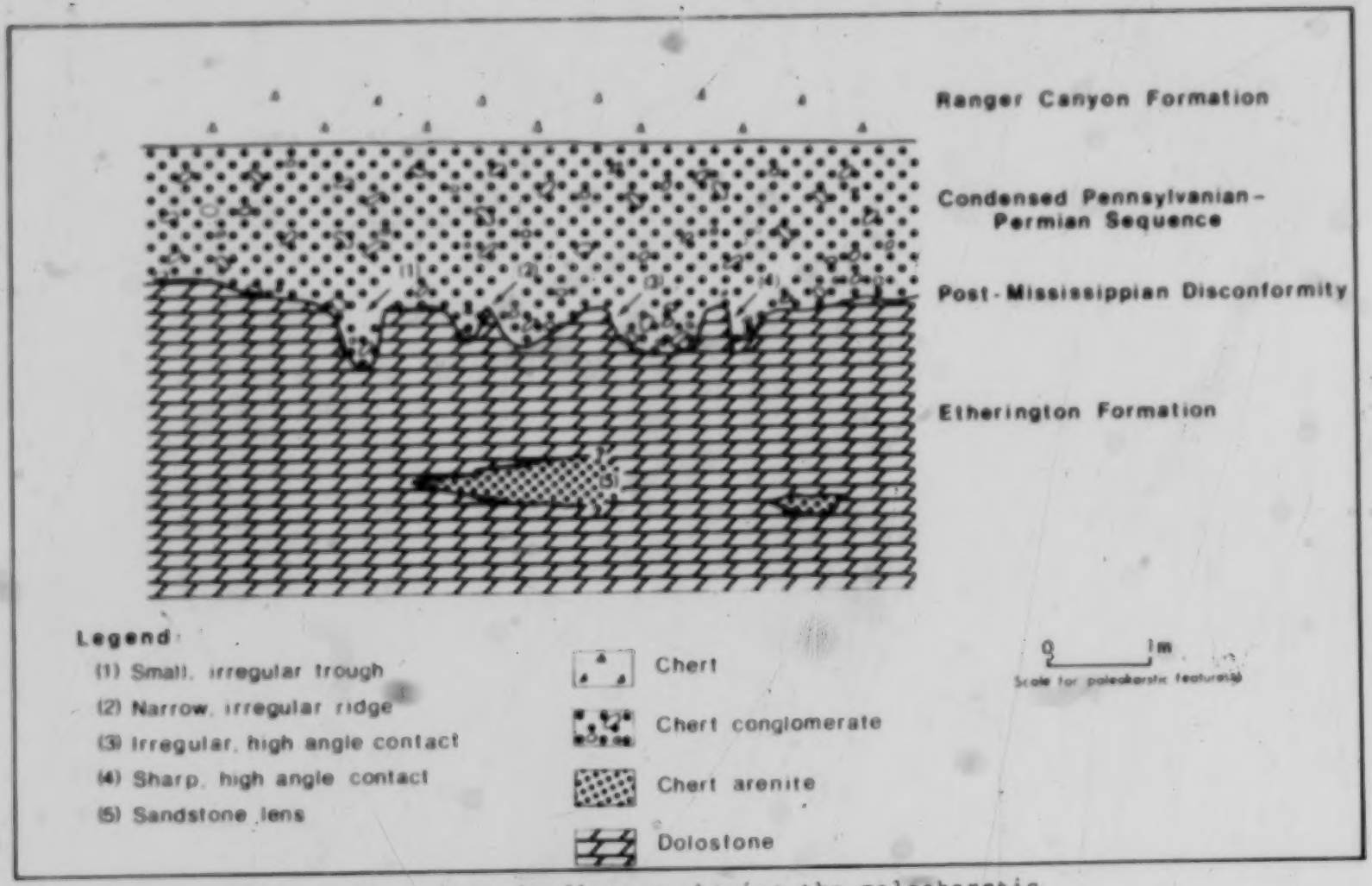

Figure 12. Schematic diagram showing the paleokarstic features on the post-Mississippian disconformity.

SOIL COVER

The environmental factors favouring maximum solution of carbonates are high partial pressure of carbon dioxide and low pH. Therefore, it is generally agreed that the solution of carbonates is most rapid under a cover of plant bearing soil because of the great abundance of carbon dioxide (Monroe, 1976). In contrast, the dissolution of bare limestone is relatively slow and usually results in the formation of sharp ridges (Read and Grover, 1977; Wright, 1982).

The trough and ridge characteristics as well as the size of the paleokarstic features are similar to that described in the scalloped surfaces by Read and Grover (1977) and Cherns (1982). Read and Grover (1977) argued that the scalloped surface developed in terrains lacking soil cover (Read and Grover, 1977). The lack of paleosol evidence in the post-Mississippian disconformity also lands support to this interpretation. The exposures in the study area are, however, far from clear to establish its definite origin. Furthermore, the soil cover may have been removed by marine transgression or wind erosion.

JOINTS AND BEDDING PLANES

At the onset of karstification, in areas underlain by intensively jointed limestone, the acidic water in the vadose zone may run rapidly down open joints and form a network of cavities at and below the water table (Ford and

Ewers, 1978). The sharp, high angle contact between the Mississippian dolostone and the overlying chert conglomerate may be related to the pre-existing joints of the host rock (Plate 11D).

The sandstone in the lenses is composed of fairly well sorted, subrounded, fine to medium sand sized quartz grains with a subordinate constituent of chert grains (10-15%). Quartz overgrowths are well developed (Plate 11G). Furthermore, its composition is similar to the sandstone in the overlying conglomerate, except that the latter has a higher chert content. Such mature sediments must have been derived from the overlying sediments and entered into the caverns through an underground network. The sorting and stratification (Plate 11F) further suggest that subterranean flowing waters were probably responsible for the transport of the sediments rather than sand fill of collapsed caverns. Moreover, the parallelism of the subhorizontal caverns (sandstone wedges) to the bedding planes, together with the interpreted high flow regime probably represent a water table cave system developed in the upper phreatic zone. If this is the case, the sandstone lenses may indicate the position of an ancient phreatic surface.

In summary, the lack of paleokarstic features is probably attributed to the absence of soil cover and the relatively unjointed rock mass. It is also possible that the preserved surfaces may have subsequently been planed by either subaerial or submarine erosion (Quinlan, 1972;

Esteban and Klappa, 1983).

C. CHERT CONGLOMERATE

The chert conglomerate apparently shows a drastic thinning from Mount Greenock to Cinquefoil Mountain which are along the same range (Figs. 9 and 11). This is likely a fictitious effect due to the thick covered interval in the former section because in transverse GU, a small outcrop of sandy chert similar to that in the Permian chert sequence is exposed at about 5 m above the Mississippian dolostone. This suggests a conglomerate thickness close to that obtained in the Cinquefoil Mountain section.

The matrix of the conglomerate is generally fairly well sorted. Medium sand sized quartz grains together with about 20-30% medium to coarse sand sized chert grains are the main constituents. They are generally subrounded and well cemented with silica (Plate 12C). The chert grains are mostly microcrystalline with minor chalcedony. Dolomite cements are subordinate and in places dissolved to give intergranular secondary porosity. Small quantities of pyrite and iron oxide are present locally.

Chert clasts, which form about 20% of the bulk of the rock are primarily microcrystalline chert and chalcedony, polymodal and poorly sorted. They are granule to boulder sized but pebbles and cobbles are most common (Plate 12A). All the clasts are well rounded and show a low degree of sphericity. Some angular fragments probably reflect the

inherited fracture pattern of the chert. The chert pebbles are mostly oblate spheroid and show no preferred orientation (Plate 12B). This implies that the clasts were not free to move relative to each other, and were unable to respond individually to fluid stresses during transport and depositional processes (Harms *et al.*, 1982).

Stratification is apparently not present; however, some vague gradings do exist. The lower basal part of the conglomerate generally contains large clasts (cobbles and boulders), while pebbles dominate the upper portion. However, it is impossible to determine whether this grading resulted from sorting of clasts due to diminishing flow strength during deposition (Blatt *et al.*, 1982), or simply represents different events and provenances.

D. BASAL INTRACLAST AND CONGLOMERATE

In the Snaring River section, the stratigraphic sequence equivalent to the chert conglomerate is an intraclastic dolostone unit that grades upward into a thin pebble conglomerate at the top (Plates 12D and 12E). Intraclasts of granule to pebble size are mostly composed of fine crystalline dolomite but the number of chert clasts increase upward. Detrital grains (approximately 20-30%) of moderately sorted, subrounded, medium to coarse sand sized quartz and chert are embedded in the fine crystalline dolomite matrix.

Distinct rim growth of clear euhedral dolomite crystals at the boundaries of the dolostone intraclasts is common (Plate 12F). These cements are usually succeeded by silica cements including microcrystalline and chalcedonic chert and megacrystalline quartz. Late fractures are generally healed by euhedral, coarse dolomite and poikilotopic clacite.

The intraclasts clearly suggest a high energy setting (Laporte, 1969; Sepkoski, 1982). The exceptional enrichment of dolostone and chert pebbles at the top of unit suggests that they are likely lag deposits or condensed layers due to frequent reworking.

E. DEPOSITIONAL ENVIRONMENTS

Paleokarstic features are thought to have formed on the carbonates which were subaerially exposed due to relative sea level drop in late Mississippian epoch. It is during this time that the disconformity developed. The subdued appearance is largely due to modification by erosion but also suggests karst development on bare carbonates lacking soil cover, indicative of arid climatic regime.

The well sorted arenite, well rounded clasts as well as the growth of silica rim cement and overgrowth over pre-exising detrital quartz grains all indicate that the conglomerate is a very mature deposit (Schmidt and MacDonald, 1979). It thus represents a condensed sequence formed by multicycled erosion, sediment reworking, and nondeposition during the Pennsylvanian to Lower Permian

period in response to several cycles of sea level change and to a lesser extent, to tidal effects. This interpretation appears to conform with the numerous unconformities and disconformities recognised in the Pennsylvanian-Permian sequence in the Southern Rockies by McGugan and Rapson (1961b, 1963a, 1963b).

In the Snaring River section, the presence of intraclasts clearly indicates physical disruption of the underlying sediments, and the detrital grains were probably reworked sediments derived from the hinterland to the east. The lag deposits at the top represent several cycles of erosion, nondeposition and reworking of sediments and probably correspond temporally to the chert conglomerates in the other sections. The overall trend from Talbot Lake to Snaring River which reflects a nearshore-offshore transect clearly demonstrates a relative decrease in the degree of physical disturbance, maturity of sediments and intensity of erosion in the further offshore, Snaring River section.

IV. PERMIAN STRATIGRAPHY AND SEDIMENTOLOGY

In the study area, the Permian strata comprise two very distinct lithologic units which are consistent with the succession described by McGugan and Rapson (1963b). Therefore, on the basis of the lithologic characteristics, the succession is divided into the Ranger Canyon and the overlying Mowitch formations (McGugan and Rapson, 1963b). Abundant sponge spicules are the only fossils present in the strata. Phosphate fragments are also common.

A. RANGER CANYON FORMATION

The Ranger Canyon Formation forms a prominent ridge in all the studied sections. It is generally well exposed and appears fairly consistent in both composition and thickness (15-20 m). McGugan and Rapson (1963b) noted that this formation has a remarkable geographic extent and is present in most sections from the Canadian-U.S. border to the Northwest Territories (McGugan and Rapson, 1963b).

BOUNDARIES

Where the boundary is exposed, the lower contact is placed at the lithologic interface of the chert conglomerate and the overlying Ranger Canyon chert. Tracing this contact along strike shows that it has no appreciable relief (Figs. 9, 10 and 11). The conglomerate may have been planed by a marine transgression prior to the sedimentation or may simply be an evened out deposition. In the Mount Greenock

section, a cherty sandstone unit (average 1-5 m thick) marks the base of the formation. This unit grades upward into the 'typical' Ranger Canyon chert.

The upper boundary with the sandstone of the Mowitch Formation (Plate 13A) appears conformable but gradational. Interfingering of chert and sandstone characterizes the uppermost one or two meters of the formation.

LITHOLOGIES AND FAUNA

Chert forms most of the Ranger Canyon Formation (Figs. 5, 6, 7 and 8). Quartzitic sandstone is usually subordinate as patches or thin beds and interfingers with chert near the top (Plates 13B and 13C).

The variable whitish grey (Talbot Lake) to bluish grey (Snaring River) colour of the chert reflects the variation in the allochemical constituents. The unit is usually thinly bedded and highly fractured or brecciated. Bedding planes generally vary from planar to irregular. The principal constituents of the cherts are microcrystalline and chalcedonic silica and sponge spicules. Detrital quartz grains, fine crystalline dolomite and phosphate fragments are minor components, but in places form a significant portion of the rock. These minor constituents show a distinct trend in the transect from Talbot Lake to Snaring River.

Dolomite patches which are thought to have survived pervasive silicification increase towards the Snaring River

section. Likewise, phosphate components which commonly appear pale brown and isotropic in thin section follow the same pattern. In the Snaring River section, these components commonly form 20% or more of the chert and gives it a bluish colour. Furthermore, vertebrate debris such as teeth and bone fragments (Plates 13D and 13E) are present only in the Snaring River section. Elsewhere in other sections, round, elliptical or rod-shaped grains (Plate 13F) are the principal phosphates. Detrital silt and sand sized quartz grains exhibit a reverse trend and are particularly dominant in the Talbot Lake section. There is also a general upward increase in the detrital quartz content. The various combinations of these minor constituents and to a lesser extent disseminated iron oxide gives a patchy colored to the chert which is monotonously white in colour.

Sponge spicules are the only fossils found in the Ranger Canyon Formation and are primarily monoaxons (Plate 13G). They are generally quite easy to identify in thin sections either from their conspicuous central canals or from their walls which are commonly replaced by chalcedonic silica. Biogenic silica released from the sponge spicules is thought to be the main silica source for the diagenetic silicification of the original carbonates (Wise and Weaver, 1974). Where common, the spicules show preferred orientation and arrangement parallel to bedding. Such alignments and concentrations may indicate current induced transport and reworking (Imoto, 1983). Moreover, spiculitic chert may be

an indicator of nearshore sedimentation (Cavaroc and Ferm 1968; Rapson-McGugan, 1970).

Small, columnar, stacked hemispheroidal laminae embedded in the microcrystalline chert may be algal stromatolites (Plate 14A). These laminae are primarily formed of fine crystalline dolomite. The dark coloration is probably due to the presence of organic or carbonaceous materials. By analogy, other dark grey, wavy, discontinuous patches probably also represent fossil stromatolites.

Scattered hollow and calcite rhombs are locally present in the chert. The rhombs are probably leached dolomite and replacement of dolomite by calcite. In other words, they represent dedolomitization of previous existing dolomites (Shearman *et al.*, 1961; Evamy, 1967). The rectangular hollows, which commonly occur with the dolomite molds, are probably leached anhydrite crystals. Shearman *et al.* (1961), Evamy (1963), Goldberg (1967) and Folkman (1969) all proposed that dedolomitization is based on the dolomite-calcium sulphate reaction.

In the Snaring River section, large quartz nodules (Plate 14B) up to 30 cm in diameter are present. In line with the other evidence of pre-existing anhydrites, it seems probable that these quartz nodules are silicified evaporite nodules similar to those described by Chowns and Elkins (1974) and Milliken (1979).

Chert breccias confined to the basal sandy chert sequence, are of limited lateral extent in the Mount

Greenock section (Transverses GE and GQ, Fig. 9, Plate 14C). Commonly, the fine to medium grained quartz arenite infiltrated among the white chert clasts or into fractures. Clasts are usually angular and up to 3 cm in size. The chert arenite fill has the same composition as the basal sandy sequence, suggesting brecciation was contemporaneous with deposition of sand and the fill is later cemented primarily by quartz overgrowth. These features suggest that the chert breccias were formed by chemical changes on lithification of chert as proposed by Rapson (1962) in her studies of Kananaskis chert.

In the Snaring River section, breccias occur throughout the chert. The lower brecciated units commonly have small angular clasts of less than a centimeter across (Plate 14D). Spaces between clasts were usually filled with coarse dolomite crystals and minor sparry calcite. The upper brecciated units commonly have angular clasts of about a centimeter across (Plate 14E). These chert clasts were cemented by coarse quartz forming a mosaic texture. Some angular vugs lined with quartz crystals (Plate 14F) remain open.

Folk (1973), in a study of the Devonian Caballos novaculite suggested that the chert breccias were created by dissolution of evaporitic strata followed by collapse of overlying brittle chert. The abundance of leached anhydrite crystals and the interpreted evaporite nodules in the Snaring River section tend to suggest that dissolution of

evaporites may have played a part in the formation of the breccias. Furthermore, the well defined outlines of the rectangular hollows which remain unsilicified indicate that evaporite dissolution occurred after silica lithification. The lack of evidence of granulitization and the presence of only chert clasts are evidence against tectonic related brecciation. It is suggested, therefore, that the brecciation in the Snaring River section resulted from the dissolution of evaporitic strata associated with the flushing of low salinity meteoric water.

DEPOSITIONAL ENVIRONMENTS

Although pervasive silicification of the originally carbonate sediments has obliterated most of the lithologic characteristics of the Ranger Canyon Formation, there is ample lithologic and faunal evidence to suggest a very shallow water intertidal to supratidal depositional environment. Such evidence includes: (1) the lack of invertebrate fossils other than sponge spicules suggests an environment in the upper intertidal zone or higher (Heckel, 1972); (2) the abundance of sponge spicules which can be a useful indicator of the nearshore zone (Caravoc and Ferm, 1968; Rapson-McGugan, 1970); (3) the accumulation and preferred orientation of spicules indicate current reworking (Imoto, 1983); (4) the well rounded phosphate grains also suggests current agitation; (5) the presence of small scale algal stromatolites is a good indicator of upper intertidal

to supratidal environment (Shinn, 1983; James, 1984); (6) the presence of fine crystalline dolomite also provides evidence for upper intertidal to supratidal environment (Curtis *et al.*, 1963; Friedman, 1980); and (7) the abundance of detrital sand grains and lack of terrigenous clay also imply a nearshore setting.

Several diagenetic characteristics provide evidence for subsurface vadose/shallow phreatic zones, namely, (1) leached pre-existing evaporite minerals (Lucia, 1972; James, 1984; Kendall, 1984), (2) microstalactitic calcite cement (Muller, 1971; Jones *et al.*, 1984), and (3) dedolomite (de Groot, 1967; Folkman, 1969). These are also useful indicators of higher tidal flat settings.

It is suggested, therefore, that the rocks of the Ranger Canyon Formation originated in the upper intertidal to supratidal zones. This represents a relatively slow rise of sea level and an associated seaward progradation of sediments (Kendall and Schlager, 1981; James, 1984). The shallowing-upward sequence probably follows a rapid transgression over the shallow shelf during which the last episode of reworking, erosion and deposition of the conglomerate sequence was taken place.

The transect from Talbot Lake to Snaring River again demonstrates a transition from nearshore to offshore depositional environment. This trend is shown by a gradual decrease in detrital quartz but an increase in phosphate fragments towards the Snaring River section.

B. MOWITCH FORMATION

The Mowitch Formation is composed of cliff forming sandstone (Plate 15A) in the Talbot Lake, Mount Greenock and Cinquefoil Mountain areas. It only occurs in and north of the Jasper area (McGugan and Rapson, 1963b).

BOUNDARIES

The lower contact is gradational and is placed at the stratigraphically highest occurrence of interfingering, laterally continuous chert.

The upper contact is hidden in a thick covered interval between the underlying prominent Permian quartzitic sandstone and the overlying relatively recessive Triassic siltstones of the Spray River Formation. Abundant vertical burrows are present in the bedding planes at or near the top of the Permian sandstone. The Permian and Triassic strata appear to have concordant attitudes. This upper boundary is variably interpreted as a disconformable (Walcott *et al.*, 1964) and paraconformable (McGugan and Rapson-McGugan, 1976) contact. In either case it represents a hiatus.

LITHOLOGIES AND FAUNA

The predominant lithotype of the Mowitch Formation is a brown weathering, quartz arenite. It is formed of clean, well sorted, fine to medium grained quartz grains with minor chert and phosphate fragments. Chert grains are equally well sorted and subrounded whereas the phosphate grains are

usually elliptical in shape (Plate 15D). Sponge spicules are locally present.

The sandstone varies from thinly to thickly bedded and has a uniform composition. Small scale cross-lamination occurs throughout the unit but is most common in the uppermost part of the unit.

Large, generally subrounded, boulder sized chert patches are common (Plate 15B). On eroded surfaces, they have a porous texture. These features are apparently silicified carbonates and may be of algal origin.

Rare, small (<1 cm) black phosphatic nodules are present in the arenite (Plate 15C). In thin sections, they are isotropic, microcrystalline and commonly show corroded boundaries with the surrounding quartz grains. These nodules also contain some phosphate fragments and corroded quartz grains. Shark teeth occur in the topmost bed.

Vertical burrow structures of 2 to 5 millimeters in diameter are common near the top of the formation (Plate 15E). These burrows were probably formed by sessile suspension feeders. The limited variety of the biogenic sedimentary structures as well as their confined occurrence near the top of the sequence indicates a change of depositional environment near the end of the arenite sedimentation.

Quartz overgrowths (Plate 15D) and minor microcrystalline chert are the most common agents for lithification. Carbonate cementation occurs locally. Thus,

the porous sandstone patches may have been formed by dissolution of carbonate cements.

DEPOSITIONAL ENVIRONMENTS

The clean, well sorted quartz arenite suggests that the sediments were commonly reworked (Blatt *et al.*, 1972). It appears that the clastic components were primarily derived from the hinterland to the east. Furthermore, it is suggested that rivers were responsible for transporting the sediments to the depocentre. The cleaning and sorting of the sediments were therefore related to both river and marine processes (Coleman and Prior, 1982).

Except for rare, small scale cross-lamination, the sequence is devoid of any large scale sedimentary structures. The fine to medium sized sands are also useful indicators of a shallow water depth, nearshore depositional environment (Allen, 1967). The lack of trace fossils in the lower sequence and absence of megafauna suggest a mobile substrate associated with a high rate of sedimentation (Heckel, 1972).

The uppermost beds are characterized by (1) bioturbated sedimentary structures such as vertical burrows and (2) presence of small phosphate nodules. Phosphate nodules probably formed in association with slow or nondeposition in shallow marine clastic deposits (Johnson, 1978). The sudden increase in suspension feeders which produced the burrows (Seilacher, 1967) may indicate a diminishment of sediment

supply.

On a shallow extensive carbonate shelf with high clastic supply, a relative sea level drop causes deltaic encroachment from a landward direction (Kendall and Schlager, 1981). Thus, it is suggested that the mature sandstone of the Mowitch Formation represents a deltaic progradation over the high tidal Ranger Canyon chert (carbonate). Furthermore, the clean, well sorted sands and also the lack of sedimentary feature may suggest that the sand unit was deposited as a distributary-mouth bar (Coleman and Prior, 1982). Channel switching or avulsion is probably responsible for cutting off the sediment supply (Elliott, 1978). Therefore, the burrowed bedding planes in the uppermost unit probably represent the abandonment surfaces due to channel migration.

V. STRATIGRAPHY AND SEDIMENTOLOGY: SYNOPSIS

A. INTRODUCTION

Sedimentary structures and grain size are of importance in the interpretation of terrigenous depositional environments, whereas in ancient carbonate sequences, it is the succession of lithologies and fauna which record the environment of deposition. Similar to their clastic counterpart, fining upward and coarsening upward cycles are also recognised in carbonate sequences (Reeckman and Friedman, 1982)

James (1984) proposed the use of the term 'shallowing-upward sequence' for situations where carbonate sediments accumulate at rates faster than the rate of subsidence of the sedimentary basin. As a result, each subsequent unit is deposited in progressively shallower water. It is important to note that such shallowing-upward or shoaling-upward carbonates are formed during relative sea level rises (Kendall and Schlager, 1981; James and Mountjoy, 1983; James, 1984)

This section discusses the stratigraphic correlation over the study area, the environmental reconstruction of the succession, and the correlation with global sea level changes.

B. STRATIGRAPHIC CORRELATION

Tremendous structural shortening of the Rocky Mountain thrust-fold belt where the study area is located resulted from the thrusting during the Laramide Orogeny. This horizontal displacement is responsible for present proximity of the strata (Fig. 13b).

The palinspastic reconstruction of the depositional environment prior to thrusting (Fig. 13a) indicates two important features. Firstly, sediment wedges thicken seaward; and secondly, water depth increases gradually seaward. The four studied locations thus represent an inshore-offshore transect in an ancient epeiric sea. This pattern is reflected by the changes of lithologies and fauna in each section. Based on these characteristics, it is possible to correlate the strata across the study area (Fig. 14). The distinct variation in the stratigraphy is thought to indicate an overall shallow water depositional environment, where facies changes were reponsive to slight changes in sea level.

In the Turner Valley Formation, there is a distinct difference in facies between the Talbot Lake and Mount Greenock sections. The grainstone in the latter is primarily composed of echinoderm and bryozoan fragments, while the skeletal grainstone in the Talbot Lake location encompasses more diverse allochems in addition to echinoderm and bryozoan fragments. This skeletal grainstone grades upward into a well sorted oölitic grainstone. It is suggested,

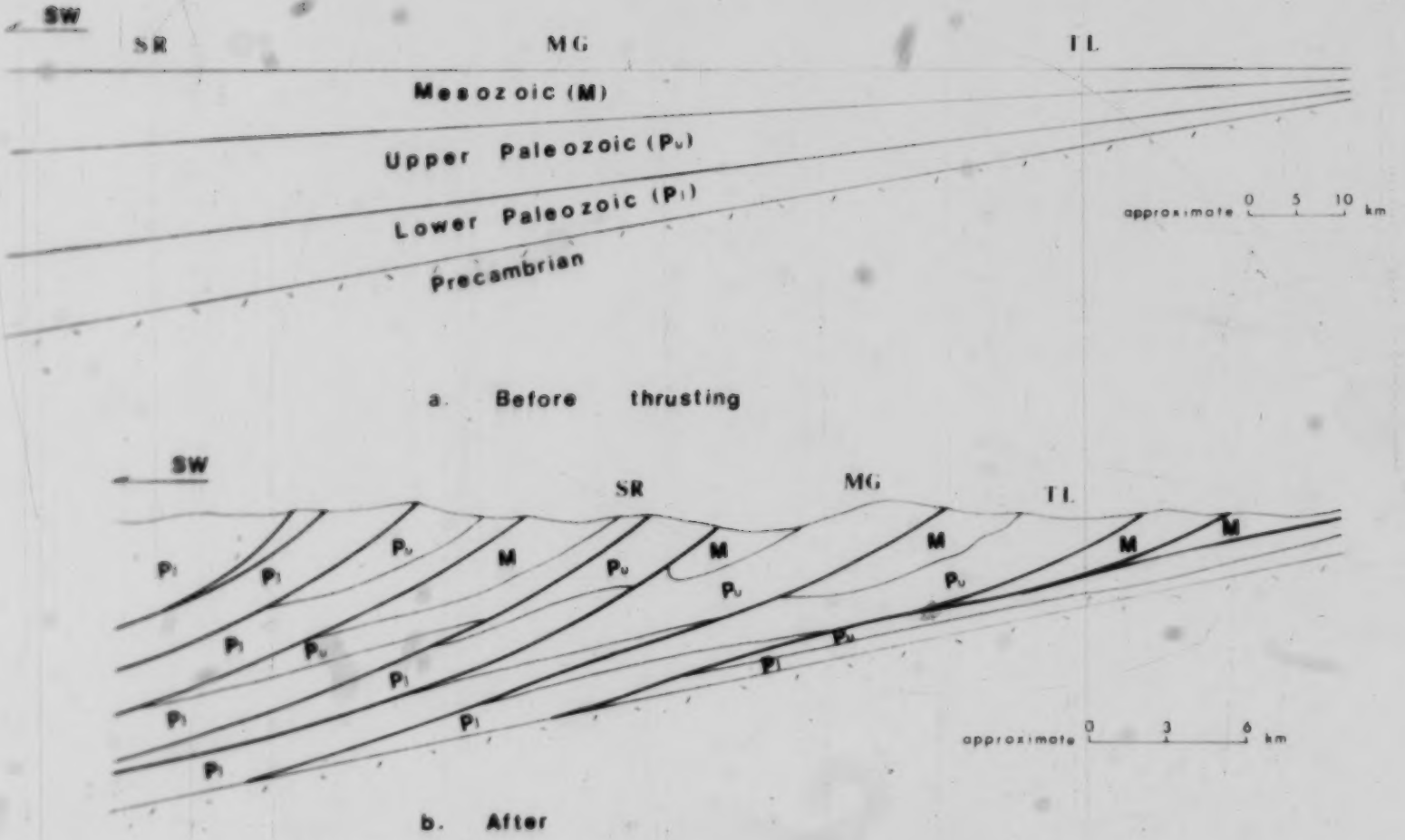

Figure 13. Schematic representation of the sedimentary strata before and after thrusting (Laramide Orogeny) showing the structural shortening of the strata.

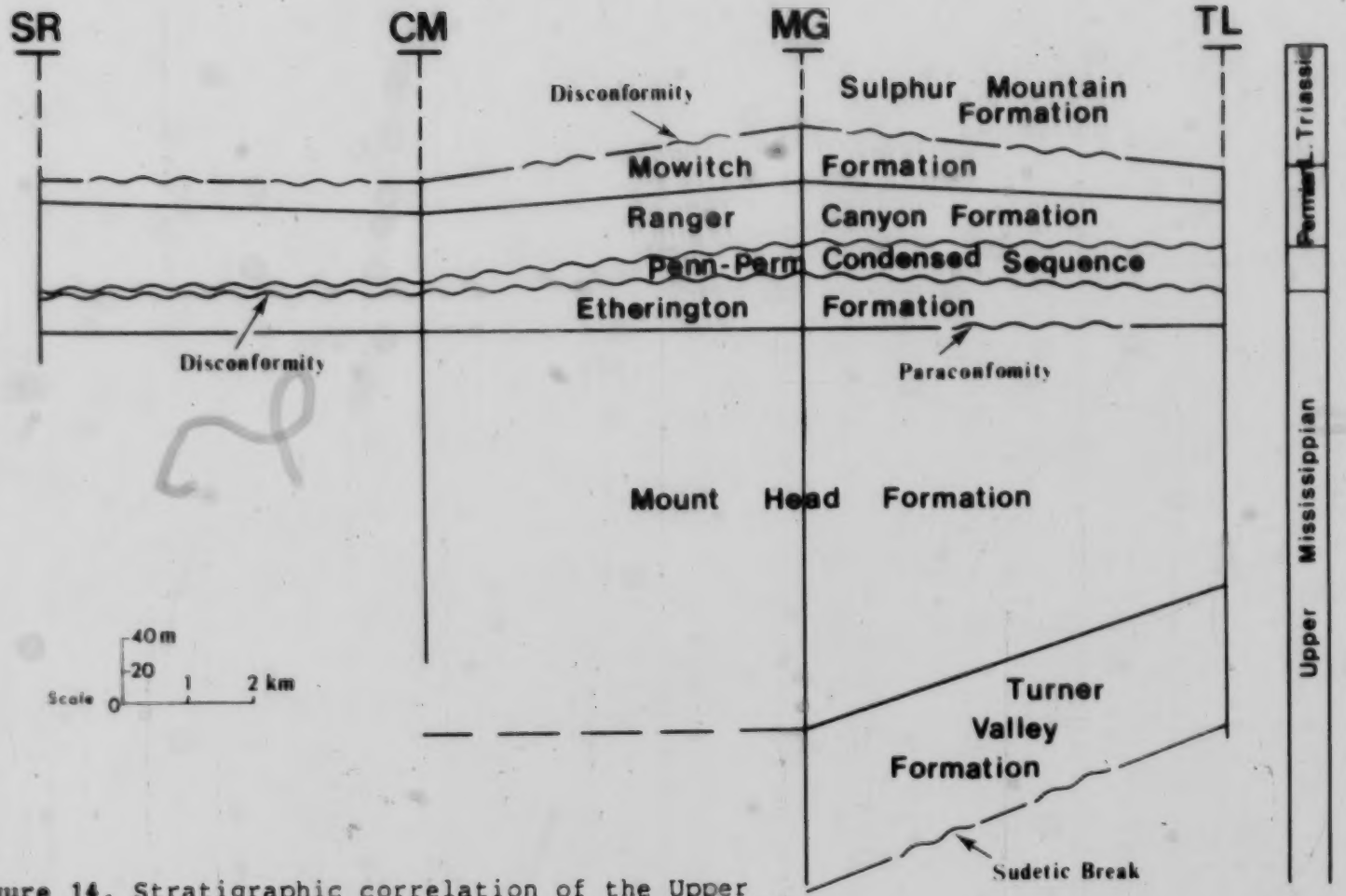

Figure 14. Stratigraphic correlation of the Upper Mississippian to Lower Triassic successions of the studied sections.

therefore, that the Talbot Lake locality was located close to a carbonate shoal where high energy deposits prevailed.

The prominent cherty ridges of essentially bryozoan stems and algal laminae in the Mount Head Formation provide an excellent control in the correlation of an otherwise monotonous, unfossiliferous sequence. The obvious thickening in the Greenock Range appears to be the consequence of the wedging of sediments. The lithologic succession and repetitive phenomenon are correlatable between the Talbot Lake and Greenock Range areas.

A distinct facies change exists in the uppermost 10 m of the Mount Head Formation between the Mount Greenock and Snaring River sections. The former is characterized by tidal deposits of alternating dolostone and argillaceous dolostone. In contrast, the stratigraphically equivalent strata in the Snaring River section is formed of a massive dolostone that contains a hardground surface and an overlying bioturbated, laminated dolostone unit. The presence of the hardground surface and bioturbation suggest a subtidal setting. Furthermore, the abundance of pyrite and quartz crystals in the Snaring River section is thought to indicate bacterial degradation of now vanished evaporite minerals, which would imply a hypersaline lagoonal environment.

The lowermost unit (E1) of the Etherington Formation shows a distinct inshore-offshore depositional pattern across the transect from the proximal (Talbot Lake) to the

distal (Snaring River) section. In the Talbot Lake area, the microkarsting in the chert pebble bed suggests carbonate solution during a short period of subaerial exposure. The stratigraphically equivalent basal unit in the Mount Greenock section is represented by a high energy deposits of interbebbed intraclastic and intralaminated dolostone. The distal section (Snaring River) is marked by a reworked pseudoanticlinal hardground surface which indicates a submarine setting. These basal units thus show a distinct trend of progressive change from upper supratidal to subtidal environment across the epeiric shelf sea.

The gradual change in water depth persisted into the Etherington Formation. Lithologies of the proximal Talbot Lake and Greenock Range sections are characterized by stromatolitic dolostone and siliceous dolostone with quartz pseudomorphs after evaporite minerals. The intraclastic brachiopod bed and the thin greenish grey shale unit present in the distal section (Snaring River) again indicate an intertidal to subtidal lagoonal environment.

The condensed sequence directly above the Mississippian carbonate succession is made up of abundant immature dolostone clasts in the Snaring River section, while mature chert clasts dominant in the other areas. This is thought to reflect a lesser degree of erosion and reworking in the distal shelf location. Likewise, the paleokarstic and erosional features at the post-Mississippian disconformity are only recognised in the proximal sections.

In the Upper Permian Ranger Canyon Formation, chert is the principal constituent; however, the subordinate components are different from section to section. Besides the vertebrate remains such as tooth and bone fragments, the Snaring River section has a distinctively higher phosphate content. Detrital quartz grains are the most abundant accessory element in the nearshore sections.

The thick sections of chert breccias and large quartz nodules which are considered to have formed by dissolution of evaporitic strata and replacement of evaporite nodules agrees with the shallow subtidal interpretation for the Snaring River section. Evaporitic strata are commonly formed in subaqueous environment (Kendall, 1984). In the other locations, only leached anhydrite molds are present which are believed to represent interstitial growth of evaporites in the supratidal environment.

C. ENVIRONMENTAL RECONSTRUCTION

On the basis of lithologies, lithologic succession, faunal association and sedimentary structures, the environments of deposition can be reconstructed. The Snaring River section is not included because it represents a relatively deeper water environment where deposits are less sensitive to sea level variations and are therefore difficult to diagnose from lithologic changes.

The carbonate succession of the Upper Mississippian period (Meramecian and Chesterian) was deposited in a

shallow epeiric sea in response to relative sea level rise. Superimposed on this marine transgressive phase are several shallowing-upward sequences (Fig. 15). They are formed as a result of high rate of carbonate sedimentation which exceeded relative rise in sea level and caused a seaward progradation of the sedimentary facies (Fig. 16).

The shallowing-upward sequence (Fig. 15) formed during the Early Meramecian (Turner Valley Formation) occurs in the Talbot Lake area where lagoonal deposits (TV4) overlie open marine sediments (TV1 and TV2). The grainstones, which indicate the carbonate shoal development, was succeeded by the bioturbated wackestones which represent sedimentation on the lee side of the shoal. The physical barrier created by the carbonate shoal is particularly evident in the Mount Greenock section where the hypersaline conditions for the anhydrite formation were developed in the lagoonal setting.

The intraclast unit at the base of the Mount Head Formation denotes the onset of a marine transgression. Two repetitive shallowing-upward sequences occur in this formation (Fig. 15). These vertical sequences show a range of depositional settings from subtidal to high tidal flat environments related to corresponding decrease in water depth (Fig. 16). The subtidal lithologies comprise thin echinoderm-bryozoan grainstone and slightly bioturbated skeletal wackestone. The skeletal sands are interpreted as tidal channel deposits. High energy intertidal deposits consist of ramose bryozoan dolostone grading upward into

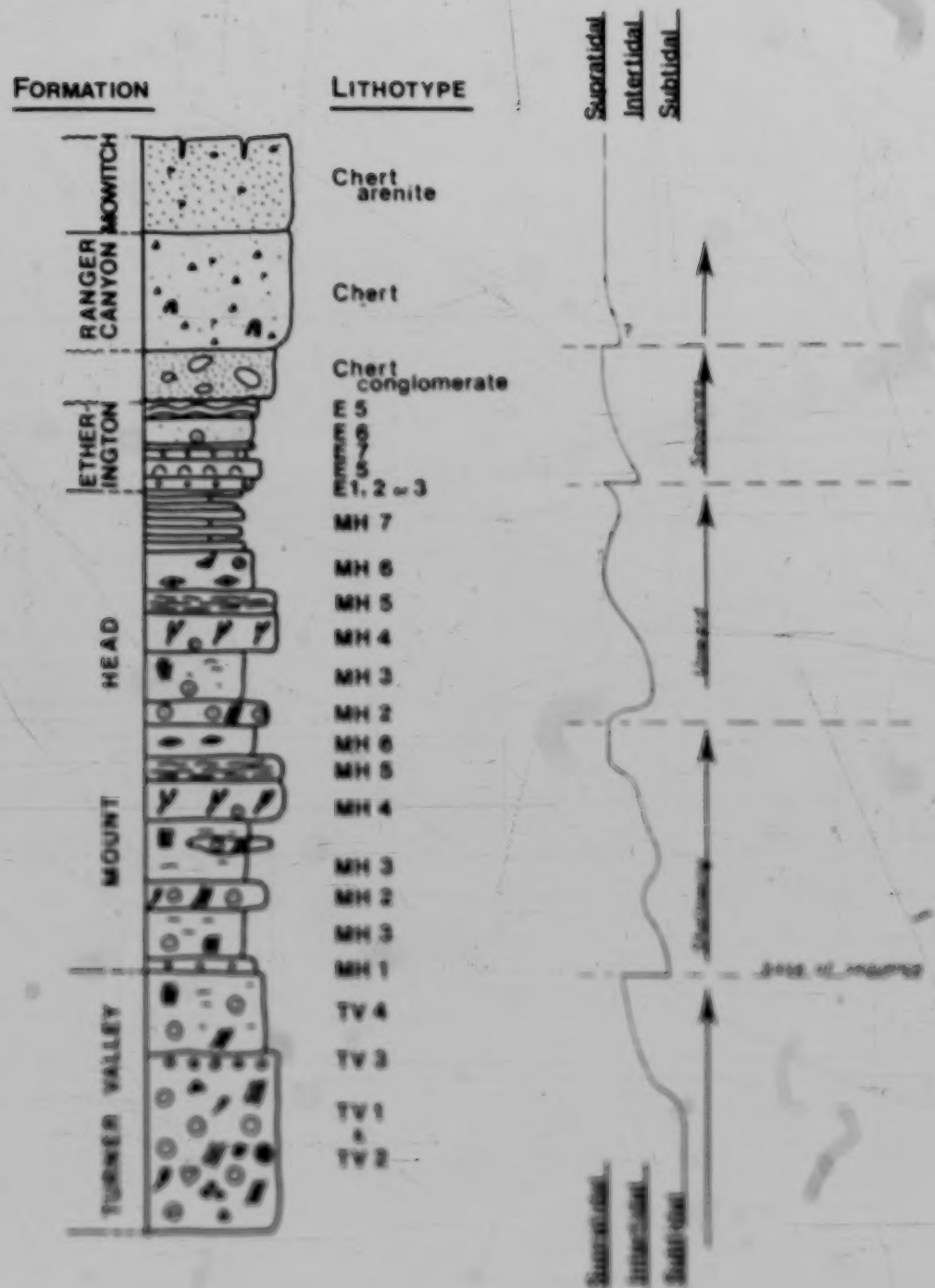

Figure 10. Composite stratigraphic column of the study area showing the major lithotypes and the corresponding shallowing-upward sequences.

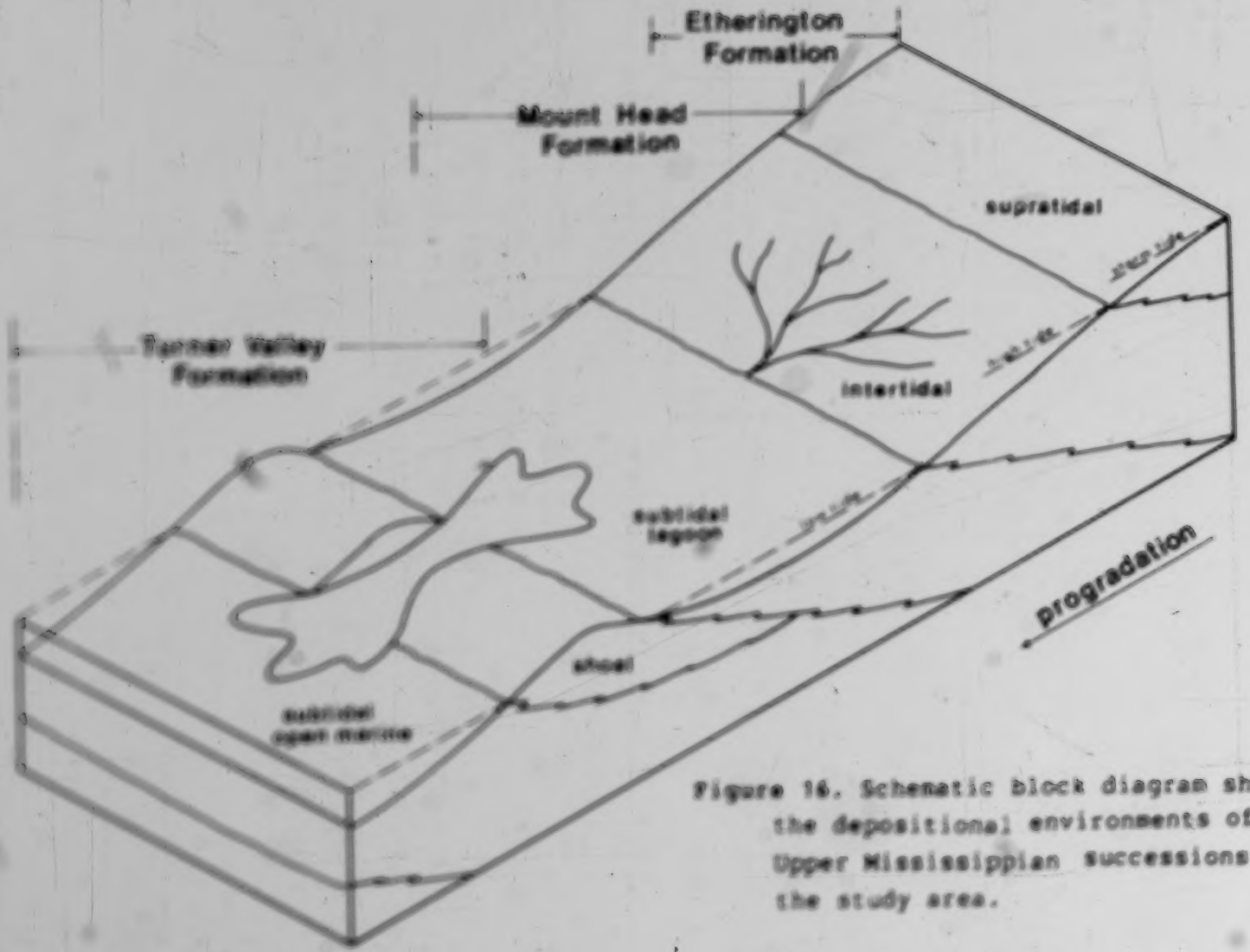

Figure 16. Schematic block diagram showing the depositional environments of the Upper Mississippian successions in the study area.

algal dolostone. Deposits of the low energy upper intertidal to supratidal fine crystalline dolostone are characterized by bird's-eye structures and small, thin shelled gastropods and bivalves. The tidal flat environmental interpretation is substantiated by the presence of interbedded dolostone and argillaceous dolostone in the uppermost beds of the Mount Head Formation. The brief period of subaerial exposure at the upper boundary in the proximal section (Talbot Lake) probably resulted from rapid progradation which outpaced relative sea level rise, and thus the low sea level is unable to reach the shelf interior.

Another episode of transgression formed the pebble bed and intraclast unit and marks the commencement of Chesterian deposition. The shallowing-upward sequence of the Etherington Formation (Fig. 15), ranging from upper intertidal to supratidal environment (Fig. 16), is well exemplified by the upward grading of low relief domal stromatolites into algal mats. This environmental interpretation is supported by the presence of quartz pseudomorphs after supratidal evaporites. The upward decrease of detrital quartz in the shallowing-upward sequence agrees with Hite's (1970) observation that regressive phases of carbonate succession have a lower detrital quartz content.

The widespread disconformity capping the Upper Mississippian carbonates developed in response to a sea level drop during late Mississippian time. The exposed

carbonate shelf was then subjected to subaerial karsting and erosion. Overlying the karsted erosional surface is a condensed sequence formed of mature arenites and well rounded clasts, which are thought to represent multicycled erosion, sediment reworking, and nondeposition in response to several episodes of marine transgression and regression during Pennsylvanian and Lower Permian times.

Pervasive chertification has obliterated most of the textures in the Upper Permian Ranger Canyon Formation. Relic structure, however, show evidence of high tidal depositional environment. These features include the presence of sponge spicules, small scale algal stromatolites, detrital quartz grains and rounded phosphate fragments. The interpretation of a supratidal setting is strengthened by the vadose diagenetic signatures which include empty molds of anhydrite and dolomite and microstalactitic cements.

At the end of the Permian time, a sea level drop coupled with high clastic influx from the hinterland resulted in deltaic progradation on the high tidal carbonate shelf when the sandstone of the Mowitch Formation was deposited. The mature quartz arenite may have been deposited as a distributary mouth bar which was later abandoned by channel switching or avulsion.

D. CORRELATION WITH GLOBAL SEA LEVEL CHANGES

The unconformities present in the Upper Mississippian to Permian strata at the Talbot Lake area show a striking correlation with those defined by Sloss (1963) and Vail *et al*. (1977, 1979) (Fig. 17). Sloss (1963) identified six craton-wide inter-regional unconformities in the North America successions. The global cycles of sea level changes and their associated coastal onlaps constructed by Vail *et al*. (1977, 1979) are determined on seismic data tied to well information for age and environmental control covering the six continental margins. Thus correlating the documented global unconformities with those recognised in the study area provides a useful framework for the stratigraphic analysis.

The post-Meramecian onlap unconformity identified by Vail *et al*. (1977, 1979) probably corresponds with the maximum shallowing during late Osagean time when the carbonaceous shale was deposited in the Talbot Lake section. Channelling was also noted by Mountjoy (1965) in the vicinity of the Mount Greenock pipeline road section.

Sloss's (1963) post-Mississippian unconformity which denotes the closing regressive phase of the Kaskaskia sequence when the sediments are exposed to erosion is probably correlatable with the disconformity which occurs in the Talbot Lake area. It also conforms with Vail *et al*.'s (1977, 1979) post-Mississippian global relative sea level drop.

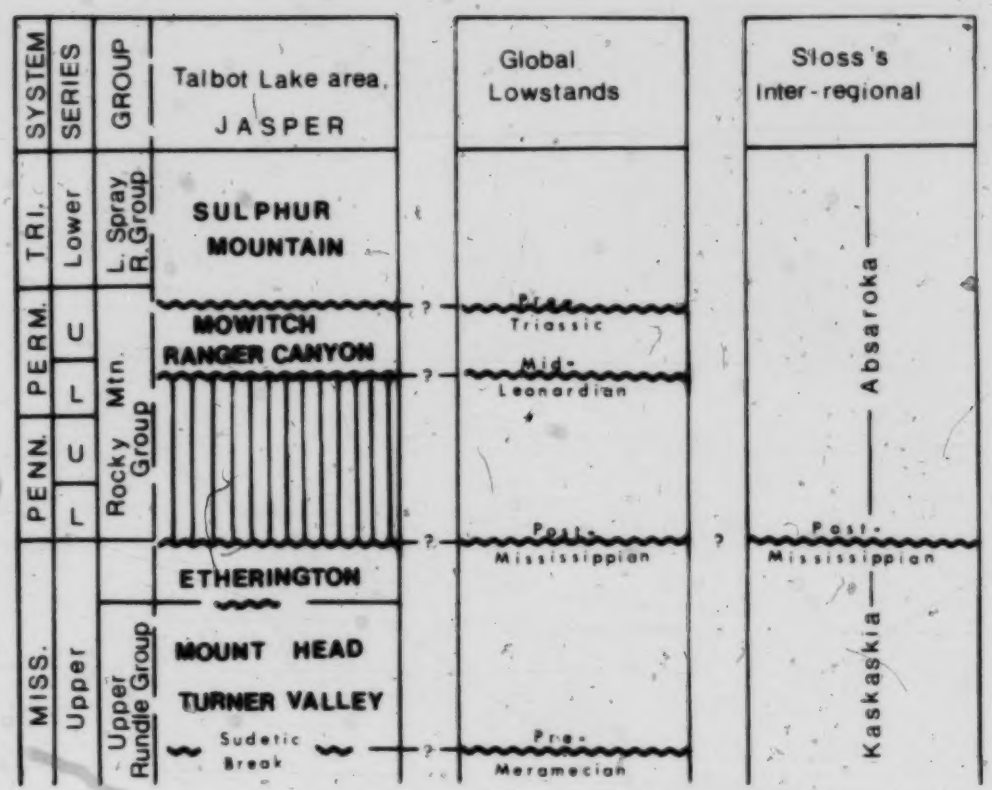

Figure 17. Correlation of the sedimentary breaks in the study area with the Global sea level lowstands (from Vail *et al.*, 1977, 1979) and Sloss's inter-regional unconformities (from Sloss, 1963).

Althought the Permian-Triassic contact is covered in the study area, McGugan and Rapson-McGugan (1976) and Walasko *et al.* (1964) reported paraconformable and disconformable contact respectively at other localities of the Rocky Mountain Front Range. These observations together with the interpreted relative sea level drop during Late Permian time (Mowitch Formation) is thought to agree with Vail *et al.*'s (1977, 1979) pre-Triassic onlap unconformity.

VI. REPLACIVE DOLOMITIZATION

On the basis of degree of dolomitization, there are two main types of replacive dolomitization in the Mississippian carbonate succession. Firstly, the selective dolomitization which occurs primarily in the partially dolomitized limestones of the lower Turner Valley Formation. Secondly, the pervasive dolomitization which occurs throughout the rest of the sequence regardless of the lithology or stratigraphic position (Fig. 18).

A. SELECTIVE DOLOMITIZATION

PETROGRAPHY OF DOLOMITE

This type of dolomite generally replaces micrite and peloids of the echinoderm-bryozoan grainstone (lithotype TV1) and skeletal grainstone (TV2) of the lower Turner Valley Formation. The euhedral dolomite rhombs are 0.05-0.1 mm in size (Plate 16A) and commonly exhibits hypidiotopic crystalline fabric (Plate 16A). Dark micrometer-sized inclusions are ubiquitous in the dolomite crystals. These inclusions are probably calcite relics or black organic material that were in the original lime muds.

TIMING OF SELECTIVE DOLOMITIZATION

The fact that the dolomite-rhomb growth ceased upon abutting the calcite cement (Plate 16A) clearly suggests that the selective dolomitization occurred after calcite

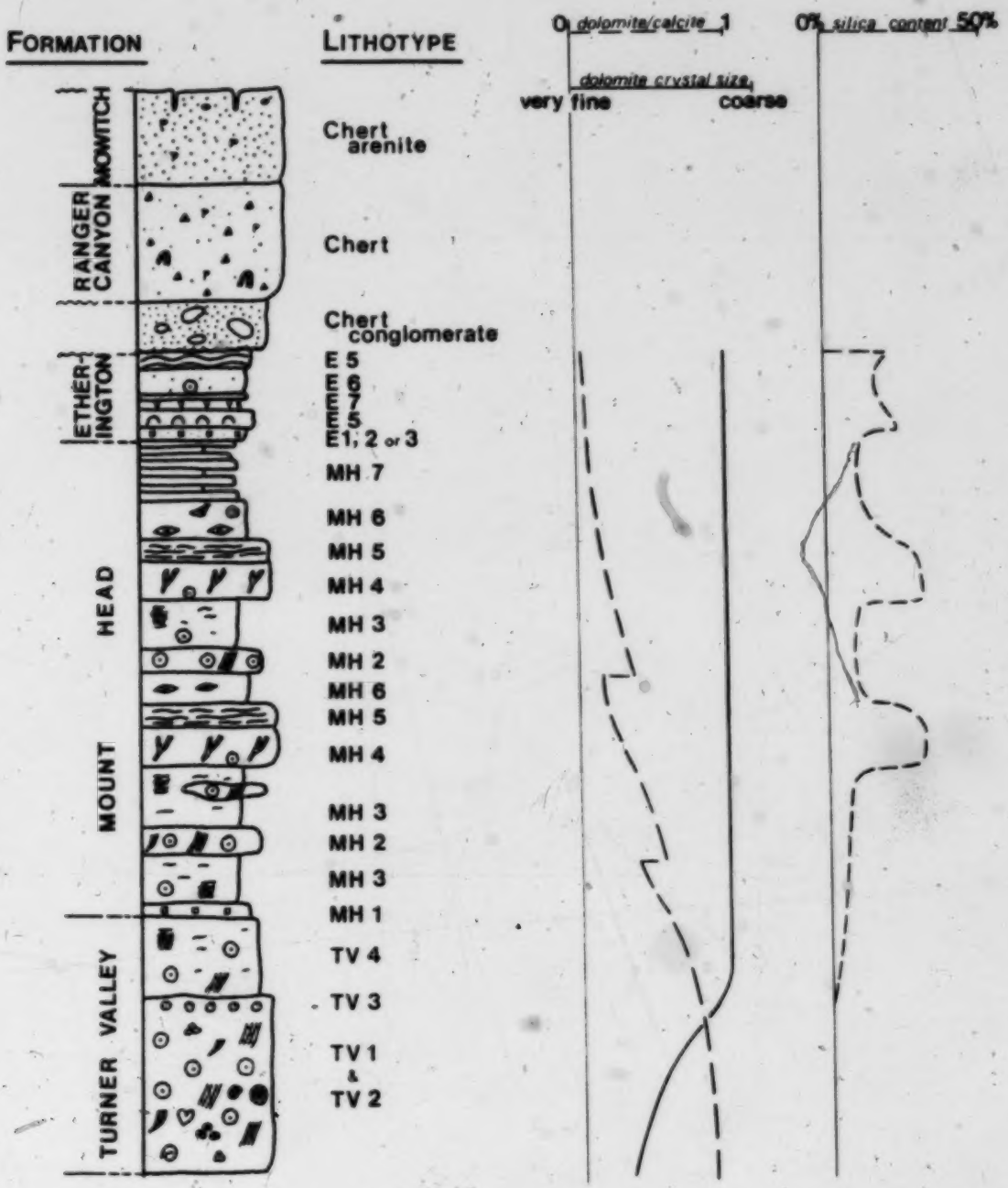

Figure 18. Composite diagram showing the variations of the dolomite/calcite ratio, dolomite grain size and silica content of the Upper Mississippian strata.

cementation. Dolomitization was incomplete and many peloids were only partially dolomitized. The selective alteration of micrites probably occurred before the matrix porosity was reduced by lithification process and before the micrite was converted to the stable phase of low magnesium calcite. Furthermore, peloids cut by fractures or stylolites remain undolomitized. In one situation, dolomite crystal in a peloid, which was cut by a stylolite, was partially dissolved (Plate 16B). These evidence suggests that this phase of dolomitization was probably an early diagenetic process.

MECHANISM OF SELECTIVE DOLOMITIZATION

The selective replacement of micrite by dolomite in partially dolomitized limestones has been noted by numerous workers (Murray, 1960; Thomas and Glaister, 1960; Lucia, 1962; Lucia and Murray, 1967). Murray and Lucia (1967), in their study of the Mississippian Turner Valley Formation at Moose Mountain in Alberta, suggested that the fabric selectivity was caused by the physical and chemical nature of the sediments rather than the difference in water composition. They further suggested two possible factors that might cause the preferential replacement, namely: (1) the difference in solubility between the crinoid particles and lime mud, and (2) the difference in particle size.

Although an understanding of the origin of the lime mud is far from complete, lime mud in modern carbonate

environments commonly contain a high percentage of aragonite (Bathurst, 1975). Thus, it can be suggested that the micrite of the Mississippian may also have been formed of aragonite. On the other hand, the high-magnesium echinoderm fragments probably underwent early transformation to low-magnesium calcite. This is a simple exchange of calcium for magnesium in an unsaturated solution and shows little change of structural detail in the bioclasts (Land, 1967). Experimental studies have demonstrated that the dolomitization rate is fastest for aragonite, followed by high-magnesium calcite, and slowest for low-magnesium calcite (Gaines, 1974). This result is compatible with the observed selective dolomitization of lime mud.

Lime muds, which have a large surface area relative to the bioclasts, provide numerous nucleation sites. This allows more dolomite crystals per unit volume to nucleate in the mud (Murray and Lucia, 1967). In addition to reducing the surface area, the early syntaxial rim growth probably rendered the crinoidal sands less permeable to the dolomitizing fluid.

B. PERVASIVE DOLOMITIZATION

PETROGRAPHY OF DOLOMITE

The dolomite occurs as a mosaic of equant dolomite crystals, forming a xenotopic to hypidiotopic crystalline fabric. Rhombs are 0.01 to 0.1 mm in size. Under plane

light, these dolomite crystals are brown and cloudy (Plate 16C), probably because of minute inclusions from the precursor carbonate. The 'typical' intercrystalline (sucrose dolomite) porosity is scant and may have been obliterated by late stage dolomite growth or recrystallization.

The dolomite crystal size appears to correlate with the lithotypes in each individual upward shallowing sequence (Fig. 18). In the Mount Head Formation, each of the two successive cycles show a gradual upward decrease in crystal size from an average of 0.02 mm in lithotype MH2 to about 0.01 mm in lithotype MH6. Crystal size variation in the Etherington Formation is generally small and commonly lies in the range of 0.05 mm to less than 0.01 mm.

There are minor occurrences of larger (approximately 0.1 mm), clearer, more euhedral crystals in the matrix dolomites, which show no evidence of progressive crystal enlargement. They were probably formed by replacement of small allochems of indiscernible origin.

There is a distinct difference in crystal size between the intraclasts which are commonly formed of dolomite crystals less that 0.01 mm in size and the matrices which have an average crystal size of 0.05 mm (Plate 16E). The intraclast-matrix boundaries are poorly defined which implies that dolomitization process occurred after deposition of the lithified clasts.

The crinoid fragments which were not leached out were replaced by three mechanisms (Plate 16D): (1) pseudomorphic

replacement, (2) internal replacement, and (3) external replacement. Similar replacement features were noted by Lucia (1962) in the crinoidal rocks of the Andrew South Devonian Field in Texas. In the pseudomorphic replacement, the single calcite crystal of the original crinoid fragment was replaced by a single, optically continuous dolomite crystal. Internal replacement is probably a type of selective replacement of the lime mud filling the axial canals of the crinoid fragments. Such dolomite crystals are generally smaller than the dolmite crystals formed by external replacement, which have approximately the same crystal size as the matrix dolomite.

TIMING OF PERVASIVE DOLOMITIZATION

There is ample evidence to suggest that the dolomites in the Mississippian carbonate succession resulted from dolomite replacement of calcium carbonate sediments. The presence of the completely dolomitized or silicified marine fauna, such as crinoids and bryozoan, supports this contention.

Although it is difficult to determine the onset of the dolomitization, there are several lines of evidence which suggest that it occurred at an early stage in diagenesis. Early diagenesis is used in the sense that the sediment was buried at shallow depth such that it could still be affected by processes operating on the depositional surfaces. The indicators include: (1) the fine crystalline nature of

dolomite crystals; (2) the evidence for pre-existing evaporites; and (3) the preservation of original fabrics in the crinoid fragments.

The preservation of fine- to micrometer-sized dolomite crystals (0.05 to <0.01 mm) is indicative of early diagenetic dolomitization (Curtis, *et al.*; Friedman, 1980). Such dolomites are common in lithotypes MH5 to MH7 and E5 to E7 which were probably deposited in high tidal flat settings. Holocene dolomites in the modern carbonate environments commonly are of micrite sized (Deffeyes *et al.*; Hardie, 1977). They may have formed by penecontemporaneous replacement of aragonite in the supratidal zone. Examples of Holocene supratidal dolomites occurrence are, the Persian Gulf (Curtis *et al.*, 1963; Illing *et al.*, 1965); Bonaire in the Netherland Antilles (Deffeyes *et al.*, 1965); Andros Island in the Bahamas (Hardie, 1977); South Australia (von der Borch and Lock, 1979) and the Florida Keys (Shinn, 1968b).

Although the remnants of pre-existing evaporites are slight compared to the typical tidal flats of the Persian Gulf, the evidence of their presence unequivocally indicates a hypersaline condition. For dolomite formation in modern carbonate environments, hypersalinity of the evaporated waters is a prerequisite. Furthermore, the relics of the evaporite minerals may not represent the actual quantity of evaporites formed at the time of dolomitization. Gypsum might have formed during the dry seasons only to be flushed

out during the wet seasons. Such is true on the humid tidal flats of Andros Island (Shinn, 1983). Muir *et al.* (1980), in a study of the dolomite formation in the Proterozoic Yalco Formation, also suggested that the lack of evaporite minerals in an ancient dolomite sequence may have been a result of flushing by a reflux mechanisms. Similar suggestions were made by Lucia (1972).

The dolomitization of the crinoid fragments with retention of their structures further supports an early diagenetic timing for the dolomite formation since the preservation of original fabrics is generally good in early dolomitization. Land and Epstein (1970) and Sibley (1980) noted that when dolomite replaces a high-magnesium calcite grain, the grain's fabric and crystallographic orientation are retained. Grains originally formed of low-magnesium calcite or aragonite, however, are usually destroyed during dolomitization. If this is so, the high-magnesium crinoid fragments were probably dolomitized before being converted to low-magnesium calcite. Furthermore, there is no evidence of selective dolomitization nor dolomite growth at or near the stylolites, which is thought to be a late diagenetic feature (Wanless, 1979).

STAGES OF PERVASIVE, MATRIX DOLOMITIZATION

On the basis of the fabrics in the coarser dolomites, at least two phases of pervasive dolomitization are recognised. They are herein termed Phase I and II matrix

dolomitization.

The medium sized, dolomite crystals commonly have a cloudy centre (Plate 16C) encased by a relatively clear pheriphery. The inclusion rich centre probably formed early in the diagenetic replacement of a carbonate precursor. This phase of dolomitization probably occurred contemporaneous with the fine crystalline dolomite (MH6 and E6) that formed in the upper intertidal to supratidal zone. The cloudy centre is probably the Phase I dolomite, whereas the clearer rim is the Phase II syntaxial growth around the Phase I dolomite crystal.

These two phases of dolomitization are also exemplified by dolomite replacement of the crinoid fragments. The crinoid fragments were commonly replaced internally by small dolomite crystals (Plate 16D). This was followed by pseudomorphic replacement of the crinoid fragments with single dolomite crystals. The fine grained crystalline dolomites were probably formed by early replacement (Phase I) of the aragonitic lime mud infilling the axial canals of the crinoid fragments. The pseudomorphic replacement is considered to represent the Phase II volume for volume replacement of the high-magnesium calcite. Lucia (1962) suggested that the single crystal replacement reflects the difficulty for dolomite to nucleate in a solid calcite crystal.

The two stages of dolomite replacement probably resulted from varying fluid chemistry. The Phase I dolomite

represents rapid crystallization from a supersaturated, saline solution. Slower and probably more ordered growth forming clearer and coarser crystal structure are suggested for the Phase II dolomitization. This interpretation is in consistent with that of Folk and Land (1975). They concluded that rapid crystal growth rate favours the development of aphanitic and poorly ordered dolomite. Dolomite formed by slow, careful precipitation from dilute solution is characteristically limpid and has more perfect stoichiometry and ionic ordering (Folk and Land, 1975).

MECHANISM OF PHASE I MATRIX DOLOMITIZATION

The style of the Phase I dolomitization is related to the original depositional facies. As a consequence, it varies between different formations.

TURNER VALLEY FORMATION

In the Mount Greenock area, the abundant relic inclusions of anhydrite in the authigenic quartz crystals (Plate 16F) provide the most convincing evidence for the hypersaline conditions that existed during the deposition of the lagoonal deposits (Lithotype TV4). These inclusions appear as high birefringence laths arranging in a pattern that roughly follows the outline of the crystal (Plate 16F). This type of anhydrite arrangement suggests that the quartz crystals probably grew in an unconsolidated anhydritic sediments.

Farther east in the Talbot Lake area, there is no evidence of relic anhydrites; however, the presence of dedolomite may also indicate a hypersaline condition. Yanateva (1955; reviewed by Chilingar, 1965) suggested that calcium sulphate is an active agent of dedolomitization at low partial pressure of carbon dioxide. This dolomite-sulphate reaction was also cited by numerous workers (Shearman *et al.*, 1961; Evamy, 1963; Goldberg, 1967; Folkman, 1969). Thus, the dedolomite may be connected to the now vanished evaporites, and hence, suggests the hypersaline conditions.

The evidence of hypersalinity in a lagoonal environment suggests that the Phase I dolomitization may have been formed by seepage reflux as proposed by Adams and Rhodes (1960). In the Reflux Model, the hypersaline brines in a shallow lagoon are generated by evaporation, which eventually become dense enough to infiltrate the underlying sediments and move seaward (Adams and Rhodes, 1960).

Deffeyes *et al.* (1965) in their studies of the dolomitized carbonate sediments of Bonaire in the Netherland Antilles showed that evaporated waters having a high Mg/Ca ratio can be generated by evaporite precipitation. Furthermore, the increase in the CO_3^{2-}/Ca ratio in the solution during evaporite formation would be an additional aid for dolomitization (Morrow, 1982a)

It is suggested, therefore, that the initial phase of the dolomitization of the Turner Valley Formation was

probably formed by seepage reflux of the hypersaline brines generated by evaporation in a barred shallow shelf. The presence of marine fauna argues against penecontemporaneous precipitation. In the reflux model, the increase in the Mg/Ca ratio can at least overcome the kinetic constraints of nucleation (Land, 1983). The lack of knowledge regarding the dynamics of subsurface water movement (Morrow, 1982b) has rendered it difficult to evaluate the effectiveness of the reflux model in dolomitizing rocks of the Turner Valley Formation.

MOUNT HEAD FORMATION

The Mount Head Formation comprises two successive upward shallowing sequences, each represented by various depositional environments ranging from subtidal upward into supratidal setting. The hypersaline condition is indicated by the presence of chert-dolomite laminations and quartz nodules.

In the Mount Geenock area, the evenly laminated chert and dolomite (Plate 4F) in the lithotype MH3 of the lower shallowing-upward sequence resembles the pin-stripe laminations described in the Devonian Caballos chert by Folk (1973). Folk (1973) suggested that such laminations probably represent silicified varved evaporites and dolomites formed in a shallow water lake or lagoon, where water chemistry varies seasonally. Finely laminated dolomite-gypsum laminae interpreted as very shallow strandline lagoonal accumulation

were also described by Hardie and Eugsten (1973) in the Upper Miocene Solfifera Series of Sicily. Thus, the pin-stripe laminations provided evidence for the hypersaline conditions. The restricted occurrence (<1 m thick) of the laminated chert-dolomite unit indicates that the hypersalinity was probably of limited magnitude.

Also in the lower sequence, the spheroidal quartz nodules (Plate 6F) which occur in the uppermost bed of the cherty algal dolostone (MH5) in the Cinquefoil Mountain section are probably silicified evaporite nodules that formed in supratidal deposits. Morphologically, these nodules average 3-10 cm in diameter are formed of an outer shell of chalcedony lined with drusy euhedral quartz crystals. These silicicied quartz nodules are similar to those described by Chowns and Elkins (1974) and Milliken (1979) who concluded that the quartz nodules from the Mississippian dolostones in Tennesse and Kentuchy were pseudomorphs after early diagenetic anhydrite nodules formed in an arid tidal flat environment. Quartz nodules after evaporites were also noted by Geeslin and Chafetz (1982) in the Ordovician Aleman Formation in Southwestern New Mexico and by Siedlecka (1972) in the Upper Carboniferous dolostone of Bear Island in Svalbard.

The presence of evaporite nodules in the tidal flat setting argues for the presence of hypersaline conditions akin to those in the sabkha of the present day Persian Gulf (Illing, 1965). In the sabkha model, the kinetic constraints

upon dolomite formation are overcome by the high ratio of Mg/Ca, thus facilitating dolomitization of a calcium carbonate precursor (Morrow, 1982b; Land, 1983). The high ratio of Mg/Ca resulted from large scale removal of calcium and sulphate ions as gypsum, which is precipitated as nodules in the dolomitized carbonates (Kendall, 1984). The evaporite development in the dolostones of the Mount Head Formation appears slight compared to the typical sabkha model of the Persian Gulf (Shinn, 1983). This implies that the deposition of the Mount Head Formation probably occurred in a relatively milder climatic regime than that of the sabkha. Although it is not clear whether this model can operate on a regional scale (Morrow, 1982b; Land, 1983), the association of the evaporite nodules with the fine crystalline dolomite in the supratidal zone provides compelling evidence that the Phase I dolomitization was probably developed in a setting akin to the sabkha area of Persian Gulf.

ETHERINGTON FORMATION

The upper intertidal and supratidal deposits of the Etherington Formation possess several features indicative of hypersaline conditions, namely: (1) the very small dolomite crystals, (2) the presence of quartz pseudomorphs after evaporites, and (3) the presence of length-slow chalcedony.

The preservation of micrometer-sized dolomite crystals (<0.01 mm) in the formation compares favourably with the

supratidal dolomites found in modern carbonate environments (Curtis *et al.*, 1963; Deffeyes *et al.*, 1965; Illing *et al.*, 1965; Hardie, 1977). Holocene supratidal dolomites probably originated by the concentration of magnesium-enriched brines through evaporation. Furthermore, the distribution of the very finely crystalline dolostone is tied to the distribution of quartz and length-slow chalcedony. The latter two are both thought to reflect now vanished evaporites. The corroded detrital quartz grains in the basal units also suggest a high pH dolomitization fluids.

In the quartzitic dolostones (lithotype E7), evidence of pre-existing evaporite minerals includes quartz crystals showing cleavage planes, saw tooth, right angled grain boundaries, and quartz crystals that have a well defined rectangular outline. Such crystal fabrics suggest that they are probably quartz pseudomorphs after sulphates and/or halites.

The length-slow chalcedony probably formed after evaporites. Folk and Pittman (1971) noted that length-slow chalcedony is closely associated with rocks containing evaporites and forms most commonly when silica replaces sulphate.

The evidence for the pre-existing evaporites coupled with the interpreted supratidal depositional setting strongly suggest an early dolomitization in response to hypersalinity caused by evaporation. The kinetic constraints upon dolomite replacement of the calcium carbonate precursor

are overcome by the high Mg/Ca ratio (Morrow, 1982b; Land, 1983), which is achieved by massive removal of calcium ion as gypsum and anhydrite forms. The abundant evidence for the hypersaline conditions further suggests that the early supratidal dolomitization was an active process in the replacement of the calcium carbonate sediments of the Etherington Formation. Thus, the Phase I dolomitization of the rocks of the Etherington Formation probably occurred in a sabkha setting similar to that in the present day Persian Gulf.

RANGER CANYON FORMATION

Several characteristics suggest that hypersaline conditions existed while the supratidal sediments of the Ranger Canyon Formation were being deposited, namely: (1) the presence of fine grained dolomite in the chert, (2) the presence of rectangular pores which are probably leached anhydrites, (3) the presence of hollow and calcite rhombs and rhombohedral pores which probably represent dedolomite, (4) the presence of quartz nodules which are probably silicified evaporite nodules, (5) the chert breccia in the Snaring River section which probably formed by collapse due to evaporite solution. The close association of the anhydrite molds and dedolomite is probably related to the dolomite-calcium sulphate dedolomitization process similar to that described by Shearman *et al*. (1961), Evamy (1963), Goldberg (1967) and Folkman (1969). Thus, a Sabkha Model,

similar to that proposed for the Etherington Formation, is probably responsible for the early diagenetic dolomitization of the rocks in the Ranger Canyon Formation.

MECHANISM OF PHASE II MATRIX DOLOMITIZATION

Recent reviews by Morrow (1982b) and Land (1983) emphasized that the reflux and sabkha models can account for the initial formation of many evaporite-related dolomites, but are unlikely to be operational on a regional scale. Both models suffer from poor knowledge of the dynamics of the subsurface flow pattern. Zenger (1972) also cautioned that supratidal dolomitization has been applied to ancient dolomites where evidence of hypersaline brines is lacking.

Taking heed of these comments and in light of the feeble presence of the pre-existing evaporites, the proposed reflux and sabkha models for the Phase I dolomitization were probably of limited effectiveness in dolomitizing the thick sequence of carbonates. It probably acts as an incipient dolomitization process by forming micrite-sized dolomites. These early dolomites, however, became the nuclei for the Phase II dolomitization.

The clear dolomite crystals and the pseudomorphic replacement of unit calcite crystal of crinoid fragments are indicative of slow rates of dolomite growth. Folk and Land (1975) suggested that clear, euhedral, coarse dolomite forms in solutions of low salinity providing the Mg/Ca ratio is above unity. Dolomitization in a low salinity circumstance

was first studied by Hanshaw *et al.* (1971). Hanshaw *et al.* (1971) postulated that dolomite may be forming in zones of brackish water due to mixing of potable water and sea water or reflux brines. The model is based on the principle that the solubility curve of calcium carbonate is nonlinear, and hence, undersaturation and supersaturation can result when solutions of contrasting concentration are mixed (Runnells, 1969). The Dorag model (better known as meteoric mixing) first proposed by Badiozamani (1973) showed that a meteoric ground water and sea water (up to 30%) mixture can cause undersaturation with respect to calcite but saturation with respect to dolomite. Therefore, in the range of 5-30% sea water, dolomitization by replacement can occur in such a mixed solution. In the mixing model, dolomite formation requires a relatively low Mg/Ca ratio once nucleation starts.

The advantage of the mixing model is that it is independent of extensive evaporation and high Mg/Ca ratios; nevertheless, dolomitization of regional extent may result (Badiozamani, 1973). The model requires, however, a period of uplift and subaerial exposure in order that the mixed realm of fresh meteoric and marine ground water can move through the system (Badiozamani, 1973; Sibley, 1980). Except for the Etherington Formation which is overlain by an unconformity, there is no evidence for such an uplift during or after the sedimentation of the Turner Valley or Mount Head formations. As a matter of fact, the characteristics of

the dolostone in the Etherington Formation suggest that Phase I dolomitization was probably the active dolomite replacement process. Land (1983) also noted that most of the present day mixed waters dolomites occur as cement.

Morrow's (1978) proposal of mixing evaporative brines and normal marine water appears to be an interesting alternative. In this modified mixing model, Morrow (1978) suggested that dolomite replacement can result from mixing between brines and sea water providing the latter is 11.5 times less than the brine. A similar conclusion was drawn by Pierre *et al.* (1984) in the studies of dolomite formation in supratidal evaporite flats at the southernmost edge of the Ojo de Liebre evaporitic complex in Baja California, Mexico. Pierre *et al.* (1984) demonstrated that dolomite precipitation is governed by the mixing of Mg-rich, marine-derived brines and calcium bicarbonate continental waters, which are modified by capillary evaporation.

The upward shallowing sequences grading into the supratidal environment in the sea-marginal setting together with the evidence of hypersaline conditions attest favourably to the brine-sea water mixing model. This also suggests that dolomitization proceeded from the top of the shallowing-upward cycles downward under the influence of solutions formed at or near the sediment-water interface. Therefore, this implies that the dolomite replacement was early and occurred at shallow burial depth. The textural and compositional homogeneity of the Phase II dolomite also

suggests the presence of a large and homogenous reservoir of magnesium. In the mixing model, there is an ample supply of magnesium from sea water. Furthermore, it conforms with the inferred slower growth process for the formation of clearer dolomites and single crystal replacement of crinoid fragments.

Several other factors that do not alter the equilibrium relations are thought to have significance in overcoming the kinetic problems. Baker and Kastner (1981) suggested that the transformation of opal-CT to quartz favours the formation of dolomite due to the release of magnesium ion taken up by the opal-CT. The common association of chert with dolomite in the Mount Head and Etherington formation apparently conforms with Baker and Kastner's (1981) observation.

In the Snaring River section, the uppermost 3 m (lithotype MH9 and MH10) of the Mount Head Formation contains 1-3% pyrite crystals. Berner (1970) suggested that pyrite may have formed by sulphate-reducing bacteria attacking organic matter. Furthermore, Baker and Kastner (1981) noted that sulphate ion in solution is a very effective inhibitor of dolomitization and that sulphate reduction promotes dolomitization by production of alkalinity. Therefore, the pyrite crystals present in the Snaring River section probably were formed in response to sulphate removal by microbial reduction in organic rich sediments. The consumption of the sulphate ion in solution

may lower the kinetic constraints to initiate the dolomitization.

The dolomitization process may have been partly aided by the oxidation of organic materials. Gaines (1980) demonstrated that certain organic material as well as soluble animal proteins inhibit dolomitization. Removal of this rate inhibiting effect can occur in fresh-water mixing zones and in supratidal environments (Gaines 1980). Furthermore, algal processes were invoked by Gebelein (1973) as being able to cause dolomitization by preferentially concentrating magnesium in thin sheaths. This organic factor is particularly noteworthy in the algal and stromatolitic dolostone (MH5 and E5) as well as the dolomitized algal stromatolites in the Ranger Canyon chert.

Finally, it is imperative to note that many of these fabrics probably were modified by later diagenetic events. For example, Land (1983) noted that recrystallization of early formed dolomite phases is very common.

VII. SILICIFICATION - REPLACEMENT AND CEMENTATION

In this study, the process of silicification encompasses silica replacement and cementation. The former includes silica replacement of precursor carbonates and evaporites, while the latter covers filling of cavities and fractures by silica cement.

As a result of their resistance to weathering, the silicified elements form distinct features in the outcrops. In the Mississippian carbonates, bedded cherts composed of silicified ramose bryozoans, algal laminae and stromatolites form prominent ridges. Chert nodules also are common. The Permian Ranger Canyon Formation is primarily formed of thin bedded chert.

Besides these macroscopic features, petrographic studies revealed interesting chert fabrics and textures. In view of their widespread occurrences in the sequences and their intriquing fabrics and textures, it is necessary to examine the distribution, timing, silica source and mechanism of the silicification.

A. CHERT DISTRIBUTION IN MISSISSIPPIAN CARBONATES

The cherts in the Mississippian carbonates have the following features (Fig. 18):

1. an overall increase in chert content in the Mount Head and Etherington formations relative to the Turner Valley Formation;
2. the first appearance of silicified fossil fragments

coincides with the first completely dolomitized unit in the Turner Valley Formation (Fig. 18);

3. the occurrence of chert nodules begins at the base of the Mount Head Formation;
4. there is an obvious selective silicification of the bioclasts. This is particularly evident in lithotypes MH4, MH5, and E5, where the ramose bryozoan, algal laminae, and stromatolites were selectively silicified;
5. the silica replacement of the micritic matrix is most significant in the Etherington Formation.

From these observations, it appears that (1) there is a strong relationship between silicification and the occurrence of bioclasts (Fig. 18). This selective silicification of the fossils is probably due to the fossil fragments having a higher porosity than the surrounding matrix. This caused preferential penetration of silica-rich fluid into the skeletal materials.

(2) There is a distinct correlation between silicification and the completely dolomitized units (Fig. 18). This suggests that the two diagenetic processes may have been operative at the same time.

(3) Perhaps the most important feature is that matrix silicification is more intense in the Etherington Formation than in the Mount Head and Turner Valley formations. The close proximity of the Etherington Formation to the post-Mississippian disconformity certainly seems to suggest that the matrix silicification may be related to that

unconformity.

B. PETROGRAPHY OF CHERTS

Microscopically, four types of chert fabrics occur: (1) microcrystalline quartz, (2) length-fast chalcedony, (3) quartzine, and (4) megacrystalline quartz. This terminology is adapted from Milliken (1979). Although both replacement and void-filling cherts are present, the former is more common. The silica content is roughly correlatable with the lithotypes and formations (Fig. 18).

MICROCRYSTALLINE QUARTZ

The microcrystalline quartz is formed of equant, anhedral crystals (<0.01 mm in diameter) that commonly have undulose extinction. The quartz replacing bioclastic fragments is usually slightly coarser grained (>0.02 mm) than the matrix (Plate 17A). Microcrystalline quartz (<0.02 mm) also forms isopachous rims as void-lining (Plate 17B). In such a situation, it commonly grades into length-fast chalcedony and/or megacrystalline quartz.

The microcrystalline quartz is the major chert component in the replacement of the ramose bryozoans, algal laminae, stromatolites and in the nodules of the Upper Mississippian carbonates. The Permian Ranger Canyon chert also consists of predominately microcrystalline quartz. The best evidence attesting to the replacement origin of the chert nodules is the fact that laminations pass through the

nodules from the matrix dolostone with no apparent disruption (Plate 17D). Dolomite rhombs scattered in the chert also suggest the replacement nature of the chert (Plate 17C) which preferentially replaced the undolomitized portion of the sediment.

LENGTH-FAST CHALCEDONY

The chalcedony commonly forms very well arranged spherulitic structures of delicate length-fast fibres (<0.2 mm in length) normal to the cavity walls (Plate 17G). A single cavity may be lined by successive layers of length-fast chalcedony. The boundary between the layers is usually very sharp and is marked by a thin black line under crossed-nicols (Plate 17F). This thick development of length-fast chalcedony generally exhibits a colloform habit. Locally, the spherulitic structures may not develop; instead, a layer of fibres radiating normal to the host rock is formed (Plate 17E). Commonly, the chalcedony grades into megacrystalline quartz towards the centre of the cavity (Plates 17F and 17G).

The length-fast chalcedony occurs only as cavity-filling and most commonly lines fractures, fissures (Plate 17F), and cavities between intraclasts (Plate 17G). There is no relic inclusions associated with the fibres. The fact that the length-fast chalcedony did not replace skeletal fragments or carbonate matrix further supports that it is a cement.

QUARTZINE

Quartzine, or length-slow chalcedony as it is more commonly known, is the least common of the four types of chert. These length-slow fibres are usually coarser and the spherules less well organised than the length-fast variety.

The most spectacular arrangement of the quartzine occurs in some of the chert fragments in the chert pebble bed (lithotype E1). These chert fragments are formed of large aggregates of spherules having polygonal outlines (Plate 18A). Folk and Pittman (1971) and Milliken (1979) associated this type of texture with replacement of evaporite nodules. Therefore, these chert fragments may have been derived from quartz nodules (inferred evaporite nodules) similar to those present in the Mount Head Formation.

The quartzine also occurs as replacement chalcedony in the pisolitic structures in the Etherington Formation (lithotype E6). It also is formed of spherules, but the fibres are coarse and appear to be intermediate between the usual chalcedonic and quartz spherules (Plates 18B and 18C). Under plane light, the outer margin of the spherules is circumscribed by a zone of several very sharp, thin, parallel lines (Plate 18D). These lines commonly crenulated at 90°. On the basis of the right-angled trace and the length-slow characteristic, it appears that the spherules were probably pseudomorphs after cubic minerals such as halite or anhydrite. The spherules are commonly free of

inclusions whereas the surrounding megacrystalline quartz usually contains dolomite inclusions (Plate 18B). This implies that the length-slow chalcedony and the megacrystalline quartz replaced different precursor minerals.

MEGACRYSTALLINE QUARTZ

The most common type of megacrystalline quartz appears as a clear mosaic of equigranular quartz grains (0.05-0.4 mm in diameter). Extinction is generally uniform. The megacrystalline quartz commonly occurs as a post-chalcedony continuation of void filling and shows a gradual increase in crystal size towards the cavity centre (Plate 19A). Cavities formed by leaching of allochems were filled with coarse, clear crystals of quartz up to 0.5 mm in length. Where megacrystalline quartz replaced fossil fragments, it generally appears as flamboyant quartz (Plate 19B). The crystals show undulose extinction and have indistinct crystal boundaries.

Quartz with euhedral terminations is typically of replacement origin. Locally, the euhedral crystals grade into coarse anhedral quartz. Anhydrite or dolomite relics (Plates 16F and 19D) are common in the quartz, suggesting that the quartz is of replacement origin. Of particular interest are the anhydrite laths which are arranged parallel to the crystal faces (Plate 16F). This suggests that the growth of the quartz crystals was in unconsolidated

anhydritic sediments (Nissenbaum, 1967).

Megacrystalline quartz spherules occur in the stratigraphically lower quartzitic dolostone unit (lithotype E7). The quartz spherules are formed of radiating quartz crystals with euhedral terminations, while the central portions commonly consist of partly microflamboyant anhedral megacrystalline quartz (Plate 19C). Individual quartz crystals in the spherules usually display uniform extinction. The spherules are clear with only minor amounts of dolomite relics around their edges. In the Mississippian rocks of south-central Kentucky and Tennessee, megaquartz spherules occur in close association with quartzine spherules in the quartz nodules (previously evaporite nodules) (Milliken, 1979). It is not known, however, whether the spherules in the quartzitic dolostone are related to vanished evaporites as those described by Milliken (1979).

Quartz crystals having cubic crystal faces are present in the stratigraphically higher quartzitic dolostone unit (E7). The quartz crystals commonly contain minor amounts of very fine inclusions of indeterminate origin. Despite the zoning, the entire crystal shows unit extinction (Plate 19F). The outer zone commonly has relics of fine fibres radiating normal to the crystal faces (Plate 19F). These relic fibrous structures probably represent an initial centripetal growth of chalcedony replacing a precursor mineral, possibly halite or anhydrite. A later phase of silica emplacement replaced the cubic crystals

pseudomorphically. If this is the case, the zoning was caused by replacement process and does not represent the growth pattern of the original crystal.

Fibrous quartz was also growing on the cubic crystal faces. This grades outward into elongated megacrystalline quartz (Plates 19E and 19F). The fibrous and megacrystalline quartz also form zonations parallel to the cubic crystal faces. These zonations support the contention that the internal zonation resulted from replacement of the original material.

C. SOURCE OF SILICA

Siliceous sponge spicules are common in the cherts of the Mississippian Mount Head and Etherington formations and the Permian Ranger Canyon Formation. All the spicules appear to be simple monoaxons that have a readily discernible axial canal (Plate 20A). They are best preserved in the cherts, but are rarely found in the dolostones.

Siliceous sponge spicules have been considered the principal source of diagenetic silica since Mid-Paleozoic times (Wilson, 1966; McGugan *et al.*, 1968; Namy, 1974; Meyers, 1977; Milliken, 1979; Geeslin and Chafetz, 1982). The biogenic silica is thought to provide the main source of free silica because of its high solubility in sea water (Heath, 1974). Most of the spicules in the study material have an enlarged central canal rimed by microcrystalline quartz (Plate 20A). The enlargement of the central canal

provides evidence of silica solution of the spicules. Another feature suggesting silica mobilization is the dislocated central canal (Plate 20A). The decoupling of the canal from the rest of the spicule probably resulted from silica solution. The lack of identifiable occurrence of the sponge spicules in the dolostone is probably due to the destruction of the microfossils by silica solution. The biogenic silica probably provided most of the silica for the chertification in the Mississippian and Permian strata.

The detrital quartz in the Etherington Formation may have provided an additional source of indigenous silica. Most of the quartz grains have etched outlines due to the dolomitization in the surrounding carbonates. This source of silica, however, probably contributed little to the chertification of the sequence. The idea that the post-Mississippian disconformity may act as a feeder for silica rich fluid is also unlikely. Most of the quartz grains in the matrix of the overlying chert conglomerate sequence were cemented by quartz overgrowth and show no evidence of solution etching (Plate 20C).

The cause of such high productivity of siliceous sponges in the Late Mississippian and Late Permian times is unclear. The main area of siliceous oozes on the modern ocean floors corresponds to areas where ocean current upwellings cause nutrient-laden deep waters to rise into the warm photic zone (Calvert, 1974). Morger *et al*. (1972) noted that the Late Devonian/Early Mississippian time marked the

first evidence of eastward shedding of clastic materials from the west plate margin. This clastic influx may have provided the silica source for the growth of the siliceous sponges. Sheldon (1980) suggested that the major phosphogenic episode in the late Paleozoic was due to the trade-wind-belt upwelling related to glacial episodes. This upwelling of fertile waters may have caused the blooming of marine life as well as siliceous sponges in the Permian time. Furthermore, from the studies of phosphatic black shales facies in Pennsylvanian, Heckel (1977) proposed a model of vertical density stratification which explains the extension of phosphate deposits into an epeiric shallow sea.

D. TIMING OF SILICIFICATION

Like other diagenetic events, the exact timing of silica replacement of precursor carbonate sediment is difficult to define. Petrographic evidence does indicate, however, that the silicification occurred early in the diagenetic history of the sediment, probably before complete dolomitization. The early chertification in the Mississippian succession is also supported by the presence of chert clasts which were derived from the underlying strata.

RANGER CANYON FORMATION

Petrographic features present in the chert clearly indicate that pervasive silicification of the original

carbonate sediment took place before complete dolomitization of the carbonate. It also suggests that the silicification probably occurred after the early Phase I (incipient) dolomitization.

Most of the dolomite crystals scattered in the Ranger Canyon chert are euhedral and have sharp contacts with the surrounding chert. The dolomites are usually uniformly fine crystals and appear cloudy. There is no evidence of relic inclusions of silica in the dolomite crystals. Hollow rhombs, which probably resulted from dolomite leaching, still have their rhombic shape (Plate 20B). These features suggest that the silicification process was post-Phase I incipient dolomitization and selectively replaced the undolomitized portion of the parent sediment. Similar dolomite-silica textural relations were noted by Dietrich *et al.*, (1963) in the Cambrian-Ordovician Knox Group of Virginia. Dietrich *et al.* (1963) suggested that the entry of silica probably caught the dolomitization process "in the act". Scattered euhedral dolomite rhombs were also noted by Dunham and Olson (1980) in the chert stringers of the Ordovician-Silurian Hanson Creek Formation. Dunham and Olson (1980) suggested that selective silica replacement of the original calcium carbonate mud may have been related to the fact that dolomite is generally less soluble than calcite in most natural solutions.

The random orientation of the euhedral dolomite rhombs also suggests early replacement. Dietrich *et al.* (1963)

pointed out that it would be more likely for this type of scattered arrangement to form in the soft carbonate mud than in the coherent siliceous medium.

Commonly, there are also leached rectangular crystals (Plate 20D) which are closely associated with the dolomite crystals and/or dolomite molds. These hollow rectangles are probably leached cubic minerals, perhaps anhydrites formed early in the diagenetic history in a hypersaline condition. If so, the well preserved anhydrite crystal shape further attests to the contention that the pervasive silicification of the precursor calcium carbonate was post-Phase I dolomitization.

MISSISSIPPIAN CARBONATES

The preservation of euhedral dolomite rhombs in the microcrystalline quartz (Plate 17C), which replaced the bioclastic fragments, and matrix carbonate (nodules), indicates that silica replacement probably occurred after the early Phase I dolomitization. In contrast, dolomites outside the chert are usually subhedral to anhedral (Plate 17C). This texture is probably due to the Phase II pervasive dolomitization of the matrix carbonates.

The delicate fibrous structure of the brachiopod shells, preserved by chertification (Plate 17E), also indicates that silica replaced the original shell material prior to complete dolomitization. Similarly, the preservation of chertified bioclastic fragments including

sponge spicules (Plate 17A) in chert nodules suggests that those in the dolostone were probably destroyed by dolomitization.

Authigenic quartz replacement of anhydrite and dolomite (Plates 16F and 19D) probably represents quartz growth in an early stage. Steinitz (1977) suggested that the preservation of anhydrite laths in silica indicates an equilibrium between anhydrite and the surrounding solutions. Likewise, quartz pseudomorphs after cubic minerals probably occurred at an early stage.

Late silicification also occurred. Coarse dolomite cements having prominent rhombohedral cleavages were selectively chertified along the cleavage traces (Plate 20H). This fabric was also noted by Kuslansky and Friedman (1981) in the chertification of calcitic crinoid ossicles.

Some features present in the chert pebble bed (lithotype E1) provide additional evidence of early chertification. The chert clasts are mostly angular (Plate 8B) indicating that the clasts were chert before they were reworked from the underlying strata. The tabular shape of the chert clasts (Plates 8A and 8B) may imply that they were originally chertified algal laminae. Microfractures in the chert were filled with fine crystalline dolomite like that of the matrix (Plate 20F). This indicates that the cherts were lithified prior to resedimentation. Furthermore, one chert clast has a dislocated chalcedonic rim (Plate 20G). This suggests that the dislocation was probably caused by

redeposition after the clast was chertified. The chert cobbles and boulders in the condensed sequence overlying the post-Mississippian disconformity probably were chertified stromatolite heads or nodules derived from the underlying strata.

The silica cement precipitation was apparently not a single event, but occurred over a wide time span. The early phase of silica cementation was probably allochem mold filling (Plate 19A). Healing of microfractures and cementation of chert breccias (Ranger Canyon Formation in the Snaring River section) were probably the last phase of silica cementation.

E. MECHANISM OF SILICIFICATION

Much of the present knowledge on chert diagenesis has been gained from research on silicification of ocean sediments. The generally accepted stepwise maturation sequence is: opal-A (biogenic opal) to opal-CT (porcellanite/cristobalite) to chalcedony or quartz (chert) (Wise and Weaver, 1974; Kastner *et al.*, 1977; Kastner and Gieskes, 1983). The transformation of opal-A to opal-CT involves a solution-reprecipitation mechanism which causes the destruction of the microfossil tests. The opal-A corresponds to the biogenic silica released from sponge spicules in the study area. A solution-recrystallization process is also involved in the opal-CT to quartz transformation.

In ocean sediments, quartz and opal-CT are the principal silica phases. The intermediate metastable opal-CT phase commonly occurs in the form of lepispheres, a spherical microcrystalline aggregate (Wise and Kelts, 1972; Kastner *et al.*, 1977). Meyers (1977) noted the presence of microspherules (0.025-0.04 mm in diameter) in the cherts of the Mississippian Lake Valley Formation. These structures are probably ancient counterparts of cristobalite lepispheres of the Tertiary deep sea chalks (Meyers, 1977).

Unfortunately, no such microspherules were found in the cherts of the study area. The absence of opal-CT is not sufficient proof for the direct replacement of the carbonates by quartz since the transformation process may not have preserved the opal-CT precursor. Land (1979) noted that the chert in the down-faulted part of the slope in the north coast of central Jamaica consists of opal-CT, whereas the subaerial exposed nodules are composed of quartz. Specifically, Land (1979) stated that although it appears convincing that an opal-CT precursor existed before transformation to quartz, it is not an unequivocal justification. Furthermore, Kastner *et al.* (1977) noted that in Mesozoic clayey sediments, opal-CT predominates, while in carbonate sediments, quartz is most common. Experimental studies showed that the transformation rate is much higher in carbonate because of the alkalinity formed by the dissolution of carbonate; this favours the formation of magnesium hydroxide which is an important component in the

precipitation of opal-CT (Kastner *et al.*, 1977).

The spicule dissolution evidently shows that the transformation of biogenic silica (opal-A) to crystalline silica (opal-CT or quartz) was a dissolution-reprecipitation process. The different in the equilibrium solubility between the various forms of silica is probably the major driving mechanism for chertification (Meyers, 1977). At 25° C, opal-A has an equilibrium solubility of 100-140 ppm (Jones and Segnit, 1971), opal-CT is 40-70 ppm (Knauth, 1979), and quartz is about 6 ppm (Morey *et al.*, 1964). This means that the highly soluble opal-A will continue to dissolve until the silica concentrations reach 40-70 ppm. As the pore waters become supersaturated with respect to opal-CT, opal-CT begins to precipitate.

It has already been shown that most of the cherts are of replacive origin and formed during early diagenesis prior to complete dolomitization. This implies that the pore waters were simultaneously undersaturated with respect to calcite and supersaturated with respect to opal-CT or quartz. Runnells (1969) demonstrated that mixing of supersaturated waters may result in undersaturation. This principal was invoked by Badiozamani (1973) to show that undersaturation of solutions with respect to calcite and simultaneous supersaturation with dolomite can be accomplished through mixing of fresh water with 5 to 30% sea water. Recent studies of Phanerozoic nodular cherts using stable isotope analyses showed a major meteoric water

component in their formation (Knauth and Epstein, 1976; Kolodney *et al.*, 1980). Thermodynamically, Knauth (1979) indicated that the mixed meteoric-marine ground waters can be simultaneously supersaturated with respect to quartz and opal-CT and undersaturated with respect to calcite. This model explains the meteoric component present in the nodular chert. Knauth (1979) postulated that the silica is collected by the meteoric waters as it moves through the sediment pile and is concentrated in the mixing zone.

This mixed-waters model is particularly attractive in explaining the silicification of the study area. The inferred tidal flat setting together with the numerous seaward prograding sequences (shallowing-upward) would have provided ample opportunity for the recharge of meteoric water. Furthermore, the relative drop in sea level during Late Mississippian and Late Permian times may have provided vast areas for the recharge. Silicification at or near erosion surface has long been recognized by geologists (Leith, 1925; Krumbein, 1942). Chafetz (1972) also noted that the replacement of carbonate by silica appears to be related to weathered bedding plane surfaces. It is thought, however, that the majority of the silicification occurred before subaerial exposure as shown by the chert clasts in the chert pebble bed. The only indication for unconformity related silicification is from the more intense matrix silicification in the Etherington Formation which lies directly underneath the post-Mississippian disconformity.

Knauth's (1979) model also provides an explanation for silica cementation. Knauth (1979) suggested that if the system is open with respect to carbon dioxide, the waters in the mixing zone would not necessarily be undersaturated with respect to calcite. Thus, silica cementation might occur.

In addition to mixed-waters diagenetic environments, it appears that the nature of sediments is equally important. Selective silicification of the bioclastic components apparently is controlled by their porous texture. Preferential replacement of fossils by silica has been noted by Siedlecka (1972), Jacka (1974), Hatfield (1975), Geeslin and Chafetz (1982). Jacka (1974) suggested that selective silicification of skeletal components was probably due to organic decomposition which creates a micro-environment conducive to silica replacement. Magnesium is an important agent in the transformation of opal-A to opal-CT (Baker and Kastner, 1981). Thus, the preferential concentration of magnesium by algae (Gebelein, 1973) may have aided in the silica diagenesis.

Silica replacement of evaporites probably follows a similar solution (evaporites) and precipitation (quartz) pattern. The preservation of anhydrite relics in the megacrystalline quartz indicates that the silicification occurred when the anhydrite was in equilibrium with the surrounding solutions (Steinitz, 1977). Steinitz (1977) further suggested that the diagenetic replacement probably occurred in a normal marine to hypersaline condition. This

interpretation agreed with data from oxygen isotopes and boron α-track mapping (Kolodney *et al.*, 1980). Therefore, the anhydrite inclusions in the megacrystalline quartz probably indicates early silicification from unconsolidated anhydritic carbonates.

The various forms of chert fabrics are dependent on kinetic factors such as nucleation and the rate of precipitation of crystalline silica (Folk and Pittman, 1971). Folk and Pittman (1971) suggested that the formation of microcrystalline quartz corresponds to the gradual decrease in silica concentration and the rate of precipitation. The formation of length-slow chalcedony was proposed by Folk and Pittman (1971) to indicate a high pH or a sulphate-polluted (evaporitic) diagenetic environment. More recent studies (Kastner, 1980; Keene, 1983) suggest that both sulphate and magnesium are essential for the formation of length-slow chalcedony. The sequence of chert types in the study area agree with that cited by Folk and Pittman (1971). It generally follows the order, from oldest to youngest: (1) microcrystalline quartz, (2) chalcedonic quartz, and (3) megacrystalline quartz.

VIII. CARBONATE CEMENTATION

A. INTRODUCTION

Cementation generally accounts for the greatest porosity loss from porous sediment. Such voids are filled by chemically precipitated authigenic minerals on an intergranular or intragranular free surface (Bathurst, 1975).

In the partially dolomitized limestones of the Turner Valley Formation (lithotype TV1 and TV2), most of the primary porosity was obliterated by syntaxial overgrowths around the echinoderm fragments and by sparry calcite cement (Plate 21A). They are both clear and nonferroan. Following the studies by Evamy and Shearman (1964), Meyers (1974) and Longman (1980), the syntaxial and calcite spar cements probably represent an early phase of cementation in the fresh water phreatic zone.

It is the cementation in the secondary pores that is of particular interest because of the intriguing variability of dolomite, calcite and more rarely, quartz cements (Fig. 19). Secondary porosity includes allochem molds, open fractures, and bird's-eye structures. On the basis of crystal morphology, clarity and iron content, there are five distinct types of cement, namely: (1) clear, nonferroan dolomite, (2) ferroan dolomite, (3) coarse dolomite spar, (4) microstalactitic calcite and (5) coarse calcite spar. The distribution of these cements (Fig. 19) shows no

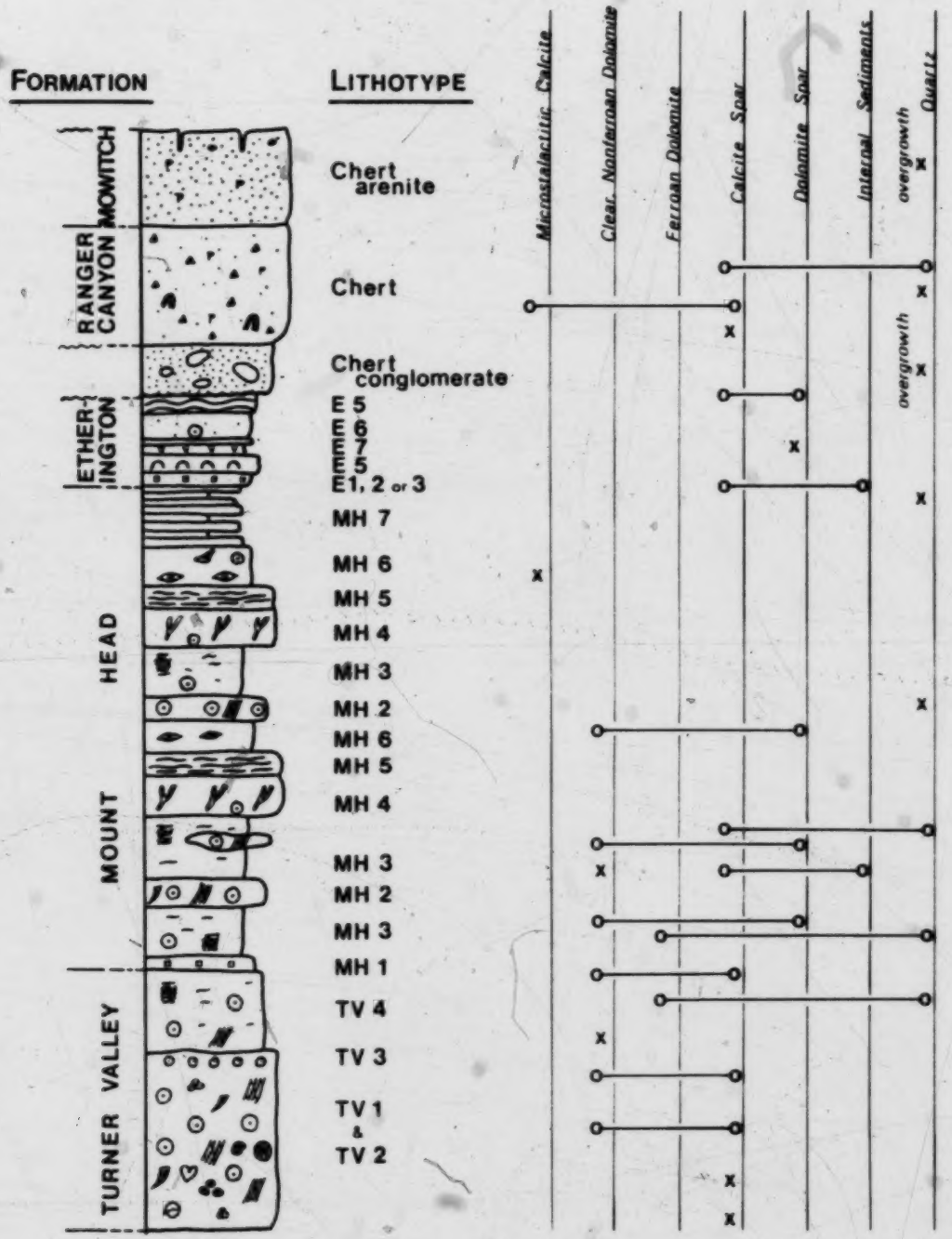

Figure 19. Composite diagram showing the major occurrences of cements. 'x' indicates that only one type of cement occurs in the cavity. 'o—o' indicates that the two indicated cement types (o) occur in the same cavity.

apparent order or pattern and probably records a complex diagenetic history.

B. LEACHING

In addition to the fracture porosity and bird's-eye vugs, most of the secondary porosity was created by preferential dissolution of the allochems. The allochem precursors were probably formed of the less stable aragonite or high magnesium calcite. The euhedral texture of the matrix dolomite lining the unfilled voids (Plate 21B) suggests that the replacement dolomite probably grew on a free surface. This means that the selective leaching occurred before the completion of the matrix dolomitization (Phase I and II dolomitization).

The environmental factors favouring solution of calcium carbonate are high partial pressure of carbon dioxide and low pH. Also, the amount of calcium carbonate removed is directly determined by the rate of fluid flow (Bathurst, 1975). This is because carbonate removal by leaching or addition by precipitaton depends on the degree of saturation of the pore fluids with respect to the minerals comprising the allochems. Land (1983) noted that a dolomitizing solution can either cause net cementation or net solution, depending on the total dissolved carbonate content of the solution as it moves though the rocks.

The diagenetic regimes, which are conducive of leaching of skeletal fragments, are the shallow phreatic zone

(Longman, 1980) and the mixing zone where marine pore fluids are diluted by meteoric waters (Buchbinder and Friedman, 1980). Thus, it would appear that the leaching of the allochems in the Mississippian carbonates probably occurred in these regimes.

C. PETROGRAPHY OF CARBONATE CEMENTS

CLEAR, NONFERROAN DOLOMITE

The euhedral, nonferroan dolomite typically developed as the first phase of cement lining the allochem molds and bird's-eye vugs. The dolomite crystals commonly formed a single layered rind and rarely filled up all the available space of the voids. It is absent in the cavities in the Permian Ranger Canyon chert where the groundmass is microcrystalline quartz.

The euhedral dolomite rhombs, 0.05-0.1 mm in size, are of two types. The commonest type is formed of water-clear crystals which have minor concentrations of inclusions in the crystal cores (Plate 21C). This is similar to limpid dolomite as described by Folk and Land (1975). The second type of dolomite is also euhedral, but the crystal are usually more cloudy and some are zoned (Plate 21D).

There are several features suggesting that the crystals were formed by direct precipitation and not by replacement of a calcite precursor: (1) the dolomite crystals have planar crystal faces, (2) the crystals line cavity walls,

(3) the intercrystalline boundaries between adjacent rhombs are planar, (4) the absence of undulose extinction, and (5) the presence of crystal zonation. These features suggest that the nonferroan dolomite is formed by cement growth, since replacive growth would give a homogeneous, xenotopic crystalline fabric.

FERROAN DOLOMITE

The ferroan dolomite is the only ferrous iron bearing carbonate component present in the rocks of the sequence. It is rare and occurs only in the skeletal medium crystalline dolostone (lithotype MH3) near the base of the Mississippian Mount Head Formation (Fig. 19)

The dolomite crystals have planar crystal faces and have a mean crystal size of up to 0.5 mm. It shows a marked uniform extinction under crossed-nicols. Where present, the ferroan dolomite commonly occurs as one or a few coarse crystals that occupy a major portion of the cavities (Plates 21E and 21F)

Another interesting feature of the ferroan dolomites is their close association with silica. Commonly, the cavities were lined with a rim of coarse microcrystalline quartz before the growth of the ferroan dolomite. In one situation, the remaining space was filled with coarse euhedral quartz crystals (Plate 21F).

Partial solution along cleavage planes is common. Furthermore, the ferroan dolomite was also replaced by

dolomite that grew out from the matrix (Plates 21E and 21F). Thus, the ferroan dolomite appears to be a rather unstable variety.

COARSE DOLOMITE SPAR

The dolomite spar is coarse, cloudy and nonferoan. It is a late phase cement which succeeded the cavity lining, clear, nonferroan dolomite and occluded all the available space in the cavities.

It commonly occurs as a single crystal measuring up to 1 mm in length (Plate 22A) and displays uniform extinction. When the cavities were filled by several crystals, the dolomite spars have an average diameter of 0.2 mm and exhibit planar, intercrystalline boundary (Plate 22C). The latter type is commonly found filling of bird's-eye vugs and healing of microfractures (Plate 22B).

MICROSTALACTITIC CALCITE

The microstalactitic calcite cement is present in only two samples. One of them is in the cavities of the Permian Ranger Canyon chert, while the other is in the bird's-eye vugs in the Mississippian Mount Head Formation. In both cases, it displays an asymmetrical growth, hanging from the roof of the cavities and terminating in a bulbous shape.

In the Ranger Canyon chert, the microstalactitic calcite rooted on the mosaic quartz exhibits a remarkable concentric laminations being formed of alternating dark,

thin (0.01 mm) laminae and clear, thicker (0.05 mm) calcite laminae (Plates 22E and 22F). The dark coloration of the thin bands is pobably due to the presence of high iron and/or organic inclusions. The maximum length of the long axis of the microstalactites is about 0.15 mm. It is of particular interest to note that almost all of the laminae are fairly continuous and follow the contour of the cavities. Each of the bulbous terminations correspond to a proturberance on the cavity roof (Plate 22E).

These pendulous calcite cements also display an internal radiating pattern which strongly suggests that they were at one time formed of radiating crystals. They show a sweeping radial extinction under crossed-nicols (Plate 22G).

The microstalactitic cements in the bird's-eye vugs are rooted on matrix dolomite crystals as well as dolomite cements (Plate 22D) which were partially silicified. Partial leaching of the microstalactitic cements seems to follow the radial and concentric structures of the grains. It is believed, therefore, that the partial solution was a selective process which attacked the relatively unstable inclusions.

COARSE CALCITE SPAR

The coarse calcite spar is a late phase cement which commonly fills all or most of the available space that remained after the precipitation of other types of cement. Commonly, in the Mississippian dolostone, the coarse calcite

spar succeeded the clear, euhedral, nonferroan dolomite (Plates 21C and 21D) and the cavity is filled with a single, clear calcite crystal. In places, the cavity may be filled with several crystals having sharp intercrystalline boundaries. Microfractures filled by coarse sparry calcite are also common (Plates 23A and 23B).

There are also other minor occurrences of the sparry calcite. In one case, the calcite spar cement is rooted on the coarse microcrystalline quartz crystals which line the cavity wall (Plate 23D). The outer crystal surface appears to be rounded and bounded by a thin (0.01 mm), dark calcite laminae. In another situation, the calcite crystals were partially dissolved thereby producing a pitted crystal surface. These irregularities were later filled by two phases of internal sediments (Plate 23E).

In the Ranger Canyon chert, the microstalactitic calcite is succeeded by coarse, sparry calcite which occluded all available space in the cavities (Plate 22E). Commonly, the coarse calcite spar enclosed poikilitically the detrital quartz grains, sponge spicules, and phosphate fragments (Plate 23C).

D. MECHANISM OF CARBONATE CEMENTATION

The five different types of cements having variable composition, morphology and texture apparently reflect the changes in the pore water chemistry with respect to the different diagenetic regimes. These diagenetic signatures

should provide, therefore, important data for resolving the series of events which the sediments underwent following the pervasive dolomitization of the original carbonates. Unfortunately, there is not a single cavity that contains all the five types of cement. This poses a severe limitation in understanding the paragenetic sequence of the cementation.

The characteristics of the clear, euhedal, nonferroan dolomite resemble those of the limpid dolomite described by Folk and Siedlecka (1974), Kaldi and Gidman (1982), and Jones *et al*. (1984). Therefore, their presence in the cavities of the Mississippian dolostone probably indicate a mixed marine and fresh water regime as invoked by the above authors to account for the formation of the limpid dolomites in other carbonate sequences. Folk and Land (1975) noted that the physical perfection and chemical stability of the limpid dolomites probably resulted from a more perfect stoichiometry and better ionic ordering. From a thermodynamic standpoint, Badiozamani (1973) showed that in the range of 5-30% sea water, the mixed meteoric-marine solution can cause dolomite formation. Also, Folk and Land (1975) showed that the lowering of salinity favours dolomitization because of the associated lowering of the ionic strength. Thus, the ability of the mixed solution to cause dolomite formation must be related to the ionic dilution produced by the mixing effect (Land, 1983). The lower salinity and Mg/Ca ratio of the solution in the mixing

zone can therefore result in slow rate of dolomite crystallization which, in turn, allows the formation of perfect crystals.

It is suggested, therefore, that the clear, euhedral, nonferroan dolomites were formed in the mixing zone of marine and meteoric fresh water. The interpreted shallowing-upward sequences in the Mississippian carbonates also favour the mixing model since additional areas may be available for recharge of meteoric water in a seaward prograding tidal flat. In such a setting, the clear, euhedral dolomites may be formed by further dilution of the sea water after the pervasive dolomitization. Furthermore, the dolomite precipitation in the cavities may be related to land emergence during Late Mississippian time. The absence of dolomite cement in the Permian Ranger Canyon chert is probably due to the low carbonate and magnesium ion concentrations in the associated hydrogeologic regime.

The ferroan dolomites probably formed due to the presence of ferrous ion in the crystal lattice. In general, the amount of ferrous ion required to generate response to the artificial staining by potassium ferricyanide is in the order of 100 ppm (Evamy, 1969). Iron content in sea water and aerated surface water are virtually all in the ferric iron state because of the chemical instability of the ferrous ion in an oxidizing environment. Furthermore, Evamy (1969) noted that once incorporated in a calcite lattice, ferrous ion can normally survive subsequent passages through

oxidizing media. Therefore, the presence of the ferroan dolomite provides a good indicator of a reducing condition.

Choquette (1971) suggested that ferroan dolomite is precipitated from heated water using carbonate and cations derived from the host rock. In the studied sequence, there is no evidence, such as sulphide mineralization, to indicate that such a hydrothermal diagenetic environment was present. Meyers (1974) and Richter and Fuchtbauer (1978) suggested that in shallow groundwater, the ferrous/calcium ratio level is generally high enough to form the ferroan zone in calcite crystals. In the studies of the Mississippian Lake Valley Formation in Sacramento Mountain of New Mexico, Meyers (1974) suggested that the reducing condition required for the ferrous ion inclusion into the calcite lattice can be accomplished by having a deeper flow path. In this connection, the ferroan dolomite in the study area may have been precipitated in the deeper part of the mixing zone where a reducing diagenetic environment prevailed. The deep mixing zone was probably developed in association with the sea level drop during the Late Mississippian time.

The instability of the ferroan dolomite as shown by the partial solution and replacement by overgrowth of matrix dolomites is probably due to the ferrous iron concentration in the dolomites crystal lattice. Frank (1981) suggested that the relative concentration of iron in the dolomite crystal lattice directly affects the susceptibility of dolomite crystal to dedolomitization. This effect is

particularly enhanced in an oxidizing environment (Al-Hashimi and Hemingway, 1973).

The coase texture and stable nature of the coarse dolomite spar probably reflect a slow rate of crystallization and stable uniform conditions during its precipitation. A type of coarse dolomite termed saddle dolomite was suggested by Radke and Mathis (1980) to have formed in association with sulphate reduction at elevated temperature. There is, however, no petrographic evidence, such as undulose extinction and curved crystal faces, to suggest that the coarse dolomite spar is a saddle dolomite. Furthermore, there is no indication of sulphide mineralization which is commonly associated with the saddle dolomite.

On the basis of their coarse texture and uniform composition, it is suggested that the coarse dolomite spar cements were formed during burial diagenesis. The healing of microfractures with coarse dolomite spar also supports this contention. Mattes and Mountjoy (1980) and Kaldi and Gidman (1982) also reported dolomite spar formed by late burial diagenesis. Zenger (1983) argued that the increased temperature, the greater stability and the less stringent time limitation in the deep burial environment can cause dolomitization despite the lower flow rate and lower magnesium ion concentration.

The crystal morphology of the microstalactitic cements suggests that they formed in cavities that were not

completely filled with water and probably represent precipitation in a vadose diagenetic environment. The vadose water in such pore spaces tends to settle at grain contacts or hangs from the bases of grains; cement precipitation is induced by subsequent loss of carbon dioxide (Dunham, 1971; Muller, 1971).

Vadose cement fabrics were studied primarily in subaerial exposed rocks - beach rock or eolian dune sand (Muller, 1971; Dunham, 1971; Ward, 1975). The vadose conditions required for their formation were also demonstrated in the experimental studies (Badiozamani *et al.*, 1977). Therefore, the presence of the microstalactitic cement in the bird's-eye vugs in the Mississippian carbonates and the cavities in the Permian chert provide excellent evidence for a vadose diagenetic regime. This observation is compatible with the suggested higher tidal flat depositional environment for both units. The microstalactitic cements probably formed early in the diagenetic history prior to burial.

The fresh water phreatic environment is generally perceived as the conditions for precipitation of coarse, sparry calcite. (Folk, 1974; Folk and Land, 1975; Kaldi and Gidman, 1982; Jones *et al.*, 1984). Its clarity and coarse texture are the result of slow precipitation in cavities that are completely water-filled (Folk and land, 1975). Therefore, the succession of the clear, euhedral dolomite by the coarse, sparry calcite represents the change from the

mixed water diagenetic environment to the fresh water phreatic realm. This situation probably corresponds with the expansion of groundwater lens in response to the Late Mississippian relative sea level drop.

In the Permian Ranger Canyon chert where the microstalactitic calcite is succeeded by the coarse, sparry, poikilotopic calcite crystals reflects the change from the vadose diagenetic environment to the fresh water phreatic realm. This is probably conformed to the slight sea level rise during the deposition of Ranger Canyon chert (carbonates).

As discussed previously, there are also other minor occurrences of sparry calcite that show no particular pattern. Thus, the calcite spar probably has a very wide time span that ranges from early to late stage diagenetic history.

IX. DEDOLOMITIZATION AND OTHER DIAGENETIC PROCESSES

In addition to dolomitization, silicification and carbonate cementation, the rocks experienced further diagenetic modifications which were generally less extensive. These diagenetic signatures, however, provide supplementary information for assessing the diagenetic history which the rocks underwent.

A. DEDOLOMITIZATION

Dedolomite is a secondary calcite formed by the replacement of dolomite by calcite. Dedolomitization is a diagenetic process related to physico-chemical changes in the pore water system (Katz, 1971). Thus, demonstration of its presence should provide a valuable information about the diagenetic environments. Furthermore, dedolomitization can convert a low porosity rock into a porous state (Evamy, 1967; Al-Hashimi and Hemingway, 1973).

PETROLOGY OF DEDOLOMITE

In the Mississippian sequence, the occurrence of dedolomite is particularly common and distinctive near the top of the Turner Valley Formation and in the lower half of the Mount Head Formation (Fig. 20). It occurs more widely throughout the Permian Ranger Canyon Formation, especially in the Snaring River section.

Several distinct petrographic textures of dedolomite were illustrated by Shearman *et al.* (1961), Evamy (1967) and

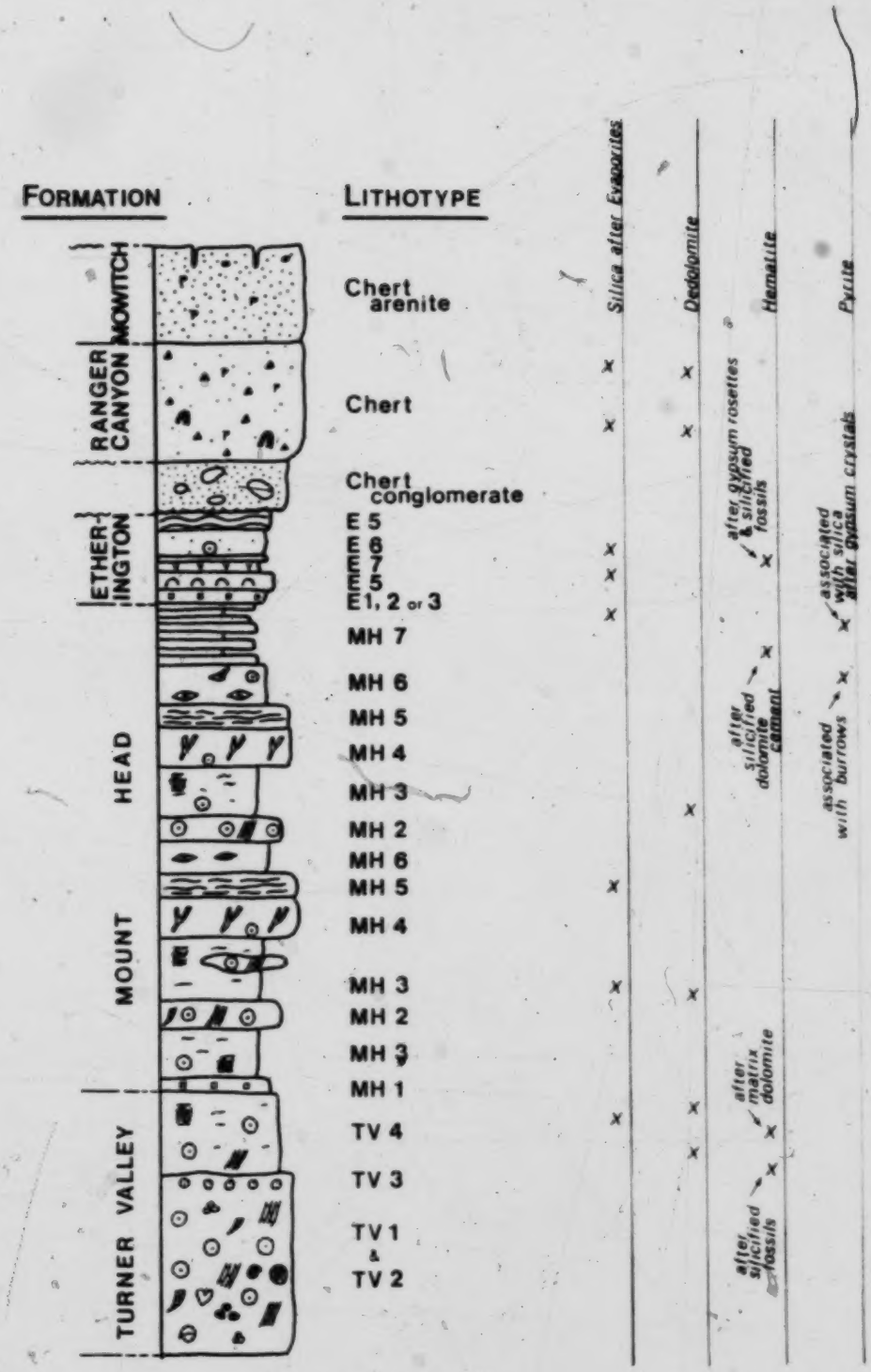

Figure 20. Composite diagram showing the occurrences of silica after evaporites, dedolomite, hematite and pyrite. Also note the close relationship of silica, dedolomite and hematite.

Katz (1971). Dedolomite can be recognized by: (1) the presence of relics of incompletely replaced dolomite crystals (Plates 24A and 24B), (2) the presence of polycrystalline calcite mosaic pseudomorphs after dolomite (Plate 24C), (3) the presence of coarse calcite crystals poikilitically enclosing rounded and corroded relics of dolomite crystals (Plate 24D), (4) the presence of rhombohedral pores (Plate 24E), and (5) the presence of calcite zones in dolomite crystals (Plate 24F).

MECHANISM OF DEDOLOMITIZATION

Although the exact mechanism of dedolomitization is not known, through field relationships, petrographic studies and experimental works, three hypothesis have been proposed for this phenomenon:

1. Dedolomitization is a surface phenomenon related to weathering surfaces (Golberg, 1967; Folkman, 1969; Chafetz, 1972; Al-Hashimi and Hemingway, 1973). Laboratory experiments performed by de Groot (1967) suggested that dedolomitization is promoted by waters having a high Ca/Mg ratio, a temperature below 50°C and a very low partial pressure of carbon dioxide. Such conditions are a characteristic of near-surface meteoric waters.
2. Dedolomitization is a process based on dolomite-calcium sulphate reaction (Shearman *et al.*, 1961; Evamy, 1963; Goldberg, 1967; Folkman, 1969). Yanateva (1955, reviewed

by Chilingar, 1956) demonstrated that calcium sulphate is an active agent of dedolomitization only at low partial pressure of carbon dioxide. Based on field observations and petrographic studies, Evamy (1963) proposed that the required sulphate can be generated by oxidation of pyrite in a calcareous medium.

3. Dedolomitization is a diagenetic process related to physico-chemical changes in the interstitial water system as well as the original composition of dolomite (Katz, 1968, 1971; Al-Hashimi and Hemingway, 1973; Frank, 1981). Katz (1968, 1971) noted that dedolomitization occurs preferentially in calcian dolomite when the chemical system crosses the dolomite stability field. Katz (1971), Al-Hashimi and Hemingway (1973) and Frank (1981) also concluded that dedolomitization of ferroan dolomite is caused by their metastability in the surface or oxidizing environment. This results in the alteration of the iron-rich dolomite to magnesian calcite and iron oxide.

In the study area it appears that most of the strata containing dedolomite is associated with or closely related to evaporitic strata (Fig. 20). The dedolomite-bearing beds in the Upper Turner Valley Formation at the Talbot Lake section is stratigraphically equivalent to strata containing quartz pseudomorphs after anhydrite in the Mount Greenock section. Similarly, the dedolomite-bearing unit in the lower part of the Mount Head Formation of the Mount Greenock

section is directly overlain by a chertified, pin-striped evaporite-dolomite unit. In the Permian Ranger Canyon Formation, the dedolomite is intimately associated with the anhydrite molds.

There is no direct evidence to indicate that the dedolomites in the Mississippian sequence are related to the subaerial exposure at the Late Mississippian time. This is deduced from the fact that dedolomites are not recognised in the Etherington Formation or in the upper half of the Mount Head Formation. It is, however, difficult to assess the effect of the Late Permian relative sea level drop on the dedolomitization in the Ranger Canyon Formation.

To a certain extent the dedolomitization was apparently connected to the composition of the dolomite. The calcite zones in the dolomite crystals may be attributed to the preferential dedolomitization of the originally calcian dolomite. Also, the rhombic hematite may be a product of the dedolomitization of ferroan dolomite.

In summary, it seems that the dedolomitization was related to a dolomite-calcium sulphate reaction. Since most of the evaporites were either leached out or replaced by silica, the calcium sulphate thus released may provide the required source of calcium sulphate. It appears that the original composition of the dolomite also plays an important role in controlling the formation of dedolomite. Furthermore, since some of the dedolomites replaced the dolomite cements, the process was probably a late diagenetic

event. If a low partial pressure of carbon dioxide is required to promote the activity of the calcium sulphate (Yanateva, 1955 - reviewed by Chilingar, 1956), is valid, it would imply that the dedolomitization probably occurred in a near-surface meteoric diagenetic environment. This contention is corroborated by the close association of the dedolomite and the coarse, sparry calcite.

B. HEMATITE REPLACEMENT ("HEMATITIZATION")

Hematite is the most common iron oxide present in the sequence. Its translucent, red colour is distinctive in thin section. Commonly, the hematite and the other varieties of iron oxides were disseminated in the dolomite matrix as fine dust. Although minor, hematite replaced dolomite, silica, and gypsum (Fig. 20).

Rhombohedral hematite pseudomorphs after matrix dolomite (Plate 25A) is a rare form of replacement. Al-Hashimi and Hemingway (1973) suggested that dedolomitization of ferroan dolomite produces iron oxide in a surface environment. The susceptibility of ferroan dolomite to dedolomitization is directly related to the relative concentration of iron in the dolomite lattice (Frank, 1981). Therefore, the hematite rhombs may reflect the presence of the originally metastable ferroan dolomite.

The hematite replacing silicified fossils commonly has a hexagonal crystal form (Plate 25C). The "hematitization" of the silicified dolomite cements shows preferential

replacement along the cleavage planes (Plate 25B). Another spectacular form of hematite is the radiating clusters of bladed crystals (Plate 25D). The crystal morphology clearly indicates that they are hematite pseudomorphs after stellate array of gypsum crystals.

The actual mechanism which causes the hematite replacement is not clear, but it apparently follows a solution-reprecipitation process. The very fact that the hematite replaced the diagenetic dolomite, silica, and gypsum suggest that the "hematitization" was a relatively late diagenetic event.

C. PYRITE FORMATION

Pyrite crystals are particularly common in the upper 2 m of the Mount Head Formation of the Snaring River section (Fig. 20). They are typically brassy yellow in colour and cubic or granular in habit. These pyrite crystals are closely associated with burrows (Plate 25E) or quartz crystals (Plate 7E). In addition to forming anhedral aggregates (Plate 25F), the quartz crystals also displays crystal forms of pinacoid and diametral prism (Plate 25G). These crystal shapes suggest that they were originally gypsum and were replaced by silica pseudomorphically.

The association of authigenic pyrite with burrows is an indicator of an anaerobic environment. Experimental studies by Berner (1970) indicated that bacterial sulphate reduction is the first major step in the process of sedimentary pyrite

formation. Furthermore, Berner (1970) concluded that organic matter is needed as an energy source for the sulphate reducing bacteria. Apparently, the burrows must have a higher organic content than the surrounding matrix. If so, the pyrite was probably an early diagenetic product.

The coarse, euhedral texture of the gypsum crystals (now quartz) suggests a slow growth rate in the sediment. The sulphate source is probably the same as that consumed by the sulphate reduction. Berner (1970) suggested a continuous diffusion of sulphate into the sediments from the overlying sea water. A similar pyrite-gypsum association was found in the silty clays recovered from the South West African continental slope. In this case, Seisser and Rogers (1976) suggested that the calcium was derived from the dissolution of the carbonate sediments. In the present study, it is thought that the calcium ions were probably released from the sediments during dolomitization. Thus, the gypsum formation may be concomittant with the dolomitization, and hence, an early diagenetic event.

D. INTERNAL SEDIMENTATION

In all the 150 thin sections examined, only two show internal sediments filling cavities. They occur near the base (Mount Greenock section) and the top (Snaring River section) of the Mount Head Formation (Fig. 19). In both cases, the internal sediments overlie the coarse sparry calcite and are composed of dark grey, silt sized grains

with abundant calcite and/or dolomite fragments (Plate 23E). No cavities were completely filled by the sediments.

The one present in the Mount Greenock section is of particular interest. A time gap between the precipitation of the calcite cement and the internal sedimentation is represented by the partial dissolution of the calcite forming a pitted crystal surface (Plate 23E). The irregularities were later filled by two phases of internal sediments having different shades and grain size.

Petrographic studies indicate that the internal sediments are lacking the criteria for vadose geopetal silt described by Dunham (1969b). Furthermore, stratigraphic data show no evidence of land emergence. Therefore, the sediments are probably of ordinary marine sediments introduced into the sedimentary framework by tidal waters. Presumably, they were brought in shortly after the precitation of the coarse, sparry calcite.

E. PRESSURE SOLUTION

Pressure solution is due to selective solution at those grain contacts excessively stressed by overburden or tectonic stress (Bathurst, 1975). In the study area, stylolites are the most common pressure solution feature. The stylolites occur as well defined, continuous sutured seams (Plates 8H and 26A) with amplitudes rarely greater than 5 mm. The interpenetrating style represents pressure solution response of a structurally resistant carbonates

with very little clay content (Wanless, 1979).

The best demonstration of carbonate dissolution is shown by the exceptional concentration of detrital quartz grains along the stylolites (Plate 26B). Dunnington (1967) showed that the amplitude of the interpenetration is an approximate measure of the amount of carbonate dissolved. Besides the usual concentration of iron oxide and organic residue (Plate 26C), there is no evidence of carbonate reprecipitation in the immediate vicinity of the stylolites. This means that the thickness reduction must have accompanied with the escape of carbonate from the system. Geiser and Sansone (1981) proposed that microfractures may act as conduits for the transport of the dissolved phases.

There is no indication of selective dolomitization near the proximity of the stylolites as was suggested by Wanless (1979). Thus, the stylolite formation was probably formed by late burial diagenesis after the pervasive matrix dolomitization.

F. FRACTURING

Microfractures, less than 0.2 mm wide are common in the sequence. In the Mississippian carbonate strata, they were commonly healed by calcite and/or dolomite (Plates 22B and 23B) or more rarely by silica cements. Silica is the dominant fracture filling agent in the Ranger Canyon chert. Petrographic evidence indicates that the brecciation in the dolostone and chert sequence occurred after dolomitization

and silicification respectively (Plate 26D). The breccias were cemented by calcite and quartz in the Mississippian dolostone and Permian chert respectively.

The cause of the brecciation in the Upper Turner Valley Formation, particularly in the Talbot Lake section, is not clear. It may be due to preferential dissolution along pre-existing joints or a result of overburden or tectonic stress. On the basis of the evidence for the hypersaline conditions during the deposition of the Ranger Canyon Formation, the chert breccia occurred in the Snaring River section probably was formed in response to the evaporite dissolution.

G. PHOSPHATIZATION

Rare, black phosphate nodules (<1 cm in diameter) occur in the uppermost beds of the Permian Mowitch Formation. The contact of the phosphate nodule and the surrounding arenite is not sharp (Plate 26E) as it appears in hand specimen (Plate 15C). In thin sections, these nodules are isotropic, microcrystalline and contain some phosphate fragments as well as highly corroded quartz grains (Plate 26F). All the above features clearly suggest that they are of replacive origin. Unfortunately, the actual mechanism of phosphate diagenesis is poorly understood.

Petrographic studies of the Permian Phosphoria Formation revealed that phosphatization of calcite and silica is a widespread diagenetic process (Cook, 1970). Cook

(1970) demonstrated that phosphate replacement of calcite and silica favours a high pH (7-10) environment. Mobilization of phosphorus can be accomplished by rain water leaching during a sea level lowstand (Fairbridge, 1983). This appears to be in agreement with the inferred Late Permian relative sea level drop. Pushing this line of thought a bit further, the phosphatization may be unconformity control, and hence, a telogenesis (Choquette and Pray, 1970)

X. DIAGENESIS: SYNOPSIS

The rocks in the Upper Mississippian to Upper Permian sequence of the Talbot Lake area have undergone a very complex diagenetic history. The major diagenetic processes were: (1) two phases of replacive dolomitization, (2) multi-stage silicification (replacement and cementation), (3) leaching, (4) complex arrays of carbonate cementation, (5) dedolomitization, (6) stylolitization, and (7) fracturing. Other relatively minor diagenetic characters include hematite replacement, pyrite formation, and internal sedimentation. The arenite of the Mowitch Formation is characterized by phosphatization in the uppermost beds.

Evidence from the diagenetic signatures - fabric and mineralogy - clearly indicate a gradual change in the pore water chemistry, and hence, the diagenetic environment. The suggested diagenetic pathways for the Mississippian sequence (Figs. 21 and 22) and the Permian Ranger Canyon strata (Fig. 23) are admittedly an over-simplified model. Much of the diagenesis is probably sequential and it is not possible to determine the exact timing of each individual process. The proposed diagenetic history of the sequence is an attempt to assemble the diagenetic events into a logical sequence in accordance with the inferred diagenetic environments.

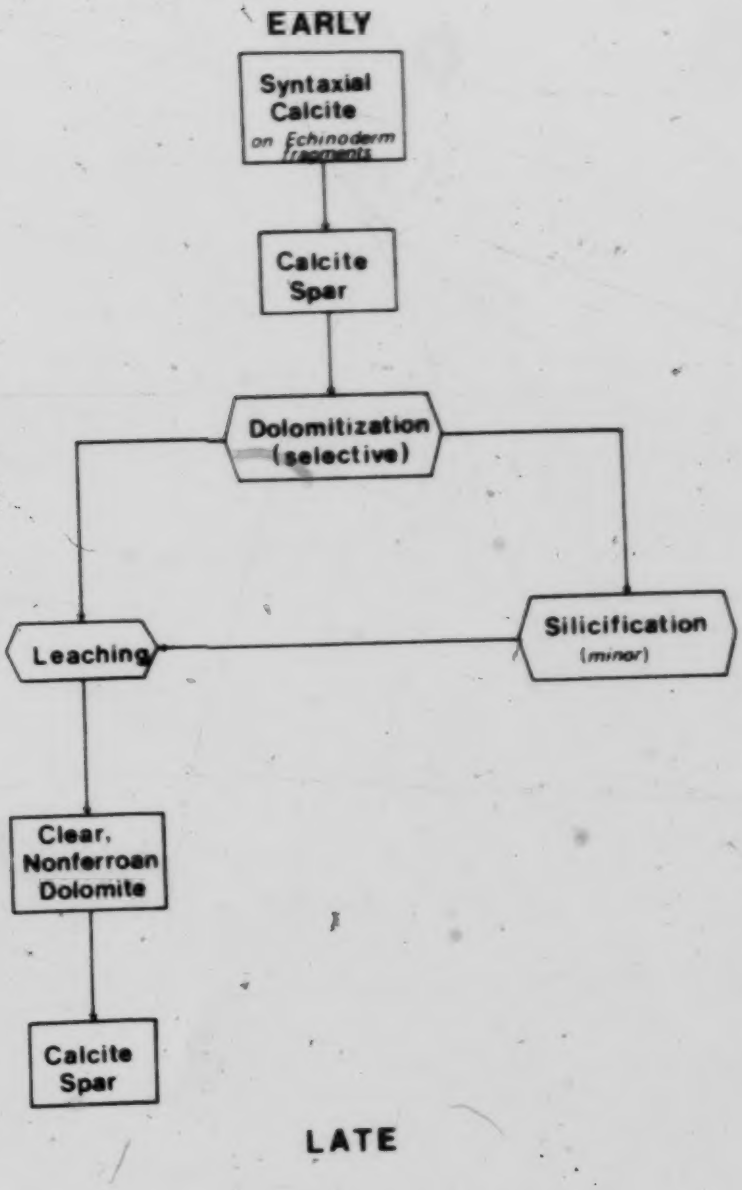

Figure 21. Suggested diagenetic pathway of dolomitic limestone in the lower part of the Turner Valley Formation.

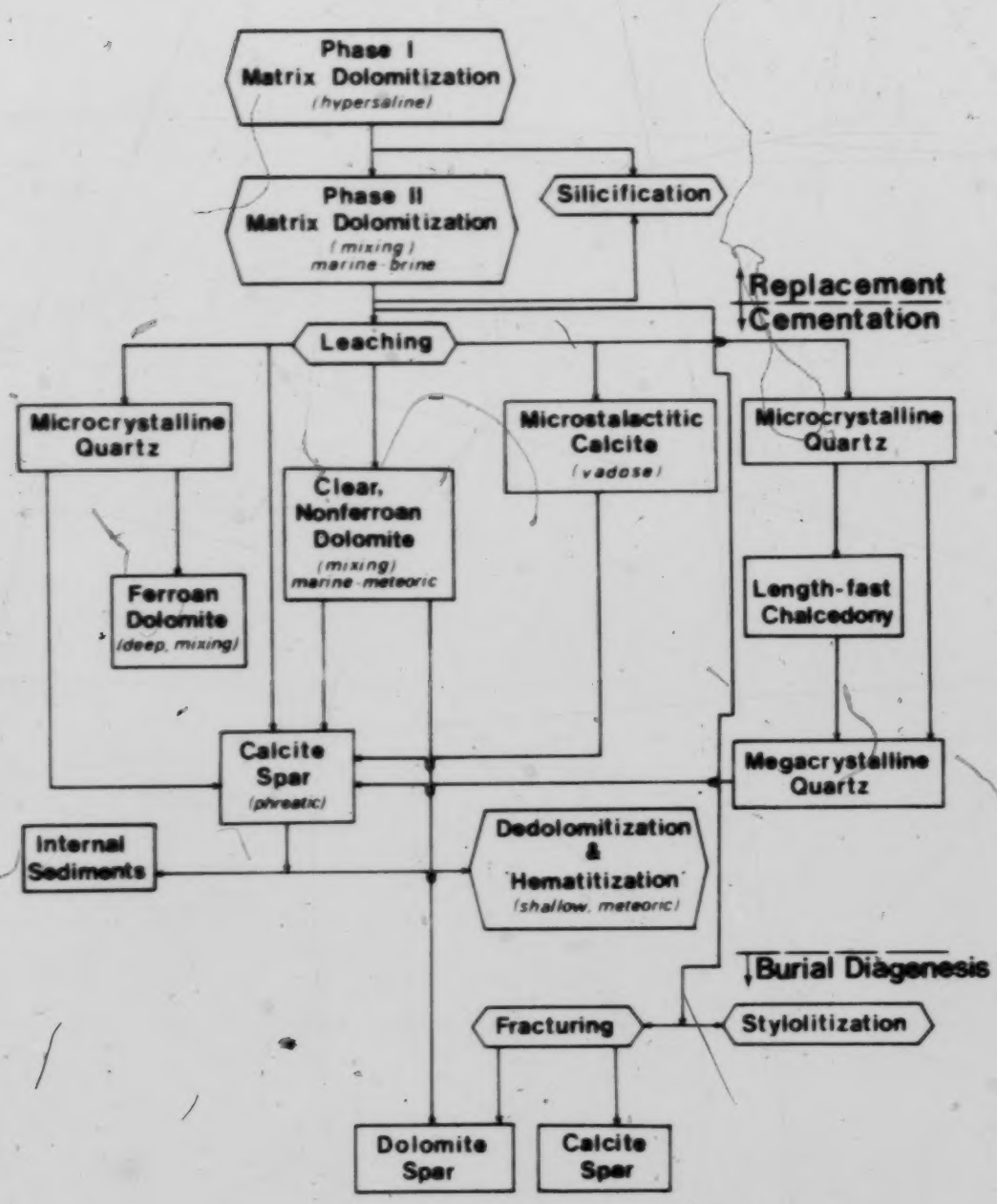

Figure 22. Suggested diagenetic pathway of dolostone in the upper part of the Turner Valley to Etherington formations (Upper Mississippian).

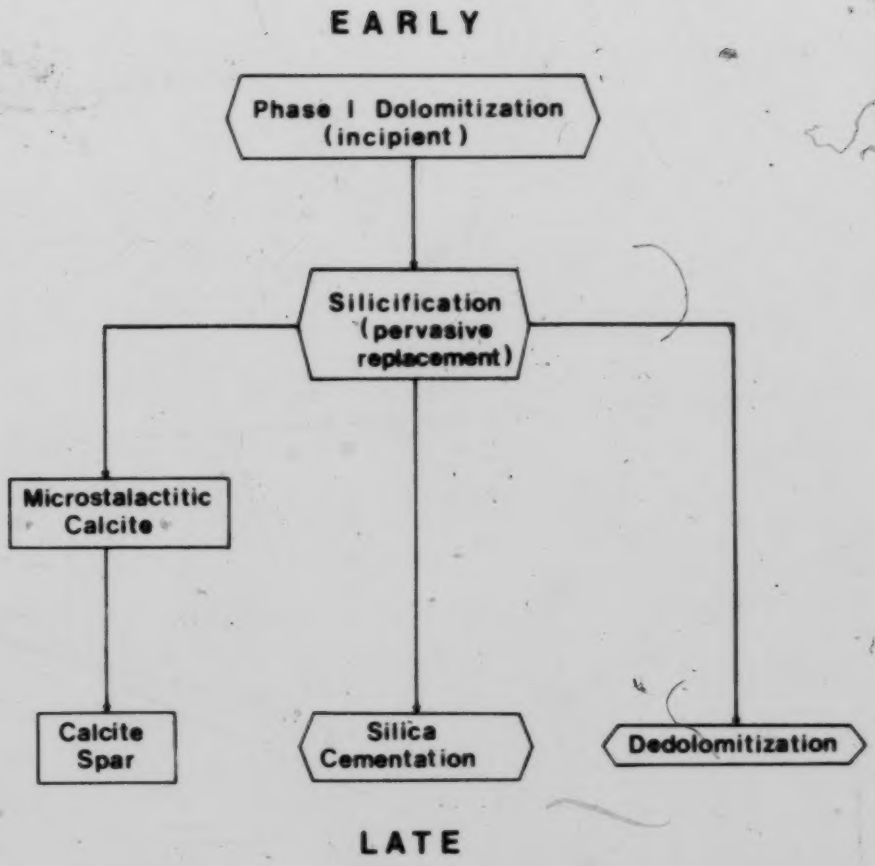

Figure 23. Suggested diagenetic pathway of the rocks in the Upper Permian Ranger Canyon Formation.

A. EFFECT OF THE DEPOSITIONAL ENVIRONMENTS

It is not difficult to envisage that the complicated diagenetic patterns were probably related to the complex depositional settings. The upward shallowing sequences mean that the sediments were affected by numerous stages of ground water fluctuation. Furthermore, these shallowing-upward sequences culminating in the upper intertidal to supratidal zone permit the development of the hypersaline conditions. These prograding tidal flats also provide an additional land area in the shoreward direction for the recharge of meteoric fresh water. Thus, the mixing of the meteoric fresh water and/or hypersaline brine with the marine water in a series of cycles is unequivocal. Furthermore, the sea-marginal depostional setting is particularly effective for mixed water diagenetic processes.

Further complicating the circumstances are the Late Mississippian and Late Permian relative sea level changes. In addition to the obvious effect of karsting at the top of the Mississippian carbonate sequence, the emerged land mass provides a vast area for the intake of meteoric fresh water. Probably more important is the fact that these major sea level fluctuations also caused major expansion and contraction of the ground water lens as well as shifting of the mixing zone.

Pore water movement in the subsurface flow system is a function of the porosity and permeability of the sediments. It is also clear that many of the diagenetic processes,

specifically, the dolomitization, silicification, and leaching, exhibit a distinct preference for certain sediment types. Therefore, the distribution of the original sediments apparently played an important role in controlling the diagenetic pattern.

B. DOLOMITIZATION VERSUS SILICIFICATION

Since both dolomitization and silica diagenesis are solution-reprecipitation process, they are influenced by a number of physico-chemical factors. Although the two diagenetic processes are temperature and pressure dependent, the effects are insignificant in the near-surface condition.

FACTORS CONTROLLING DOLOMITIZATION

Although the enigma of dolomite formation is unresolved, the dolomitization process is known to have been governed by several physico-chemical factors (Folk and Land, 1975; Gaines, 1980; Baker and Kastner, 1981; Morrow, 1982a):

1. high salinity increases crystallization rate of dolomite, but causes high disorder,
2. high pH favours dolomite precipitation,
3. high Mg^{2+}/Ca^{2+} and CO_3^{2-}/Ca^{2+} ratios favour dolomite formation;
4. low SO_4^{2-} in solution promotes dolomitization;
5. the presence of Li^+, Fe^{2+}, and NH_4^+ provides a catalytic effect;
6. the transformation of opal-A to opal-CT inhibits

dolomite formation, while opal-A to quartz favours dolomitization.

FACTORS CONTROLLING SILICIFICATION

Like dolomitization, silica diagenesis is also controlled by a number of physico-chemical factors (Wise and Weaver, 1976; Kastner *et al.*, 1980; Kastner, 1980; Baker and Kastner, 1981; Kastner and Gieskes, 1983):

1. the increase in ionic strength favours opal-CT to quartz transformation;
2. the higher the pH, the higher the solubility of silica;
3. the presence of Mg^{2+}, OH^-, and CO_3^{2-} enhances the transformation of opal-A to opal-CT;
4. the presence of SO_4^{2-} retards the transformation of opal-CT to quartz;
5. the presence of clay retards the transformation of opal-A to opal-CT;
6. the presence of Mg^{2+} and SO_4^{2-} favours the formation of length-slow chalcedony.

The factors governing silicification and dolomitization are in many respects similar. For example, high pH favours dolomite formation, whereas high pH causes silica dissolution while low SO_4^{2-} promotes dolomitization and opal-CT to quartz transformation. Of particular interest is the transformation of opal-A to opal-CT which inhibits dolomitization due to uptake of magnesium. On the other hand, the conversion of opal-CT to quartz promotes

dolomitization as a result of release of magnesium. Therefore, the close association of silica and dolomite is not surprising. It is, however, imperative to note that the available source of silica, carbonate and magnesium are of paramount significance. The controlling factors are important in the sense that they may either lower or raise the kinetic constraints of the diagenetic processes.

C. CARBONATE CEMENTATION PATTERN

Petrographic studies indicate an intricate pattern of carbonate cementation (Fig. 19). Some of the critical features are:

1. In certain beds, the allochem molds are open, whereas those in the overlying and underlying units are partially or completely filled with cement;
2. in the same thin section, some bird's-eye vugs are partially filled with the microstalactitic cement, while the adjacent vugs are completely filled with the clear, nonferroan dolomite and coarse calcite spar;
3. in certain units, the clear, nonferroan calcite is succeeded by the coarse, sparry calcite, whereas in others, it is followed by coarse, dolomite spar;
4. the seemingly close relationship of the ferroan dolomite and the silica cements;
5. the close association of the coarse, sparry calcite and dedolomite (Figs. 19 and 20).

These features undoubtedly connected to the complex depositional pattern. Based on the cement association and the interpreted diagenetic environments, the cementation sequence in the Mississippian carbonates may represent, from early to late, the followings (Fig. 22):

1. leaching of allochems and generation of bird's-eye vugs;
2. precipitation of the microstalactitic calcite in the vadose zone;
3. precipitation of the clear, nonferroan dolomite in the mixed marine and meteoric fresh water diagenetic environment;
4. precipitation of the ferroan dolomite in the deeper part of the mixing zone;
5. precipitation of the coarse, sparry calcite in the fresh water phreatic zone;
6. dedolomitization in the near-surface meteoric zone;
7. precipitation of the coarse, dolomite spar in the deep burial diagenetic environment;
8. healing of late microfractures by the sparry calcite or dolomite spar in the deep burial zone.

These sequential events appear to correspond with a complete cycle of ground water lens fluctuations in response to the marine transgression (steps 1-3) and regression (steps 3-6). It is important to note that the rocks were probably subjected to several phases of ground water lens expansion and contraction.

D. POROSITY DESTRUCTION BY DOLOMITIZATION

In general, the dolostones in the studied sequence have low porosity. This contradicts the general concept of porosity creation through dolomitization of limestone.

Murray (1960) noted that porosity in dolomite is formed by three processes: (1) the dolomitization itself, (2) the solution of relic calcite from a partially dolomitized rock, and (3) the solution of unreplaced evaporite minerals. In the study area, however, most, if not all of the allochem molds and other types of cavities were filled with calcite, dolomite and/or silica cements. Moreover, the evaporite minerals in the Mississippian carbonates were replaced by silica. Open cavities are rare. Rectangular hollows probably formed by leaching of anhydrites are present in the Ranger Canyon chert; however, these scattered molds probably do not contribute any significant permeability to the cherts.

On the basis of the carbonate source, Murray (1960) proposed two possible paths of diagenesis: (1) local source dolomitization, and (2) distant source dolomitization. In the local source dolomitization, calcite solution is accompanied by growth of sucrose (idiotopic) dolomite, thus forming and redistributing porosity. A direct mole/mole replacement of a calcite mudstone would produce a crystalline dolomite with approximately 13% intercrystalline porosity (Murray, 1960). If carbonate is brought to the site of dolomitization (from a distant source), porosity destruction will occur. This process is also called

'overdolomitization'. Powers (1962) in the study of the Arabian Upper Jurassic carbonate reservoir rocks also concluded that the porosity and permeability show a drastic decrease when the quantity of dolomite exceeds 80%.

The abundance of stylolites suggests that at least some of the carbonates derived from the carbonate dissolution due to the pressure solution. These dissolved carbonates may act as the distant source for 'overdolomitization' which may have been involved in the obliteration of the porosity. Furthermore, the generally xenotopic interlocking fabric of the dolomite suggests that the rocks also underwent recrystallization. Land (1983) noted that recrystallization of early formed dolomites is probably a norm. It is envisaged that the later stages of dolomite formation also may affect the matrix dolomite if it was still porous at those times.

XI. CONCLUSION

The present study of the Upper Mississippian to Permian strata exposed near the Talbot Lake area indicates the following:

1. The Upper Mississippian to Upper Permian carbonate-clastic successions of the Talbot Lake area encorporate into five formations, namely, the Turner valley, Mount Head and Etherington formations of the Mississippian Rundle Group, and the Ranger Canyon and Mowitch formations of the Permian Ishbel Group.
2. The Pennsylvanian and Lower Permian strata are represented by a condensed sequence (4-13 m thick) of chert conglomerate. Paleotopographic, erosional relief of up to 10 m occurs on the post-Mississippian disconformity.
3. In response to a Late Mississippian relative drop in sea level small scale surface-developed paleokarstic features such as irregular troughs and ridges developed on the subaerially exposed carbonate rocks. The lack of prominent paleokarstic landforms is probably due to the absence of soil cover and the relatively unjointed rock mass. It is also possible that some of the features may have been removed by subsequent subaerial and submarine erosion.
4. The rocks of the study area originated by sedimentation associated with numerous shallowing-upward sequences in a marginal, shallow shelf sea. Although many of the

sedimentary fabrics were obliterated by post-depositional diagenesis, the preserved fossils, lithologies, textural characters and sedimentary structures permit environmental interpretation, namely:

a. Turner Valley Formation - open marine, shoal grading to subtidal lagoonal;
b. Mount Head Formation - subtidal grading to lower supratidal;
c. Etherington Formation - upper intertidal to supratidal;
d. Ranger Canyon Formation - upper intertidal to supratidal;
e. Mowitch Formation - deltaic progradation over a shallow carbonate shelf.

5. Stratigraphic correlation of the four studied sections clearly indicates an overall shallow water depositional environment as shown by the facies changes from section to section. The lithologic and faunal data show that the sections represent an inshore-offshore transect in an ancient epeiric sea. The Talbot Lake area was located in the proximal shelf whereas the Snaring River area was situated in the distal shelf position.
6. The sedimentary breaks in the succession can be correlated with the global lowstands in sea level and Sloss's inter-regional unconformities. This correlation provides a useful framework for the stratigraphic analysis of the otherwise monotonous sequence of the

Upper Mississippian strata.

7. The dolomitic limestone of the Lower Turner Valley Formation shows selective dolomitization of micrite and peloids which probably had a high aragonite content. Petrographic studies suggest that the dolomite replacement occurred after syntaxial overgrowths on echinoderm fragments.
8. The Upper Turner valley, Mount Head, and Etherington formations are primarily dolostone. In each individual shallowing-upward sequence, the dolomite crystal size shows a gradual decrease from the subtidal to supratidal deposits. The dolomite replacement occurred in two sequential phases. Phase I dolomite is characterized by small crystal size and was associated with hypersaline conditions. This early phase dolomitization probably developed by seepage brine reflux in a barred shelf or in a setting akin to the sabkha area of the present day Persian Gulf (but in a relatively milder climatic regime). Phase II dolomite is formed of coarser, clearer crystals. This second phase pervasive dolomitization probably occurred in a diagenetic zone where sea water mixed with meteoric water or hypersaline brine.
9. There are four types of chert fabrics which developed as a cement or replaced the original sediment, namely:
   a. microcrystalline chert which is the major replacement chert of the bioclasts and matrices in the rocks of the Upper Mississippian and Permian

Ranger Canyon Formation;

b. length-fast chalcedony which typically occurs as cavity- and fracture-fill;

c. quartzine which is probably connected to the now vanished evaporites;

d. megacrystalline quartz which replaced dolomite and evaporite minerals and commonly occurs as a cement.

10. Siliceous sponge spicules are the principal source of silica for the diagenetic replacement of the Upper Mississippian and Permian rocks. Petrographic evidence suggests that most of the replacive silicification occurred early in the diagenetic history prior to complete dolomitization. The silica replacement probably occurred in a mixed zone of meteroic-marine ground waters whereas the replacement of evaporites probably took place in a normal marine to hypersaline conditions. The preferential silicification of the skeletal material was probably controlled by the more porous texture of the bioclastic components than the surrounding matrix.

11. Petrographic evidence suggests that the dolomitization and silica diagenesis probably occurred in tandem. Their close association is probably due to the fact that they are both governed by a similar set of physico-chemical factors.

12. Syntaxial overgrowths on echinoderm fragments and sparry calcite are the major types of cement in the dolomitic limestone of the Lower Turner Valley Formation. In the

stratigraphically higher strata, carbonate cementation in the secondary pores is complex. There are five distinct types of cement representing different diagenetic environments:

a. microstalactitic calcite - vadose zone;
b. clear, nonferroan dolomite - mixed marine and meteoric zone;
c. ferroan dolomite - deeper part of the mixing zone;
d. calcite spar - fresh water phreatic zone;
e. dolomite spar - deep burial diagenetic environment.

13. The dedolomitization was probably a late diagenetic event related to a dolomite-calcium sulphate reaction in the near-surface meteoric zone. This replacement of dolomite by calcite may have been connected to the original composition of the dolomite as calcium-rich and iron-rich dolomites are chemically less stable.
14. Hematite replacement of matrix dolomite, gypsum crystals and silica is a rare form of diagenesis. The 'hematitization' process was probably a late solution-reprecipitation event. The rocks in the Mississippian strata were also modified by other diagenetic processes, namely, pyrite formation, internal sedimentation, fracturing and pressure solution.
15. Early incipient dolomitization was the dominant diagenetic process that affected the rocks of the Permian Ranger Canyon Formation. Later, pervasive silicification affected the undolomitized carbonate

sediments. The Permian Mowitch Formation is characterized by phosphatization in the uppermost beds.

16. The complicated diagenetic history of the rocks appears to be related to the complex depositional settings. The successive shallowing-upward sequences culminating in the supratidal zone or barred, shallow shelf permit the development of hypersaline conditions. These prograding tidal flats also provide additional land area for the recharge of meteoric fresh water. Thus, diagenetic processes involving sea water, fresh water and hypersaline brine were probably in operation for the modifications of the rocks in the strata.

Ground water lens expansion and contraction in response to Late Mississippian and Late Permian maximum regressions are of significant consequences. In addition to providing a vast area for meteoric fresh water recharge as a result of land emergence, these fluctuations of ground water table also caused changes in the diagenetic regimes. Therefore, it is clear that the diagenetic patterns are directly connected to the depositional environments as well as the early lowerings of relative sea level.

XII. LIST OF PLATES: Plates 1 to 26

NOTA BENE: All photographs of thin sections, which have been impregnated with blue epoxy and stained with Alizarin Red-S, are taken under plane-polarized light unless otherwise specified.

Plate 1

Field photograph of the Talbot Lake section showing the lower part of the Turner Valley Formation. The basal contact (dashed line) with the underlying Shunda Formation is marked by a thin (<10 cm) carbonaceous, calcareous shale unit. The strata comprise prominent, thick bedded skeletal (SG) and echinoderm grainstones (EG) and recessive, thin bedded skeletal wackestone (R); v = vuggy interval. Scale bar equals 4 m.

SW
SG
Turner Valley Formation

Plate 2

Field photograph of the Talbot Lake section showing the boundary between the lower Turner Valley Formation and the overlying Mount Head Formation. The contact is placed at the base of a thin intraclastic dolostone unit (ID). The uppermost units of the Turner Valley Formation is composed of thin bedded echinoderm packstone-wackestone (EP). The rocks in the lower part of the Mount Head Formation are predominantly fine to medium crystalline dolostone (FD). Scale bar equals 4 m.

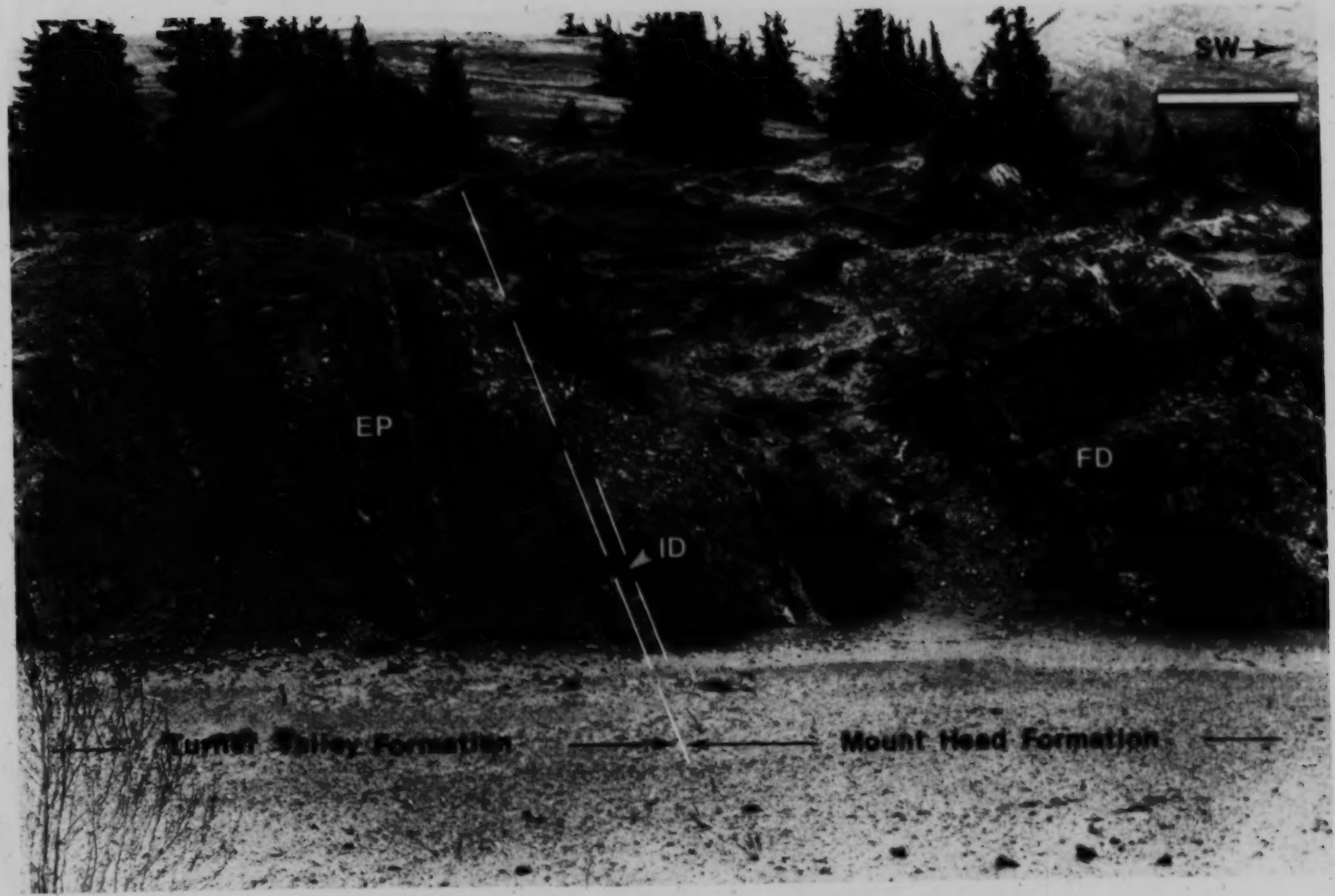
SW
EP
FD
ID
Turner Valley Formation
Mount Head Formation

Plate 3

(3A) Polished hand specimen of lithotype TV1 (Mount Greenock section) showing abundance of crinoid stems and ossicles. Scale bar equals 2 cm.

(3B) Photomicrograph of (3A) showing allochemical components of crinoid fragment (c), echinoderm spine (es), bryozoan fragment (b), and peloid (p). Scale bar equals 0.2 mm.

(3C) Polished hand specimen of lithotype TV2 (Talbot Lake section) showing diverse allochemical constituents. Scale bar equals 2 cm.

(3D) Photomicrograph of (3C) showing allochemical components of crinoid fragment (c), foraminifera (f), brachiopod (br), and peloid (p). Scale bar equals 0.2 mm.

(3E) Polished hand specimen of lithotype TV3 (Talbot Lake section) showing well sorted oöids. Scale bar equals 2 cm.

(3F) Photomicrograph of (3E) showing completely dolomitized oöids (ö). Outlines of oöids (indicated by arrows) are defined by distribution of relic inclusions in dolomite rhombs or presence of microspar cement (smaller, clear crystals) filling interstitial around oöids. Scale bar equals 0.2 mm.

A
B
C
D
p
E
F
o

Plate 4

(4A) Field photograph of lithotype TV2 (Talbot Lake section) showing a colonial coral (cc) which has been completely leached out. Lens cap (55 mm in dia.) for scale.

(4B) Polished hand specimen of lithotype TV2 (Talbot Lake section) showing cross-bedding (x) in crinoidal grainstone. Scale bar equals 2 cm.

(4C) Field photograph of lithotype TV4 (Mount Greenock section) showing burrow mottled texture (m). Scale bar equals 6 cm.

(4D) Polished hand specimen of lithotype TV4 (Talbot Lake section) showing disturbed laminations (indicated by arrows) and pseudonodules (pn) caused by bioturbation. Scale bar equals 2 cm.

(4E) Field photograph of lithotype MH1 (Talbot Lake section) showing dolostone intraclasts (i). The intraclastic dolostone unit marks the onset of marine transgression and resedimentation of underlying sediments. Lens cap (55 mm in dia.) for scale.

(4F) Field photograph showing pin-stripe laminated unit (pl) in lithotype MH3 (Mount Greenock section). The unit is formed of evenly interlaminated chert (white in colour) and dolomite (grey in colour). Hammer handle (33 cm) for scale.

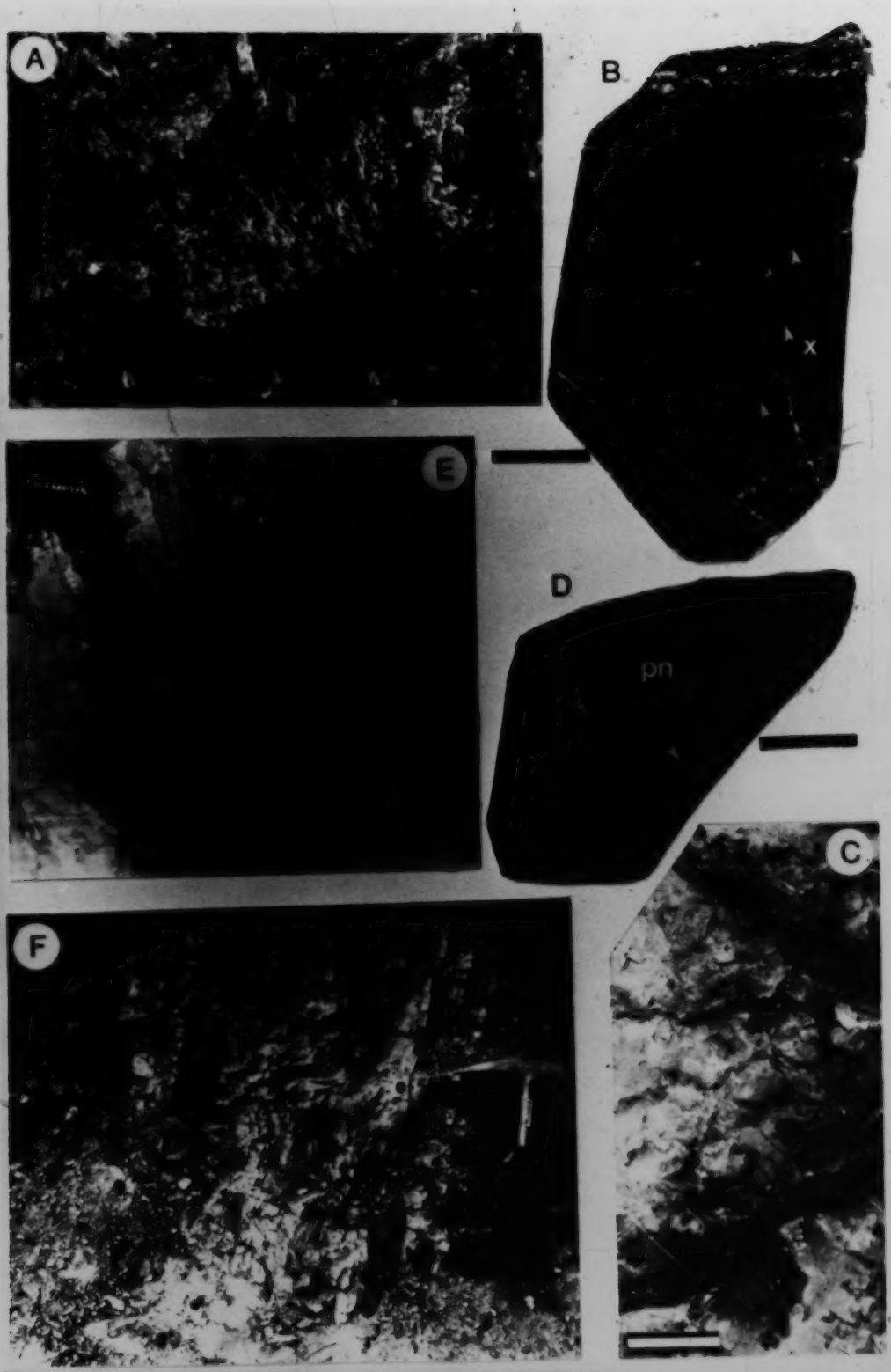
A
B
X
E
D
pn
C
F

Plate 5

(5A, B) Field photograph of lithotype MH4 (Talbot Lake section) showing chertified robust, ramose bryozoan branches (rb). Lens cap (55 mm in dia.) for scale.

(5C) Field photograph of lithotype MH4 (Talbot Lake section). Note that oblique section of ramose bryozoan branches (rb) give a nodular appearance. Lens cap (55 mm in dia.) for scale.

(5D) Field photograph of lithotype MH4 (Talbot Lake section) showing chertified bioclasts; g = gastropod, rb = ramose bryozoan branches, bi = bivalve. Lens cap (55 mm in dia.) for scale.

(5E) Field photograph of lithotype MH4 (Cinquefoil Mountain section) showing chertified brachiopod (br). Scale bar equals 1 cm.

(5F) Field photograph showing chertified sponges (s) at the uppermost beds of cherty dolostone ridge (lithotype MH4 and MH5, Mount Greenock section). Scale bar equals 10 cm.

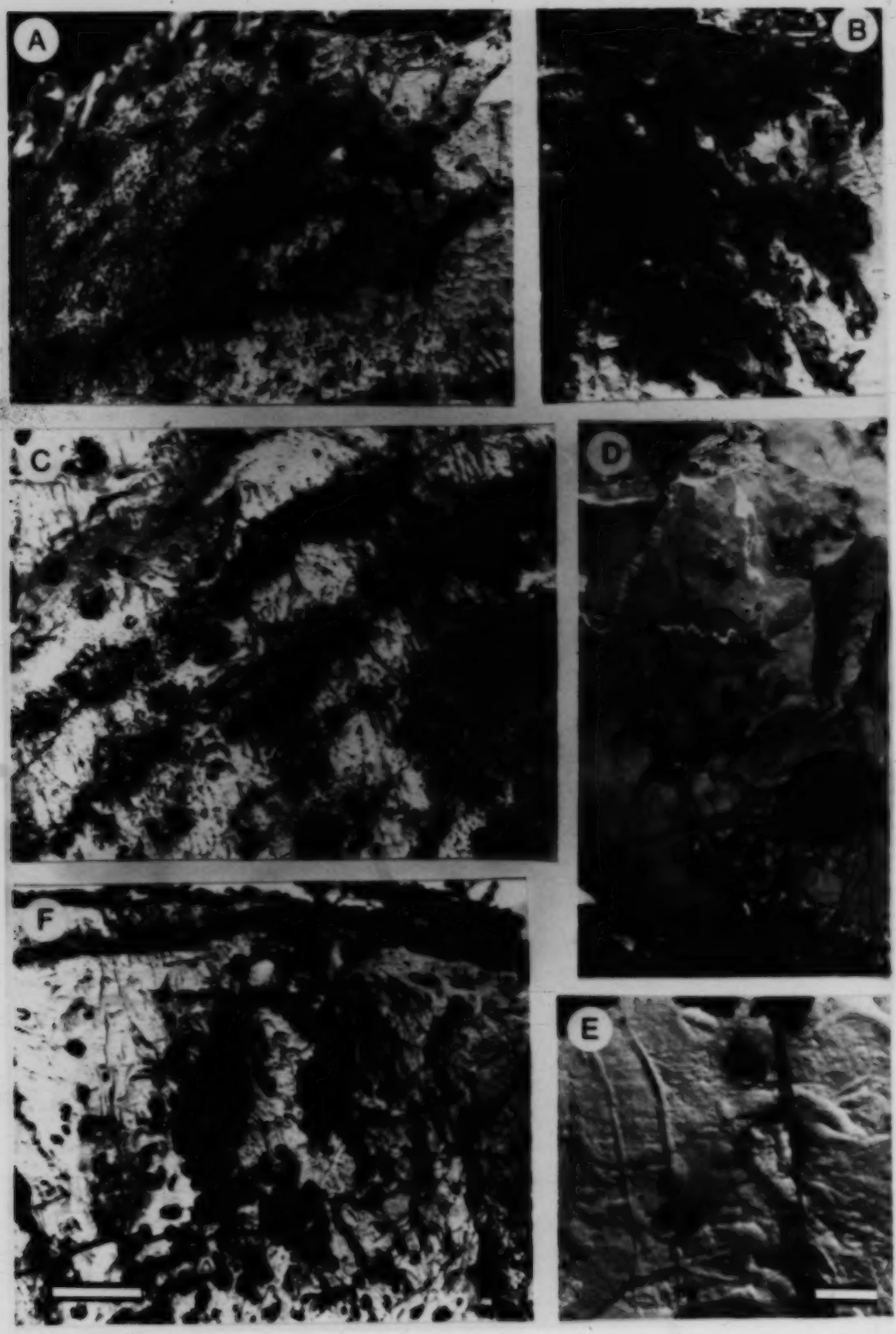
A
B
C
D
F
E

Plate 6

(6A) Field photograph showing prominent dolostone ridge which comprises lithotype MH4 and MH5 (Mount Greenock section). Scale bar equals 4 m.

(6B) Close up view of (6A) showing upward grading of cherty bryozoan (rb) dolostone (MH4) to cherty algal (al) dolostone (MH5). Hammer handle (33 cm) for scale.

(6C) Field photograph of lithotype MH5 (Talbot Lake section) showing chertified algal layers (al). Lens cap (55 mm in dia.) for scale.

(6D) Field photograph of lithotype MH5 (Mount Greenock section) showing chertified algal laminae (al). Lens cap (55 mm in dia.) for scale.

(6E) Field photograph of lithotype MH9 (Snaring River section) showing chert nodules (cn). Note that chert nodules arranged parallel to bedding. Lens cap (55 mm in dia.) for scale.

(6F) Field photograph of lithotype MH5 (Cinquefoil Mountain section) showing quartz nodules occur on upper surface of dolostone ridge in the Cinquefoil Mountain section. Scale bar equals 2 cm.

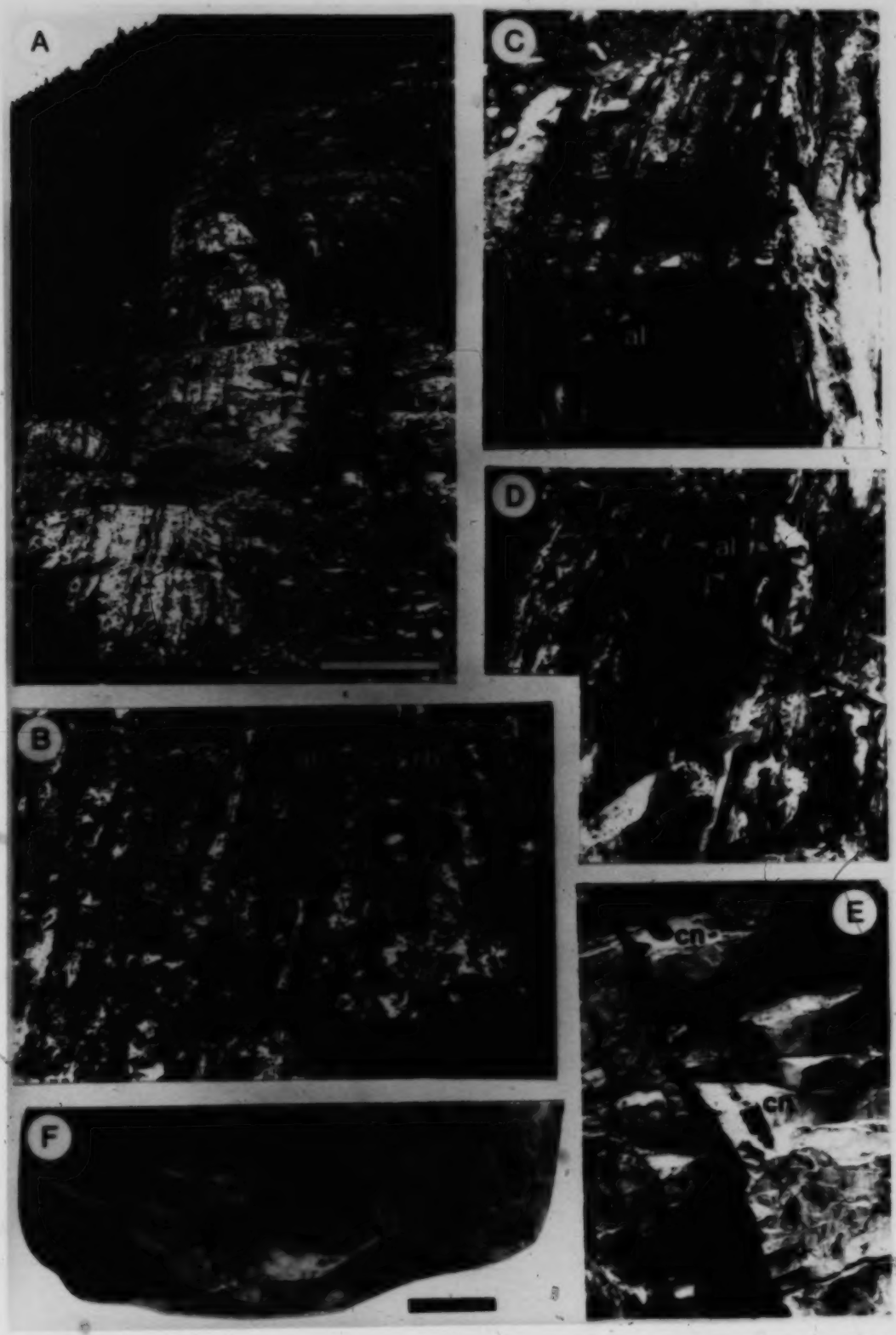
A
C
D
B
E
cn
cn
F

Plate 7

(7A) Polished hand specimen of lithotype MH6 from the Cinquefoil Mountain section showing bird's-eye structure (be). Scale bar equals 2 cm.

(7B) Polished hand specimen of lithotype MH6 from the Talbot Lake section showing bird'-eye structures (be). Note the planar arrangement of irregular, augen-shaped bird's-eye vugs. Scale bar equals 2.5 cm.

(7C) Field photograph of lithotype MH6 (Mount Greenock section) showing small sized, thin shelled gastropod (g) and bivalve (bi). Scale bar equals 1 cm.

(7D) Field photograph of lithotype MH8 (Snaring River section) showing an extensively burrowed surface. Note the abundant horizontal burrows (bu). Scale bar equals 1 cm.

(7E) Polished hand specimen of lithotype MH10 (Snaring River section) showing close association of pyrite (py) and quartz (q) crystals. Note the concentration of quartz crystals near a chert band (ch) which appears to be bioturbated. Scale bar equals 2 cm.

(7F) Field photograph of lithotype MH7 (Mount Greenock section) showing interbedded dolostone and argillaceous dolostone. Thin bedded to laminated argillaceous dolostone were preferentially weathered out. Scale bar equals 1 m.

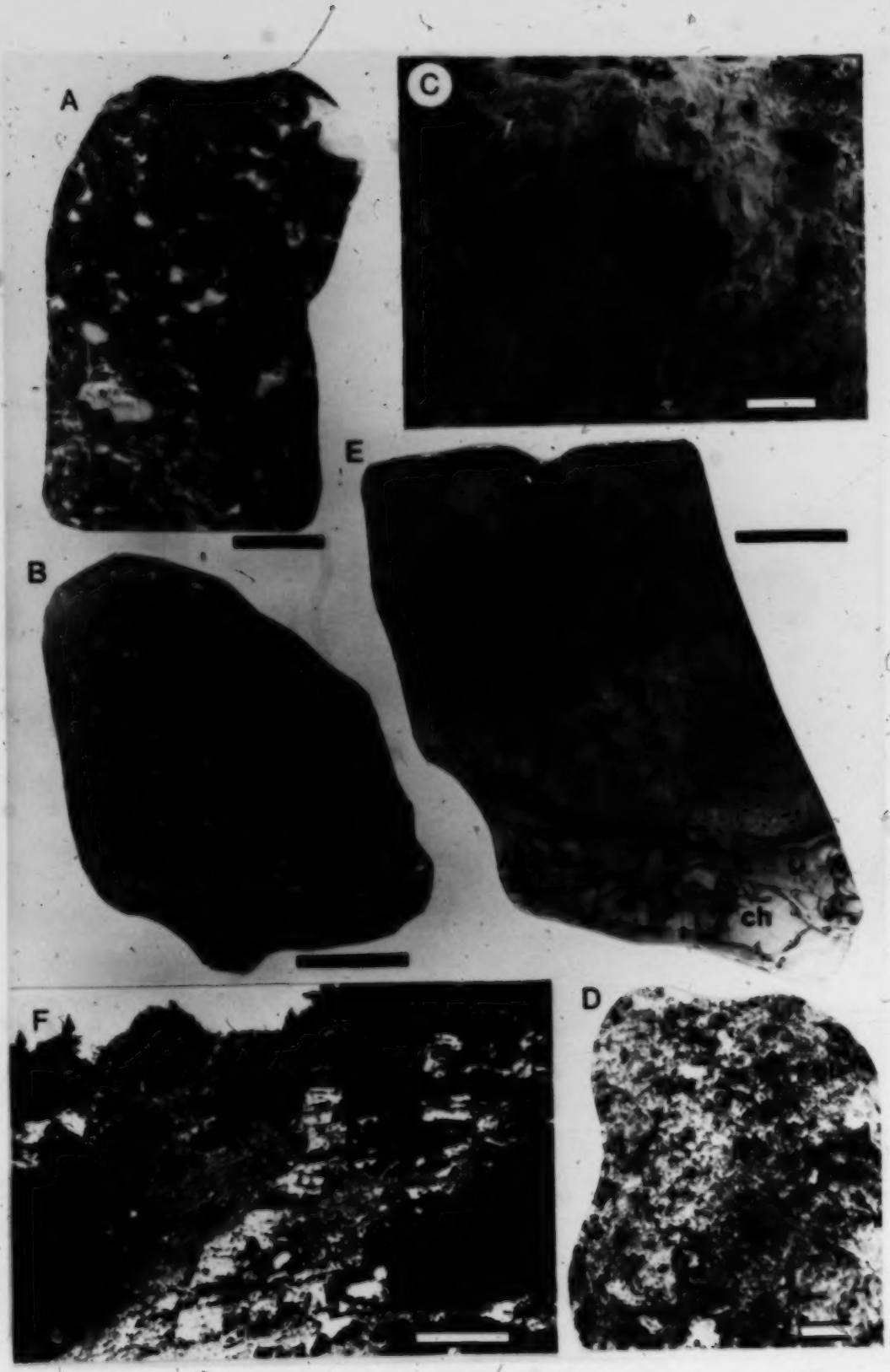
A
C
E
B
ch
F
D

Plate 8

(8A) Field photograph of lithotype E1 (Talbot Lake section) showing angular, fine crystalline dolostone clasts (di) and chert granules and pebbles (cp). Lens cap (55 mm in dia.) for scale.

(8B) Polished hand specimen of lithotype E1 (Talbot Lake section) showing angular and tabular shaped chert clasts (cp). Scale bar equals 2 cm.

(8C) Polished hand specimen of lithotype E1 (Talbot Lake section) showing small, ramifying solution channels (sc) filled with admixture of chert and dolostone fragments. Scale bar equals 2 cm.

(8D) Field photograph of lithotype E2 (Mount Greenock section) showing intercalated intraclastic (ic) and intralaminated (il) dolostone. Scale bar equals 0.2 mm.

(8E) Field photograph of lithotype E2 (Mount Greenock section) showing choatic arrangement of dolostone intraclasts (i). Lens cap (55 mm in dia.) for scale.

(8F) Polished hand specimen of lithotype E2 (Mount Greenock section) showing low angle, ripple cross-laminations (rl) and truncations. Scale bar equals 2 cm.

(8G) Polished hand specimen of lithotype E3 (Snaring River section) showing laminated dolostone intraclasts (pi) which exhibit pseudo-anticline structures. Scale bar equals 1 cm.

(8H) Field photograph of lithotype E4 (Snaring River section) showing dolostone intraclasts (i) which were partly dissolved along stylolites (st). Lens cap (55 mm in dia.) for scale.

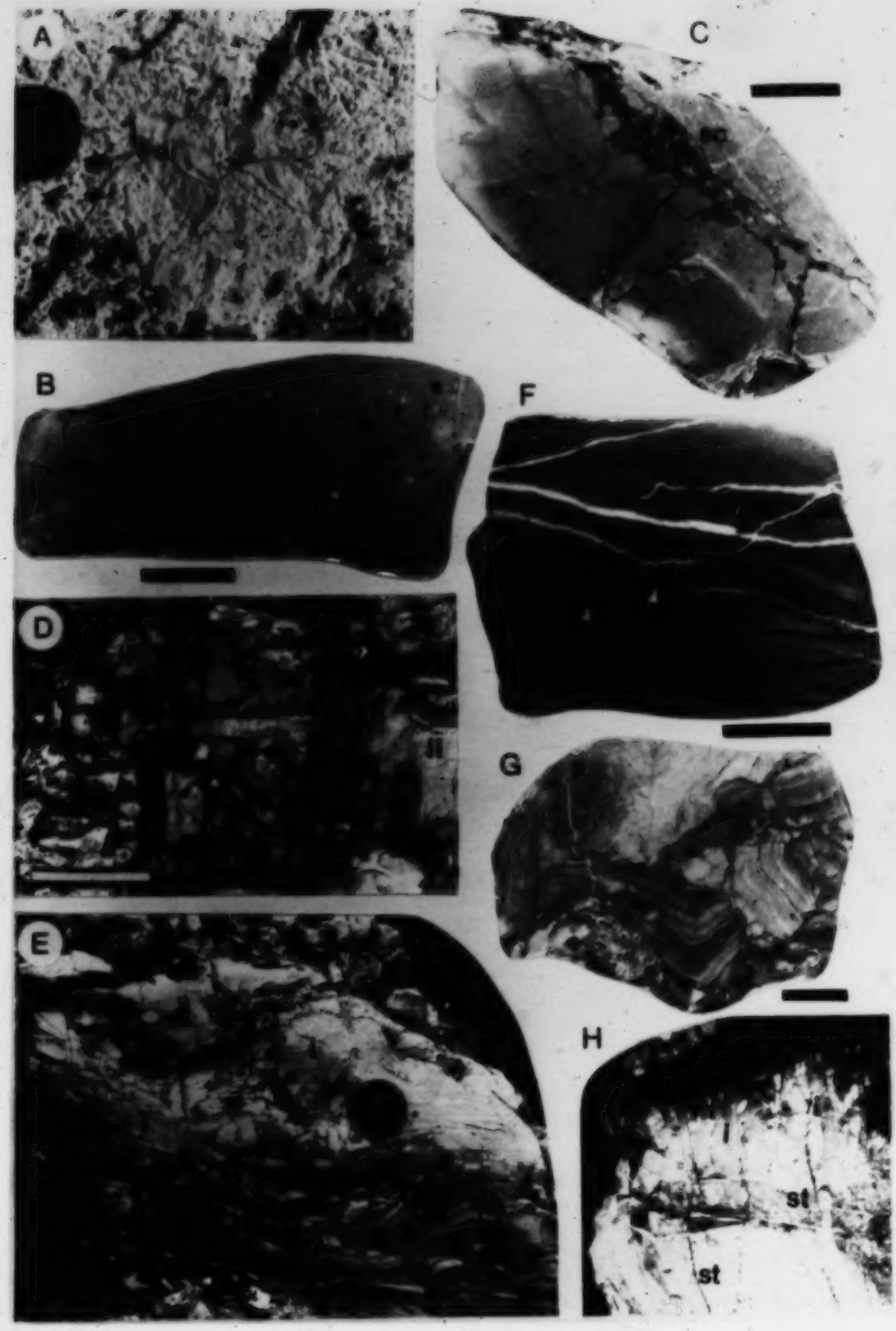
A
C
B
F
D
G
E
H
st
st

Plate 9

(9A) Field photograph of lithotype E5 (Talbot Lake section) showing laterally linked chertified algal mounds (am). Hammer handle (33 cm) for scale.

(9B) Field photograph of lithotype E5 (Cinquefoil Mountain section) showing small, isolated, chertified algal mounds (am). Scale bar equals 10 cm.

(9C) Field photograph of lithotype E5 (Cinquefoil Mountain section) showing internal ring structure (ar) of chertified algal mounds. Lens cap (55 mm in dia.) for scale.

(9D) Field photograph of lithotype E5 (Mount Greenock section) showing small, hemispherical, domal stromatolites (sl). Note the well preserved internal structure of alternating thin chert and relatively thicker dolomite laminae. Scale bar equals 10 cm.

(9E) Polished hand specimen of lithotype E6 (Talbot Lake section) showing intricate silicification pattern; d = unsilicified dolomite, mc = microcrystalline quartz, cc = cryptocrystalline quartz, fc = fibrous chalcedony. Scale bar equals 2 cm.

(9F) Polished hand specimen of lithotype E7 (Mount Greenock section) showing quartz clusters in very fine crystalline dolostone. Note that quartz clusters formed right-angled outlines. Scale bar equals 2 cm.

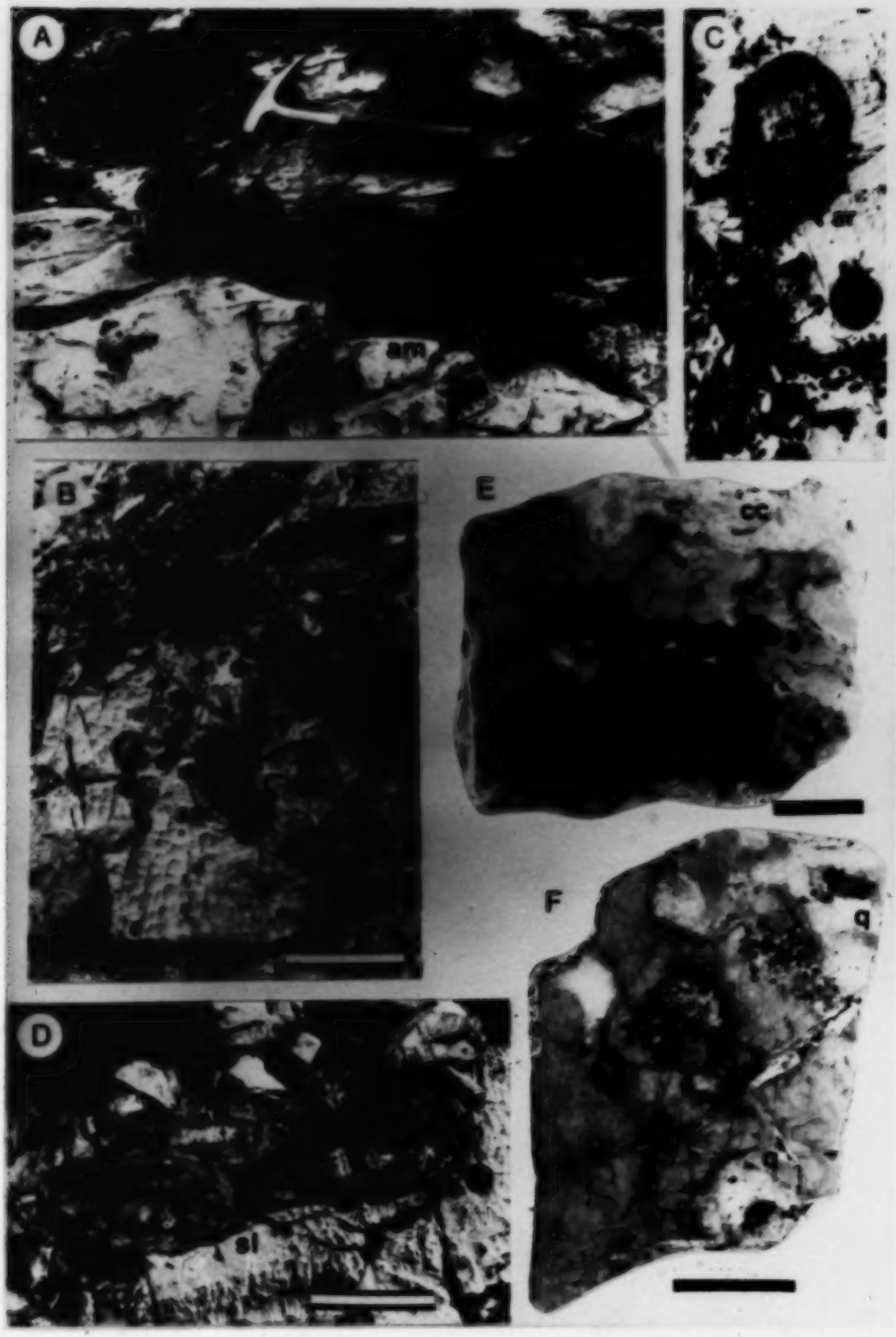
A
sm
C
B
E
cc
F
q
q
D
sl

Plate 10

(10A) Field photograph of Cinquefoil Mountain (CM). B refers to location of Plate 10B.

(10B) Field photograph of Cinquefoil Mountain exposures. Dashed line indicates top of Mississippian dolostone (Md) showing paleotopographic relief of the post-Mississippian disconformity; cs = chert conglomerate, Rc = chert of the Permian Ranger Canyon Formation, C refers to location of Plate 10C. Scale bar equals 10 m.

(10C) Field photograph of Cinquefoil Mountain section showing covered Mississippian - Upper Permian boundary. Md = Mississippian dolostone, Rc = chert of the Ranger Canyon Formation. Note that this photograph view at an angle opposite to that of Plate 10B. Jacob staff (1.5 m) for scale.

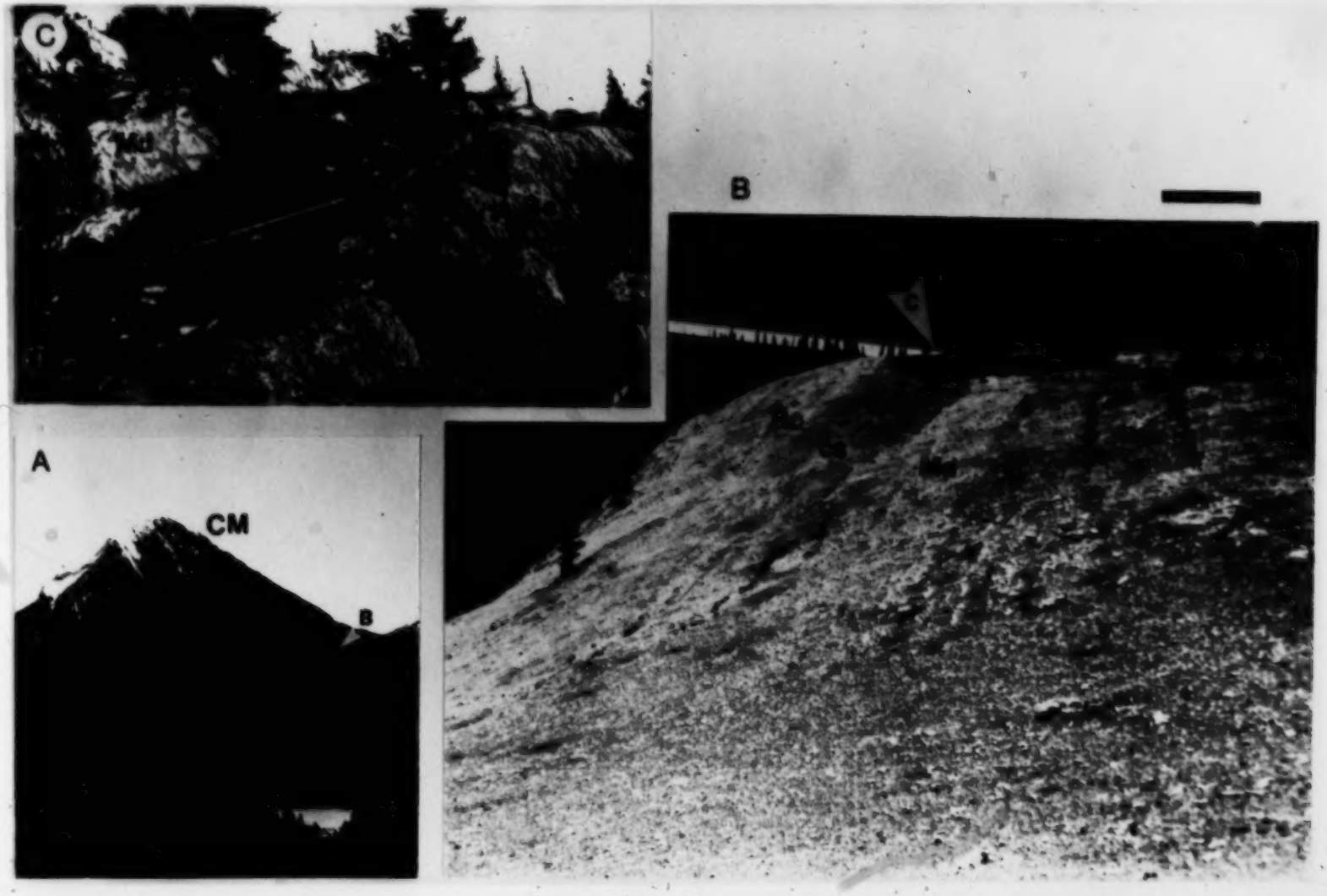
C
B
C
A
CM
B

Plate 11

Photographs of post-Mississippian disconformity (Talbot Lake section)

(11A) Field photograph showing small trough having irregular, steeply sloping walls filled with chert conglomerate (cs); Md = Mississippian dolostone. Hammer handle (33 cm) for scale.

(11B) Field photograph showing narrow, irregular dolostone ridge (Md) surrounded by chert conglomerate (cs) on both sides. Lens cap (55 mm in dia.) for scale.

(11C) Field photograph showing irregular, high angle contact between Mississippian dolostone (Md) and chert conglomerate (cs). Lens cap (55 mm in dia.) for scale.

(11D) Field photograph showing sharp, high angle contact between Mississippian dolostone (Md) and chert conglomerate (cs). Hammer handle (33 cm) for scale.

(11E) Field photograph showing sandstone lens (sl) in Mississippian dolostone (Md). Lens cap (55 mm in dia.) for scale.

(11F) Polished hand specimen of chert arenite from sandstone lens showing vague stratifications (arrows) due to concentration of dark chert grains. Scale bar equals 1 cm.

(11G) Photomicrograph of chert arenite from sandstone lens showing well sorted quartz (q) and chert (c) grains. Note the quartz overgrowths (qo). Crossed-nicols. Scale bar equals 0.1 mm.

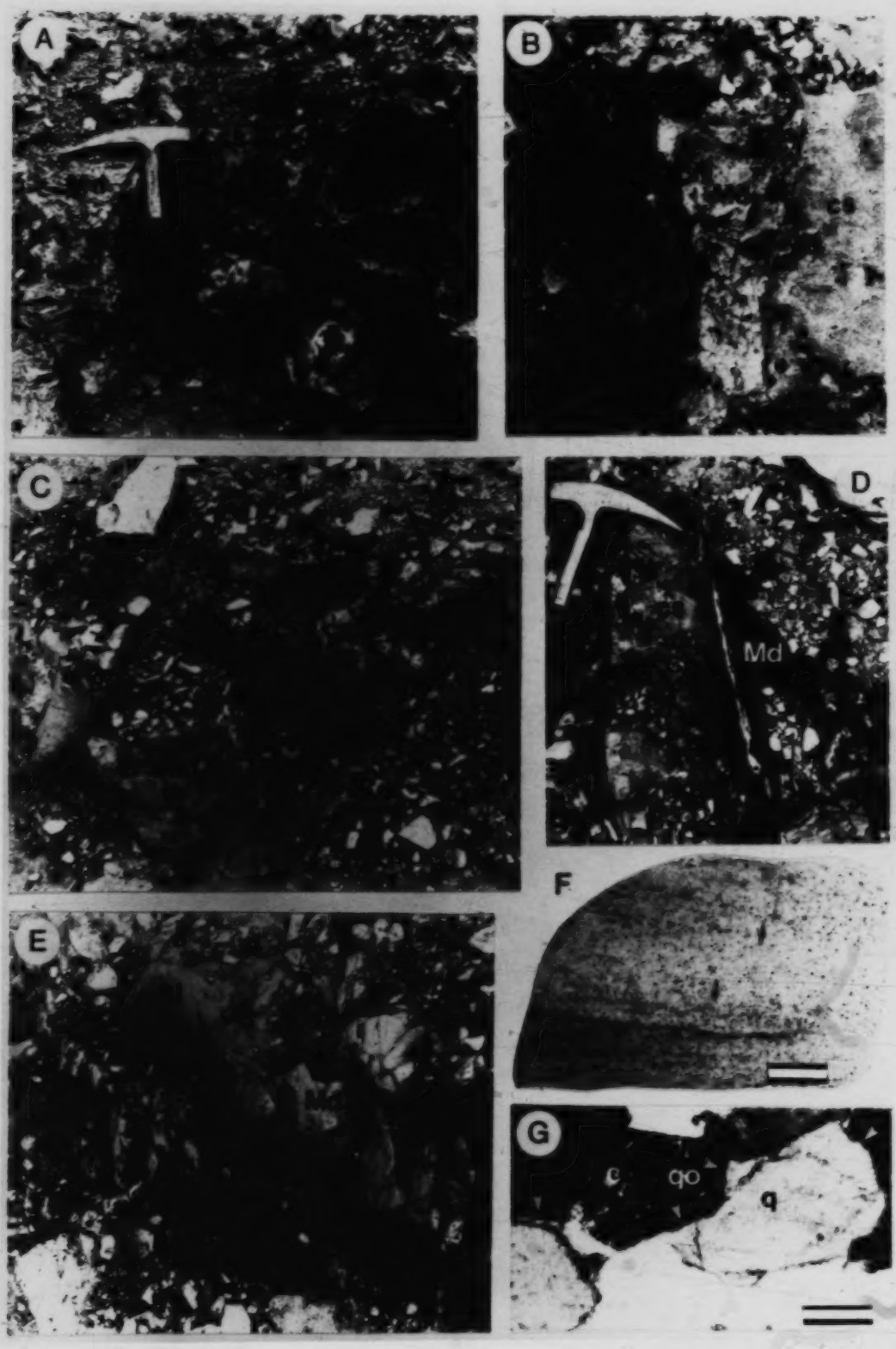
A
B
C
D
Md
E
F
G
qo
q

Plate 12

(12A) Field photograph of chert conglomerate (Talbot Lake section); c = chert cobbles, s = sandstone matrix. Lens cap (55 mm in dia.) for scale.

(12B) Field photograph of chert conglomerate (Talbot Lake section); c = chert cobbles and pebbles, s = sandstone matrix. Note the oblate spheroidal shape of chert pebbles. Hammer handle (33 cm) for scale.

(12C) Photomicrograph of chert arenite from chert conglomerate (Talbot Lake section). Note the quartz overgrowths (qo). Crossed-nicols. Scale bar equals 0.2 mm.

(12D) Field photograph of basal intraclast and conglomerate (Snaring River section). Note the abundant angular dolostone clasts (di). Lens cap (55 mm in dia.) for scale.

(12E) Field photograph showing top surface of basal intraclast and conglomerate (Snaring River section). Note the exceptional enrichment of dolostone and chert pebbles. Lens cap (55 mm in dia.) for scale.

(12F) Polished hand specimen of basal intraclast and conglomerate (Snaring River section); di = dolostone clast, c = chert clast, cv = calcite vein. Note the dolomite rim growths on dolostone clasts. Scale bar equals 1 cm.

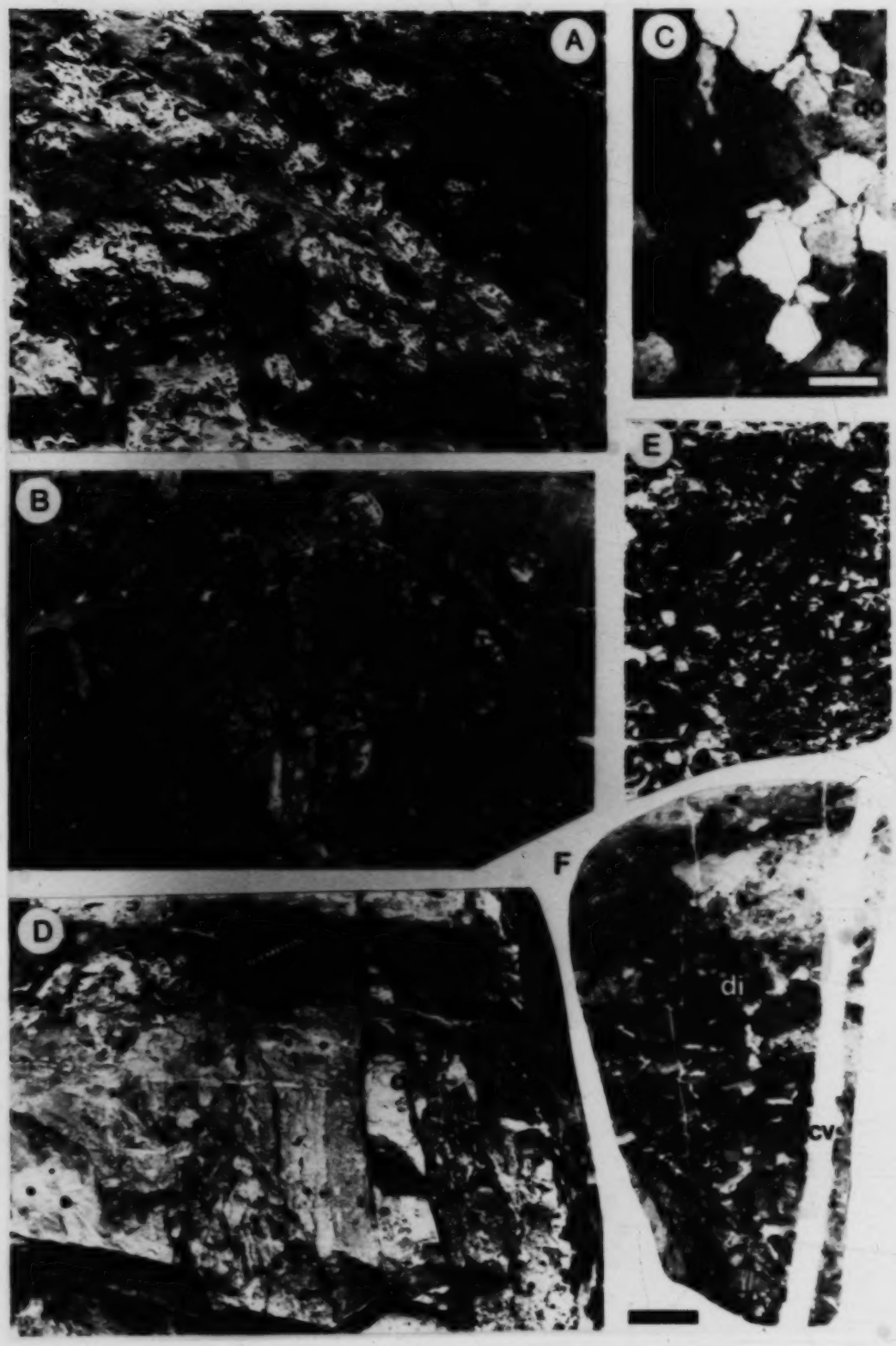
A
C
C
go
B
E
F
D
di
cv

Plate 13

(13A) Field photograph showing contact between the Ranger Canyon Formation (Rc) and the overlying Mowitch Formation (Ms) in the Mount Greenock section. Hammer handle (33 cm) for scale.

(13B) Field photograph showing chert (ch) of the Ranger Canyon Formation with sandstone (s) patches (Mount Greenock section). Lens cap (55 mm in dia.) for scale.

(13C) Field photograph showing interfingering of sandy chert (sc), sandstone (ss) and cherty sandstone (cs) near top of Ranger Canyon Formation (Mount Greenock section) Lens cap (55 mm in dia.)

(13D) Photomicrograph of Ranger Canyon chert (Snaring River section) showing tooth-like structure (t) and quartz (q) grains in microcrystalline chert (mc). Crossed-nicols. Scale bar equals 0.2 mm.

(13E) Photomicrograph showing bone tissue (bt) in sandy chert (Snaring River section). Crossed-nicols. Scale bar equals 0.2 mm.

(13F) Photomicrograph of Ranger Canyon chert (Mount Greenock section) showing circular and elliptical phosphate fragments (ph) in microcrystalline chert. Scale bar equals 0.05 mm.

(13G) Photomicrograph showing monoaxon sponge spicules (sp) in microcrystalline chert (Snaring River section). Note the distinct central canals of sponge spicules. Scale bar equals 0.2 mm.

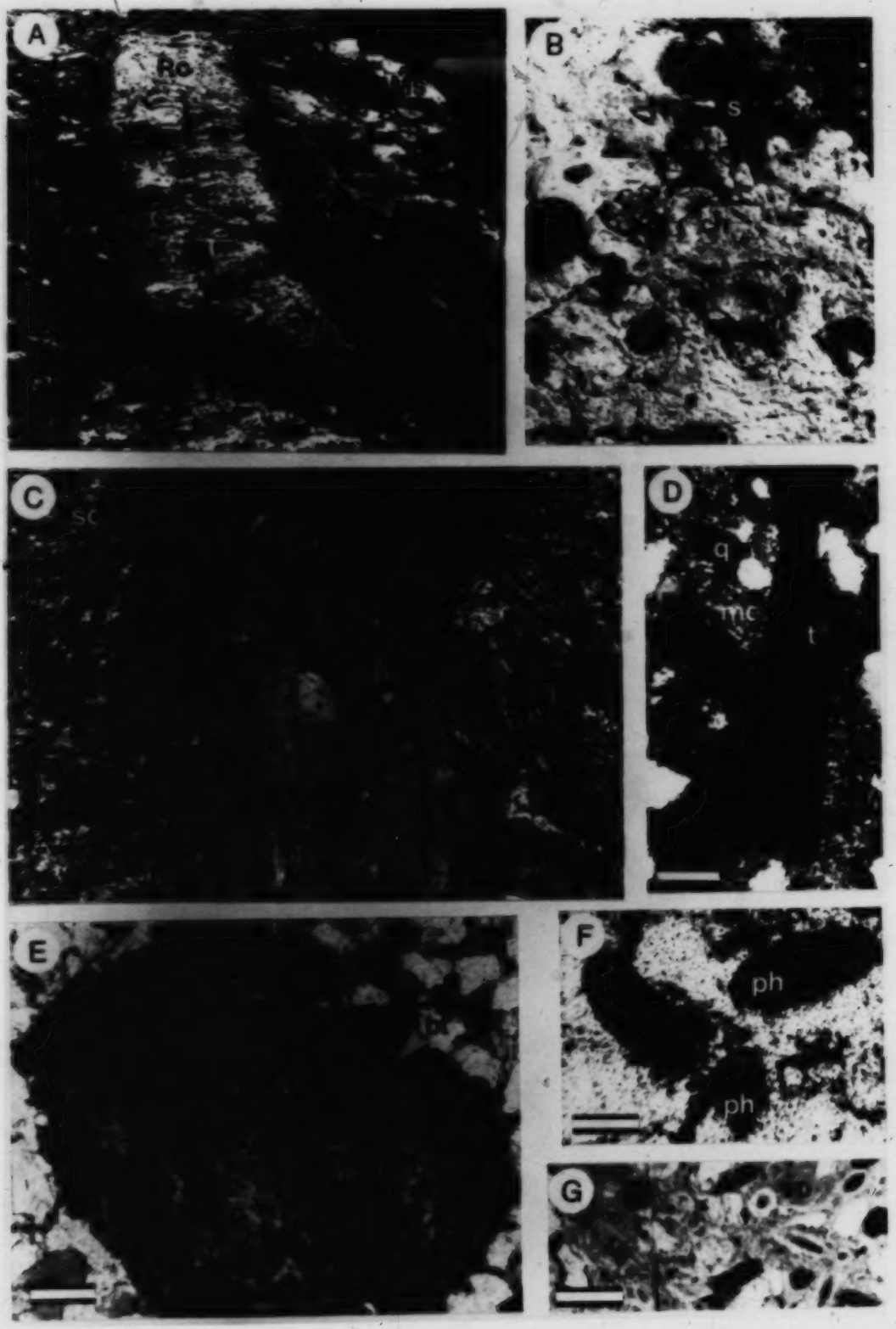
A
Rc
B
s
C
sc
D
q
mc
t
E
F
ph
ph
G

Plate 14

(14A) Polished hand specimen showing small, columnar, stacked laminae of algal stromatolites (sl) in Ranger Canyon chert (Snaring River section). Scale bar equals 1 cm.

(14B) Field photograph of Ranger Canyon Formation (Snaring River section) showing quartz nodules (qn). Lens cap (55 mm in dia.) for scale.

(14C) Field photograph of chert breccia (Mount Greenock section). Note the sandstone (ss) and chert fragments (ch) infiltrated among brecciated chert. Lens cap (55 mm in dia.) for scale.

(14D) Polished hand specimen of chert breccia (Snaring River section). Spaces between angular chert clasts filled with dolomites. Scale bar equals 1 cm.

(14E) Polished hand specimen of chert breccia (Snaring River section). Angular chert clasts cemented by quartz crystals forming a mosaic texture. F refers to the location of Plate 14F. Scale bar equals 1 cm.

(14F) Close up view of (14E) showing small, euhedral quartz crystals grew in open vugs between chert clasts. Scale bar equals 1 cm.

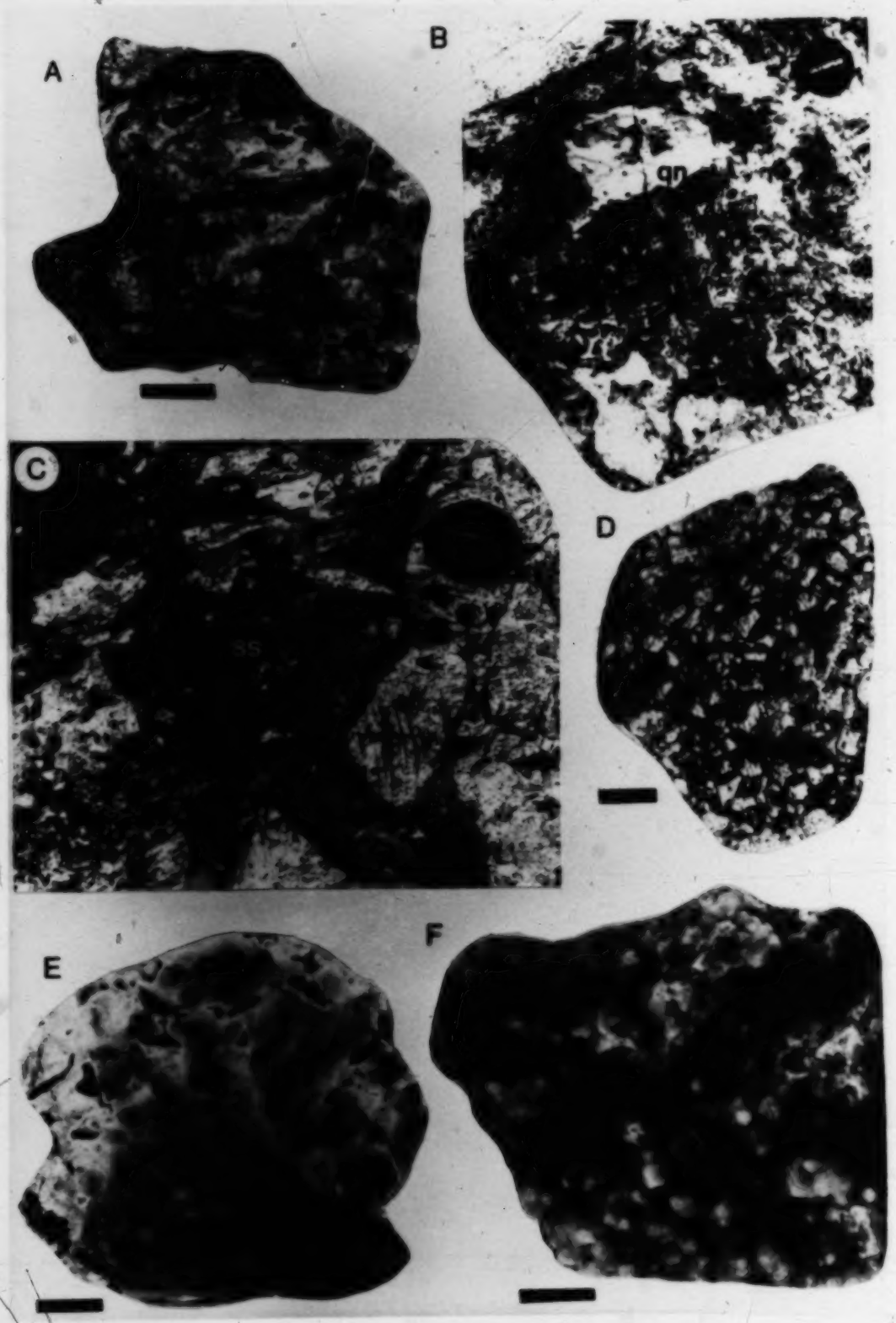
A
B
qp
C
D
E
F

Plate 15

(15A) Field photograph showing cliff forming sandstone of the Mowitch Formation (Cinquefoil Mountain section); Mount Greenock (MG) in background. Scale bar equals 4 m.

(15B) Field photograph showing chert (c) patches in sandstone (Ms) of the Mowitch Formation (Mount Greenock section). Lens cap (55 mm in dia.) for scale.

(15C) Polished hand specimen showing black, phosphate nodule (pn) in sandstone of the Mowitch Formation (Mount Greenock section). Scale bar equals 1 cm.

(15D) Photomicrograph of chert arenite of the Mowitch Formation (Mount Greenock section). Note the well sorted quartz grains with quartz overgrowths (qo) and phosphate fragments (ph). Crossed-nicols. Scale bar equals 0.2 mm.

(15E) Field photograph of uppermost beds of the Mowitch Formation (Mount Greenock section) with abundant vertical burrows (vb). Scale bar equals 10 cm.

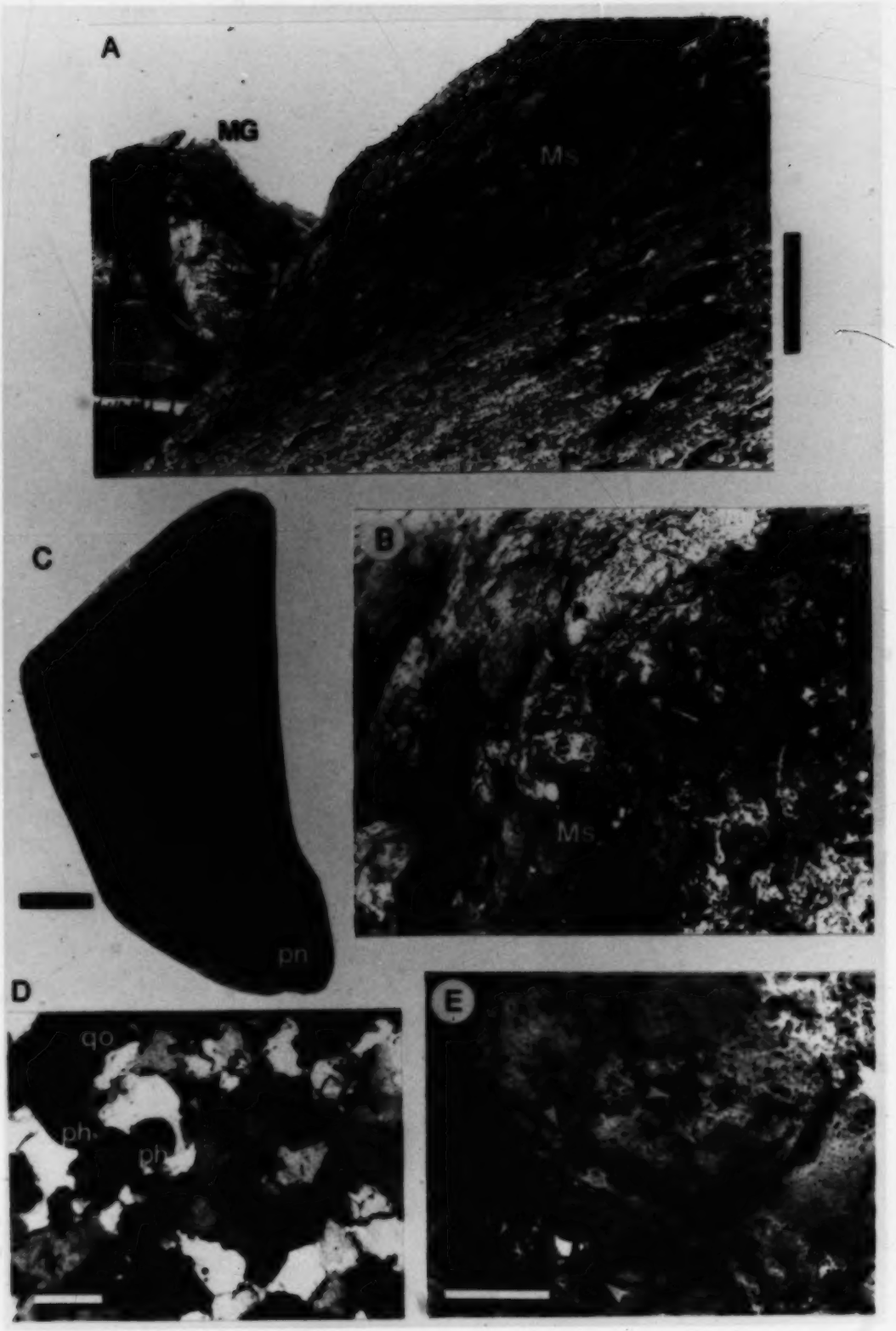
A
MG
Ms
B
Ms
C
pn
D
qo
ph
ph
E

Plate 16

Photomicrographs

(16A) Euhedral to subhedral dolomite crystals (d) showing hypidiotopic crystalline fabric; dolomite rhombs abut upon coarse calcite spar (c). Specimen of lithotype TV2 (Talbot Lake section). Scale bar equals 0.2 mm.

(16B) Selective replacement of micritic peloids (p) by euhedral dolomite (d) crystals. Note the partial dissolution of dolomite crystal and peloid cut by stylolite (st); c = calcite spar. Specimen of lithotype TV2 (Talbot Lake section). Scale bar equals 0.1 mm.

(16C) Crystalline dolomite with cloudy centre (a) encased by clear periphery (b). Specimen of lithotype TV4 (Talbot Lake section). Scale bar equals 0.2 mm.

(16D) Dolomite replacement of crinoid fragment. Internal replacement by small dolomite crystals (d_1); external impingement by matrix dolomite (d_2); pseudomorphic replacement by a single dolomite crystal (d_3). Specimen of lithotype TV4 (Talbot Lake section). Scale bar equals 0.2 mm.

(16E) Note the poorly defined boundaries of intraclasts (i) and matrix dolomite (d). Specimen of lithotype E2 (Mount Greenock section). Scale bar equals 0.2 mm.

(16F) Authigenic quartz crystal (q) with abundant relic inclusions of anhydrite lath (a). Note that some laths (arrows) arranged parallel to crystal faces of quartz crystal. Specimen of lithotype TV4 (Mount Greenock section). Crossed-nicols. Scale bar equals 0.1 mm.

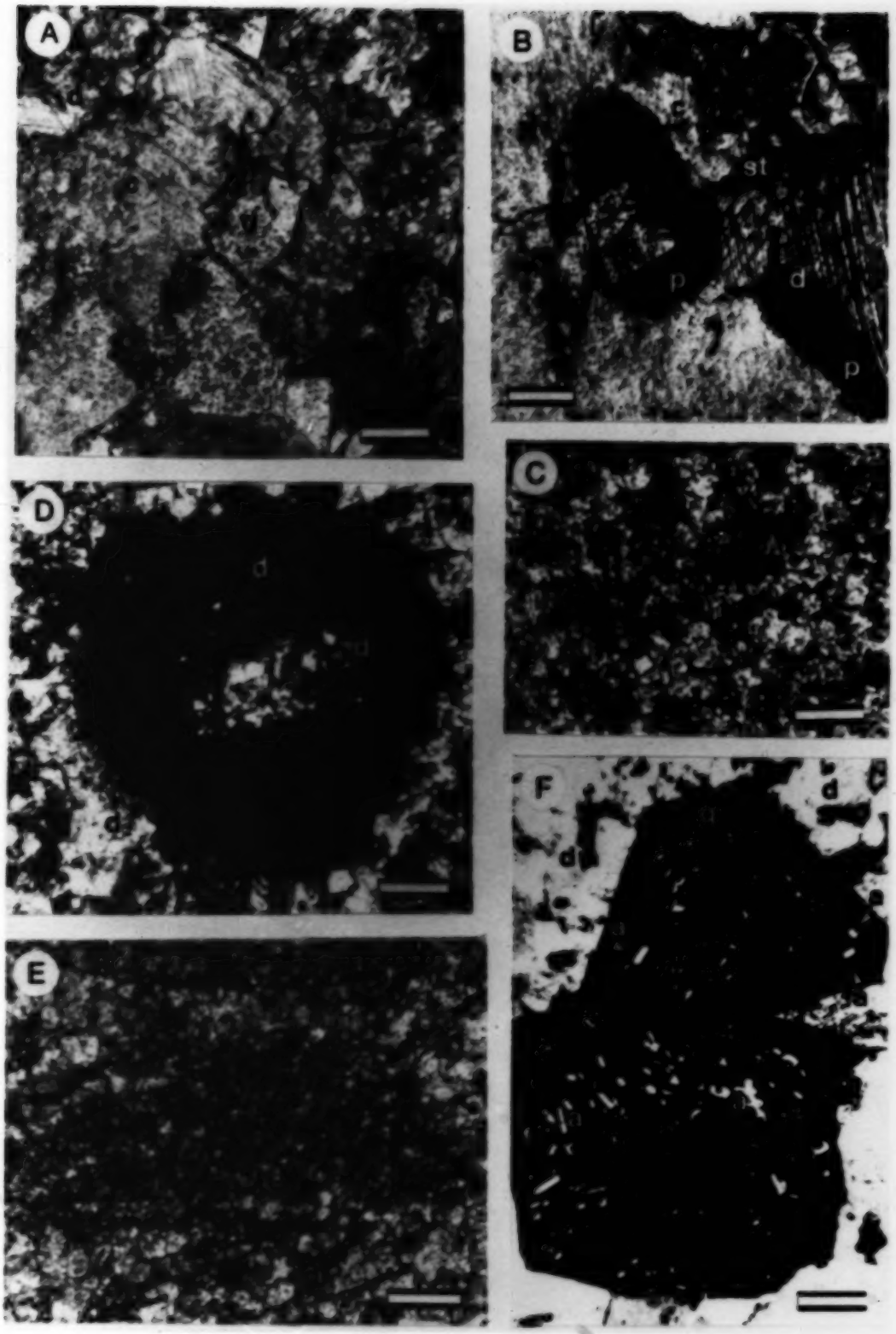
A
d
B
st
p
d
p
C
D
d
E
F
d
d

Plate 17

(17A) Photomicrograph showing microcrystalline quartz (c) with coarser grained quartz (m) which replaces bioclastic fragments. Specimen of lithotype MH3 (Mount Greenock section). Cross-nicols. Scale bar equals 0.2 mm.

(17B) Photomicrograph showing microcrystalline quartz (m) lining cavity walls. Note the sawtooth, right-angled (arrows) grain boundaries of megacrystalline quartz (q) which may be related to precursor evaporite minerals. Specimen of lithotype E7 (Mount Greenock section). Crossed-nicols. Scale bar equals 0.2 mm.

(17C) Photomicrograph showing dolomite rhombs (r) scattered in microcrystalline chert (c). d indicates the dolomitized portion of the rock remains unchertified. Specimen of lithotype MH4 (Mount Greenock section). Scale bar equals 0.1 mm.

(17D) Polished hand specimen of lithotype E6 (Snaring River section) showing fine laminations (arrows) pass through chert nodule (cn) from matrix dolostone with no apparent disruption. Scale bar equals 1 cm.

(17E) Photomicrograph showing length-fast chalcedonic fibres (f) radiating normal to the surface of a microcrystalline chert (c) clast. Specimen of lithotype E1 (Talbot Lake section). Crossed-nicols. Scale bar equals 0.2 mm.

(17F) Photomicrograph showing fissure filled with two layers of length-fast chalcedony (f_1 and f_2); followed by megacrystalline quartz (q). Specimen of lithotype E6 (Cinquefoil Mountain section). Crossed-nicols. Scale bar equals 0.1 mm.

(17G) Photomicrograph showing cavity between intraclasts (di = dolostone clasts, ci = chert clasts) filled with length-fast chalcedony; followed by megacrystalline quartz (q). Note the well arranged spherulitic structures (arrows). Specimen of basal intraclasts and conglomerate (Snaring River section). Crossed-nicols. Scale bar equals 0.1 mm.

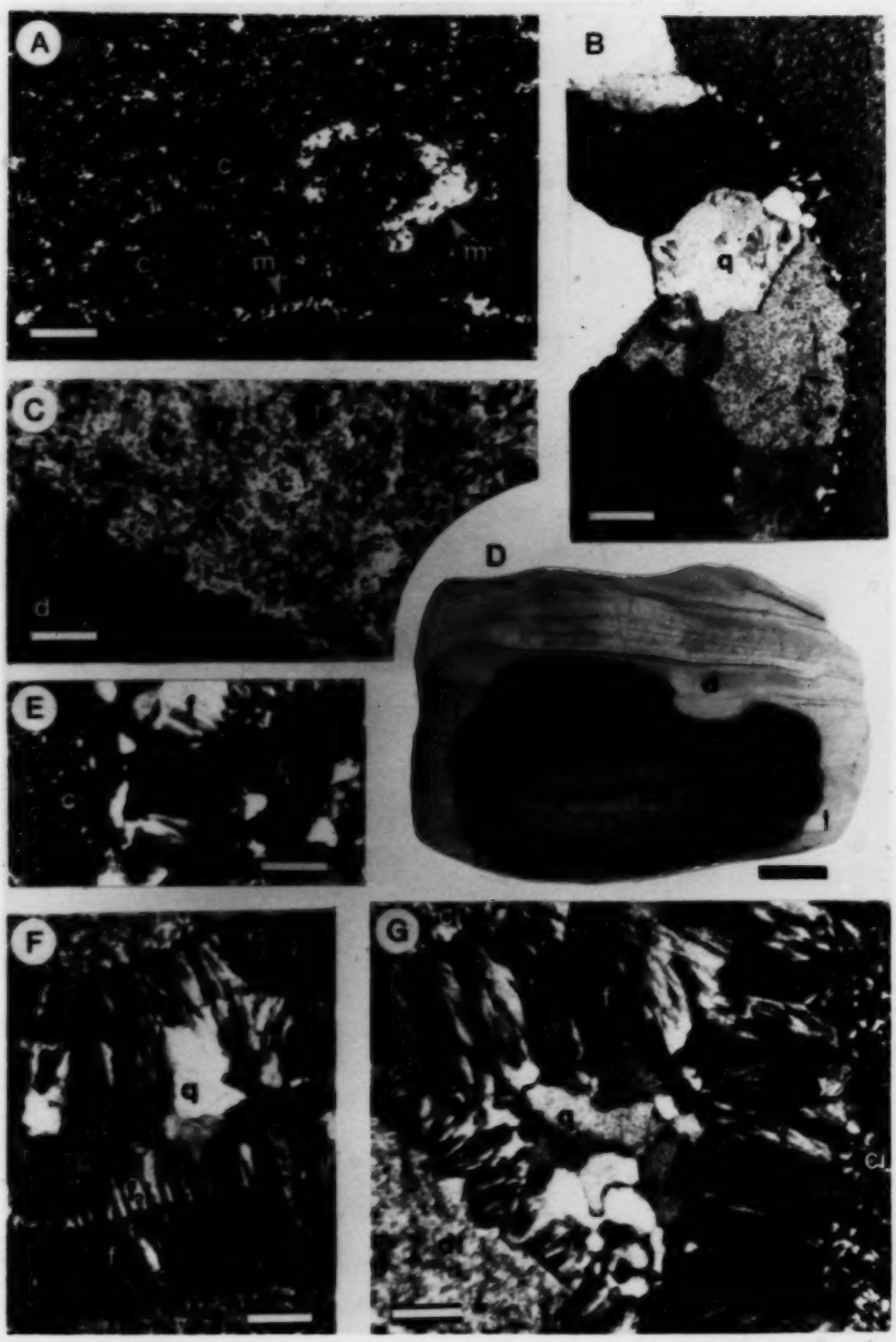
A
c
c
m
m'
B
q
C
d
D
E
c
F
q
G
c
c
c

Plate 18

(18A) Photomicrograph showing aggregates of length-slow spherules (s) having polygonal outlines (arrows). Specimen of lithotype E1 (Talbot Lake section). Crossed-nicols. Scale bar equals 0.2 mm.

(18B,18C,18D) Photomicrographs showing length-slow spherules (s) in pisolitic structures. Specimen of lithotype E6 (Talbot Lake section). (18B) shows compound structures of pisoliths. Note the spherules grade outward to megacrystalline quartz (q) and dolomite crystals. Crossed-nicols. Scale bar equals 0.1 mm. (18C) shows spherules (s) with coarse length-slow fibres; outer margin of spherules circumscribed by a zone of thin, parallel lines (z). Crossed-nicols. Scale bar equals 0.1 mm. (18D) shows right-angled crenulations (arrows) of parallel lines (z) circumscribing length-slow spherules (s). Scale bar equals 0.05 mm.

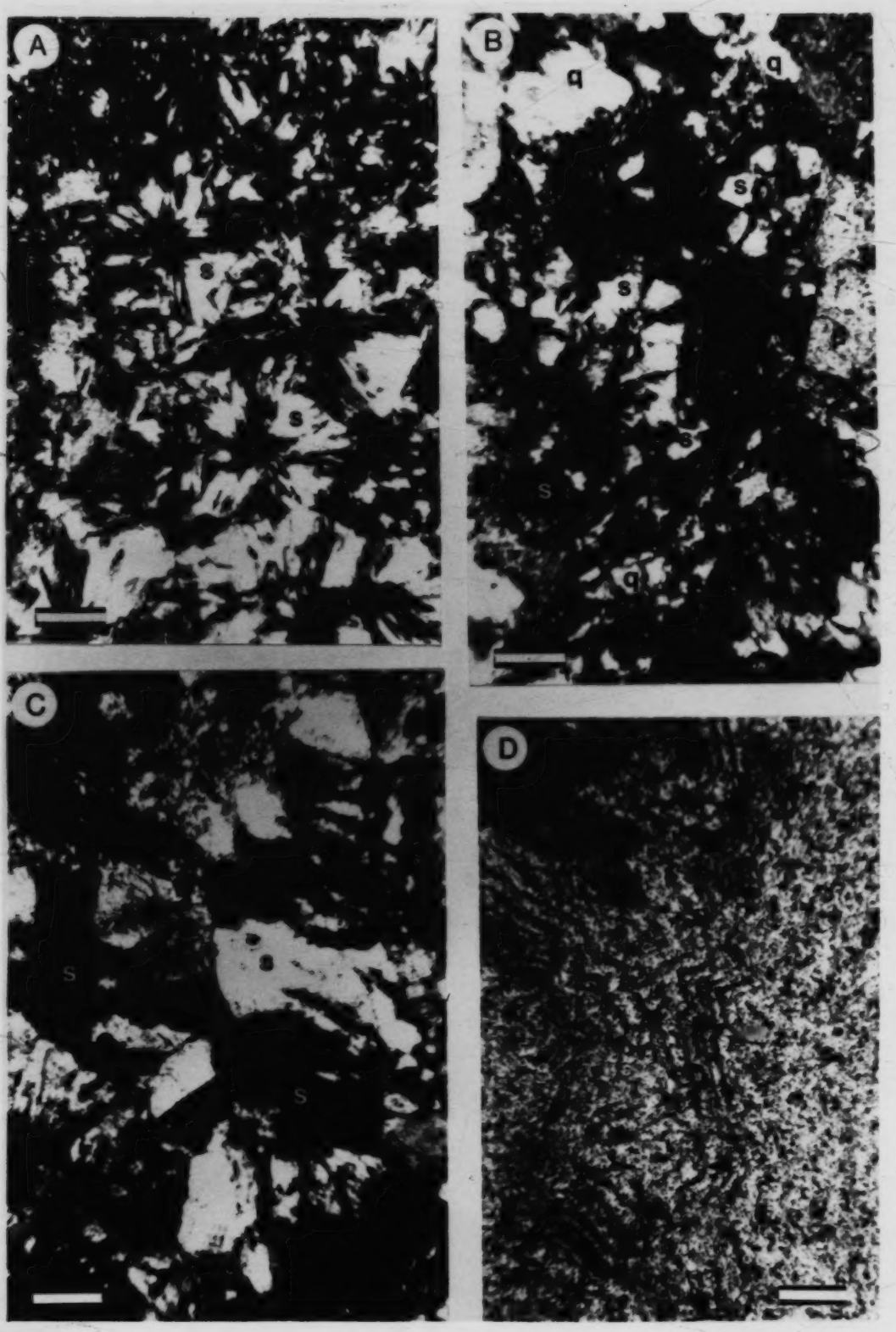
A
B
q
q
s
s
s
s
C
s
s
D

Plate 19

(19A) Photomicrograph showing allochem molds filled with megacrystalline quartz (q); c = microcrystalline quartz with sponge spicules (sp). Specimen of chert of the Ranger Canyon Formation (Mount Greenock section). Crossed-nicols. Scale bar equals 0.2 mm.

(19B) Photomicrograph showing a fossil fragment replaced by flamboyant megacrystalline quartz (q); d = medium crystalline matrix dolomite. Specimen of lithotype MH1 (Talbot Lake section). Crossed-nicols. Scale bar equals 0.2 mm.

(19C) Photomicrograph showing quartz spherules (qs) in very fine crystalline dolomite (d); mf = megacrystalline quartz with microflamboyant fabric. Specimen of lithotype E7 (Mount Greenock section). Crossed-nicols. Scale bar equals 0.2 mm.

(19D) Photomicrograph showing authigenic quartz (q) replaces matrix dolomite (d) and dolomite spar (dc); r = dolomite relics. Specimen of lithotype E6 (Talbot Lake section). Crossed-nicols. Scale bar equals 0.1 mm.

(19E) Photomicrograph showing cubic quartz crystal (q). Note the external zonations of fibrous quartz (f) and elongated megacrystalline quartz (q). Specimen of lithotype E7 (Mount Greenock section). Crossed-nicols. Scale bar equals 0.2 mm.

(19F) Photomicrograph showing external zonations similar to (19E); f = fibrous quartz, q = megacrystalline quartz, arrows indicate the zonations. Note the internal zonation with indication of relic fibres growing centripetally. Crossed-nicols. Scale bar equals 0.2 mm.

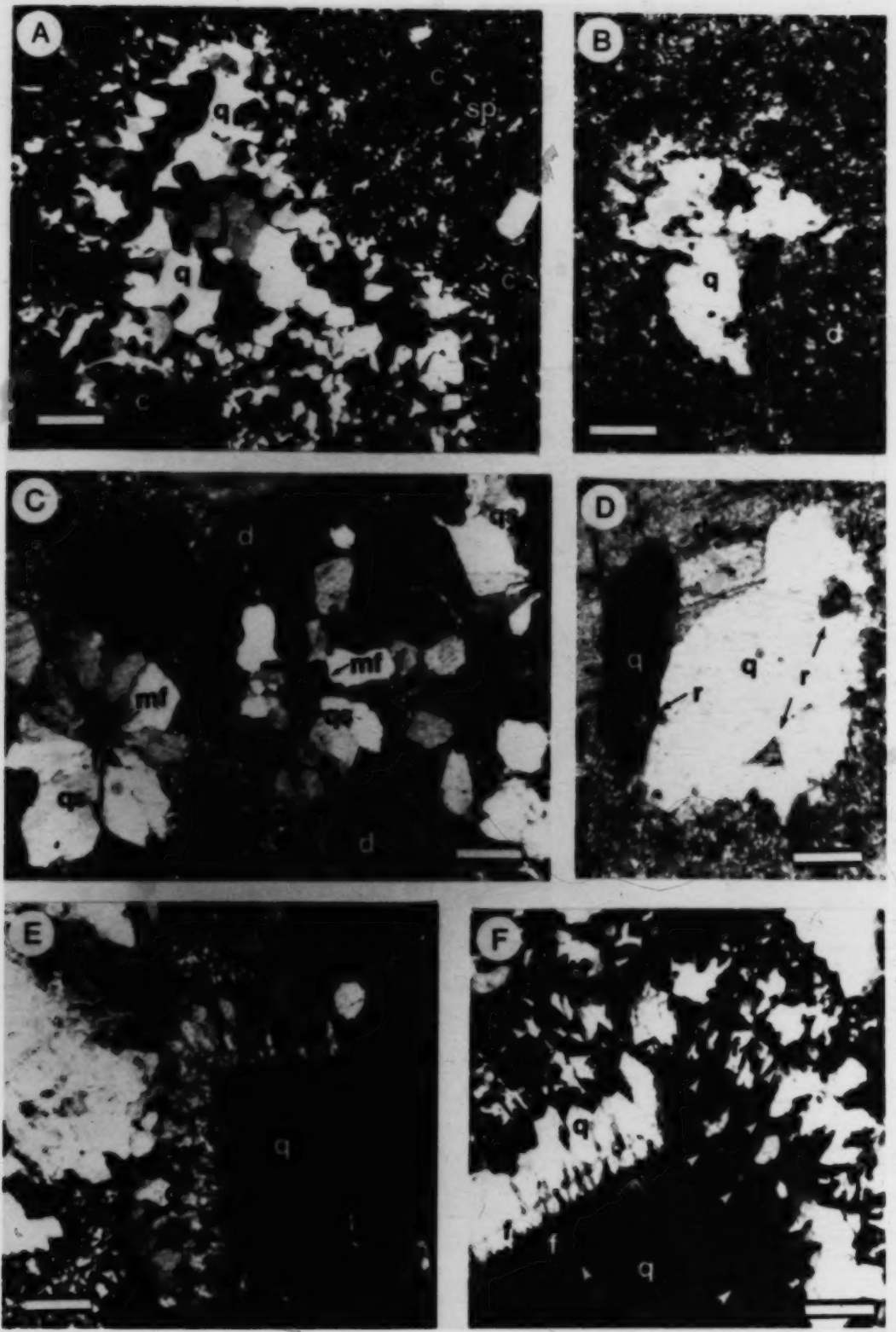
A
q
c
sp
q
c
c
B
q
d
C
d
ml
ml
q
d
D
q
q
r
r
E
q
F
q
q

Plate 20

Photomicrographs

(20A) Evidence of silica solution of monoaxon sponge spicules. 'a' indicates enlargement of central canals, 'b' indicates decoupling of central canal from the spicule. Specimen of Ranger Canyon chert (Snaring River section). Scale bar equals 0.1 mm.

(20B) Scattered, hollow euhedral rhombs (r) and calcite rhombs (ca) in microcrystalline quartz (c). Specimen of Ranger Canyon chert (Snaring River section). Scale bar equals 0.1 mm.

(20C) Quartz overgrowths (qo) on quartz grains. Specimen of chert arenite matrix of the chert conglomerate (Talbot Lake section). Crossed-nicols. Scale bar equals 0.1 mm.

(20D) Scattered hollow rectangles (a) and calcite rhombs (ca) in microcrystalline quartz (c). Specimen of Ranger Canyon chert (Snaring River section). Crossed-nicols. Scale bar equals 0.1 mm.

(20E) Chertified brachiopod shell with well preserved fibrous structure; d = medium crystalline dolomite. Specimen of lithotype E4 (Snaring River section). Crossed-nicols. Scale bar equals 0.1 mm.

(20F) Microfractures in chert clast (c) filled with fine crystalline dolomite (arrows) like that of matrix (d). Specimen of lithotype E1 (Talbot lake section). Crossed-nicols. Scale bar equals 0.2 mm.

(20F) Chalcedonic rim (r) dislodged from a chert clast which is formed of quartz spherules (qs) encased by chalcedony (ch); d = fine crystalline matrix dolomite. Specimen of lithotype E1 (Talbot Lake section). Crossed-nicols. Scale bar equals 0.2 mm.

(20G) Selective silicification of coarse dolomite (d) cement along rhombohedral cleavages (arrows). Specimen of lithotype MH6 (Cinquefoil Mountain section). Scale bar equals 0.1 mm.

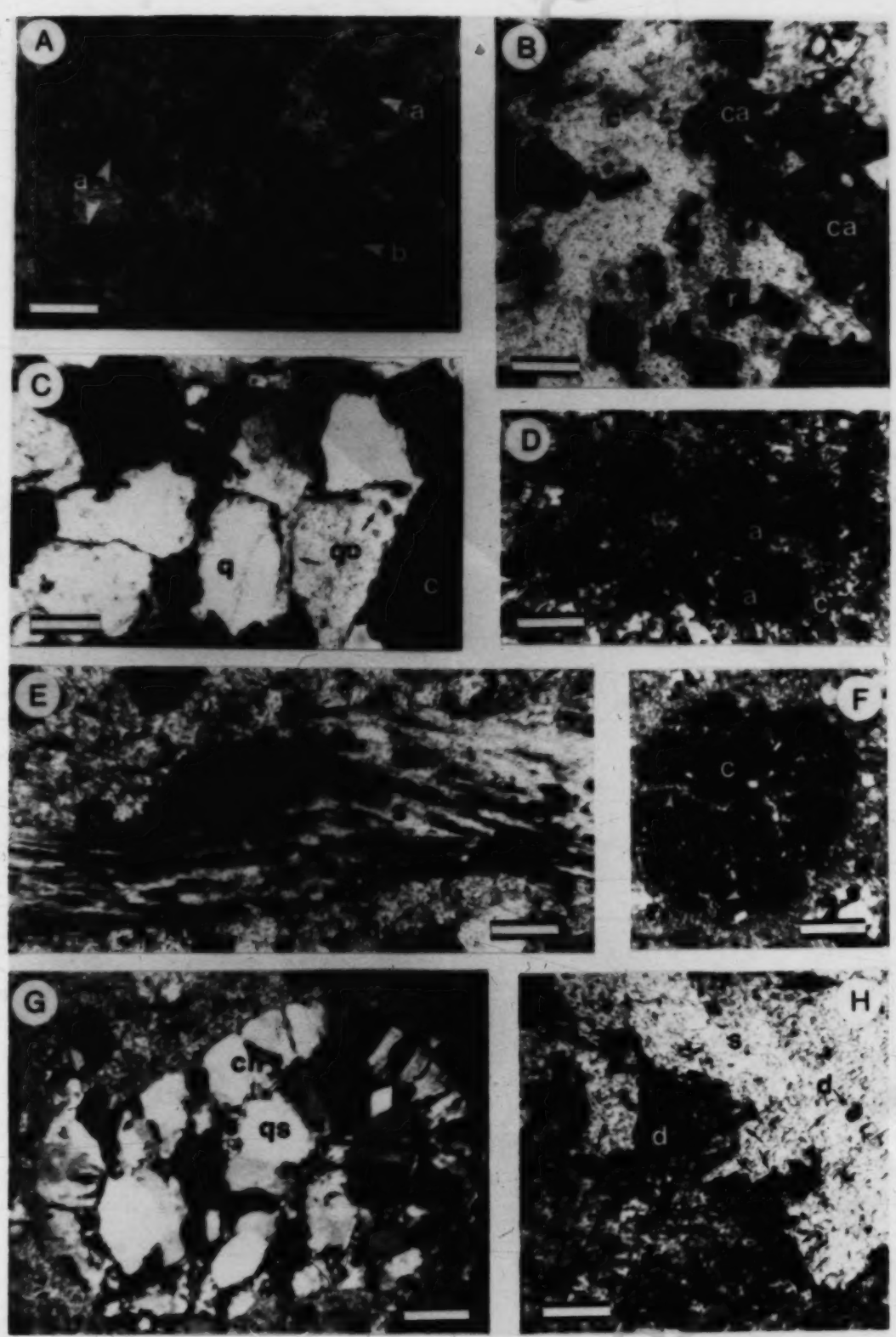
A
a
a
b
B
ca
ca
C
q
qp
c
D
a
a
c
E
F
c
G
ch
qs
H
s
d
d

Plate 21

Photomicrographs

(21A) Sparry calcite (sc) and syntaxial overgrowths (c) on crinoid fragments obliterated all primary porosity of the rocks. Specimen of lithotype TV2 (Talbot Lake section). Scale bar equals 0.2 mm.

(21B) Euhedral matrix dolomite (arrows) lines an unfilled fossil mold (v); d = fine to medium crystalline matrix dolomite. Specimen of lithotype MH3 (Talbot Lake section). Scale bar equals 0.2 mm.

(21C,21D) Cavity lined with euhedral, clear, nonferroan dolomite (nd) crystals; followed by a coarse calcite spar (sc). d = medium crystalline matrix dolomite, v = void. Note the zonation of nonferroan dolomite (nd) in (21D). Specimen of lithotype TV2 (Talbot lake section). Scale bar for (21C) equals 0.1 mm; for (21D) equals 0.2 mm.

(21E,21F) Thin sections stained with potassium ferricyanide solution. Cavities lined with microcrystalline quartz (q); followed by coarse, ferroan dolomite (fd). Note that ferroan dolomite (fd) replaced by dolomite (dr) that grew out from matrix; also note partial solution of ferroan dolomite (fd) in (21E), cavity in (21F) filled with euhedral quartz crystals (q). Specimens of lithotypes MH1 (Plate 21E) and MH3 (Plate 21F) from the Talbot Lake section. Scale bars for (21E) and (21F) equal 0.2 mm.

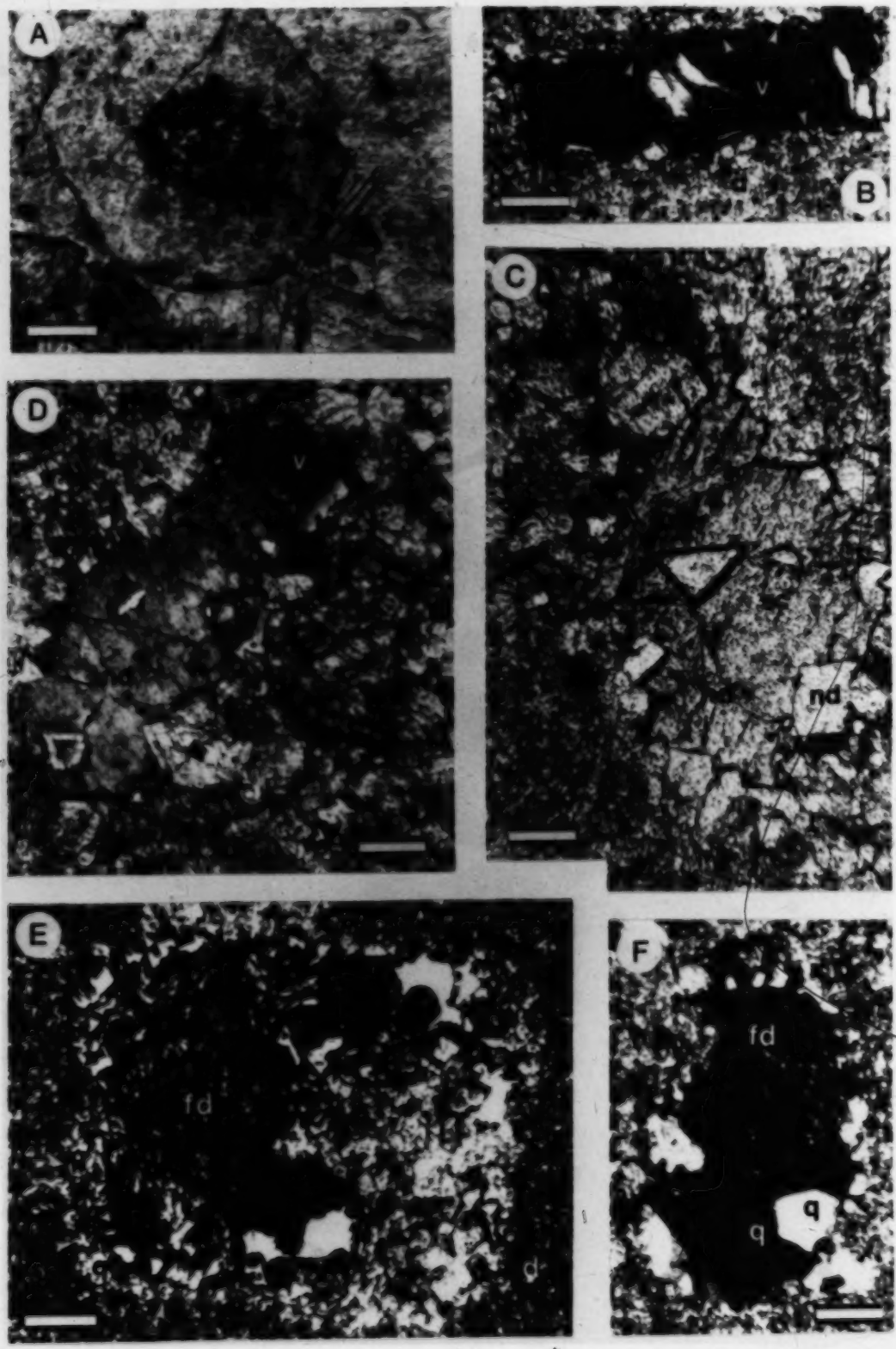
A
B
v
C
nd
D
v
E
fd
d
F
fd
q
q

Plate 22

Photomicrographs

(22A) Cavity lined with clear, nonferroan dolomite (nd); followed by a coarse dolomite spar (ds). d = fine crystalline matrix dolomite. Specimen of lithotype MH3 (Mount Greenock section). Scale bar equals 0.2 mm.

(22B) Fracture filled with coarse dolomite spar (ds); d = fine crystalline matrix dolomite. Specimen of lithotype E4 (Snaring River section). Scale bar equals 0.2 mm.

(22C) Bird's-eye vug lined with clear, nonferroan dolomite (nd); followed by euhedral dolomite spar (ds). d = fine crystalline matrix dolomite. Specimen of lithotype MH6 (Talbot Lake section). Crossed-nicols. Scale bar equals 0.2 mm.

(22D) Roof of bird's-eye vug lined with microstalactitic calcite (mc); v = void, d = fine crystalline matrix dolomite. Note the partial solution of microstalatitic calcite. Specimen of lithotype MH6 (Cinquefoil Mountain section). Scale bar equals 0.1 mm.

(22E) Cavity roof in Ranger Canyon chert (c) lined with microstalactitic calcite (mc); followed by coarse calcite spar (sc). Note the continuity of laminae which followed contour of cavity roof. Specimen from the Mount Greenock section. Scale bar equals 0.1 mm.

(22F,22G) Enlarged view of microstalactite showing alternating dark, thin and clear, thicker calcite laminae. (22G) shows sweeping radial extinction under crossed-nicols. Scale bar for (22F) and (22G) equal 0.05 mm.

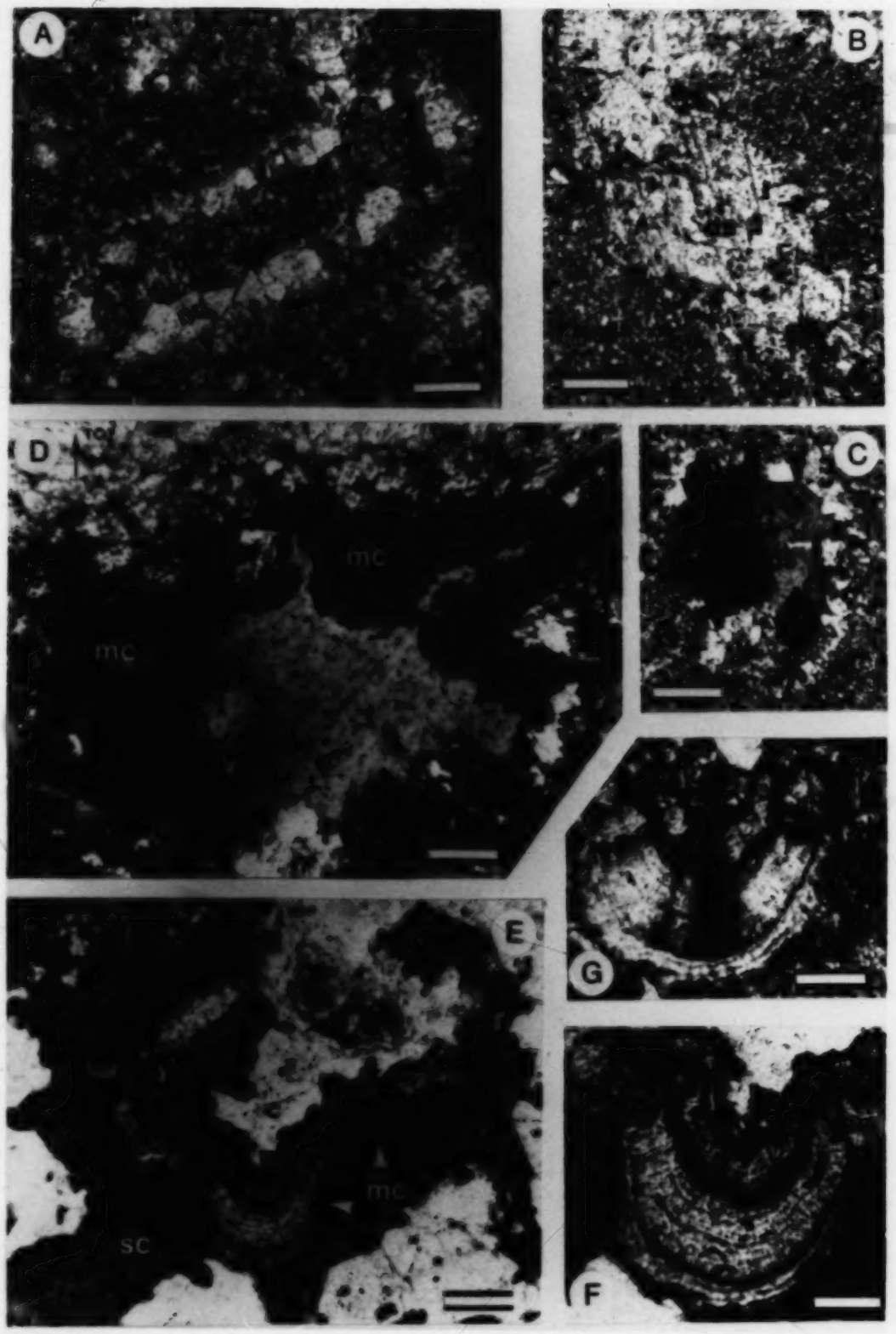
A
B
C
D
mc
mc
E
mc
sc
F
G

Plate 23

Photomicrographs

(23A) Fracture in sandy dolomite (d = matrix dolomite, q = quartz grains) filled with euhedral dolomite spar (d) and coarse bar (sc). Specimen of basal intraclast and conglomerate (Snaring River section). Scale bar equals 0.2 mm.

(23B) Fractures in fine crystalline dolomite (d) filled with coarse calcite spar (sc). Specimen of lithotype MH8 (Snaring River section). Scale bar equals 0.2 mm.

(23C) Coarse calcite spar (sc) in Ranger Canyon chert (c) poikilitically enclosing sponge spicules (sp) and phosphate fragments (p). Specimen from the Snaring River section. Scale bar equals 0.1 mm.

(23D) Cavity lined with microcrystalline quartz (arrows); followed by sparry calcite (sc) which is bounded by a thin calcite lamina (c). v = void. Specimen of lithotype MH3 (Mount Greenock section). Scale bar equals 0.2 mm.

(23E) Partial solution of sparry calcite (sc) cement forming pitted crystal surface (arrows); subsequently filled with two phases of internal sediments (ia and ib). v = void. Specimen of lithotype MH3 (Mount Greenock section). Scale bar equals 0.2 mm.

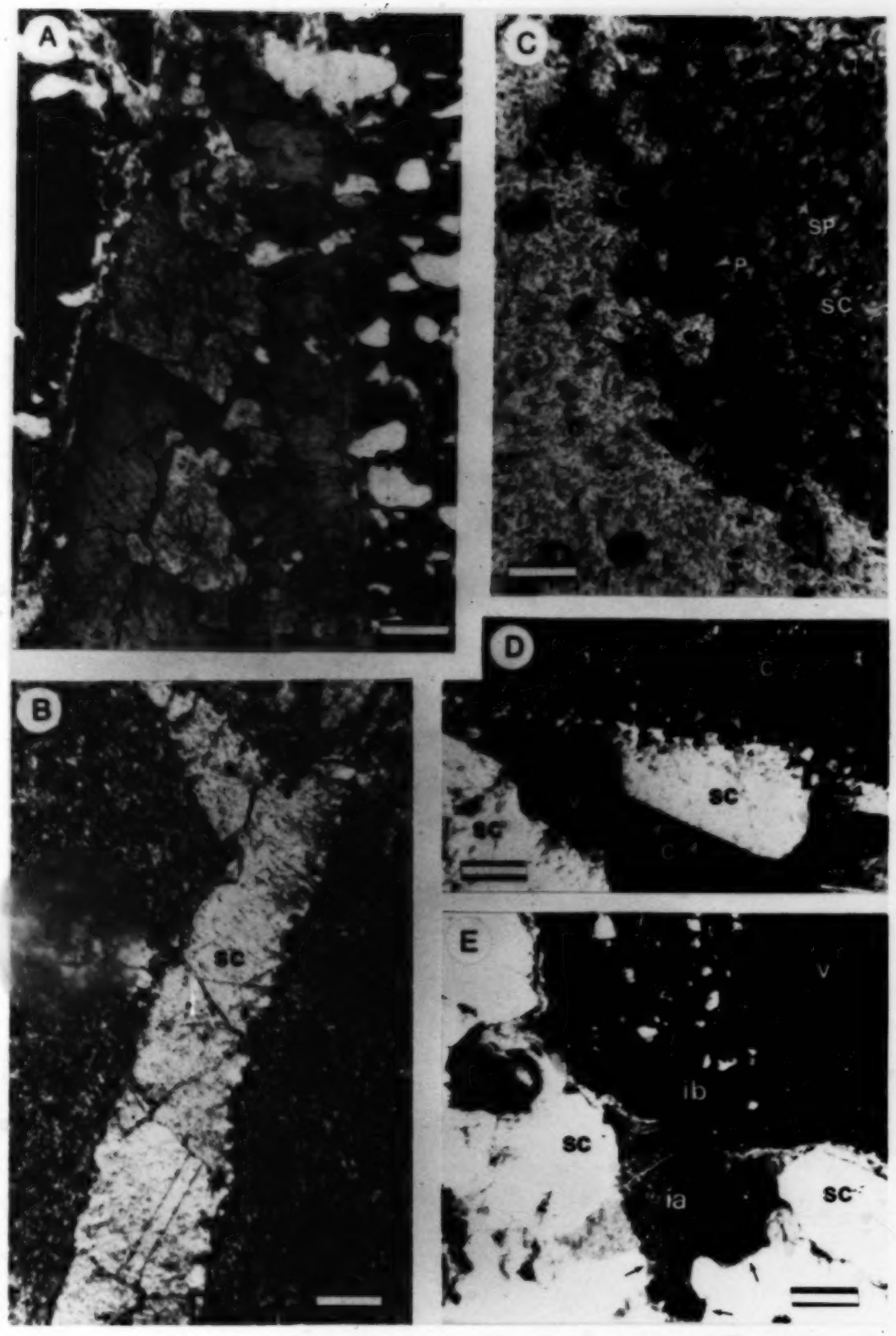
A
B
sc
C
SP
P
sc
D
C
sc
sc
C
E
V
ib
sc
ia
sc

Plate 24

Photomicrographs

(24A) Dolomite replaced by calcite (c) leaving only dolomite remnants (d). Arrows indicate outlines of original dolomite rhombs. Specimen of lithotype TV4 (Talbot Lake section). Scale bar equals 0.05 mm.

(24B) Dolomite (d) cement in fracture partially replaced by calcite (c). Specimen of lithotype MH2 (Mount Greenock section). Scale bar equals 0.05 mm.

(24C) Polycrystalline calcite (c) pseudomorphs after dolomite (d) crystals. Arrows indicate outlines of calcite rhombs. Specimen of lithotype TV4 (Talbot Lake section). Scale bar equals 0.1 mm.

(24D) Coarse calcite spar (c) poikilitically enclosing rounded and corroded relics of dolomite (d). Specimen of lithotype TV4 (Talbot Lake section). Scale bar equals 0.1 mm.

(24E) Scattered calcite rhombs (c) and dolomite molds (r) in microcrystalline chert (ch). Specimen of Ranger Canyon chert (Snaring River section). Scale bar equals 0.1 mm.

(24F) Zonal replacement of dolomite crystals; d = unreplaced dolomite, c = calcite zone. Specimen of lithotype MH1 (Talbot Lake section). Scale bar equals 0.1 mm.

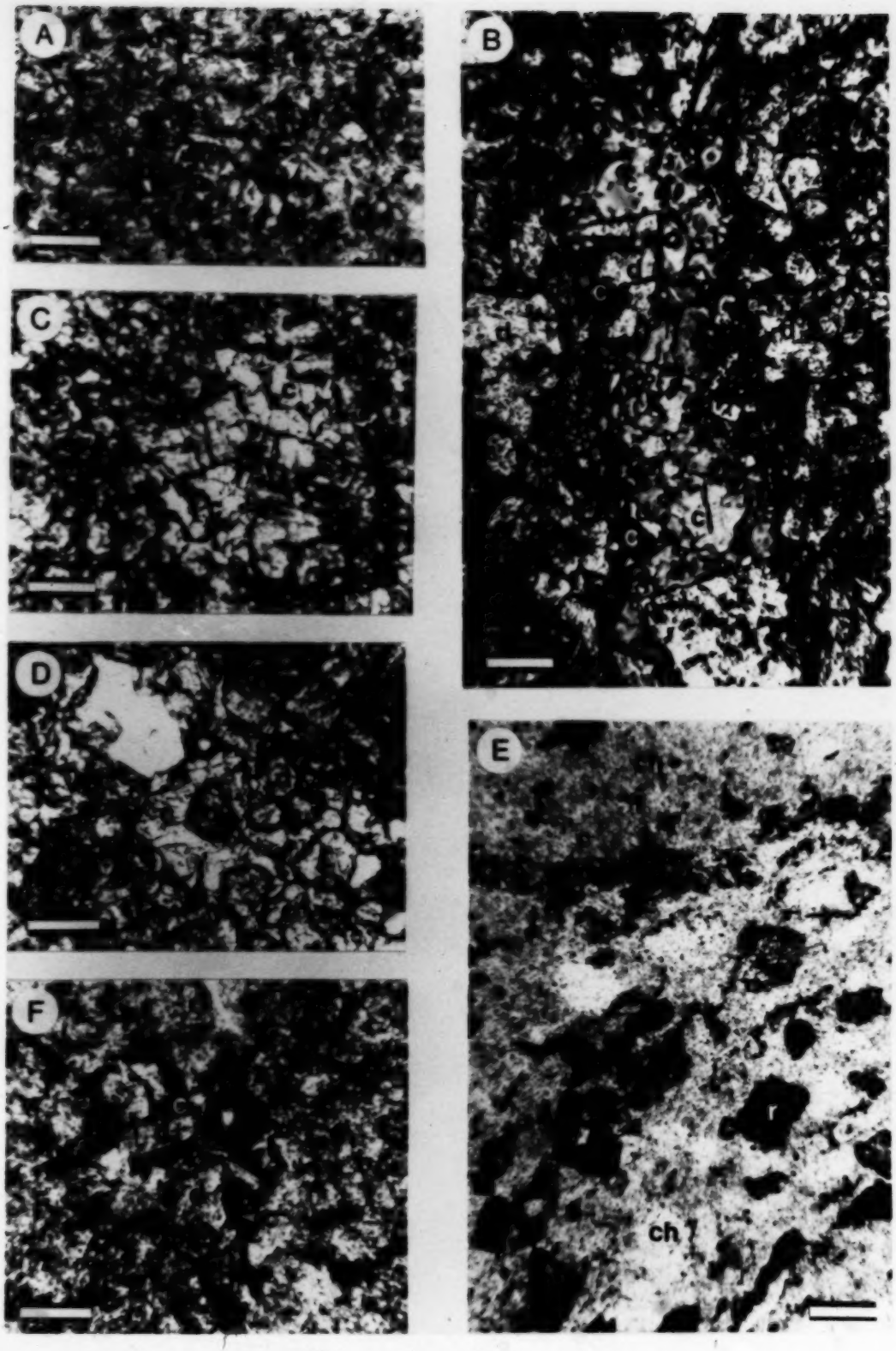
A
B
C
C
C
C
C
D
E
ch
F
C

Plate 25

(25A) Photomicrograph showing rhombohedral hematite (h) pseudomorphs after matrix dolomite (d). Specimen of lithotype TV4 (Talbot Lake section). Scale bar equals 0.05 mm.

(25B) Photomicrograph showing preferential replacement of silicified dolomite cement (s) by hematite (h) along cleavage planes; d = fine crystalline matrix dolomite. Specimen of lithotype MH7 (Cinquefoil Mountain section). Scale bar equals 0.05 mm.

(25C) Photomicrograph showing silicified fossil fragment (s) replaced by hexagonal hematite (h) crystals; d = fine crystalline matrix dolomite. Specimen of lithotype TV4 (Talbot Lake section). Scale bar equals 0.1 mm.

(25D) Photomicrograph showing hematite (h) pseudomorphs after stellate array of gypsum crystals; d = fine crystalline matrix dolomite. Specimen of lithotype E4 (Snaring River section). Scale bar equals 0.05 mm.

(25E) Polished hand specimen of lithotype MH9 showing pyrite (py) crystals associated with a burrow (b) in fine crystalline dolomite (d). Specimen of lithotype MH9 (Snaring River section). Scale bar equals 0.5 mm.

(25F) Photomicrograph showing anhedral aggregates of quartz crystals (q); d = fine crystalline matrix dolomite. Specimen of lithotype MH9 (Snaring River section). Scale bar equals 0.2 mm.

(25G) Photomicrograph showing quartz crystals having pinacoid and diametral prism crystal forms; d = fine crystalline matrix dolomite. Specimen of lithotype E3 (Snaring River section). Scale bar equals 0.2 mm.

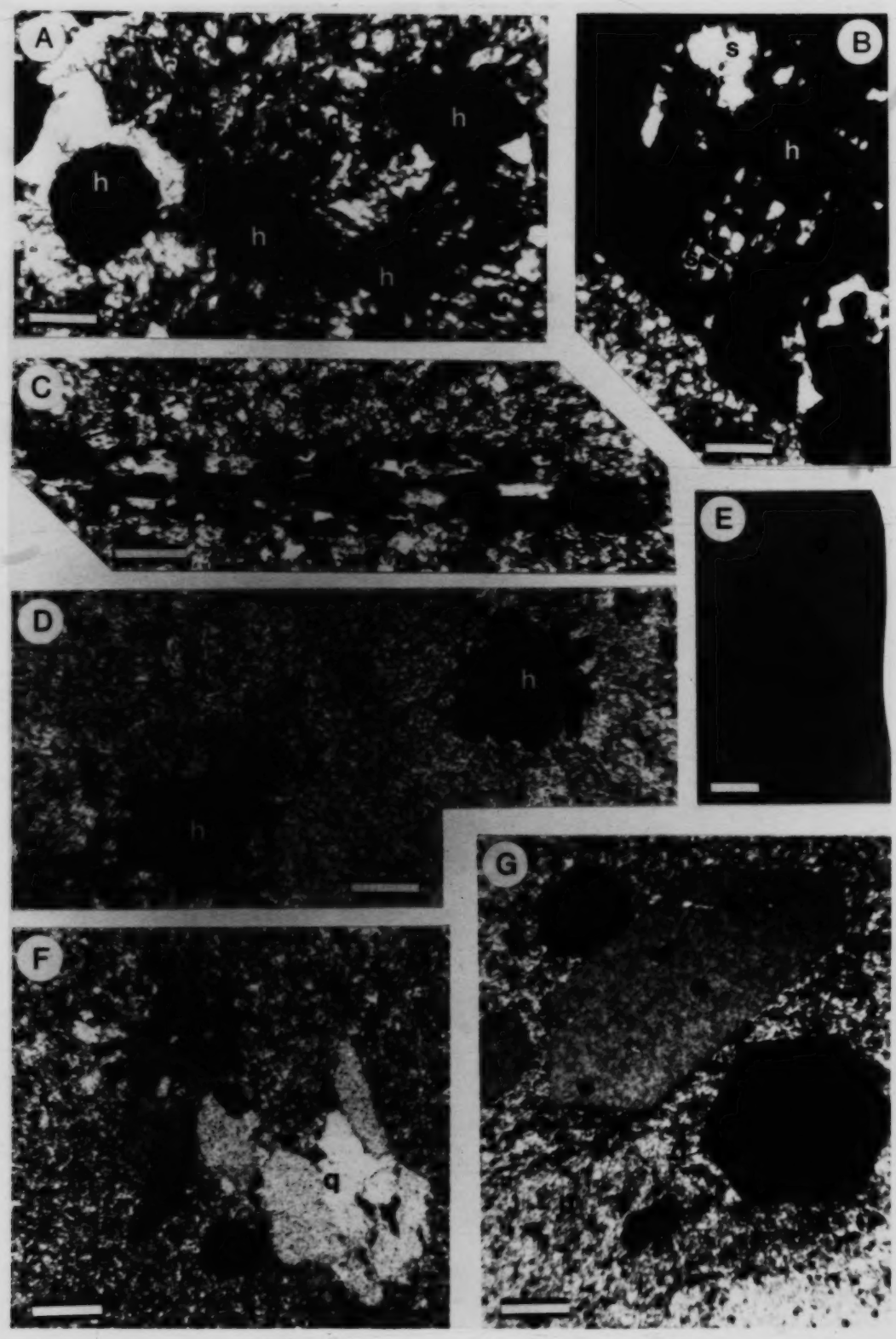
A
h
h
h
h
B
s
h
C
D
h
h
E
F
q
G

Plate 26

(26A) Field photograph of lithotype MH3 (Talbot Lake section) showing well developed stylolite (st) in crinoid dolostone.

(26B) Photomicrograph showing concentration of detrital quartz grains (q) along stylolite (st); d = fine crystalline matrix dolomite. Specimen of lithotype E2 (Mount Greenock section). Scale bar equals 0.1 mm.

(26C) Photomicrograph showing concentration of iron oxide and organic residue along stylolite (st); d = fine crystalline matrix dolomite. Specimen of lithotype MH1 (Talbot Lake section). Scale bar equals 0.1 mm.

(26D) Polished hand specimen of lithotype TV2 (Talbot Lake section) showing brecciated dolostone (d) cemented by calcite (c). Scale bar equals 1 cm.

(26E) Photomicrograph showing phosphate nodule in chert arenite of the Mowitch Formation (Mount Greenock section). Note the irregular contact of black phosphate nodule (p) with surrounding arenite (q), and corroded quartz grains (q) in phosphate. Scale bar equals 0.2 mm.

(26F) Enlarged view of (26E) showing corroded quartz grains (q) and tooth-like phosphate (t) in black phosphate nodule (p). Scale bar equals 0.1 mm.

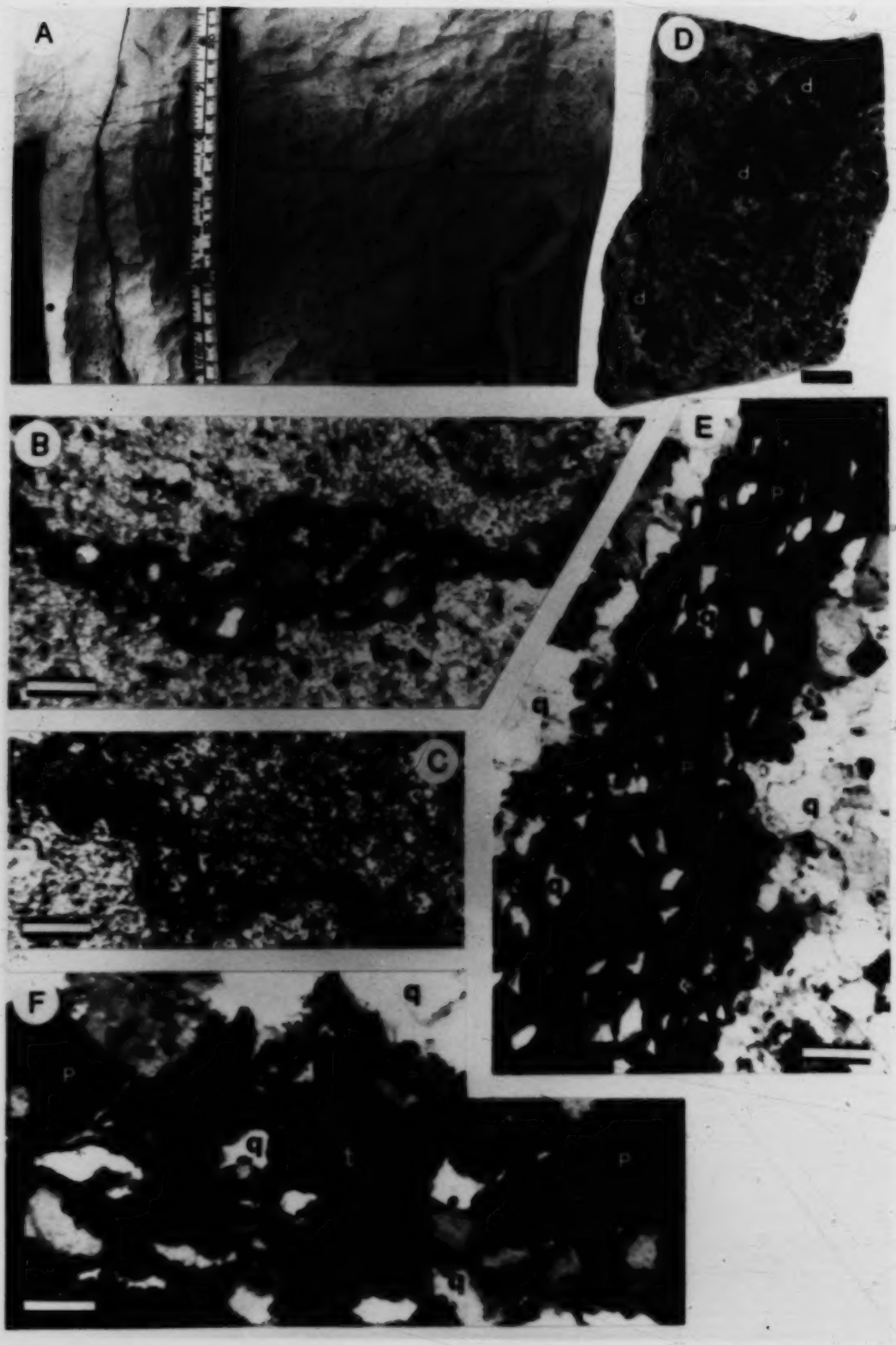
A
D
d
d
d
B
E
P
q
q
q
C
F
q
P
q
P
q

XIII. REFERENCES

Adams, J. E. and Rhodes, M. L. 1960. Dolomitization by seepage refluxion. Bulletin of American Association of Petroleum Geologists, v. 44, p. 1912-1920.

Al-Hashimi, W. S. and Hemingway, J. E. 1973. Recent dedolomitization and the origin of the rusty crust of Northumberland. Journal of Sedimentary Petrology, v. 43, p. 82-91.

Allen, J. R. L. 1967. Depth indicators of clastic sequences. Marine Geology, v. 5, p. 429-446.

Allen, J. R. L. 1970. Studies in fluvialtile sedimentation: a comparison of fining upwards cyclothems, with special reference to coarse member composition and interpretation. Journal of Sedimentary Petrology, v. 40, p. 298-323.

Assereto, R. L. and Kendall, C. G. St C. 1977. Nature, origin and classification of peritidal tepee structures and related breccias. Sedimentology, v. 24, p. 153-210.

Badiozamani, K. 1973. The Dorag dolomitization model - application to the Middle Ordovician of Wisconsin. Journal of Sedimentary Petrology, v. 43, p. 965-984.

Badiozamani, K., MacKenzie, F. T. and Thorstenson, D. C. 1977. Experimental carbonate cementation - salinity, temperature and vadose-phreatic effects. Journal of Sedimentary Petrology, v. 47, p. 529-542.

Baker, P. A. and Kastner, M. 1981. Constraints on the formation of sedimentary dolomite. Science, v. 213, p. 214-216.

Bamber, E. W., Macqueen, R. W. and Ollerenshaw, N. C. 1981. Mississippian stratigraphy and sedimentology, Canyon Creek (Moose Mountain), Alberta. Field Guides to Geology and Mineral Deposits, Geological Association of Canada, p. 177-194.

Ball, S. M. 1971. The Westphalia Limestone of the Northern Midcontinent: A possible ancient storm deposit. Journal of Sedimentary Petrology, v. 41, p. 217-232.

Bally, A. W. 1975. A geodynamic scenario for hydrocarbon occurences. 9th World Petroleum Congress Proceedings, p. 33-43.

Bally, A. W., Gordy P. L., and Steward, G. A. 1966. Structure, seismic data, and orogenic evolution of Southern Canadian Rocky Mountain. Bulletin of Canadian

Petroleum Geology, v. 14, p. 537-381.

Bathurst, R. G. C. 1975, Carbonate sediments and their diagenesis. Elsevier Publishing Co., Amsterdam, Development in Sedimentology, 12, 658p.

Becher, J. W. and Moore, C. H. 1976. The Walker Creek Field: A Smackover diagenetic trap. Transactions Gulf Coast Association of Geological Societies, v. 26, p. 34-56.

Berner, R. A. 1970. Sedimentary pyrite formation. America Journal of Science, v. 268, p. 1-23.

Blatt, H., Middleton, G. V. and Murray, R. C. 1972. Origin of Sedimentary Rocks. Prentice Hall Inc., New Jersey, 634p.

Boardman, R. S. 1960. Trepostomatous bryozoa of the Hamilton Group, New York State. United States Geological Survey, Professional Paper no. 340, 83p.

Brown, R. A. C. 1952. Carboniferous stratigraphy and paleontology in the Mount Greenock aea, Alberta. Geological Survey of Canada, Memoir264, 119p.

Buchbinder, L. G. and Friedman, G. M. 1980. Vadose, phreatic, and marine diagenesis of Pleistocene-Holocene carbonates in a borehole: Mediterranean coast of Israel. Journal of Sedimentary Petrology, v. 50, p. 395-408.

Calvert, S. E. 1974. Deposition and diagensis of silica in marine sediments. Special Publications of the International Association of Sedimentology, 1, p. 273-299.

Cavaroc, V. V. Jr. and Ferm, J. C. 1968. Siliceous spiculites as shoreline indicators in deltaic sequence. Bulletin of Geological Society of America, v. 79, p. 263-271.

Chafetz, H. S. 1972. Surface diagenesis of limestone. Journal of Sedimentary Petrology, v. 52, p. 325-329.

Cheetham, A. H. 1971. Functional morphology and biofacies distribution of Cheilostome Bryozoa in the Danian Stage (Paleocene) of Southern Scandinavia. Smithsonian Contribution to Paleobiology, no. 6, 87p.

Chenoweth, P. A. 1972. Unconformity traps. *In* King, E. A. (*Ed.*) Stratigraphic Oil and Gas Fields - Classification, Exploration Methods and Case Histories. American Association of Petroleum Geologists, Memoir16, p. 42-46.

Cherns, L. 1982. Paleokarst, tidal erosion surfaces and

stromatolites in the Silurian Eke Formation of Gotland, Sweden. Sedimentology, v. 29, p. 819-833.

Chilingar, G. V. 1956. Dedolomitization - a review. Bulletin of American Association of Petroleum Geologists, v. 40, p. 762-778.

Choquette, P. W. 1971. Late ferroan dolomite cement, Mississippian carbonates, Illinois Basin, U.S.A.. *In* Bricker, O. P. (*Ed.*) Carbonate Cement. Johns Hopkins University, Studies in Geology, no. 19, p. 339-345.

Choquette, P. W. and Pray, L. C. 1970. Geologic nomenclature and classification of porosity in sedimentary carbonates. Bulletin of American Association of Petroleum Geologists, v. 54, p. 207-250.

Chowns, T. M. and Elkins, J. E. 1974. The origin of quartz geodes and cauliflower cherts through the silicification of anhydrite nodules. Journal of Sedimentary Petrology, v. 44, p. 885-903.

Coleman, J. M. and Prior, D. B. 1982. Deltaic environments of deposition. *In* Scholle P. A. and Spearing, D. (*Eds.*) Sandstone Depositional Environments. American Association of Petroleum Geologists, Memoir31, p. 139-178.

Cook, P. J. 1970. Repeated diagenetic calcitization, phosphatization, and silification in the Phosphoria Formation. Bulletin of Geological Society of America, v. 81, p. 2107-2116.

Curtis, R., Evans, G., Kinsman, D. J. J. and Shearman, D. J. 1963. Association of dolomite and anhydrite in recent sediments of the Persian Gulf. Nature, v. 197, p. 679-680.

Dahlstrom, C. D. A. 1970. Structural geology in the eastern margin of the Canadian Rcoky Mountains. Bulletin of Canadian Petroleum Geology, v. 18, p. 332-406.

Davies, G. R. 1970. Algal-laminated sediments, Gladstone Embayment, Shark Bay. *In* Logan, B. W., Davies, G. R., Read, J. F. and Cebulski, D. E. (*Eds.*) Carbonate sedimentation and environments, Shark Bay, Western Australia. American Association of Petroleum Geologists, Memoir 13, p. 169-205.

de Groot, K. 1967. Experimental dedolomitization. Journal of Sedimentary Petrology, v. 37, p. 1216-1220.

Deffeyes, K. S., Lucia, F. J. and Weyl, P. K. 1965. Dolomitization of Recent and Plio-Pleistocene sediments

by marine evaporate waters on Bonaire, Netherland Antilles. *In* Pray, L. C. and Murray, R. C. (*Eds.*) Dolomitization and Limestone Diagenesis. Society of Economic Paleontologists and Mineralogists, Special Publication no. 13, p. 71-88.

Dickson, J. A. D. 1965. A modified staining technique for carbonates in thin section. Nature, v. 205, p. 587.

Dietrich, R. V., Hobbs, J. R. B. Jr. and Lowry, W. D. 1963. Dolomitization interrupted by silicification. Journal of Sedimentary Petrology, v. 33, p. 646-663.

Douglas, R. J. W. 1953. Carboniferous stratigraphy in the southern Foothills of Alberta. Alberta Society of Petroleum Geologists, 3rd Annual Field Conference and Symposium, p. 68-88.

Douglas, R. J. W. 1958. Mount Head map area, Alberta. Geological Survey of Canada, Memoir291, 241p.

Douglas, R. J. W., Gabrielse, H., Wheeler, J. D., Stott, D. F. and Belyea, H. R. 1976. Geology of Western Canada. *In* Douglas, R. J. W. (*Ed.*) Geology and Economic Minerals of Canada. Part B, p. 365-488.

Douglas, R. J. W. and Harker, P. 1958. Mississippian succession in Mount Head area, Alberta. *In* J. A. Allan Memorial Volume, Jurassic and Carboniferous of Weatern Canada, American Association of Petroleum Geologists, p. 177-189.

Drummond, J. M. 1961. Detailed Carboniferous correlations between Mount Greenock and Box Canyon, Southern Canadian Rockies. Edmonton Geological Society, 3rd Annual Field Trip Guide Book, p. 43-64.

Dunbar, C. O. and Rodgers, J. 1957. Principle of Stratigraphy. John Wiley and Sons, New York, 356p.

Dunham, R. J. 1962. Classification of carbonate rocks according to depositional texture. *In* Ham, W. E. (*Ed.*) Classification of Carbonate Rocks. American Association of Petroleum Geologists, Memoir1, p. 108-121.

Dunham, R. J. 1969a. Vadose pisolite in the Capitan Reef (Permian), New Mexico and Texas. *In* Friedman, G. M. (*Ed.*) Depositional Environments in Carbonate Rocks. Society of Economic Paleontologists and Mineralogists, Special Publication no. 14, p. 182-191.

Dunham, R. J. 1969b. Early vadose silt in Townsend mound (reef), New Mexico and Texas. *In* Friedman, G. M. (*Ed.*) Depositional Environments in Carbonate Rocks. Society of

Economic Paleontologists and Mineralogists, Special Publication no. 14, p. 139-181.

Dunham, R. J. 1971. Meniscus cement. *In* Bricker, O. P. (*Ed.*) Carbonate Cement. Johns Hopkins University, Studies in Geology, no. 19, p. 297-300.

Dunham, J. B. and Olson, E. R. 1980. Shallow subsurface dolomitization of subtidally deposited carbonate sediments in the Hanson Creek Formation (Ordovician-Silurian) of central Nevada. *In* Zenger, D. H., Dunham, J. B. and Ethington, R. L. (*Eds.*) Concepts and Models of Dolomitization. Society of Economic Paleontologists and Mineralogists, Special Publication no. 28, p. 139-161.

Dunnington, H. V. 1967. Aspects of diagenesis and shape change in stylolitic limestone reservoirs. 7th World Petroleum Congress Proceedings, v. 49, p. 339-352.

Elliott, T. 1978. Deltas. *In* Reading, H. G. (*Ed.*) Sedimentary Environments and Facies. Elsevier, New York, p. 97-142.

Enos, P. 1983. Shelf. *In* Scholle, P. A., Bebout, D G. and Moore, C. H. (*Eds.*) Carbonate Depositional Environments. American Association of Petroleum Geologists, Memoir33, p. 267-296.

Esteban, M. and Klappa, C. F. 1983. Subaerial exposure environment. *In* Scholle, P. A., Bebout, D G. and Moore, C. H. (*Eds.*) Carbonate Depositional Environments. American Association of Petroleum Geologists, Memoir33, p. 1-54.

Evamy, B. D. 1963. The application of a chemical staining technique to a study of dedolomitization. Sedimentology, v. 2, p. 164-170.

Evamy, B. D. 1967. Dedolomitization and the development of rhombohedral pores in limestones. Journal of Sedimentary Petrology, v. 37, p. 1204-1215.

Evamy, B. D. 1969. The precipitational environment and correlation of some calcite cements deduced from artificial staining. Journal of Sedimentary Petrology, v. 39, p. 787-793.

Evamy, B. D. and Shearman, D. J. 1964. The development of overgrowths from echinoderm fragments. Sedimentology, v. 5, p. 211-233.

Fairbridge, R. W. 1983. Syndiagenesis - anadiagenesis - epidiagenesis: phases in lithogenesis. *In* Larsen, G. and

Chiligar, G. V. (*Eds.*) Diagenesis in Sediments and Sedimentary Rocks, 2, Elsevier Publishing Co., Amsterdam, Development in Sedimentology., 25B, p. 17-114.

Flemming, N. C. and Roberts, D. G. 1973. Tectono - Eustatic changes in sea level and seafloor spreading. Nature, v. 243, p. 19-22.

Folk, R. L. 1962. Spectral subdivision of limestone types. *In* Ham, W. E. (*Ed.*) Classification of Carbonate Rocks. American Association of Petroleum Geologists. Memoir1, p. 62-84.

Folk, R. L. 1968. Petrology of sedimentary rocks. Austin, Texas, Hemphills Book, 170p.

Folk, R. L. 1973. Evidence for peritidal deposition of Devonian Caballos novaculite, Marathon Basin, Texas. Bulletin of American Association of Petroleum Geologists, v. 57, p. 702-725.

Folk, R. L. 1974. The natural history of crystalline calcuim carbonate: effect of magnesium content and stability. Journal of Sedimentary Petrology, v. 44, p. 40-53.

Folk, R. L. and Land, L. S. 1975. Mg/Ca ratio and salinity - two controls over crystallization of dolomite. Bulletin of American Association of Petroleum Geologists, v. 59, p. 60-68.

Folk, R. L. and Pittman, J. S. 1971. Length-slow chalcedony: a New Testament for vanished evaporites. Journal of Sedimentary Petrology, v. 41, p. 1045-1058.

Folk, R. L. and Siedlecka, A. 1974. The Schizohaline environments: its sedimentary and diagenesis fabrics as exemplified by Late Paleozoic rocks of Bear Island. Sedimentary Geology, v. 11, p. 1-15.

Folkman, Y. 1969. Diagenetic dedolomitization in the Albian-Cenomanian Yagur Dolomite on Mount Carmel (Northern Israel). Journal of Sedimentary Petrology, v. 39, p. 380-385.

Forbes, C. I. and McGugan, A. 1959. A lower Permian fusulinid fauna from Wapiti Lake, B.C. Journal of Alberta Society of Petroleum Geologists, v. 7, p. 33-42.

Ford, D. C. and Ewers, P. D. 1978. The development of limestone cave systems in the dimensions of length and depth. Canadian Journal of Earth Science, v. 15, p. 1783-1798.

Frank, J. R. 1981. Dedolomitization in the Taum Sauk Limestone (Upper Cambrian), southeast Missouri. Journal of Sedimentary Petrology, v. 51, p. 7-18.

Friedman, G. M. 1965. Terminology of crystallization textues and fabrics in sedimentary rocks. Journal of Sedimentary Petrology, v. 35, p. 643-655.

Friedman, G. M. 1980. Dolomite is an evoporite mineral: evidence from the rock record and from the sea-marginal ponds of the Red Sea. *In* Zenger, D. H., Dunham, J. B. and Ethington, R. L. (*Eds.*) Concepts and Models of Dolomitization. Society of Economic Paleontologists and Mineralogists, Special Publication no. 28, p. 69-80.

Friedman, G. M. and Sanders, J. E. 1978. Principle of Sedimentology. John Wiley & Sons, New York, 792p.

Gaines. A. M. 1974. Protodolomite synthesis at 100°C and atmospheric pressure. Science, v. 183, p. 518-520.

Gaines, A. M. 1980. Dolomitization kinetics: recent experimental studies. *In* Zenger, D. H., Dunham, J. B. and Ethington, R. L. (*Eds.*) Concepts and Models of Dolomitization. Society of Economic Paleontologists and Mineralogists, Special Publication no. 28, p. 81-86.

Gebelein, C. D. 1973. Algal origin of dolomite lamination in stromatolitic limestone. Journal of Sedimentary Petrology, v. 43, p. 603-613.

Geeslin, J. H. and Chafetz, H. S. 1982. Ordovician Aleman ribbon cherts: an example of silicification prior to carbonate lithification. Journal of Sedimentary Petrology, v. 52, p. 1283-1293.

Geiser, P. A. and Sansone, S. 1981. Joints, microfractures, and the formation of solution cleavage in limestone. Geology, v. 9, p. 280-285.

Goldberg, M. 1967. Supratidal dolomitization and dedolomitization in Jurassic rocks of Hamakhtesh Haquatar, Israel. Journal of Sedimentary Petrology, v. 37, p. 760-773.

Green, R. 1962. Zonal relationships in Lower Mississppian rocks in Alberta. Journal of Alberta Society of Petroleum Geologists, v. 10, p. 1-38.

Gregg, J. M. and Sibley, D. F. 1984. Epigenetic dolomitization and the origin of xenotopic dolomite texture. Journal of Sedimentary Petrology, v. 54, p. 908-931.

Hallam, A. 1981. Facies interpretation and the stratigraphic records. Freeman W. H. and Company, London. 291p.

Hanshaw, B. B., Back, W. and Deike, R. G. 1971. A geochemical hypothesis for dolomitization by ground water. Economic Geology, v. 66, p. 710-724.

Hardie, L. A. (*Ed.*) 1977. Sedimentation on the modern carbonate tidal flats of NW Andros Island, Bahamas. Johns Hopkins University, Studies in Geology, no. 22, 196p.

Hardie, L. A. and Eugster, H. P. 1971. The depositional environment of marine evaporites: a case for shallow, clastic accumulation. Sedimentology, v. 16, p. 187-220.

Hardie, L. A. and Ginsburg, R. N. 1977. Layering: the origin and environmental significance of lamination and thin bedding. *In* Hardie, L. A. (*Ed.*) Sedimentation on the Modern Carbonate Tidal Flats of NW Andros Island, Bahamas. Johns Hopkins University, Studies in Geology, no. 22, p. 50-123.

Harding, T. P. and Lowell, J. D. 1979. Structure styles, their plate tectonics habits, and hydrocarbon traps in petroleum provinces. Bulletin of American Association of Petroleum Geologists, v. 63, p. 1016-1058.

Harms, J. C., Southard, J. B. and Walker, R. G. 1982. Structures and sequences in clastic rocks. Society of Economic Paleontologists and Mineralogists, Short Course no. 9, p. 61-21.

Hatfield, C. B. 1975. Discussion: "Replacement of fossils by length-slow chalcedony and associated dolomitization, by Jacka, A. D. Journal of Sedimentary Petrology, v. 44, p. 421-427". Journal of Sedimentary Petrology, v. 45, p. 951-952.

Hawryszko, J. W. and Hamilton, R. S. 1964. The Permo-Carboniferous section at Mount Greenock. Bulletin of Canadian Petroleum Geology, v. 12, p. 623-631.

Heath, G. R. 1974. Dissolved silica and deep-sea sediments. *In* Hay, W. W. (*Ed.*) Studies in Paleo-oceanography. Society of Economic Paleontologists and Mineralogists, Special Publication no. 20, p. 77-93.

Heckel, P. H. 1972. Recognition of ancient shallow marine environments. *In* Rigby, J. K. and Hamblin, Wm. K. (*Eds.*) Recognition of Ancient Sedimentary Environments, Society of Economic Paleontologists and Mineralogists, Special Publication no. 16, p. 226-286.

Heckel, P. H. 1977. Origin of phosphate black shale facies in Pennsylvanian cyclothems of Mid-Continent North America. Bulletin of American Association of Petroleum Geologists, v. 61, p. 1045-1068.

Hite, R. J. 1970. Shelf carbonate sedimentation controlled by salinity in the Paradox Basin, Southeast Utah. Third Symposium on Salt, v. 1, p. 48-66.

Howard, J. D. 1972. Trace fossils as criteria for recognising shorelines in stratigraphic records. *In* Rigby, J. K. and Hamblin, Wm. K. (*Eds.*) Recognition of Ancient Sedimentary Environments. Society of Economic Paleontologists and Mineralogists, Special Publication no. 16, p. 215-225.

Illing, L. V. 1959. Cyclic carbonate sedimentation in the Mississippian at Moose Dome, Southwest Alberta. Alberta Society of Petroleum Geologists, 9th Annual Field Trip Guide Book, p. 37-52.

Illing, L. V., Wells, A. J. and Taylor, J. C. M. 1965. Penecontemporaneous dolomite in the Persian Gulf. *In* Pray, L. C. and Murray, R. C. (*Eds.*) Dolomitization and Limestone Diagenesis. Society of Economic Paleontologists and Mineralogists Special Publication no. 13, p. 89-111.

Imoto, N. 1983. Sedimentary structures of Permian-Triassic cherts in the Tamba District, Southwest Japan. *In* Iijima, A., Hein, J. R. and Siever, R. (*Eds.*) Siliceous Deposits in the Pacific region. Elsevier Publishing Co., Amsterdam, Development in Sedimentology., 36, p. 377-393.

Irwin, M. L. 1965. General theory of epeiric clear water sedimentation. Bulletin of American Association of Petroleum Geologists, v. 49, p. 445-459.

Jacka, A. D. 1974. Replacement of fossils by length-slow chalcedony and associated dolomitization. Journal of Sedimentary Petrology, v. 44, p. 421-427.

James, N. P. 1984. Shallowing-upward sequences in carbonates. *In* Walker, R. G. (*Ed.*) Facies Models. Geoscience Canada, Reprint Series 1, p. 213-228.

James, N. P. and Mountjoy, E. W. 1983. Shelf-slope break in fossil carbonate platforms: an overview. *In* Stanley, D.J. and Moore, G. T. (*Eds.*) The Shelf Break: Critical Interface on Continental Margins. Society of Economic Paleontologists and Mineralogists, Special Publication no. 33, p. 189-206.

Jeffery, D. and Alinger, T. 1982. Storm sedimentation in the Carboniferous limestones near Weston-Super-Mare (Dinantian, SW England). *In* Einsele, G. and Seilacher, A. (*Eds.*) Cyclic and Event Stratification. Springer-Verlag, New York, p. 240-247.

Johnson, H. D. 1978. Shallow siliciclastic seas. *In* Reading, H. G. (*Ed.*) Sedimentary Environments and Facies. Elsevier, New York, p. 207-258.

Jones, B., Lockhart, E. B. and Squair, C. 1984. Phreatic and vadose cements in the Tertiary Bluff Formation of Grand Cayman Island, British West Indies. Bulletin of Canadian Petroleum Geology, v. 32, p. 382-397.

Jones, J. B. and Segnit, E. R. 1971. The nature of opal: I. Nomenclature and constituent phases. Journal of Geological Society of Australia, v. 18, p. 57-68.

Kaldi, J. and Gidman, J. 1982. Early diagenetic dolomite cements: examples from the Permian Lower Magnesian Limestone of England and the Pleistocene carbonates of Bahamas. Journal of Sedimentary Petrology, v. 52, p. 1073-1085.

Kastner, M. 1980. Length-slow chalcedony: the end of the new Testaments. Transactions of American Geophysical Union, v. 61, p. 399.

Kastner, M. and Gieskes, J. M. 1983. Opal-A to opal-CT transformation-a kinetic study. *In* Iijima, A., Hein, J. R. and Siever, R. (*Eds.*) Siliceous Deposits in the Pacific region. Elsevier Publishing Co., Amsterdam, Development in Sedimentology., 36, p. 377-393.

Kastner, M., Keene, J. B. and Gieskes, J. M. 1977. Diagensis of siliceous oozes - I. Chemical controls on the rate of opal-A to opal-CT transformation-an experimental study. Geochimica et Cosmochimica Acta, v. 41, p. 1041-1059.

Katz, A. 1968. Calcian dolomites and dedolomitization. Nature, v. 217, p. 439-440.

Katz, A. 1971. Zoned dolomite crystals. Journal of Geology, v. 79, p. 38-51.

Keene, J. B. 1983. Chalcedonic quartz and occurrence of quartzine (length-slow chalcedony) in pelagic sediments. Sedimentology, v. 30, p. 449-454.

Kendall, A. C. 1984. Evaporites. *In* Walker, R. G. (*Ed.*) Facies Models. Geoscience Canada, Reprint Series 1, p. 259-296.

Kendall, C. G. St C. and Schlager, W. 1981. Carbonates and relative changes in sea level. Marine Geology, v. 44, p. 181-212.

Kinsman, D. J. J. 1969. Modes of formation, sedimentary associations, and diagenetic features of shallow water and supratidal evaporites. Bulletin of Canadian Petroleum Geology, v. 53, p. 830-840.

Knauth, L. P. 1979. A model for the origin of chert in limestone. Geology, v. 7, p. 274-277.

Knauth, L. P. and Epstein, S. 1976. Hydrogen and oxygen isotope ratios in nodular and bedded cherts. Geochimica et Cosmochimica Acta, v. 41, p. 1095-1108.

Kolodney, Y., Taraboulos, A. and Frieslander, U. 1980. Participation of fresh water in chert diagenesis: evidence from oxygen isotopes and α-track mapping. Sedimentology, v. 27, p. 305-316.

Krumbein, S. W. 1942. Criteria for subsurface recognition of unconformities. Bulletin of American Association of Petroleum Geologists, v. 26, p. 36-62.

Kuslansky, G. H. and Friedman, G. M. 1981. Chertification of crinoids may yield a product resembling "dedolomite". Journal of Sedimentary Petrology, v. 51, p. 795-798.

Land, L. S. 1967. Diagenesis of skeletal carbonates. Journal of Sedimentary Petrology, v. 37, p. 914-930.

Land, L. S. 1979. Chert - chalk diagenesis: The Miocene Island slope of North Jamaica. Journal of Sedimentary Petrology, v. 49, p. 223-232.

Land, L. S. 1983. Dolomitization. American Association of Petroleum Geologists, Course Notes Series no. 24, 20p.

Land, L. S. and Epstein, S. 1970. Pleistocene diagenesis and dolomitization, North Jamaica. Sedimentology, v. 14, p. 187-200.

Laporte, L. F. 1967. Carbonate deposition near sea level and resultant facies mosaic: Manlius Formation (Lower Devonian) of New York State. Bulletin of American Association of Petroleum Geologists, v. 51, p. 73-101.

Laporte, L. F. 1969. Recognition of transgressive carbonate sequence within an epeiric sea: Helderberg Group (Lower Devonian) of the New York State. *In* Friedman, G. M. (*Ed.*) Depositional Environments in Carbonate Rocks. Society of Economic Paleontologists and Mineralogists, Special Publication no. 14, p. 98-119.

Leith, C. K. 1925. Silicification of erosion surfaces. Economic Geology, v. 20, p. 513-523.

Lindholm, R. C. 1980. Intraclast orientation in Cambro-Ordovician limestones in Western Maryland. Journal of Sedimentary Petrology, v. 50, p. 1205-1212.

Logan, B. W. 1961. Cryptozoan and associated stromatolites from the Recent, Shark Bay, Australia. Journal of Geology, v. 69, p. 517-533.

Longman, M. W. 1980. Carbonate diagenetic texture from nearsurface diagenetic environment. Bulletin of American Association of Petroleum Geologists, v. 64, p. 461-487.

Lucia, F. J. 1962. Diagenesis of a crinoidal sediment. Journal of Sedimentary Petrology, v. 32, p. 848-865.

Lucia, F. J. 1972. Recognition of evaporite-carbonate shoreline sedimentation. *In* Rigby, J. K. and Hamblin, Wm. K. (*Eds.*) Recognition of Ancient Sedimentary Environments. Society of Economic Paleontologists and Mineralogists, Special Publication no. 16, p. 160-191.

Lucia, F. J. and Murray, R. C. 1967. Origin and distribution of porosity in crinoidal rock, 7th World Petroleum Congress Proceedings, v. 2, p. 409-423.

Macqueen, R. W. 1966. Mississippian stratigraphy and sedimentology at Cadomin, Alberta. Edmonton Geological Society, 8th Annual Field Trip Guide Book, p. 39-59.

Macqueen, R. W. and Bamber, E. W. 1968. Stratigraphy and facies relationships of the Upper Mississippian Mount Head Formation, Rocky Mountains and Foothills, southwestern Alberta. Bulletin of Canadian Petroleum Geology, v. 16, p. 225-287.

MacRae, J. and McGugan, A. 1977. Permian stratigraphy and sedimentology - Southwestern Alberta and Southeastern British Columbia. Bulletin of Canadian Petroleum Geology, v. 25, p. 752-766.

Mattes, B. W. and Mountjoy E. W. 1980. Burial dolomitization of the Upper Devonian Miette buildup, Jasper National Park, Alberta. *In* Zenger, D. H., Dunham, J. B. and Ethington, R. L. (*Eds.*) Concepts and Models of Dolomitization. Society of Economic Paleontologists and Mineralogists, Special Publication no. 28, p. 259-297.

McGugan, A. 1963. A Permian brachiopod and fusulinid fauna from the Elk Valley, British Columbia, Canada. Journal of Paleontology, v. 37, p. 621-627.

McGugan, A. 1968. Biostratigraphy and Faunas of the Permian Ishbel Group, Canadian Rocky Mountaions. Journal of Paleontology, v. 42, p. 1123-1138.

McGugan, A. and Rapson, J. E. 1961a. Stratigraphy of the Rocky Mountain Group (Permo-Carboniferous), Banff area, Alberta. Journal of Alberta Society of Petroleum Geologists, v. 9, p. 73-89.

McGugan, A. and Rapson, J. E. 1961b. Permian Stratigraphy, and the post-Carboniferous unconformity, Jasper area, Alberta. Edmonton Geological Society, 3rd Annual Field Trip Guide Book, p. 71-81.

McGugan, A. and Rapson, J. E. 1962. Permo-Carboniferous Stratigraphy, Crowsnest area, Alberta and British Columbia. Journal of Alberta Society of Petroleum Geologists, v. 10, p. 352-368.

McGugan, A. and Rapson, J. E. 1963a. Permian Stratigraphy and nomenclature, western Alberta and adjacent regions. Edmonton Geological Society, 5th Annual Field Trip Guide Book, p. 52-64.

McGugan, A., and Rapson, J. E. 1963b. Permo-Carboniferous stratigraphy between Banff and Jasper, Alberta. Bulletin of Canadian Petroleum Geology, v. 11, p. 150-160.

McGugan, A. and Rapson-McGugan, J. E. 1976. Permian and Carboniferous stratigraphy, Wapiti Lake area, Northeastern British Columbia. Bulletin of Canadian Petroleum Geology, v. 24, p. 193-210.

McGugan, A., Rapson-McGugan, J. E., Mamet, B. L. and Ross, C. A. 1968. Permian and Pennsylvanian biostratigraphy, and Permian depositional environments, petrography and diagenesis, southern Canadian Rocky Mountains. Alberta Society of Petroleum Geologists, 16th Annual Field Trip Guide Book, p. 48-66.

McKenzie, J. A., Hsu, K. J. and Schneider, J. F. 1980. Movement of subsurface waters under the sabkha, Abu Dhabi, United Emirates and its relations to evaporitive dolomite genesis. *In* Zenger, D. H., Dunham, J. B. and Ethington, R. L. (*Eds.*) Concepts and Models of Dolomitization. Society of Economic Paleontologists and Mineralogists, Special Publication no. 28, p. 69-80.

Meyers, W. J. 1974. Carbonate cement stratigraphy of the Lake Valley Formation (Mississippian) Sacramento Mountains, New Mexico. Journal of Sedimentary Petrology, v. 44, p. 837-861.

Meyers, W. J. 1977. Chertification in the Mississippian Lake

Valley Formation, Sacramento Mountain, New Mexico. Sedimentology, v. 24, p. 75-105.

Milliken, K. L. 1979. The silicified evaporite syndrome - two aspects of silicification history of former evaporite nodules from Southern Kentucky and Northern Tennessee. Journal of Sedimentary Petrology, v. 49, p. 245-256.

Monroe, W. H. 1976. The karst landforms of Puerto Rico. United States Geological Survey, Professional Paper 899, p. 1-58.

Moore, P. F. 1958. Late Paleozoic stratigraphy in the Rocky Mountains and Foothills of Alberta-a critical historical review. *In* J. A. Allan Memorial Volume, Jurassic and Carboniferous of Weatern Canada, American Association of Petroleum Geologists, Tulsa, Oklahoma, p. 145-176.

Morey, G. W., Fournier, R. O. and Rowe, J. J. 1964. The solubility of amorphous silica at 25°C. Journal of Geophysical Research, v. 69, p. 1995-2002.

Monger, J. W. H., Souther, J. G., and Gabrielse, H. 1972. Evolution of the Canadian Cordillera: A plate-tectonic model. America Journal of Science, v. 272, p. 577-602.

Morrow, D. W. 1978. The influence of the Mg/Ca ratio and salinity on dolomitization in evaporite basins. Bulletin of Canadian Petroleum Geology, v. 26, p. 389-392.

Morrow, D. W. 1982a. The chemistry of dolomitization and dolomite precipitation. Geoscience Canada, v. 9, p. 5-13.

Morrow, D. W. 1982b. Dolomitization models and ancient dolostones. Geoscience Canada, v. 9, p. 95-107.

Mountjoy, E. W. 1961. Rocky Mountain Front Ranges along the Athabasca Valley, Jasper National Park, Alberta. Edmonton Geological Society, 3rd Annual Field Trip Guide Book, p. 14-34.

Mountjoy, E. W. 1965. The Permo-Carboniferous succession of Mount Greenock and northern Jasper Park - Discussion. Bulletin of Canadian Petroleum Geology, v. 13, p. 340-348.

Muir, M., Lock, D. and von der Borch, C. 1980. The Coorong model for penecontemporaneous dolomite formation in the Middle Proterozoic McArthur Group, Northern Territory, Australia. *In* Zenger, D. H., Dunham, J. B. and Ethington, R. L. (*Eds.*) Concepts and Models of Dolomitization. Society of Economic Paleontologists and

Mineralogists, Special Publication no. 28, p. 51-67.

Muller, G. 1971. Gravitational cement. *In* Bricker, O. P. (*Ed.*) Carbonate Cement. Johns Hopkins University, Studies in Geology, no. 19, p. 301-302.

Murray, R. C. 1960. Origin of porosity in carbonate rocks. Journal of Sedimentary Petrology, v. 30, p. 59-84.

Murray, R. C. 1964. Origin and diagenesis of gypsum and anhydrite. Journal of Sedimentary Petrology, v. 34, p. 512-523.

Murray, R. C. and Lucia, F. J. 1967. Cause and control of dolomite distribution by rock selectivity. Bulletin of Geological Society of America, v. 78, p. 21-36.

Namy, J. N. 1974. Early diagenetic chert in the Marble Falls Group (Pennyslvanian) of Central Texas. Journal of Sedimentary Petrology, v. 44, p. 1262-1268.

Nelson, S. J. 1962. Upper Mississippian and Permo-Pennsylvanian terminology, southern Canadian Rocky Mountains. Journal of Alberta Society of Petroleum Geologists, v. 10, p. 22-77.

Nelson, S. J. and Rudy, H. R. 1961. Tunnel Mountain - Rundle relationships, Carboniferous of the southern Canadian Rocky Mountains. Edmonton Geological Society, 3rd Annual Field Trip Guide Book, p. 56-70.

Newell, N. D., Purdy, E. G. and Imbrie, J. 1960. Bahamian oolitic sand. Journal of Geology, v. 48, p. 481-497.

Nissenbaum, A. 1967. Anhydrite inclusions in idiomorphic quartz in gypsum concretions from Makhtesh Ramon, Israel. Israel Journal of Earth Sciences, v. 16, p. 389-392.

Oswald, D. H. 1968. Mississippian stratigraphy of the Nordegg area. Alberta Society of Petroleum Geologists, 16th Annual Field Trip Guide Book, p. 42-47.

Payton, C. E. (*Ed.*) 1977. Seismic stratigraphy - applications to hydrocarbon exploration. American Association of Petroleum Geologists, Memoir26, 516p.

Penner, D. G. 1957. The Elkton Member. Journal of Alberta Society of Petroleum Geologists, v. 5, p. 101-104.

Pierre, C., Ortlieb, L. and Person, A. 1984. Supratidal evaporitic dolomite at Ojo de Liebre Lagoon; mineralogical and isotopic arguments for primary crystallization. Journal of Sedimentary Petrology,

v. 54, p. 1049-1061.

Powers, R. W. 1962. Arabian Upper Jurassic carbonate reservoir rocks. *In* Ham, W. E. (*Ed.*) Classification of Carbonate Rocks. American Association of Petroleum Geologists, Memoir1, p. 122-192.

Quinlan, J. F. 1972. Karst-related mineral deposits and possible criteria for the recognition of paleokarsts. 24th International Geological Congress, Section 6, p. 156-167.

Radke, B. M. and Mathis, R. L. 1980. On the formation and occurrence of saddle dolomite. Journal of Sedimentary Petrology, v. 50, p. 1149-1168.

Rapson, J. E. 1962. The petrology of Pennsylvanian chert breccias and conglomerates, Rocky Mountain Group, Banff, Alberta. Journal of Sedimentary Petrology, v. 32, p. 249-262.

Rapson-McGugan, J. E. 1970. The diagenesis and depositional environment of the Permian Ranger Canyon and Mowitch Formation. Sedimentology, v. 15, p. 363-417.

Read, J. F. and Grover, G. A. Jr. 1977. Scalloped and planar erosion surfaces, Middle Ordovician Limestone, Virginia - analogues of Holocene exposed karsts or tidal rock platforms. Journal of Sedimentary Petrology, v. 47, p. 956-972.

Reeckmann, A. and Friedman, G. M. 1982. Exploration for carbonate petroleum reservors. John Wiley & Sons, New York, 213p.

Richter, D. K. and Fuchtbauer, H. 1978. Ferroan calcite replacement indicates former magnesium calcite skeletons. Sedimentology, v. 25, p. 843-860.

Runnells, D. D. 1969. Diagenesis, chemical sediments and the mixing of natural waters. Journal of Sedimentary Petrology, v. 39, p. 1188-1201.

Schmidt, V. and MacDonold, D. A. 1979. Texture and recogition of secondary porosity in sandstones. *In* Scholle, P. A. and Schulger, P. R. (*Eds.*) Aspects of Diagenesis. Society of Economic Paleontologists and Mineralogists, Special Publication no. 26, p. 209-225.

Scott, D. L. 1964. Pennsylvanian Stratigraphy. Bulletin of Canadian Petroleum Geology, v. 12, p. 460-493.

Seilacher, A. 1967. Bathymetry of trace fossils. Marine Geology, v. 5, p. 389-412.

Seisser, W. G. and Rogers, J. 1976. Authigenic pyrite and gypsum in South West African continental slope sediments. Sedimentology, v. 23, p. 567-577.

Sepkoski, J. J. Jr. 1982. Flat pebble conglomerates, storm deposits, and the Cambrian bottom fauna. *In* Einsele, G. and Seilacher, A. (*Eds.*) Cyclic and Event Stratification. Springer-Verlag, New York, p. 371-388.

Shearman, D. J., Khouri, J. and Taha, S. 1961. On the replacement of dolomite by calcite in some Mesozoic Limestones from the French Jura. Proceedings of the Geological Association, v. 72, p. 1-12.

Sheldon, R. P. 1980. Episodicity of phosphate deposition and deep ocean circulation-a hypothesis. *In* Bentor, Y. K. (*Ed.*) Marine phosphorites-geochemistry, occurrence, genesis. Society of Economic Paleontologists and Mineralogists Special Publication no. 29, p. 239-247.

Shinn, E. A. 1968a. Practical significance of birdseye structures. Journal of Sedimentary Petrology, v. 38, p. 215-223.

Shinn, E. A. 1968b. Selective dolomitization of some recent sedimentary structures. Journal of Sedimentary Petrology, v. 38, p. 612-616.

Shinn, E. A. 1969. Submarine lithification of Holocene carbonate sediments in the Persian Gulf. Sedimentology, v. 12, p. 109-144.

Shinn, E. A. 1983. Tidal flats. *In* Scholle, P. A., Bebout, D G. and Moore, C. H. (*Eds.*) Carbonate Depositional Environments. American Association of Petroleum Geologists, Memoir33, p. 171-210.

Sibley, D. F. 1980. Climate control of dolomitization, Seroe Domi Formation (Pliocene), Bonaire, N. A. *In* Zenger, D. H., Dunham, J. B. and Ethington, R. L. (*Eds.*) Concepts and Models of Dolomitization. Society of Economic Paleontologists and Mineralogists, Special Publication no. 28, p. 247-258.

Siedlecka, A. 1972. Length-slow chalcedony and relicts of sulphates: evidences of evaporitic environments in the Upper Carboniferous and Permian beds of Bear Island, Svalbard. Journal of Sedimentary Petrology, v. 42, p. 812-816.

Sloss, L. L. 1963. Sequence in the cratonic interior of North America. Bulletin of Geological Society of America, v. 74, p. 93-113.

Steinitz, G. 1977. Evaporite-chert associations in Senonian bedded chert, Israel. Israel Journal of Earth Sciences, v. 26, p. 55-63.

Tasch, P. 1973. Paleobiology of the invertebrates. John Wiley & Sons, Inc. New York, 946p.

Thomas, G. E. and Glaister, R. P. 1960. Facies and porosity relationships in some Mississippian carbonate cycles of Western Canada Basin. Bulletin of American Association of Petroleum Geologists, v. 44, p. 569-588.

Thomsen, E. 1976. Depositional environment and development of Danian bryozoan biomicrite mound (Karlby Klint, Denmark). Sedimentology, v. 23, p. 485-509.

Toomey, D. F. and Babcock, J. A. 1983. Precambrian and Paleozoic carbonates, West Texas-Southern New Mexico. Colorado School of Mines Professional Contributions no. 11, 345p.

Vail, P. R., Mitchum, R. M. Jr. 1979. Global cycles of relative changes of sea level from seismic stratigraphy. *In* Watkins, J. S., Montadent, L. and Dickerson, P. W. (*Eds.*) Geological and Geophysical Investigations of Continental Margins. American Association of Petroleum Geologists, Memoir29, p. 469-472.

Vail, P. R., Mitchum, R. M. Jr., and Thompson, S. III. 1977. Relative changes of sea level from coastal onlap. *In* Payton, C. E. (*Ed.*) Seismic Stratigraphy - application to Hydrocarbon Exploration, American Association of Petroleum Geologists, Memoir26, p. 83-98.

von der Borch, C. 1976. Stratigraphy of stromatolite occurrences in carbonate lakes of the Coorong area, South Australia. *In* Walter, J. R. (*Ed.*) Stromatolites. Elsevier, Amsterdam, p. 413-420

von der Borch, C. C. and Lock, D. 1979. Geological significance of Coorong dolomites. Sedimentology, v. 26, p. 813-824.

Walasko, J. T., Lerbekmo, J. F. and Mountjoy E. W. 1964. Petrology of a Permo-Carboniferous section in northern Jasper National Park, Alberta. Edmonton Geological Society, 6th Annual Field Trip Guide Book, p. 35-60.

Wanless, R. G. 1979. Limestone response to stress-pressure solution and dolomitization. Journal of Sedimentary Petrology, v. 49, p. 437-462.

Ward, W. C. 1975. Petrology and diagenesis of carbonate eolianites of northeastern Yucatan Peninsula, Mexico. *In*

Wantland, K. E. and Pusey, W. C. III. (*Eds.*) Belize Shelf - Carbonate Sediments, Clastic Sediments, and Ecology. American Association of Petroleum Geologists, Studies in Geology no. 2, p. 500-571.

Watson, H. J. 1982. Casablance Field offshore Spain - a paleogeomorphic trap. *In* Halbouty, M. T. (*Ed.*) The Deliberate Search for the Subtle Trap. American Association of Petroleum Geologists, Memoir32, p. 237-250.

Wilson, J. L. 1975. Carbonate facies in geologic history. Springer-Verlag, New York, 471p.

Wilson, R. C. L. 1966. Silica diagenesis in the Upper Jurassic Limestones of Southern England. Journal of Sedimentary Petrology, v. 36, p. 1036-1049.

Wise, S. W. Jr. and Kelts, K. R. 1972. Inferred diagenetic history of a weakly silicified deep sea chalk. Trans. Gulf Coast Association of Geological Societies, v. 23, p. 305-323.

Wise, S. W. Jr. and Weaver, F. W. 1974. Chertification of ocean sediments. Special Publication of International Association of Sedimentology, no. 1, p. 301-326.

Wright, V. P. 1981. Algal aragonite encrusted pisoids from a Lower Carboniferous schizohaline lagoon. Journal of Sedimentary Petrology, v. 51, p. 479-489.

Wright, V. P. 1982. The recognition and interpretation of paleokarsts-two examples from the Lower Carboniferous of South Wales. Journal of Sedimentary Petrology, v. 52, p. 83-94.

Yan, D. and Zhai, G. 1980. Exploration practice in and prospects of the buried-hill oil fields in North China. *In* Mason, J. E. (*Ed.*) Petroleum Geology of China. p. 92-100.

Zeigler, P. A. 1969. The development of sedimentary basins in Western and Arctic Canada. Alberta Society of Petroleum Geologists, 82p.

Zenger, D. H. 1972. Significance of supratidal dolomitization in the geologic record. Bulletin of Geological Society of America, v. 83, p. 1-12.

Zenger, D. H. 1983. Burial dolomitization in the Lost Burro Formation (Devonian), east-central Californian, and the significance of late diagenetic dolomitization. Geology, v. 11, p. 519-522.

XIV. APPENDIX

CARBONACEOUS SHALE

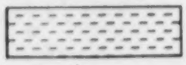
CALCAREOUS SHALE

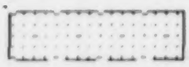
SILTY SANDSTONE

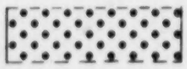
CHERT ARENITE

CHERT CONGLOMERATE

SANDY CHERT

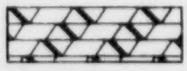
BLACK PHOSPHATIC CHERT

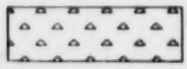
THIN BEDDED CHERT

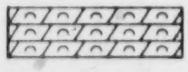
NODULAR CHERTY DOLOSTONE

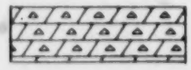
'RAGGED' CHERTY DOLOSTONE

LAMINATED CHERTY DOLOSTONE

QUARTZITIC DOLOSTONE

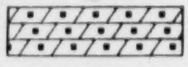
INTRACLASTIC DOLOSTONE

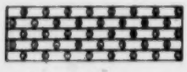
OÖLITIC DOLOSTONE

SANDY DOLOSTONE

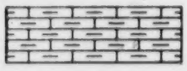
ARGILLACEOUS LIMESTONE/DOLOSTONE

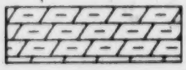
LAMINATED DOLOSTONE

THIN BEDDED DOLOSTONE

THICK BEDDED DOLOSTONE

DOLOMITIC LIMESTONE

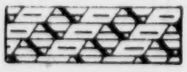
INTERLAMINATED CHERT & DOLOSTONE

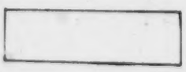
COVERED INTERVAL

PLANAR TO WAVY LAMINATION

BIRD'S-EYE TEXTURE

BRECCIA

CROSS BEDDING OR LAMINATION

CHERT NODULES

BURROWS

BIOTURBATION

PELOIDS

CALCISPHERES

BIOCLASTIC FRAGMENTS

PHOSPHATIC FRAGMENTS

SPONGE SPICULES

SPONGE

FORAMINIFERA

OSTRACOD

BIVALVE

GASTROPOD

BRACHIOPOD

CRINOID

RAMOSE BRYOZOAN

FENESTRATE BRYOZOAN

HORN CORAL

COLONIAL CORAL

Appendix 1 SYMBOLS FOR THE MEASURED SECTIONS

1 of

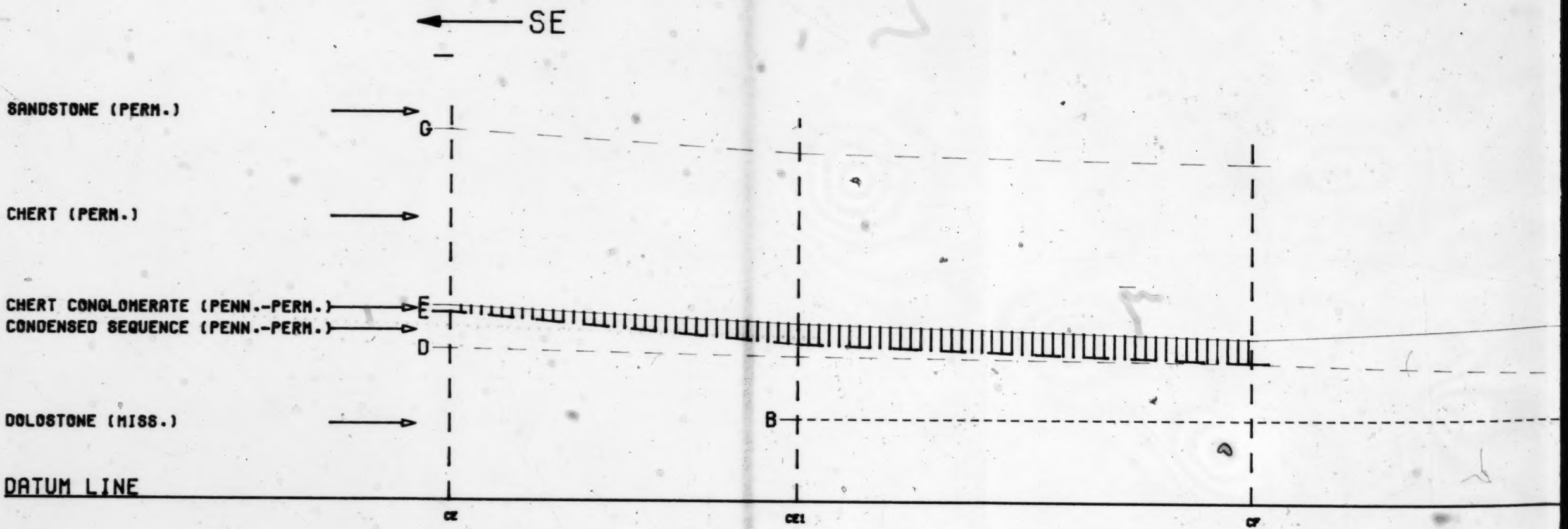
SE
SANDSTONE (PERM.)
G
CHERT (PERM.)
CHERT CONGLOMERATE (PENN.-PERM.)
CONDENSED SEQUENCE (PENN.-PERM.)
E
D
DOLOSTONE (MISS.)
B
DATUM LINE
CE2
CE1
CE

FIGURE 11. CORRELATION OF SECTIONS ON CINQUEFOIL MOUNTAIN

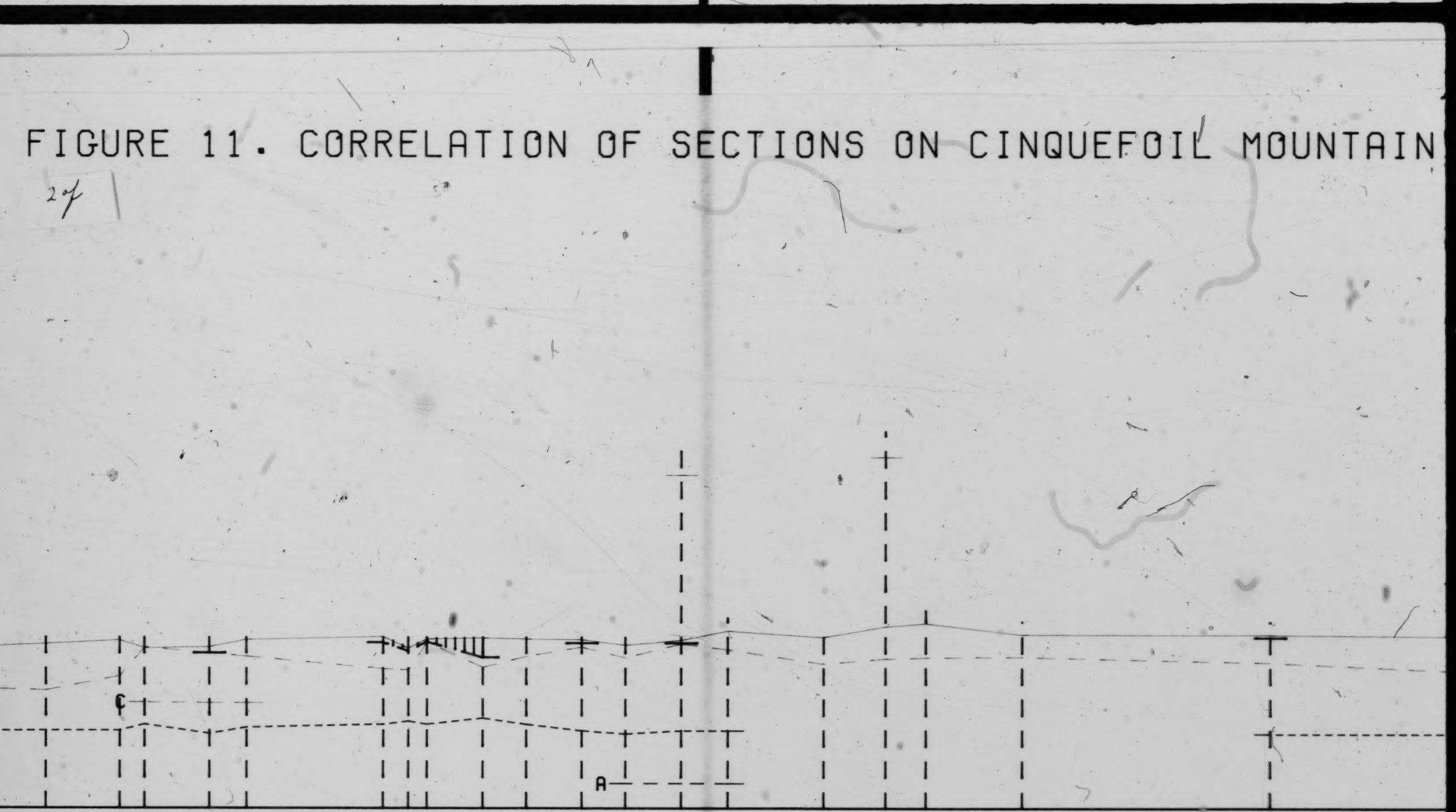

L MOUNTAIN, JASPER

3 of 3

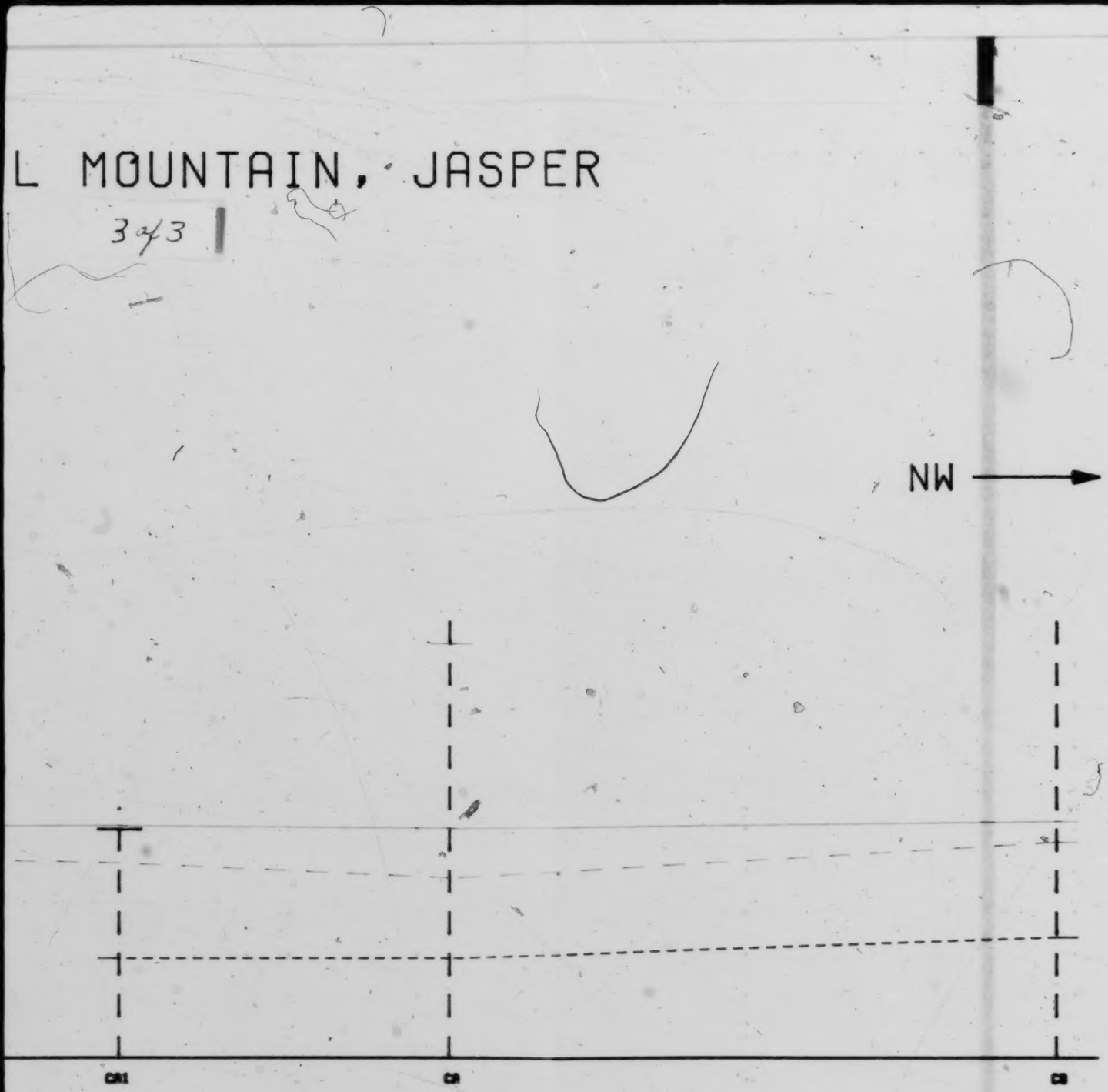

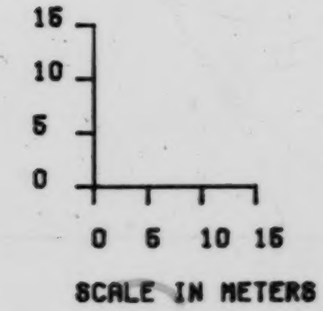

LEGEND

A	INTRACLAST UNIT A
B	INTRACLAST UNIT B
C	INTRACLAST UNIT C
D	TOP OF DOLOSTONE UNIT
E	BASE OF CHERT CONOLOMERATE
F	BASE OF CHERT
G	BASE OF CHERTY SANDSTONE

FIGURE 10. CORRELA

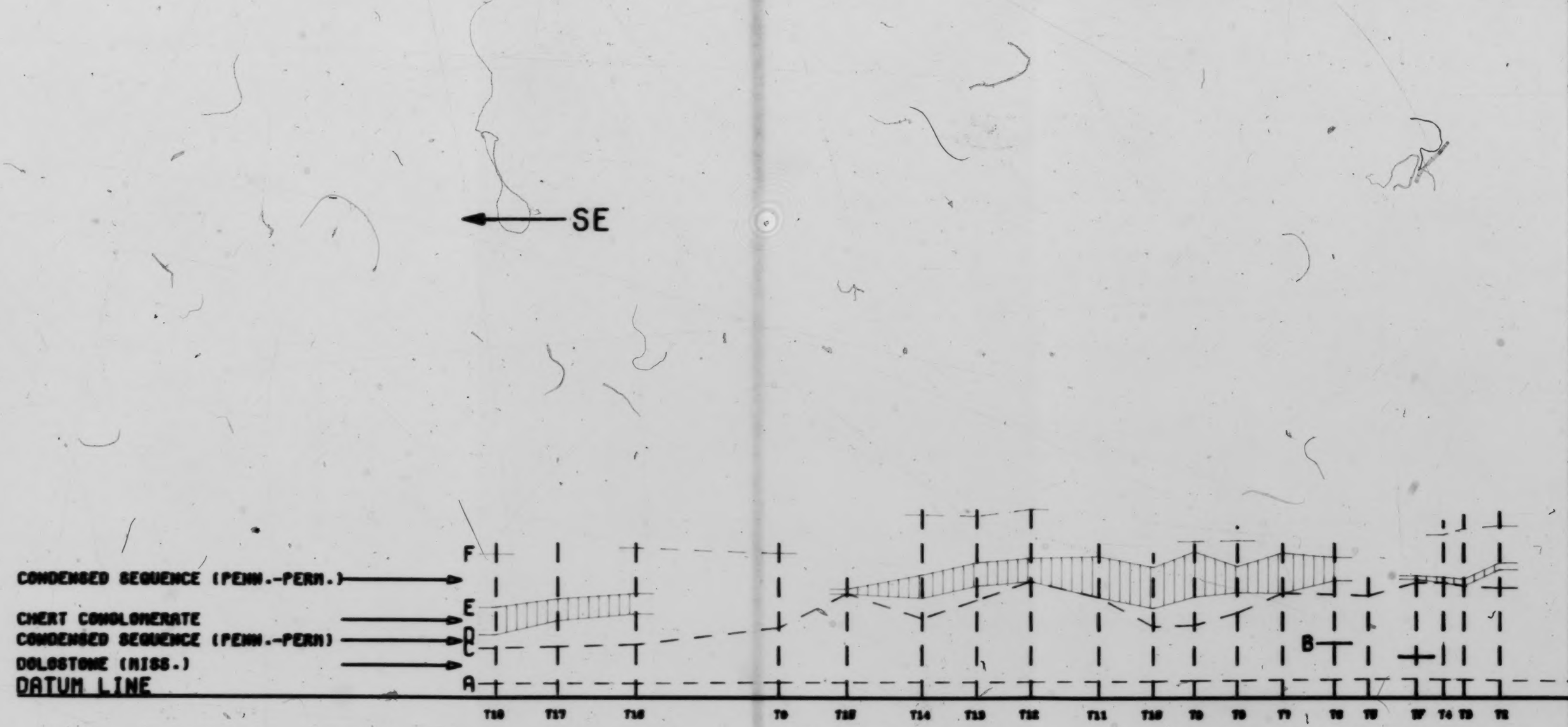

TION OF SECTIONS ON TALBOT LAKE, JASPER.

~ 2 ~

NW ⟶

15
10
5
0
0 5 10 15
SCALE IN METERS

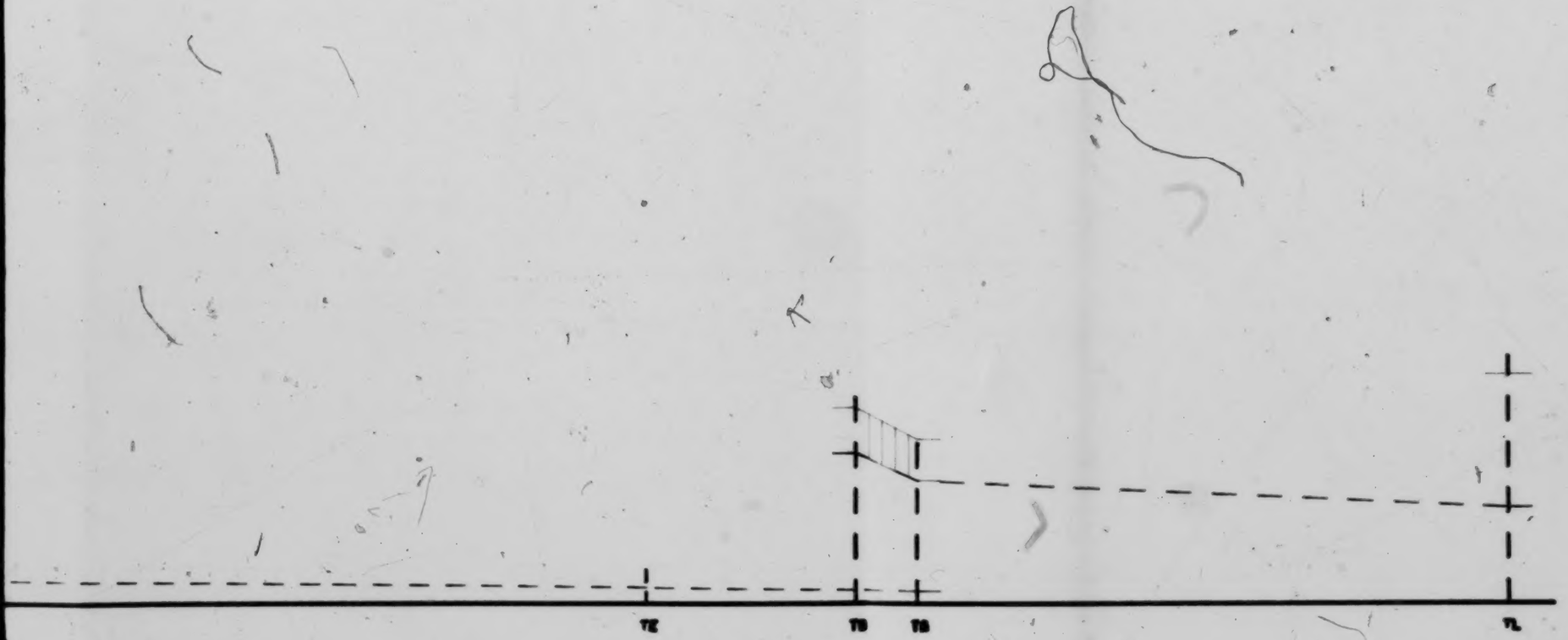

LEGEN

A TOP OF CHERT
B SANDSTONE LE
C TOP OF DOLOS
D BASE OF CHER
E TOP OF CHERT
F BASE OF CHER

TIONS ON TALBOT LAKE, JASPER.

3 of 3

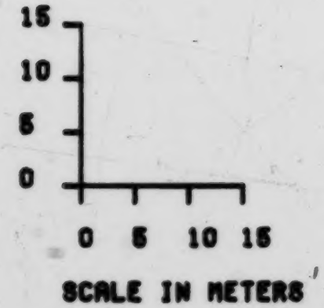

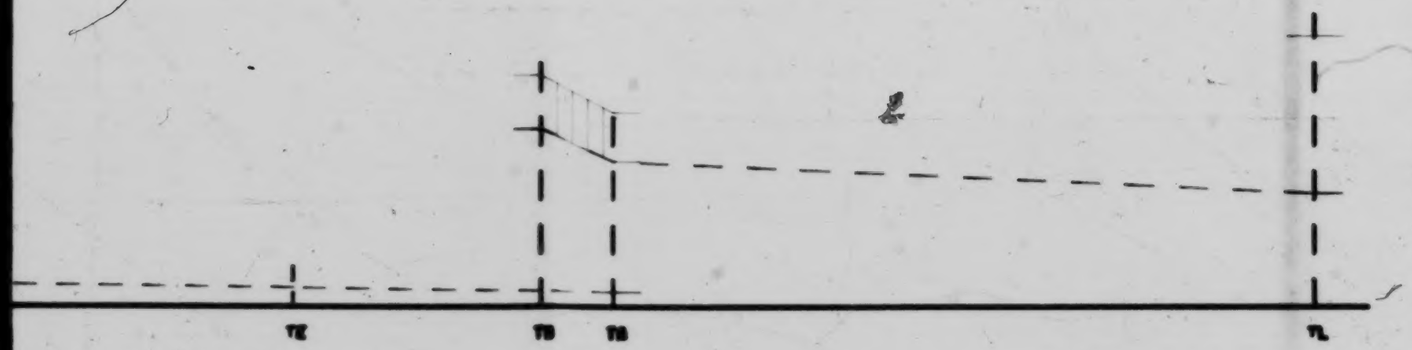

LEGEND

A	TOP OF CHERTY DOLOSTONE UNIT
B	SANDSTONE LENS
C	TOP OF DOLOSTONE UNIT
D	BASE OF CHERT CONGLOMERATE
E	TOP OF CHERT CONGLOMERATE
F	BASE OF CHERT

FIGURE 9.

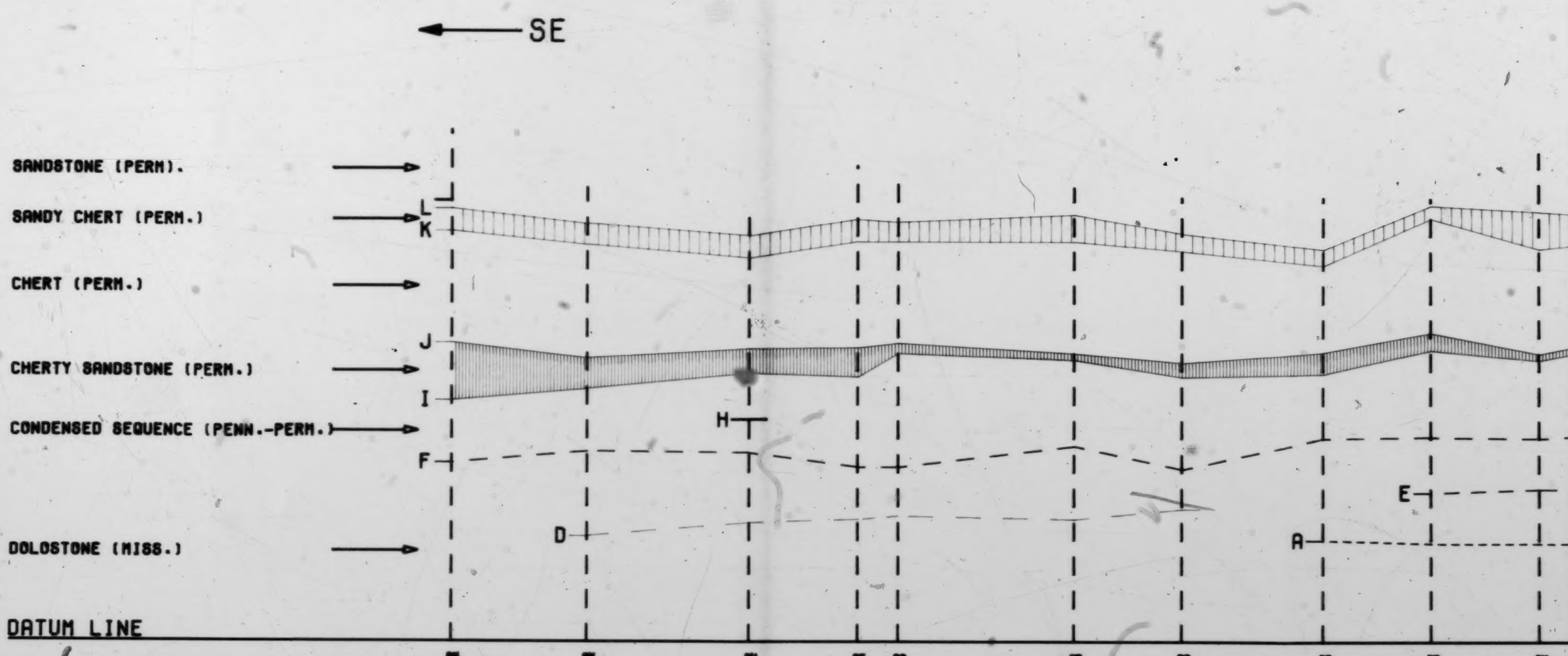
SE
SANDSTONE (PERM).
SANDY CHERT (PERM.)
CHERT (PERM.)
CHERTY SANDSTONE (PERM.)
CONDENSED SEQUENCE (PENN.-PERM.)
DOLOSTONE (MISS.)
DATUM LINE
L
K
J
I
H
F
D
E
A

9. CORRELATION OF SECTIONS ON MOUNT GREENOCK, JASPER.

27

NW —

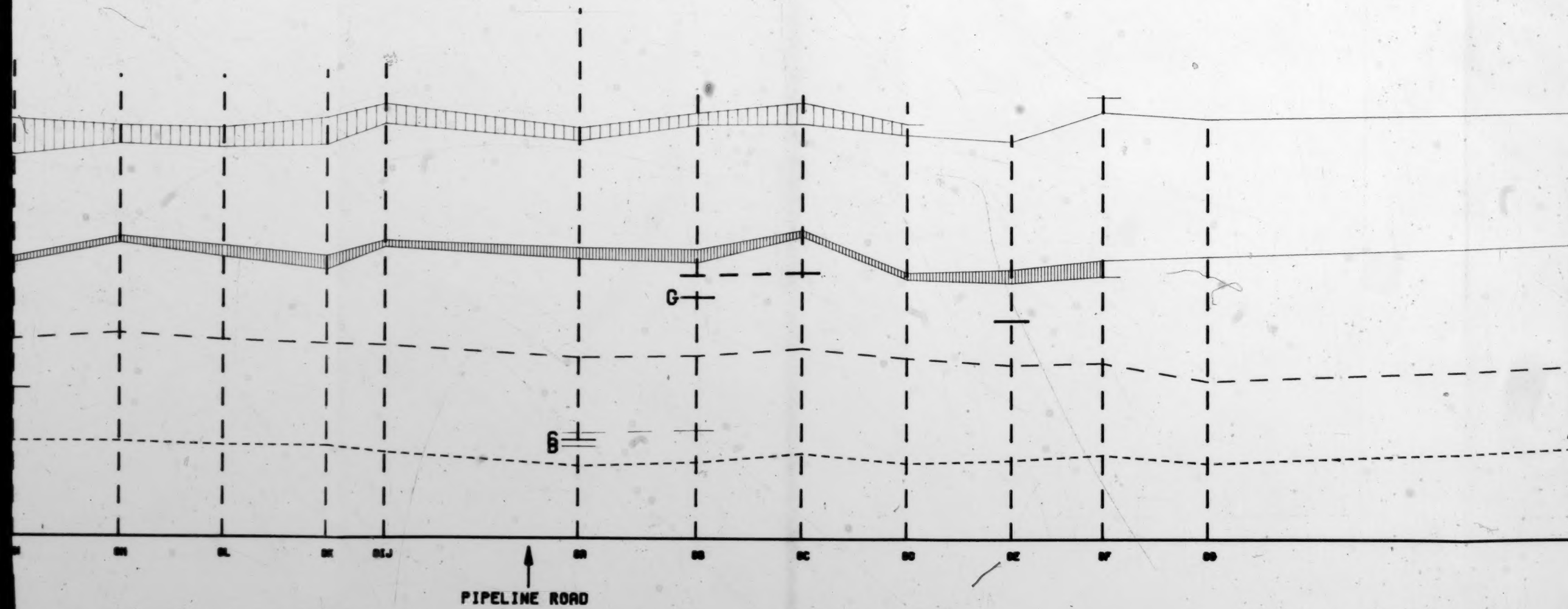

UNT GREENOCK, JASPER.

3 of 3

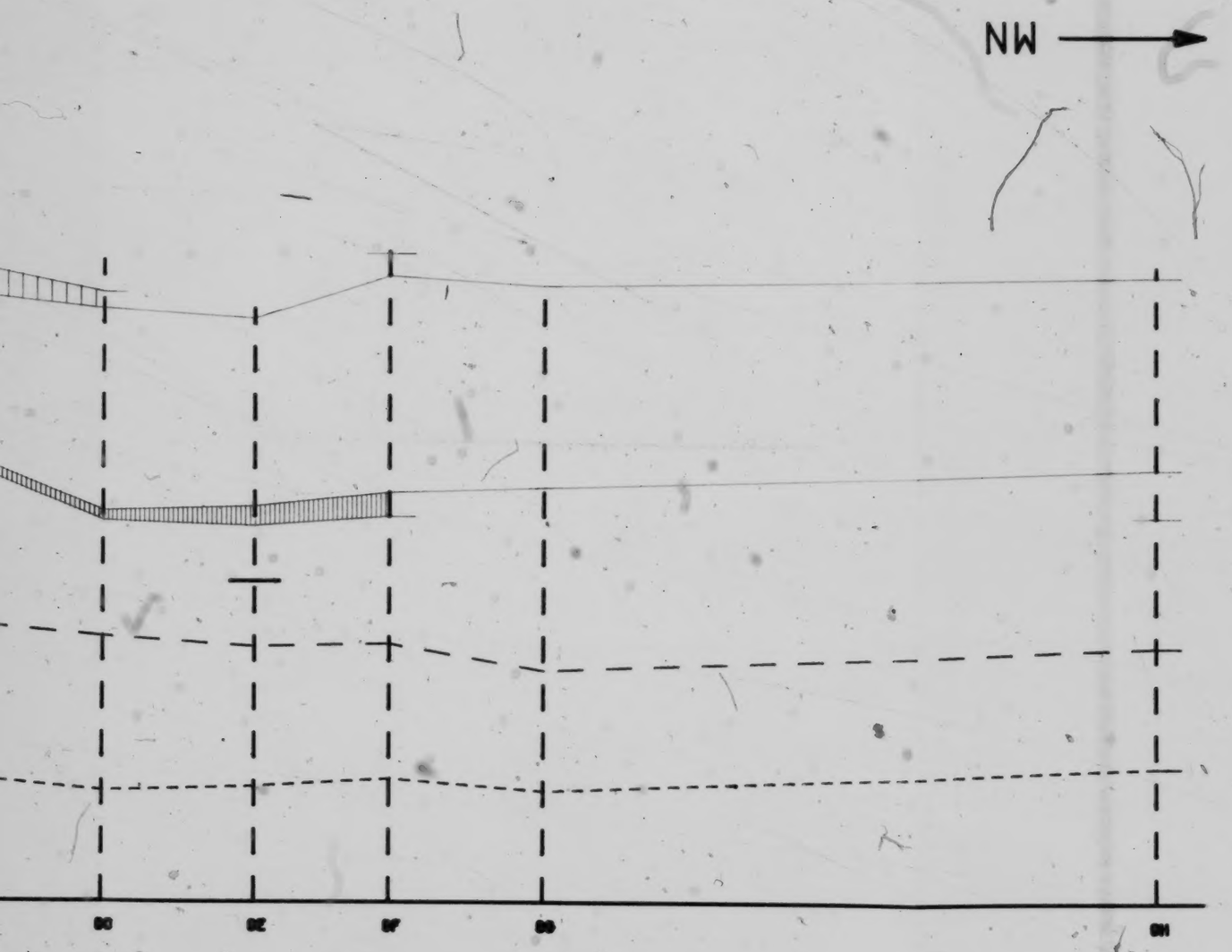

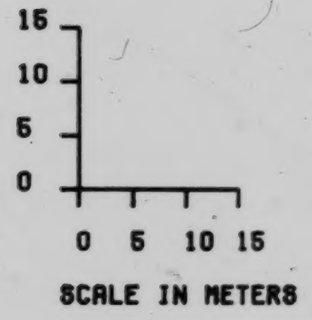

LEGEND

A	INTRACLAST UNIT A
B	QUARTZITIC DOLOSTONE A
C	INTRACLAST UNIT B
D	QUARTZITIC DOLOSTONE B
E	INTRACLAST UNIT C
F	TOP OF DOLOSTONE UNIT
G	CHERT CONGLOMERATE
H	DISCONTINUOUS CHERTY SANDSTONE
I	BASE OF CHERTY SANDSTONE/SANDSTONE
J	BASE OF CHERT
K	BASE OF SANDY CHERT
L	BASE OF SANDSTONE

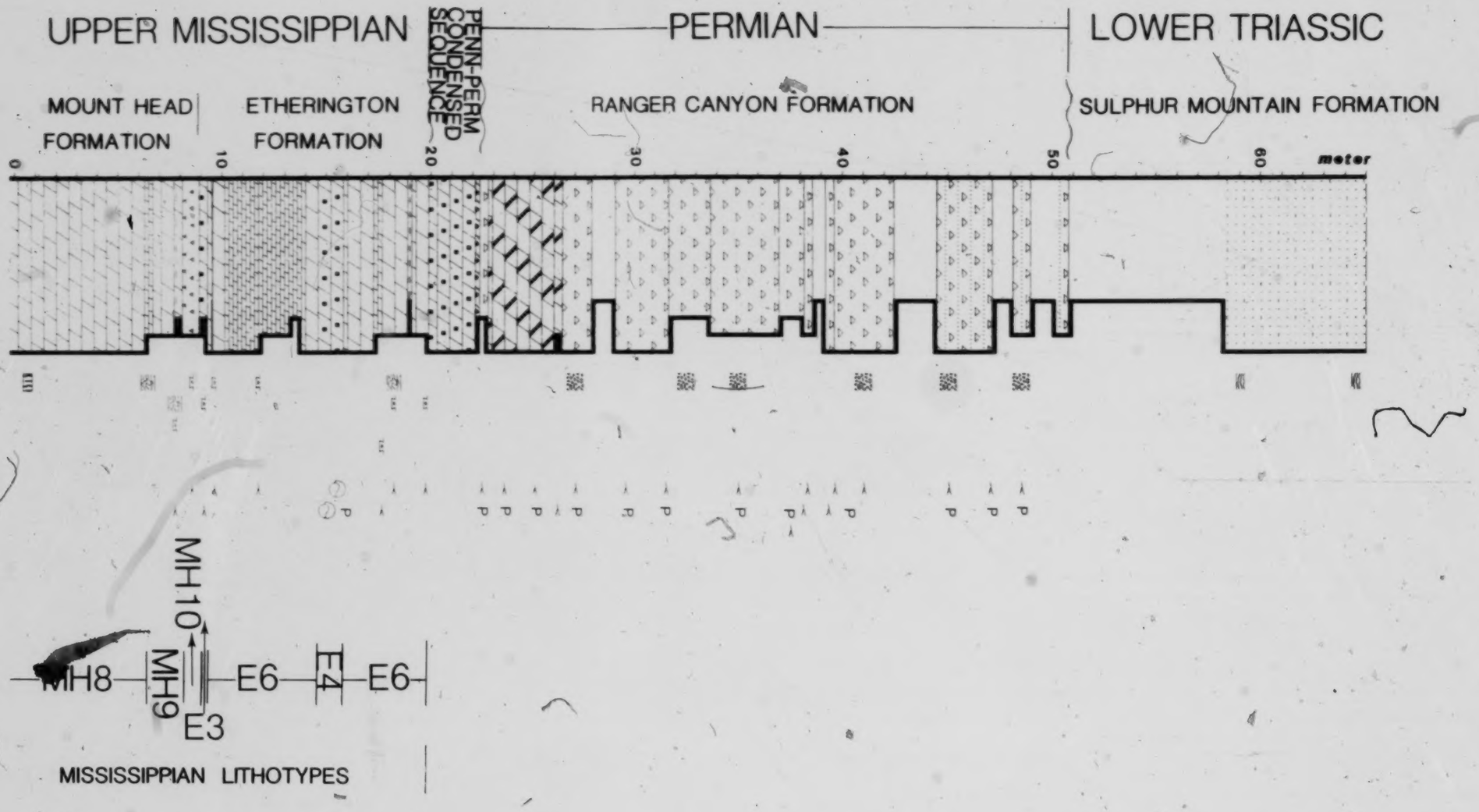

FIGURE 8. GEOLOGICAL SECTION - SNARING RIVER (symbols: see Appendix 1)

UPPER — MISSISSIPPIAN

MOUNT — HEAD — FORMATION

MH3 &2 | MH3 MH4 | MH3 MH4 | MH3 | MH3 | MH3 | MH4 | MH3

MISSISSIPPIAN LITHOTYPES DISCUSSED IN TEXT

FIGURE 7. GEOLOGICAL SECTION - CINQUEFOIL MOUNTAIN

(symbols: see Appendix 1)

272

MISSISSIPPIAN

PERMIAN

FORMATION

ETHERINGTON FORMATION

PENN-PERM CONDENSED SEQUENCE

RANGER CANYON FORMATION

MOWITCH FORMATION

70 80 90 100 110 120 130 140 meter

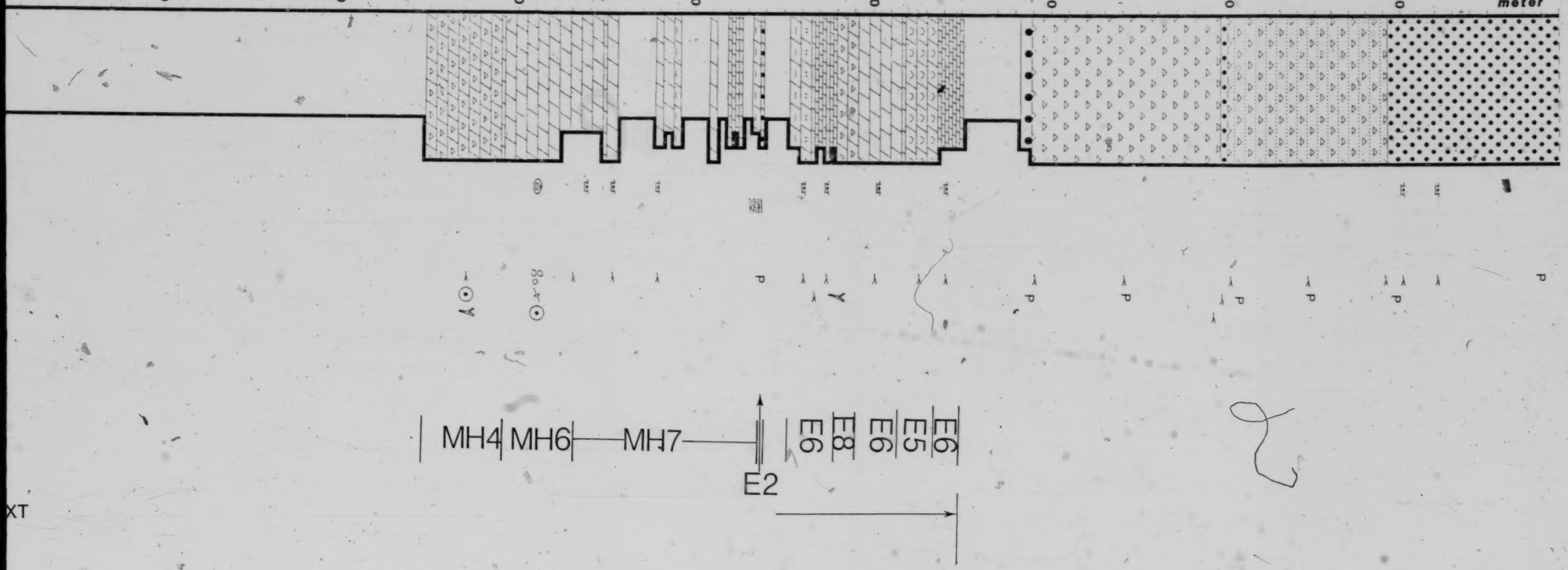

XT

UPPER

TURNER VALLEY FORMATION MOUNT

0 10 20 30 40 50 60 70 80

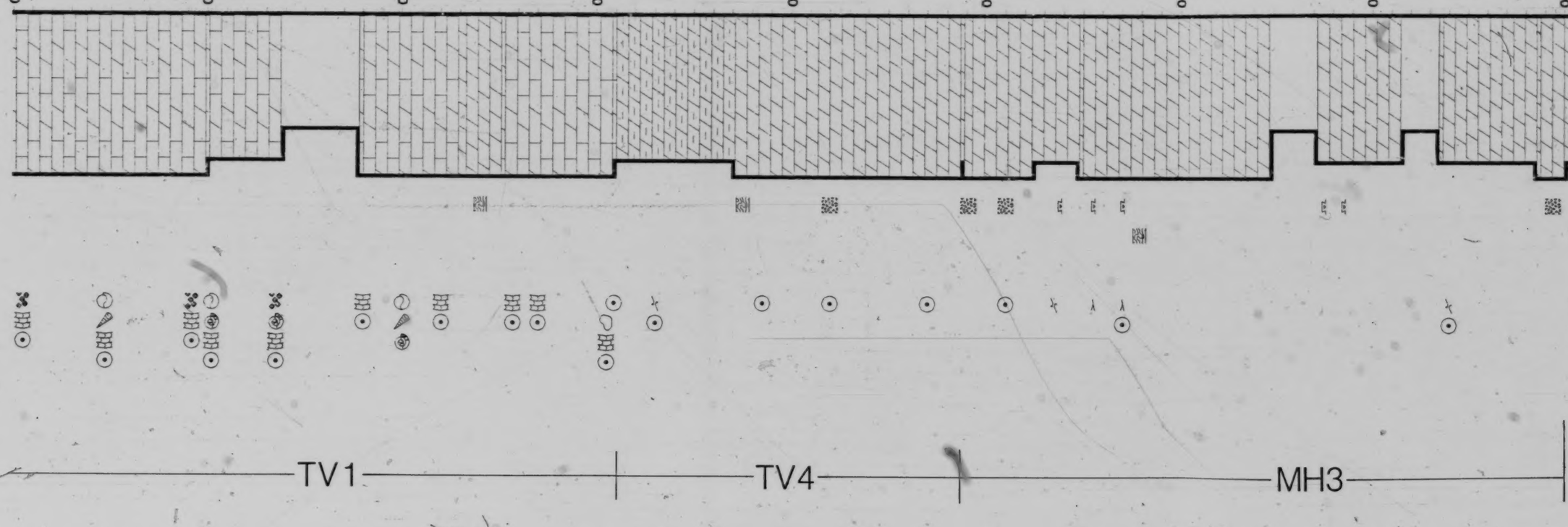

TV1 TV4 MH3 MH2

MISSISSIPPIAN LITHOTYPES DISCUSSED IN TEX

FIGURE 6. GEOLOGICAL SECTION - MOUNT GREENOCK

(symbols: see Appendix 1)

27

MISSISSIPPIAN

HEAD FORMATION ETHERINGTON

90 100 110 120 130 140 150 160 170

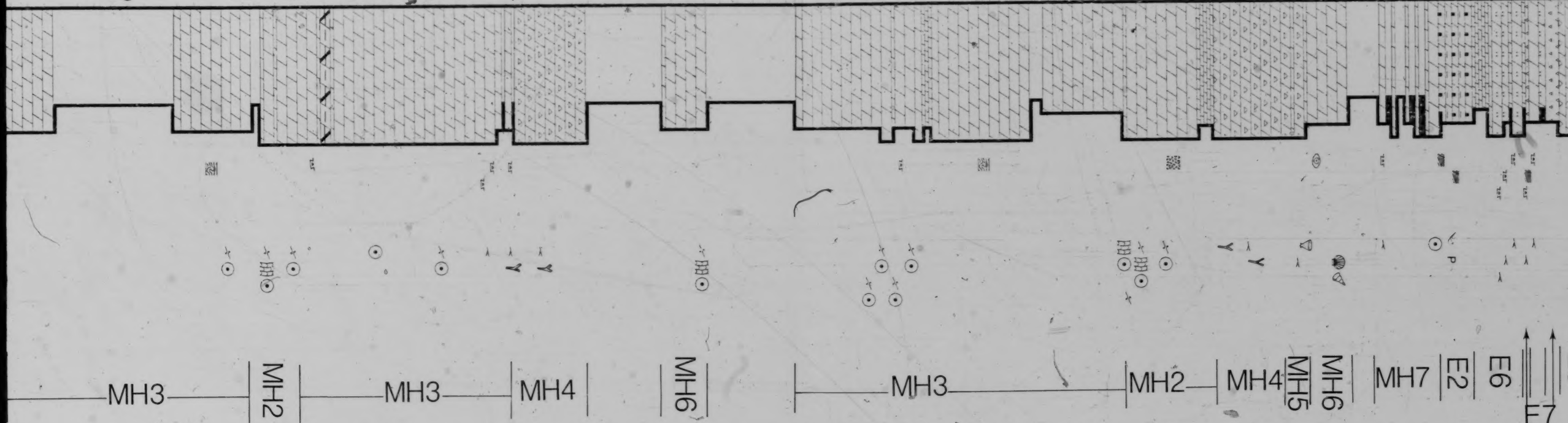

MH3 MH2 MH3 MH4 MH6 MH3 MH2 MH4 MH5 MH6 MH7 E2 E6 E7

EXT

373

PERMIAN

PENN-PERM CONDENSED SEQUENCE

ETHERINGTON FORMATION

RANGER CANYON FORMATION

MOWITCH FORMATION

150 160 170 180 190 200 210 220 230 meter

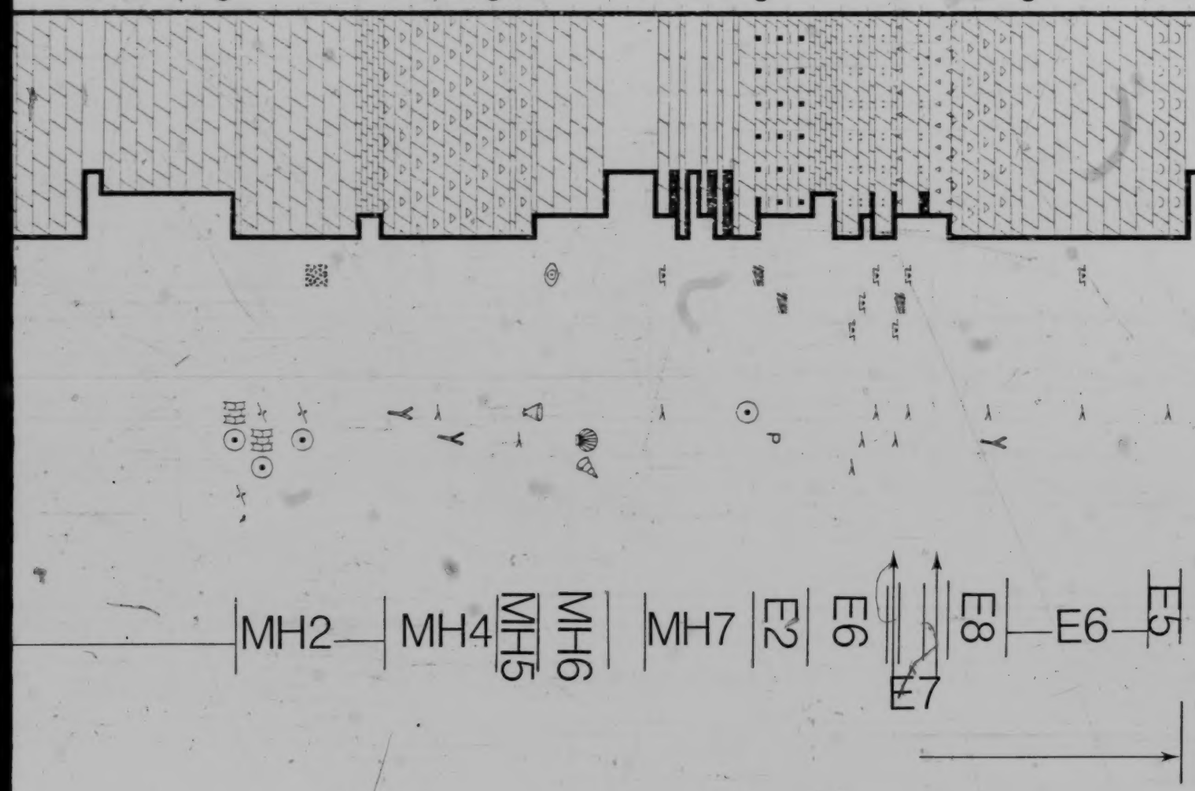

MH2 MH4 MH5 MH6 MH7 E2 E6 E7 E8 E6 E5

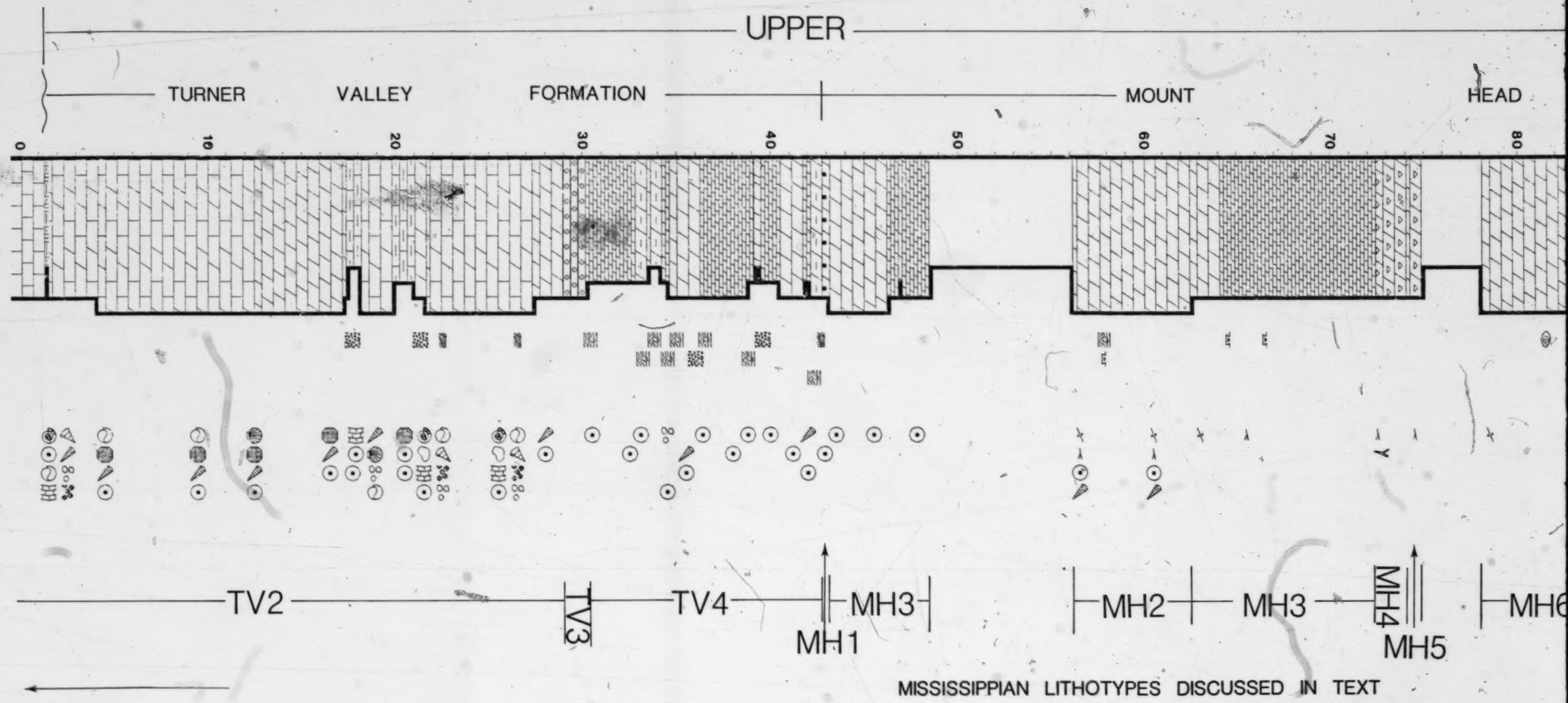

FIGURE 5. GEOLOGICAL SECTION - TALBOT LAKE

(symbols: see Appendix 1)

27

MISSISSIPPIAN

MOUNT HEAD FORMATION ETHERINGTON FORMATION PE CONDENSE

50 60 70 80 90 100 110 120 130

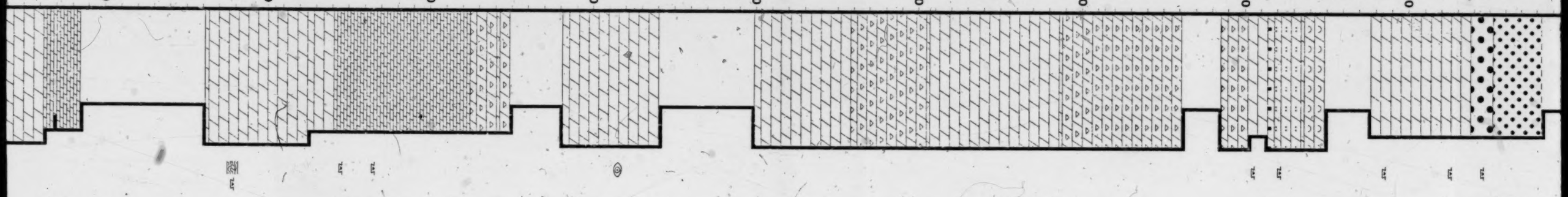

MH3 MH2 MH3 MH4 MH5 MH6 MH3 MH2 MH4 MH3 MH4 MH5 MH6 E5 E6 E6

1 E1

MISSISSIPPIAN LITHOTYPES DISCUSSED IN TEXT

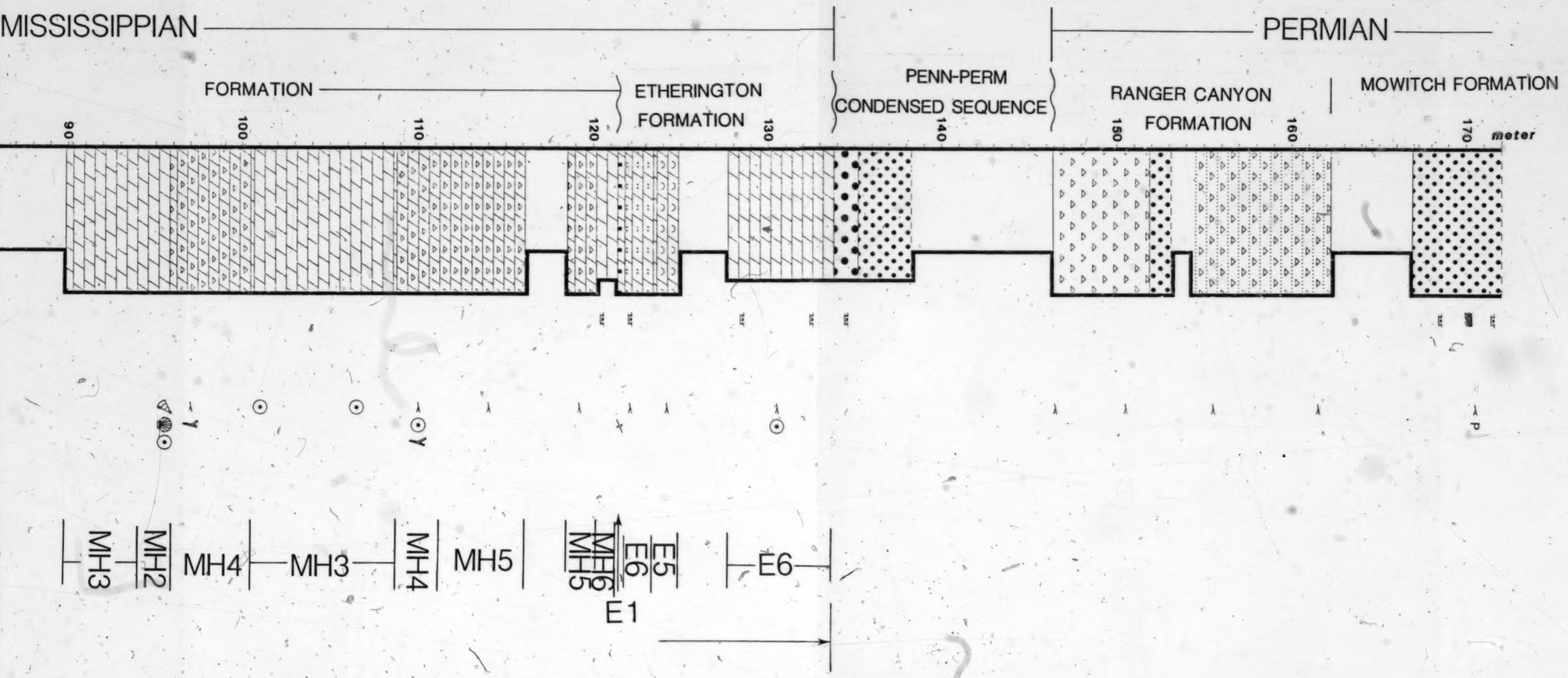
MISSISSIPPIAN
PERMIAN
FORMATION
ETHERINGTON FORMATION
PENN-PERM CONDENSED SEQUENCE
RANGER CANYON FORMATION
MOWITCH FORMATION
90
100
110
120
130
140
150
160
170
meter
MH3
MH2
MH4
MH3
MH4
MH5
MH6
E5
E6
E1
E6